University of Nevada, Reno

# Dynamics of KSHV gene expression during de novo infection and the role of LANA in immune modulation

A dissertation submitted in partial fulfillment of the requirements for the degree of

Doctor of Philosophy in Cell and Molecular Biology

By

Suhani T. Thakker

Dr. Subhash C. Verma/Dissertation Advisor

May, 2015

THE GRADUATE SCHOOL

We recommend that the dissertation
prepared under our supervision by

**SUHANI T. THAKKER**

Entitled

**Dynamics of KSHV gene expression during de novo infection and the role of LANA in immune modulation**

be accepted in partial fulfillment of the
requirements for the degree of

DOCTOR OF PHILOSOPHY

Subhash Verma, Ph.D., Advisor

Gregory Pari, Ph.D., Committee Member

David AuCoin, Ph.D., Committee Member

Thomas Kozel, Ph.D., Committee Member

Dean Burkin, Ph.D., Graduate School Representative

David W. Zeh, Ph. D., Dean, Graduate School

May, 2015

## Abstract

Kaposi's sarcoma-associated herpesvirus (KSHV) is an oncogenic human herpes virus that has been linked to the development of multiple malignancies including Kaposi's sarcoma, primary effusion lymphoma, and multicentric Castleman's disease. Like all members of the herpesvirus family, KSHV establishes a lifelong persistence in the infected host. However, immediately upon infection, the virus has to overcome many challenges in the hostile cellular environment before it can establish a long-term infection. The remarkable success of the virus in establishing lifelong persistence in the infected host indicates that the virus is well equipped to manipulate the host environment very efficiently, even before it has a chance to fully express its genome. In order to understand how KSHV manipulates the host environment immediately upon infection, we must first understand which molecules are packaged in the virions and which viral genes are expressed during the initial time points following entry of the virus into the host cells. In chapter I, we probe these questions by performing a comprehensive analysis of the viral transcriptome in the purified KSHV virions. We also examine the dynamics of viral transcriptome at very early time-points following *de novo* infection of multiple cell lines permissive to long-term infection of KSHV. For this comprehensive study of viral transcriptome analysis, we used a high throughput approach of next-generation RNA sequencing. The results of this study identified many viral transcripts that are packaged into the virions and the transcripts that are actively transcribed during the initial infection period. Overall, the results of this study lay a foundation for future research targeting the viral genes whose expression may be critical for establishing a successful viral infection.

One critical aspect of KSHV infection is its ability to persist throughout the life of the host. This can be attributed to its ability to efficiently hide from the host's immune surveillance. In chapter II, we identify a novel mechanism that helps the virus hide from the radar of host immunity. Our data sheds light on how one of the viral proteins, Latency- associated nuclear antigen (LANA), reduces the expression of major histocompatibility class II (MHC II) molecules, which are the molecules that are critical for reporting viral antigens to the immune cells of the host. We demonstrated that LANA binds with the proteins of regulatory factor X (RFX) complex, which are essential components of MHC II transcription machinery. The association of LANA with RFX complex reduces binding of the transcription factor called class II transactivator (CIITA) to the highly conserved promoters of MHC II genes. Binding of the CIITA to MHC II promoters is absolutely necessary for the expression of MHC II genes; by reducing the association of CIITA with the promoters of MHC II genes, LANA inhibits the expression of MHC II genes.

KSHV infection is known to induce multiple pro-angiogenic cytokines that aid in extensive angiogenesis associated with Kaposi's sarcoma tumors. In chapter III, we demonstrate that LANA induces expression of a secreted angiogenic cytokine epidermal growth factor-like multiple 7 (EGFL7). Our data shows that LANA induces expression of EGFL7 in B cells, suggesting that it may act in a paracrine fashion during KSHV infection. The results of this research provide insight into an additional mechanism used by KSHV to promote angiogenesis. Targeting EGFL7 in combination with other important angiogenic cytokines induced during KSHV infection may increase the effectiveness of currently available anti-angiogenic therapy for Kaposi's sarcoma.

**Acknowledgements**

I would like to express my utmost gratitude to my advisor, Dr. Subhash Verma. He has been very supportive of my efforts since my first day in his lab. It was a pleasure working with such a knowledgeable mentor with an unmatched enthusiasm and passion for research. I have learned a lot from him; one thing worth mentioning is the scientific attitude that he infused in me, as it is beyond this research.

I would also like to express my sincerest thanks to all of my committee members Dr. Gregory Pari, Dr. David Aucoin, Dr. Thomas Kozel, and Dr. Dean Burkin for their constructive feedback on my research and for their valuable time.

Many thanks go to Dr. Pari for his advice and encouragement throughout my studies at UNR. He was one of the people who encouraged me to restart my Ph.D. studies.

I express my sincere gratitude to Dr. Mick Hitchcock who provided financial patronage to me and to many other graduate students. It is great people like Dr. Hitchcock who help others achieve their true American dream.

I am thankful to all my colleagues and lab members for making the lab a pleasant place to work. Special thanks go to Dr. Purushothaman for frequently removing technical roadblocks, and to Jessica Chen for assisting me on multiple projects. I also thank Dr. Cai, Dr. Uppal, Dr. Gupta, and Allie Scurry for their contribution in this research.

Finally, I would like to thank my family. My husband Tushar and my children, Trisha and Toshaan, have given me their unconditional support. They were my motivation for getting a Ph.D. degree and their love is the reason behind my success.

## Table of Contents

# List of Tables

## List of Figures

## List of Figures

## List of Figures

**Page**

**Chapter 3**

## Introduction and Background

### 1. Herpes viruses

Herpes viruses are the leading cause of viral diseases in animals and humans. The family name 'Herpesviridae' is derived from the Greek word herpein, referring to latent, recurring infections that are characteristic of herpes viruses. They are enveloped DNA viruses containing relatively large linear double-stranded DNA genomes (~130–250 kb) with a capacity to encode 70–200 genes (35, 89). The viral DNA is encased within an icosahedral protein capsid approximately 125 nm in diameter and a tegument matrix. Viral DNA replication and capsid assembly occur in the nucleus of the infected host cell, and viral particles become enveloped by lipids as the particles leave the nucleus (8).

Herpes viruses are classified into three distinct subgroups, alpha, beta and gamma, based on genomic sequence similarities and biological properties such as tissue and host specificity (42, 43, 113). One common attribute of all of the members of the herpesvirus family is their ability to establish life-long latent infection in permissive cells, with periodic reactivation of productive, lytic replication cycles. Alpha herpes viruses establish latency in neuronal cells, beta herpes viruses establish latency in myeloid progenitor cells and/or lymphocytes, and gamma herpes viruses establish latency in cells of lymphoid origin (113).

Out of over 100 known herpes viruses, only eight are known to infect humans. These include Herpes simplex type I (HHV-1), Herpes simplex type II (HHV-2), Varicella-Zoster virus (VZV/HHV-3), Epstein-Barr virus (EBV/HHV-4), Cytomegalovirus (CMV/HHV-5), Human herpesvirus type 6 (HBLV/HHV-6), Human herpesvirus type 7 (HHV-7) and Kaposi's sarcoma-associated herpes virus (KSHV/HHV-

8). A large majority of the human population is estimated to be infected with at least one of these eight herpes viruses (165). KSHV was discovered by Patrick Moore and Yuan Chang in 1994 by using the Representational Difference Analysis (RDA) technique in biopsy samples of Kaposi's sarcoma (KS), an AIDS-associated tumor (33). Later, KSHV was found to be associated with several other malignancies including body cavity-based lymphomas. Having been linked to both lymphomas and sarcomas (104), KSHV classifies as an oncogenic virus (103).

**2. KSHV-related diseases**

Primary KSHV infection in immune-competent hosts is largely asymptomatic; however, the virus often causes cancer in immunosuppressed hosts. KSHV has been established as a causative agent of KS, a highly vascularized tumor of endothelial origin. In addition to KS, the virus also causes primary effusion lymphoma (PEL) and Multicentric Castleman disease (MCD).

**2.1 Kaposi's sarcoma (KS)**

KS was initially described by Moritz Kaposi in 1872 as an aggressive pigmented tumor of skin (34). At that time, KS was most common amongst elderly men of Mediterranean, eastern European or Middle Eastern heritage. However, following the onset of the AIDS pandemic in the 1980s, rates of KS incidence became so high in HIV co-infected individuals that KS became an AIDS-defining tumor. Since then, four subtypes of KS have been described. The first subtype, classic KS, is the one originally described by Moritz Kaposi. Classic KS is more predominant in men than in women. This form is characterized by benign lesions on the legs, ankles or soles of the feet, and is rarely aggressive (45). The second subtype, African endemic KS, is associated with HIV-

positive and HIV-negative individuals, including children, and is associated with significant mortality (54, 100). The third subtype, Iatrogenic KS, is the form that develops in organ transplant patients following immunosuppressive therapy (54, 100). The fourth subtype, AIDS-associated epidemic KS, is a highly aggressive tumor primarily associated with HIV co-infected individuals whose immune systems are severely compromised. This subtype is the most aggressive form of KS and is not restricted to the skin. The tumors frequently develop on the internal organs such as liver, spleen, gastrointestinal tract and lungs. AIDS-associated epidemic KS is the most common malignancy associated with HIV infection, and causes significant morbidity and mortality in this group of patients (54).

**2.2 Primary effusion lymphoma (PEL)**

Primary effusion lymphoma, also known as body cavity-based lymphoma, is a rare but aggressive B cell tumor that arises within the pericardial, pleural, and peritoneal body cavities (54). PEL occurs in HIV-positive as well as HIV-negative individuals, and 5- 20% of HIV co-infected patients develop PEL. It is a very aggressive form of lymphoma, with an average survival time of only 6 months from diagnosis (21, 100).

**2.3 Multicentric Castleman's disease (MCD)**

Castleman's disease is angiofollicular lymph node hyperplasia that is either unicentric (localized) or multicentric. MCD has two clinical variants – a hyaline vascular variant that is not associated with KSHV infection, and a plasmoblastic variant that is associated with KSHV infection. In KSHV/HIV co-infected patients, progression of MCD is very aggressive.

**2.4 KSHV-inflammatory cytokine syndrome (KICS)**

KICS is an inflammatory condition arising due to severe systemic lytic reactivation of KSHV. KICS is associated with high systemic viral load, KS and excessive cytokine production, notably high levels of interleukin 6 (IL-6). KICS has been proposed as a new KSHV-associated disease (132, 154).

**3. KSHV cell tropism and transmission**

KSHV is a lymphotropic gammaherpesvirus, subclassified as ϒ2-herpesvirus. However, it infects a variety of cell types *in vivo* and *in vitro*. KSHV is known to infect endothelial cells, epithelial cells, monocytes, keratinocytes and B cells *in vivo*. Whereas KSHV can infect T cells *in vivo*, KSHV infection of T cells is abortive (106). Some studies suggest that KSHV can also infect mesenchymal stem cells (MSCs) and hematopoietic progenitor cells (HPCs), which may serve as reservoirs for KSHV infection (56, 116, 169). *In vitro*, KSHV has even broader tropism. The virus can successfully infect human dermal microvascular endothelial (HMVEC-d) cells, human umbilical vein endothelial (HUVEC) cells, human foreskin fibroblast (HFF) cells, telomerase-immortalized human umbilical vein endothelial (TIVE) cells, human embryonic kidney 293 (HEK293) cells, human epithelial SLK cells, monkey kidney epithelial VERO cells, monkey kidney CV-1 cells, and mouse fibroblasts (158).

There are many transmission routes of KSHV. In KSHV-infected humans, the oropharynx is thought to be the primary site of virus replication, where the virus is shed into the saliva (106). High KSHV loads have been detected in saliva, irrespective of KSHV titers in the peripheral blood (55). Saliva is thus the main reservoir of infectious KSHV virions, and also the main route of infection in the context of both sexual and non-

sexual KSHV transmission. However, KSHV can also be transmitted through parenteral routes such as needle sharing, blood transfusion and solid-organ transplantation (54). Vertical transmission from mother to child is thought to be rare for KSHV.

**4. KSHV virion structure and assembly**

The KSHV architecture is built from conserved structural elements of herpesviruses. A typical KSHV virion is composed of a viral genomic DNA encased in an icosahedral capsid shell (~125 nm in diameter) composed of 162 capsomeres (165). KSHV capsids are made up of a repeating pattern of five viral proteins including ORF25, ORF26, ORF62, ORF17.5 and ORF65 (54, 108, 168). The envelope surrounding the capsid is a lipid bilayer spiked with the virally-encoded glycoproteins ORF8 (gB, glycoprotein B), ORF22 (gH), ORF39 (gM), ORF47 (gL), ORF53 (gN), ORF68 and ORFK8.1 (15, 54, 177). These glycoproteins mediate the attachment and entry of the virus into host cells. A KSHV virion also contains a tegument, an electron-dense, proteinaceous material located between the capsid and the envelope. KSHV tegument proteins are known to be involved in several phases of the viral life cycle including virion assembly and egress, transportation of incoming virions towards the nucleus, and immune evasion (145).

The KSHV genome is a double-stranded DNA with a typical ϒ2-herpesviruses genome structure (93, 134). The genome is circularized and maintained as an extrachromosomal episome during latent infection, but is linearized during virion packaging and replication. The length of the genome is variable, usually 160–170 Kb, containing approximately 145 kb of coding sequences. These sequences are flanked by multiple copies of 801 bp, GC-rich terminal repetitive (TR) DNA, a region that is not

known to have any coding capacity so far (93). The number of TRs varies amongst KSHV isolates, which accounts for the variation in genome sizes of KSHV isolates. The coding sequences of the KSHV genome reside in at least 89 open reading frames (ORFs), 67 of which have homologues in the closely-related ϒ2-herpes virus known as herpesvirus saimiri (93). KSHV genes are numbered from left to right as ORF1 to ORF75 (54). The KSHV genes that do not share a clear homology with herpesvirus saimiri are designated as ORFs starting with the prefix 'K'. There are 19 such genes, including ORFs K1 to K15, K4.1, K4.2, K8.1 and K 10.5. Often, these genes share homology with cellular genes and encode proteins that mimic cellular proteins involved in immune modulation, cellular growth and metabolic regulation (93). In addition, KSHV encodes several mRNAs, miRNAs and noncoding RNAs (14, 26, 88, 122, 129, 141, 152). A long (1.1 kb) noncoding RNA termed polyadenylated nuclear RNA (PAN RNA) is one of the most abundant transcripts detected in KSHV-infected cells (137). A schematic map of the KSHV genome is shown in Figure 1.

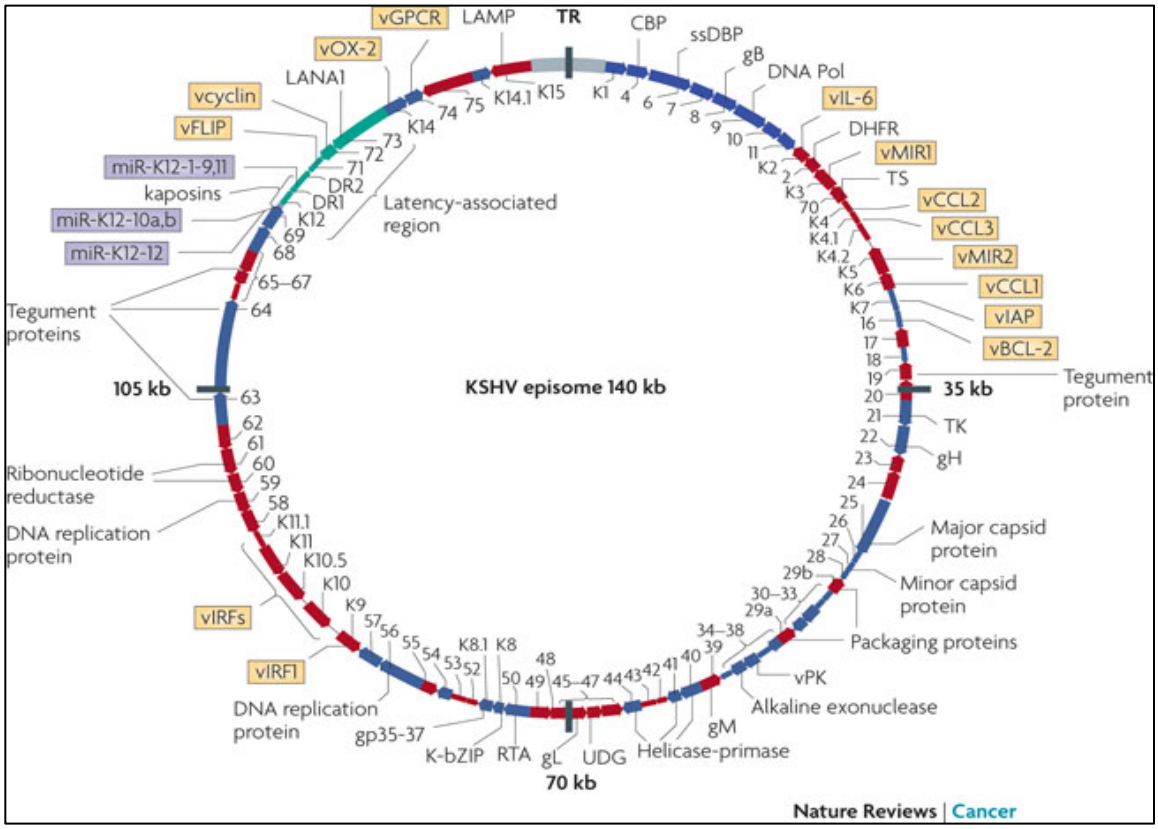


Figure 1: The KSHV episome. This image from 'Kaposi's sarcoma and its associated herpesvirus' is reprinted here with the original publisher's permission (100). KSHV encodes at least 87 open reading frames (ORFs) and 17 microRNAs (purple boxes), 14 of which are co-expressed as a cluster. A striking feature of KSHV is the number (at least 14) of ORFs that encode cellular orthologues. Identified ORFs and encoded proteins are indicated in the figure. Putative latent transcripts are indicated in green, and cellular orthologues in yellow. Infection occurs when glycoproteins on the surface of mature virions bind to receptors on the cell surface. After binding, clathrin-mediated endocytosis facilitates virion entry into the cell. Next, the viral DNA is rapidly transported into the nucleus and circularized, forming a dormant episome like other herpesviruses. Viral reactivation can occur when the promoter of ORF50 is activated (by demethylation, for example), resulting in the expression of replication and transcription activator (RTA), the main regulator for the viral lytic replication programme. Early lytic genes include those encoding viral proteins required for DNA replication or viral gene expression, whereas late lytic genes are those encoding viral structural proteins, such as envelope and capsid proteins that are required for assembly of new virions.

During the lytic phase of viral replication, when new virions are assembled, KSHV capsid proteins bind to KSHV DNA. The KSHV DNA is packaged into capsids as a single-copy linear DNA free of nucleosomes or other DNA binding proteins. The DNA-

containing capsids then acquire tegument and envelope proteins and bud through the nuclear membrane into cytoplasm. These virions are transcytosed toward the plasma membrane within vesicles that ultimately fuse with the plasma membrane to release the virions into the extracellular space (108).

**5. KSHV entry into host cells**

KSHV entry into host cells is a complex multistep process involving virion attachment, endocytosis, trafficking, and nuclear transport. Virion attachment to the host cell is itself a two-stage process mediated by KSHV envelope glycoproteins which bind to host cell surface molecules (121, 158). First, KSHV glycoproteins gB (ORF 8), gH (ORF22), ORF4, and gpK8.1A bind to heparan sulfate, a cellular proteoglycan located on a variety of host cell types. Binding to heparan sulfate serves as an initial docking event, facilitating further interactions of the virion with more cell-specific receptors (2, 17, 59, 162). One of these receptors is DC-SIGN, which facilitates binding to activated B cells, myeloid dendritic cells and macrophages (158). In addition, KSHV glycoprotein gB (ORF 8) contains a conserved integrin-binding RGD motif, enabling the protein to bind to integrins, $\alpha 3\beta 1$ $\alpha V\beta 3$, and $\alpha V\beta 5$ (158). Furthermore, the 12-transmembrane glutamate/cysteine exchange transporter protein xCT, and the tyrosine kinase receptor EphA2 also serve as entry receptors for KSHV (60, 64). The use of multiple cellular receptor molecules is responsible for KSHV's broad tropism. The interactions between KSHV envelope glycoproteins and cellular receptors trigger multiple downstream signaling cascades, leading to internalization of the virus by endocytosis or by direct fusion of the viral envelope with the plasma membrane. The viral capsid is transported

through the cytosol and the viral DNA is delivered into the host nucleus, where KSHV begins its life cycle (31).

**6. KSHV life cycle**

Following an acute primary infection, KSHV establishes life-long persistence in immune-competent individuals. As with all other herpesviruses, KSHV exhibits two distinct phases of gene expression in its life cycle – a latent phase and a lytic phase (19). During latency, only a handful of viral genes are expressed, in order for the virus to avoid detection by the host immune system. During the lytic phase, the entire KSHV genome is expressed in a highly ordered fashion in order to ensure efficient replication of viral DNA and its packaging into new virions. Whereas latency efficiently maintains the KSHV genome, periodic reactivation to lytic replication is necessary for the transmission and dissemination of KSHV into new cells and new hosts (172). Thus, both stages of the viral life cycle are essential for viral maintenance and propagation. The appropriate regulation of latent and lytic gene expression is extremely critical for viral pathogenicity, and KSHV has evolved complex regulatory mechanisms in order to ensure that the correct genes are active at the correct times.

**6.1 KSHV latency**

Latency is established rapidly following KSHV infection (within 24 hours of infection) and is considered the predominant stage of the KSHV life cycle (69). During latency, the KSHV genome persists as multi-copy circular episomes that are assembled into chromatin like nucleosomal structures; hence, the KSHV genome is chromatinized (172). KSHV episomes replicate using host cell machinery and segregate into the daughter cells during mitosis (159). As mentioned earlier, only a small proportion of

KSHV genes are transcribed during latency. Limited expression of KSHV genes during latency allow the virus to "hide," as the majority of viral epitopes are not available for detection by the host immune surveillance. The handful of KSHV genes that are transcribed during latency ensures efficient maintenance of KSHV episomes, immune evasion, regulation of the host cell cycle, inhibition of host cell apoptosis, and suppression of KSHV lytic gene expression.

The genes that are actively transcribed during latency are clustered in the latency locus of the KSHV genome (Fig 2). This locus transcribes viral genes including latency-associated nuclear antigen (LANA or LANA-1,ORF73), viral cyclin (vCyc, ORF72), viral FLICE inhibitory protein (vFLIP, ORF71), Kaposin (ORF K12) and viral microRNAs (26, 47, 143). Regulation of latent gene transcription is a complex process that involves multicistronic transcripts, several alternative promoters and epigenetic regulation (65). LANA, vCyc, and vFLICE are expressed from the same major latency 5.7 kb transcript that is differentially spliced. A separate 1.7 kb transcript contains vCyclin and vFLIP coding sequences. Transcription of the major latency mRNA encoding ORF71 to ORF73 is regulated by at least two promoters - a constitutively-active latent promoter (LTc) and an alternate inducible promoter (LTi) which is normally inactive but can be activated by KSHV replication and the transactivator protein (RTA, ORF50) (157).

In addition to these genes that are expressed in all latently-infected cells, the viral interferon regulatory factor (vIRF-3 or LANA-2, K10.5) is expressed in all latently-infected PEL cells but not in latently-infected KS spindle cells (40, 136, 166). Whereas

the above-mentioned genes are considered “classic” latent genes, some other viral genes such as K1 and vIL6 are also likely to be expressed at low levels during latency (32).

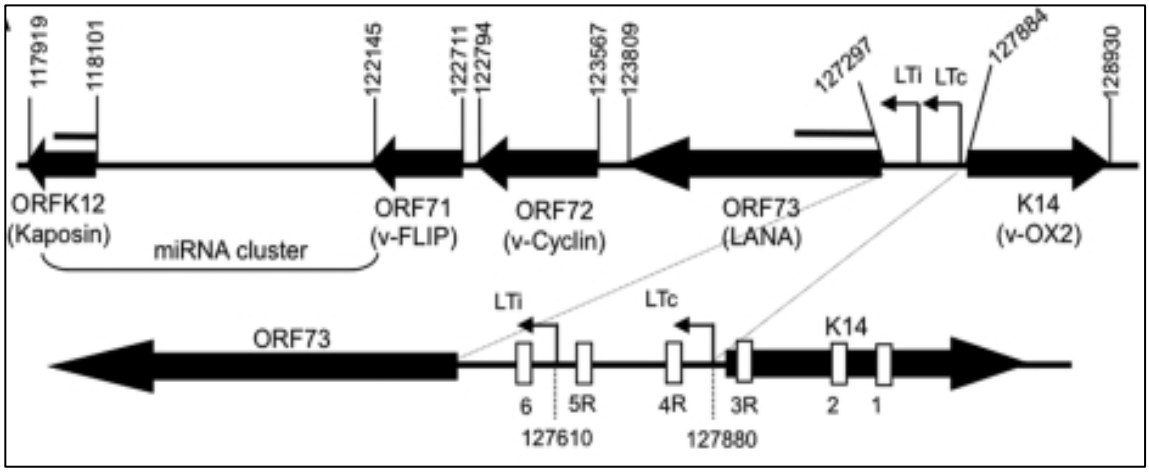


Figure 2: The KSHV latent transcript. This image from ‘Kaposi's sarcoma-associated herpesvirus latency-associated nuclear antigen induction by hypoxia and hypoxia-inducible factors’ is reprinted here with the permission from the original publisher (157). Schematic diagram of the genomic organization of the region spanning *ORFK12* (Kaposin) through *K14* (v-OX2) in the KSHV genome; this region includes *ORF71* through *ORF73* (LANA) as well as the KSHV miRNA cluster. The numbers above the closed arrows correspond to positions of initiation/termination codons of the ORFs. Two arrows between *K14* (v-OX2) and LANA denote the LANA constitutive (LTc) and RTA-inducible (LTi) mRNA start sites.

### 6.1.1 vCyclin

vCyclin, the product of KSHV ORF72, is a functional homologue of the cellular gene cyclin D2. Each protein can form active holoenzymes with cyclin-dependent kinases (CDK) 4 and 6. However, vCyclin has a broader substrate range than its cellular counterpart, possessing the ability to associate with CDK-2 and CDK-9. In addition, the vCyclin-CDK6 holoenzyme is refractory to several cell cycle control mechanisms, thus deregulating the cell cycle. Intriguingly, overexpression of vCyclin induces p53-

dependent growth arrest and cell apoptosis, activates the DNA damage response and increases autophagy (120).

### 6.1.2 vFLIP

vFLIP, encoded by K13, is a viral homologue of the cellular inhibitory protein FLICE (FADD-like interleukin-1 beta converting enzyme/caspase-8). vFLIP is capable of activating both classical and alternative NF-kB pathways, and is also known to block autophagy. Furthermore, vFLIP induces expression of inflammatory cytokines in endothelial cells in vitro (11).

### 6.1.3 Kaposins

The ORF K12 encodes three proteins, Kaposin A, Kaposin B and Kaposin C, by alternative splicing of a multicistronic transcript (140). Kaposin transcripts are some of the most abundant latency-associated viral transcripts. Kaposin A can induce cell transformation, whereas Kaposin B stabilizes AU-rich mRNAs. Since many cytokine mRNAs contain AU-rich elements, Kaposin B thus stabilizes transcripts of cytokines including IL-6 and GM-CSF (99). Knowledge regarding the function of Kaposin C is still limited. The relative expression of Kaposins A, B and C varies amongst different KSHV-infected tissues (82).

### 6.1.4 KSHV microRNAs

KSHV encodes over 12 pre-miRNAs from the latent Kaposin promoter. Cellular proteins Drosha and Dicer process these pre-miRNAs to generate more than 24 mature miRNAs. Despite having a common promoter, the levels of these miRNAs are variable in latent KSHV-infected cell lines. In PEL cell lines, KSHV miRNAs are the most predominant miRNAs, indicative of their essential functions in regulation of the viral life

cycle (26, 54). KSHV miRNAs target diverse cellular pathways in order to promote angiogenesis, regulate the cell cycle, inhibit apoptosis, evade host immunity, transform the infected cell and promote tumorigenesis (101, 124). KSHV-encoded miRNAs also suppress lytic reactivation in latently-infected cells by modulating the expression of cellular transcription factors including MYB, C/EBPα and Ets-1 (124).

**6.1.5 vIRF3**

KSHV encodes four interferon regulatory factors (vIRF1 to vIRF4) encoded by the cluster of ORFs K9, K11/11.1, K10.5/10.6, and K10. vIRFs share homology with cellular interferon regulatory factors (IRFs), and modulate the activities of cellular IRFs and interferons (IFNs). vIRF3, also known as latency-associated nuclear antigen-2 (LANA-2), is encoded by ORF K10.5 and is constitutively expressed in PEL cell lines. Expression of vIRF3 has also been detected in MCD tumors, but not in KS spindle cells. vIRF3 shares significant homology with cellular IRF4 in its C terminus and with vIRF2 in its N terminus (13, 147). vIRF3 is known to be an oncogene required for continuous proliferation and survival of PEL cells (166). vIRF3 also acts as a immune suppressor, in that it inhibits recognition of infected cells by CD4 T cells through CIITA-dependent and -independent interference with MHC II antigen presentation (138, 146, 166).

**6.1.5 LANA**

Latency-associated nuclear antigen (LANA, LANA-1), the key viral protein required for establishment and maintenance of KSHV latency, is encoded by KSHV ORF73. LANA is highly expressed in all latently-infected cells, whether normal or malignant (62, 67, 156, 161). LANA is a functional homologue of the Epstein Barr Virus

(EBV)-encoded protein EBNA1. Both are nuclear proteins that interact with numerous viral and cellular proteins (161).

The LANA protein sequence consists of 1,162 amino acids, with a theoretical molecular mass of 135 kDa, but migrates on SDS-PAGE gels as if it was 220 kDa (161). LANA can be subdivided into three major domains: an N-terminal proline-rich domain, a central domain containing a glutamine-rich region and a variable number of acidic amino acid repeats, and a conserved C-terminal domain containing a leucine zipper motif (Fig 3) (62, 110). The N-terminal domain contains a chromosome binding site (CBS) and a nuclear localization signal (NLS). LANA has another NLS in its C-terminus, the N-terminal NLS seems to be functionally dominant, as N-terminal deletion mutants of LANA accumulate in the cytoplasm (110). The C-terminal domain mediates LANA's ability to dimerize and to bind to DNA. Post-translational modifications that regulate LANA activity include phosphorylation, acetylation, PARylation (Poly ADP-ribosylation), SUMOylation (small ubiquitine-like modification), and arginine methylation ((10, 28, 29, 36, 51, 94, 111, 125).

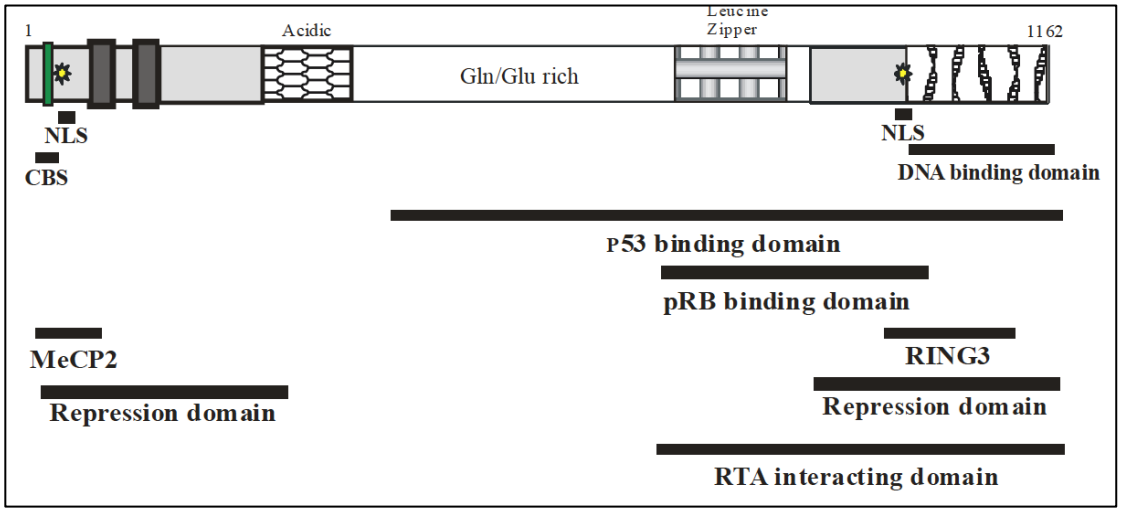

Figure 3: A schematic showing the domain structure of LANA. LANA is an 1162 aa protein containing two nuclear localization sequences (NLS). The N-terminal domain contains a chromosome-binding site (CBS), the central domain contains an acidic region rich in aspartic and glutamic acid residues, a glutamine-rich region, and a leucine zipper motif (L-ZIP). LANA forms homodimers through its C-terminal domain and facilitates binding to LANA-binding sequences (LBS) in the KSHV genome.

LANA is a multifunctional protein that interacts with many viral and cellular proteins (66) and binds to DNA. One of the main functions of LANA is the establishment and maintenance of viral episomes during latency. LANA binds to the terminal repeat region (TR) of the KSHV genome and employs host cell DNA replication machinery to replicate KSHV episomes (95). LANA also ensures the proper segregation of KSHV genomes during mitosis by tethering the episomes to host chromatin; this is accomplished by binding of the CBS to histones. LANA also binds to several cellular chromatin-binding proteins, which together aid LANA in its episome tethering function. Some of these proteins include bromodomain-containing protein Brd4, methyl-CpG binding protein MeCP2, DEK, and nuclear mitotic apparatus protein (NuMA) (12, 39, 58, 62, 87, 123, 156, 175).

In addition to its role in the maintenance of viral episomes, LANA has demonstrated roles in cellular transformation and blocking of apoptosis (3, 22, 24, 25, 53, 76, 95, 96, 142, 156), cell cycle regulation (70, 90), angiogenesis (24, 117, 163), and immune evasion (23, 37). Pro-survival and transformative activities of LANA can be partially attributed to LANA's ability to bind to and inhibit the activities of the tumor suppressor proteins p53 and Rb. LANA can also bind to glycogen synthase kinase 3β and sequester it in the nucleus, resulting in the accumulation of baccumula and consequent upregulation of pro-survival proteins cyclin D and c-Myc. Expression of

LANA in endothelial cells is known to induce expression of angiogenin, a potent stimulator of endothelial cell proliferation and angiogenesis (139). Furthermore, LANA can bind to death-domain associated protein-6 Daxx, thereby relieving Daxx's repression of Ets-1-dependent VEGF receptor expression in order to boost angiogenesis (105). LANA also promotes angiogenesis by upregulating Hey1, an essential Notch signaling pathway member (163). LANA is known to deregulate host immunity by impairing neutrophil chemotaxis to the site of infection and interfering with the TNF-α signaling, interferon signaling, MHC I antigen presentation and MHC II antigen presentation pathways (23, 37, 71, 83, 176).

LANA is a potent transcription modulator of many cellular and viral genes (133). LANA can activate or inhibit expression of many genes through direct or indirect mechanisms. For example, LANA can indirectly activate transcription of genes with promoters containing binding sites for transcription factors such as ATF, CAAT, AP-1 or SP1 (133). On the other hand, LANA can indirectly repress transcription via association with co-repressor proteins such as mSIn3, SAP30, CIR, the methyl CpG-binding protein MeCP2, and the histone methyl transferase SUV39H1. LANA can also repress expression of KSHV genes by directly associating with the viral DNA, e.g. ORFK1 (160). LANA inhibits expression of the transcription activator RTA (ORF50), the lytic master switch protein, in order to suppress the lytic replication cycle. At the same time, LANA can auto-regulate its own expression by binding directly to its own promoter. Thus, LANA serves pleiotropic roles in maintenance of KSHV latency and is indispensible for the life-long persistence of KSHV.

**6.2 KSHV lytic replication**

Whereas latent infection is important for viral persistence and for maintaining a continuous viral reservoir, lytic infection is essential for viral spread to other cells and tissues of the same individual, as well as between different individuals. Whereas the majority of KSHV-infected tumor cells harbor the KSHV genome in a latent stage, a subset (1 to 3%) of these latently-infected cells are estimated to undergo spontaneous lytic replication (18, 30, 68, 112, 115, 151). The lytic replication cycle has important pathological consequences, as many lytic proteins trigger the release of cellular inflammatory cytokines and several lytic proteins have oncogenic and angiogenic potential (5, 9, 20, 52, 77, 102, 144).

In contrast to latency, the lytic replication cycle activates most of the KSHV genes, in a highly-regulated sequential manner. KSHV lytic genes can be broadly classified into three major groups: immediate early (IE), early or delayed early (E or DE), and late (L), based on their timing of expression. As the name suggests, the immediate early genes are the first set of KSHV genes expressed during reactivation of the lytic replication cycle, or following viral entry into the host cells. In the latter case, these genes generally do not require *de novo* protein synthesis, and hence their expression is insensitive to treatment with the eukaryotic protein synthesis inhibitor cyclohexamide. The immediate early KSHV proteins predominantly serve regulatory roles. The immediate early protein RTA (ORF50) is one of the earliest KSHV proteins detected following *de novo* infection. RTA auto-regulates its own promoter and also transactivates the promoters of many viral and cellular genes. Immediate early proteins are also required for transcription of early and late genes, which are sensitive to cyclohexamide.

KSHV early genes encode accessory proteins or have enzymatic activities, and are mainly involved viral DNA replication. Some of the early proteins also regulate gene expression or promote immune evasion. Late genes typically encode virion structural proteins such as capsid and envelope proteins (130). At the end of a productive lytic cycle, the infected cell is lysed, releasing new virions into the surrounding environment.

Virally-encoded proteins ensure efficient viral DNA replication under cellular conditions that may not be favorable for viral DNA replication. Like other herpesviruses, KSHV lytic DNA replication initiates from the origin of replication and proceeds via the rolling circle mechanism. Two functional origins of lytic replication that share high sequence homology with each other have been identified in the KSHV genome. Of these two origins of lytic DNA replication, Ori-Lyt-L (located between K4.2 and K5) is sufficient to propagate the viral genome, whereas Ori-Lyt-R (located between ORF69 and vFLIP) is not sufficient propagate the viral genome (6, 171).

The switch from latent to lytic infection primarily depends on the expression of ORF50/RTA, the key initiator that has been demonstrated to be both necessary and sufficient to drive productive lytic replication by numerous studies. *In vitro* ectopic expression of RTA leads to activation of the full cycle of KSHV lytic gene expression, and deletion or inhibition of RTA prevents lytic cycle reactivation (153). Whereas the majority of factors that activate lytic replication do so by activating RTA expression, alternative pathways are likely to exist. The discovery that lytic replication can be triggered by apoptosis in the absence of RTA expression strongly suggests that KSHV has backup pathways that detect adverse cellular conditions limiting RTA expression (127, 128).

Numerous complex mechanisms are involved in lytic reactivation and many triggers can activate the lytic replication cycle. These include chemicals like sodium butyrate and TPA that are routinely used to induce lytic replication *in vitro* (97). In addition, many cellular stresses such as oxidative stress or inflammation can lead to viral reactivation (130). Other physiological factors influencing lytic reactivation include co-infection with other viruses, apoptosis and the immune status of the infected host. For example, during KSHV/Epstein-Barr virus (EBV) co-infection, EBV inhibits KSHV lytic replication, probably because the two viruses compete for the same limited cellular resources; hence, the two viruses have evolved mechanisms to inhibit lytic replication of each other (170). The immune status of the infected host is probably the most important factor controlling viral reactivation. A strong immune system limits KSHV lytic reactivation, as the immune system attacks viral epitopes and thereby keeps KSHV lytic replication in check. Conversely, lytic replication is unchecked when the immune system is compromised, as indicated by high viral titers and the resultant detection of antibodies against lytic proteins in the blood (97). As mentioned earlier, apoptotic signals can also lead to viral reactivation (127). Thus, KSHV is well-equipped to sense adverse cellular conditions that could threaten viral persistence, and the virus responds to these unfavorable conditions by producing more virions through lytic reactivation.

**Overview of the thesis**

**7.1. Transcriptome analysis of Kaposi's sarcoma-associated herpesvirus during de novo primary infection of human B and endothelial cells**

During the latent phase, the KSHV genome is silently maintained without production of functional virions. Hence, a latent phase on its own is not sufficient to

propagate viral spread in the infected host. In the absence of productive lytic replication, one can expect the virus to eventually disappear when the latently-infected cells die. Indeed, in culture, latent KSHV episomes tend to be lost from a wide variety of dividing cells (57). Accordingly, a continuous lytic replication is necessary for the spread of the virus within the infected host. Due to this necessity, a small proportion (1-5%) of the latently infected cells routinely undergo spontaneous lytic replication. Nascent virions that are released at the end of lytic replication cycle infect fresh cells in order to perpetuate viral infection. The process of nascent virions infecting fresh cells is called *de novo*, or primary, infection. *De novo* infection begins when newly-released virions bind to cell surface receptors of uninfected target cells. A successful viral infection involves virion internalization in an endosome, fusion of the viral envelope with the endosomal membrane, transport of the viral capsid to the nucleus, release of the viral DNA from the capsid in the nucleus and finally formation of latent episomes (31).

During these early events the virus has to face many challenges. For example, detection of KSHV as an intracellular pathogen may trigger innate and adaptive host immune responses that may result in apoptosis or destruction of the infected cell. A successful viral infection critically depends upon whether the virus is capable of overcoming these challenges successfully. Fortunately for the virus, it is well-equipped to face the challenges imposed by the host. During the very early period of *de novo* infection, proteins present in the virion manipulate the cellular environment to make it conducive for viral infection. In order to understand the host-virus interactions that make KSHV an extremely successful intracellular pathogen, we must first know which proteins are present in the virion and which viral genes are activated during early infection.

Hence, this calls for a clear understanding of the viral genes that play an important role during the early events of infection. Several previous studies have probed the events that happen during early KSHV infection (14, 15, 69, 107). These studies have revealed that during *de novo* infection, KSHV typically establishes latency by 24 hours post infection (15). Before that, there is an initial burst of viral gene expression that includes a subset of lytic genes. However, the lytic cycle that is induced during this period is transient and is followed by rapid establishment of latency, as indicated by the presence of latent gene transcripts. Additionally, KSHV virions are known to contain a variety of proteins and several RNA species including viral gene transcripts, cellular and viral microRNAs and noncoding RNAs (14, 88). Whereas these studies have provided significant insights into the elements present in the virion and the viral genes that are expressed immediately following infection, the complete picture has not fully emerged. The open questions necessitate further research on this process. The study included here as Chapter 1, and originally published as "Transcriptome Analysis of Kaposi's sarcoma-Associated Herpesvirus during *De Novo* Primary Infection of Human B and Endothelial cells" in the March 2015 issue of the Journal of Virology, extends the previous studies by analyzing the viral genes that are transcribed early during *de novo* infection of human peripheral blood mononuclear cells (PBMCs), CD14+ monocytes, and telomerase-immortalized vascular endothelial cells (TIVES) (129). In this study, we performed a comprehensive analysis of the KSHV transcriptome during multiple time-points of infection (0, 4, 24, 48, 72 and 120 h post infection) in these three cell types. We used unbiased RNA sequencing, followed by confirmation of the findings by quantitative real-time PCR (qPCR). We also distinguished between the transcripts that are actively transcribed upon

infection and the transcripts that are brought into the cell by the virion. Furthermore, we identified viral transcripts that appear to be selectively packaged into the virion, by comparing the relative abundance of the transcripts in the virions versus the relative abundance in the infected cells during virion assembly. The data obtained in this study have provided insights into the early events that happen during *de novo* infection by KSHV. In this study, many more transcripts were identified than reported previously. The key findings of this study include: (i) several latent and lytic transcripts co-exist, indicative of a complex pattern of gene expression during early infection. Importantly, (ii) many of the viral transcripts we detected are those required for active lytic replication, raising the possibility that the viral genome is actively replicated during early infection. In fact, we observed a significant increase in the KSHV genome copy number following *de novo* infection. This replication presumably accounts for the large number of viral episomes observed in latently-infected cells. Finally, (iii) transcripts of a larger number of latent and lytic genes were detected in this study as compared to the previous studies, possibly due to the transcripts that are packaged by the virions. Many noncoding RNAs were also detected in this study.

**7.2 KSHV LANA inhibits MHC II expression by disrupting enhanceosome assembly through binding with the RFX complex**

One important characteristic of KSHV infection is the virus's ability to persist for life in the infected host. Whereas a healthy immune system is capable of controlling KSHV infection and its associated malignancies, the immune system does not recognize latently-infected cells and thus can never fully eradicate the virus from the body. KSHV is a very sophisticated virus in terms of immune evasion. Over millions of years of co-

evolution with humans, KSHV has developed an impressive array of immune evasion and modulation strategies to protect the virus from being eliminated by the host immune response. Not surprisingly, at least 22 KSHV proteins are thought to have immune modulatory functions, many of which were copied from the host during evolution (4, 38, 135). The list of KSHV genes implicated in immune evasion/modulation is ever-increasing and not only includes proteins but also miRNAs and noncoding RNAs such as PAN RNA. Immune modulatory mechanisms employed by KSHV are elaborate and finely-coordinated, that effectively disrupt nearly every aspect of host immunity, both innate and adaptive (reviewed in (78-80, 85)).

Sustained latency in the infected host is a hallmark of KSHV infection. Whereas immune evasion is essential for KSHV at all stages of its life cycle, immune evasion is more critical during latency due to its long-term nature. A successful latency requires minimal exposure of KSHV epitopes to the host immune system and hence latency is characterized by expression of only a limited number of KSHV genes (85). Amongst the handful of genes that are expressed during latency, most have demonstrated immune modulatory roles. For example, vFLIP is involved in anti-apoptotic and anti-autophagy activities (16, 49, 81, 91). Furthermore, expression of vFILIP in endothelial cells in transgenic mice has been shown to cause immune dysfunction by interfering with germinal center formation and Ig maturation (11). The miRNAs miR-k9 and miR-k5 have been demonstrated to regulate TLR/IL1R signaling (1, 78). miR-K-12-10 inhibits expression of the pro-inflammatory chemokines IL-8 and MCP-1 by blocking the activity of TWEAKR (tumor necrosis factor-like weak inducer of apoptosis receptor) (131). vIRF3 can interfere with the interferon pathway, a critical component of innate immunity,

by associating with nuclear interferon regulatory factors 3, 5 and 7 (IRF-3, IRF-5 and IRF-7). vIRF3 also interferes with adaptive immunity by down-regulating MHC II expression, at least in part through inhibition of class II transactivator (CIITA) expression, a critical transcription factor for MHC II genes (178). LANA, being an essential multifunctional protein for establishing and maintaining KSHV latency, can be expected to play important roles in immune evasion by the virus during latency. Indeed, several immune evasive/modulatory roles for LANA have been identified, and many more are likely to exist. For example, LANA regulates its own expression and acts *in cis* to inhibit transcription of other viral genes, reducing the number of epitopes available for detection (176). LANA also interferes with neutrophil recruitment, TNF-α signaling and INF-ϒ signaling (37, 83).

Adaptive host immunity plays a critical role in controlling KSHV infection and progression of KSHV-associated tumors. However, efficient activation of the adaptive immune system requires the processed antigens to be displayed in conjugation with either MHC I (expressed on all cells) or MHC II (expressed on antigen-presenting cells such as macrophages and B cells). Interestingly, B cells are the primary reservoir of KSHV latency. LANA has previously been shown to inhibit both MHC I and MHC II antigen presentation pathways (23, 71, 176). Expression of MHC II genes, which is predominantly controlled at the level of transcription, requires binding of CIITA to the highly-conserved promoters of the MHC II genes. Transcription of CIITA itself is activated by interferon regulatory factor 4 (IRF-4). LANA binds to IRF-4, preventing it from activating CIITA transcription, decreasing the levels of CIITA protein, which decreases transcription of MHC II genes and thereby decreases antigen presentation (23).

In Chapter 2 of this thesis, originally published as 'KSHV LANA Inhibits MHC II Expression by Disrupting the Enhanceosome Assembly through Binding with the RFX Complex' in the March 2015 issue of the Journal of Virology, we describe yet another mechanism employed by LANA that interferes with the MHC II antigen presentation pathway. The mechanism that we have elucidated appears to be operating one step downstream of the inhibition of CIITA transcription by LANA. We show that LANA also interacts with the proteins of the regulatory factor X complex, proteins critical for recruitment of CIITA to the MHC II promoters. When LANA binds to the regulatory factor X complex, it impedes recruitment of CIITA to the MHC II promoters, a process that is mandatory for the expression of MHC II genes (155). The fact that LANA employs multiple mechanisms to target the MHC II pathway emphasizes the importance of avoiding MHC II antigen presentation during KSHV latency.

**7.3 KSHV LANA induces expression of EGFL7 to promote angiogenesis**

KSHV is named after Kaposi's sarcoma, a highly angiogenic multifocal malignancy caused by its infection. Angiogenesis refers to the formation of new blood vessels from pre-existing ones. KS is a highly-vascularized tumor of endothelial cell origin that contains high levels of multiple inflammatory cytokines and pro-angiogenic molecules which contribute to the pathogenesis of the disease (46). The importance of angiogenesis in KS tumor progression is highlighted by the fact that KS tumors are highly vascularized even at the early stages of the tumor development. Several well-known angiogenic cytokines including vascular endothelial growth factor (VEGF), basic fibroblast growth factor (b-FGF), angiopoietin-2, angiogenin and cyclooxygenase-2

(COX-2) are known to be induced during KSHV infection (107, 119, 126, 139, 148-150, 173, 174).

Epidermal growth factor-like protein 7 (EGFL7), also known as vascular endothelial statin (VE statin), is a small (~30 kDa) secreted pro-angiogenic cytokine that is highly conserved in vertebrates (109). Under physiological conditions, its expression is normally restricted to actively-proliferating endothelial cells during wound healing, pregnancy and embryonic development (27, 50, 109). However, in many solid tumors, which depend on angiogenesis for survival, tumor cells secrete EGFL7 to promote angiogenesis (44, 63, 167). A number of independent observations when taken together suggest that EGFL7 upregulation might have important implications during KSHV infection. For example, a few recent studies have established EGFL7 as a gene regulated by oxygen levels, with hypoxia being an inducer of EGFL7 expression (7, 84, 92). Interestingly, KS tumors frequently arise at locations with low oxygen levels such as the feet (41). Furthermore, hypoxia induces lytic reactivation of KSHV, which contributes to the progression of KS tumors. Additionally, EGFL7 seems to execute its pro-angiogenic effects through the activation of MAPK, PI3K and Notch signaling pathways (98). Interestingly, KSHV also targets these same signaling pathways in order to modulate cellular functions for its own advantage (48, 61, 72-75, 86, 114, 163). Collectively, these findings point towards an important role for EGFL7 during KSHV infection.

LANA has been shown to promote endothelial cell proliferation and angiogenesis through manipulation of multiple signaling pathways (25, 118, 164). In particular, LANA is known to modulate the Notch signaling pathway in order to promote angiogenesis (163), similar to EGFL7. In an unbiased sequencing screen to identify cellular genes

modulated by LANA in KSHV-negative BJAB cells, we identified EGFL7 as a cellular gene induced by LANA. Considering the biological importance or EGFL7 in promoting angiogenesis in a variety of cancers, and based on the indirect evidence that points towards the role of EGFL7 in KSHV-induced angiogenesis, we aimed to study the regulation of EGFL7 expression by LANA.

In the study described in Chapter 3 of this thesis, we show that LANA upregulates expression of EGFL7. Whereas this study is still in its early stages, we have convincing data that LANA positively regulates expression of EGFL7. Interestingly, in addition to inducing EGFL7 expression in endothelial cells, LANA also induces expression of EGFL7 in B cells. Since B cells are not known to be directly involved in the process of angiogenesis, an involvement of paracrine mechanisms for promotion of angiogenesis by KSHV is highly plausible. Our data show that KSHV-positive tissues and KSHV-positive PEL cells show increased expression of EGFL7. The mechanism of EGFL7 up-regulation by LANA seems to involve sequestration of DAXX (a suppressor of Ets-1 expression) by LANA. Ets-1 is a transcription factor required for the expression of EGFL7. We further show that increased expression of EGFL7 contributes to the promotion of angiogenesis by LANA, as knockdown of EGFL7 in LANA-expressing endothelial cells using siRNA results in decreased *in vitro* tubulogenesis. Further research is required to fully elucidate the detailed mechanism and significance of LANA-mediated upregulation of EGFL7 expression.

**References:**

1. **Abend, J. R., D. Ramalingam, P. Kieffer-Kwon, T. S. Uldrick, R. Yarchoan, and J. M. Ziegelbauer.** 2012. Kaposi's sarcoma-associated herpesvirus microRNAs target IRAK1 and MYD88, two components of the toll-like

receptor/interleukin-1R signaling cascade, to reduce inflammatory-cytokine expression. Journal of virology **86:**11663-11674.

2. **Akula, S. M., N. P. Pramod, F. Z. Wang, and B. Chandran.** 2002. Integrin alpha3beta1 (CD 49c/29) is a cellular receptor for Kaposi's sarcoma-associated herpesvirus (KSHV/HHV-8) entry into the target cells. Cell **108:**407-419.
3. **An, F. Q., N. Compitello, E. Horwitz, M. Sramkoski, E. S. Knudsen, and R. Renne.** 2005. The latency-associated nuclear antigen of Kaposi's sarcoma-associated herpesvirus modulates cellular gene expression and protects lymphoid cells from p16 INK4A-induced cell cycle arrest. The Journal of biological chemistry **280:**3862-3874.
4. **Areste, C., and D. J. Blackbourn.** 2009. Modulation of the immune system by Kaposi's sarcoma-associated herpesvirus. Trends in microbiology **17:**119-129.
5. **Arvanitakis, L., E. Geras-Raaka, A. Varma, M. C. Gershengorn, and E. Cesarman.** 1997. Human herpesvirus KSHV encodes a constitutively active G-protein-coupled receptor linked to cell proliferation. Nature **385:**347-350.
6. **AuCoin, D. P., K. S. Colletti, Y. Xu, S. A. Cei, and G. S. Pari.** 2002. Kaposi's sarcoma-associated herpesvirus (human herpesvirus 8) contains two functional lytic origins of DNA replication. Journal of virology **76:**7890-7896.
7. **Badiwala, M. V., L. C. Tumiati, J. M. Joseph, R. Sheshgiri, H. J. Ross, D. H. Delgado, and V. Rao.** 2010. Epidermal growth factor-like domain 7 suppresses intercellular adhesion molecule 1 expression in response to hypoxia/reoxygenation injury in human coronary artery endothelial cells. Circulation **122:**S156-161.
8. **Baines, J. D.** 2007. Envelopment of herpes simplex virus nucleocapsids at the inner nuclear membrane. *In* A. Arvin, G. Campadelli-Fiume, E. Mocarski, P. S. Moore, B. Roizman, R. Whitley, and K. Yamanishi (ed.), Human Herpesviruses: Biology, Therapy, and Immunoprophylaxis, Cambridge.
9. **Bais, C., B. Santomasso, O. Coso, L. Arvanitakis, E. G. Raaka, J. S. Gutkind, A. S. Asch, E. Cesarman, M. C. Gershengorn, and E. A. Mesri.** 1998. G-protein-coupled receptor of Kaposi's sarcoma-associated herpesvirus is a viral oncogene and angiogenesis activator. Nature **391:**86-89.
10. **Bajaj, B. G., S. C. Verma, K. Lan, M. A. Cotter, Z. L. Woodman, and E. S. Robertson.** 2006. KSHV encoded LANA upregulates Pim-1 and is a substrate for its kinase activity. Virology **351:**18-28.
11. **Ballon, G., G. Akar, and E. Cesarman.** 2015. Systemic Expression of Kaposi Sarcoma Herpesvirus (KSHV) Vflip in Endothelial Cells Leads to a Profound Proinflammatory Phenotype and Myeloid Lineage Remodeling In Vivo. PLoS pathogens **11:**e1004581.
12. **Barbera, A. J., J. V. Chodaparambil, B. Kelley-Clarke, K. Luger, and K. M. Kaye.** 2006. Kaposi's sarcoma-associated herpesvirus LANA hitches a ride on the chromosome. Cell cycle **5:**1048-1052.

13. **Baresova, P., P. M. Pitha, and B. Lubyova.** 2013. Distinct roles of Kaposi's sarcoma-associated herpesvirus-encoded viral interferon regulatory factors in inflammatory response and cancer. Journal of virology **87:**9398-9410.
14. **Bechtel, J., A. Grundhoff, and D. Ganem.** 2005. RNAs in the virion of Kaposi's sarcoma-associated herpesvirus. Journal of virology **79:**10138-10146.
15. **Bechtel, J. T., R. C. Winant, and D. Ganem.** 2005. Host and viral proteins in the virion of Kaposi's sarcoma-associated herpesvirus. Journal of virology **79:**4952-4964.
16. **Belanger, C., A. Gravel, A. Tomoiu, M. E. Janelle, J. Gosselin, M. J. Tremblay, and L. Flamand.** 2001. Human herpesvirus 8 viral FLICE-inhibitory protein inhibits Fas-mediated apoptosis through binding and prevention of procaspase-8 maturation. Journal of human virology **4:**62-73.
17. **Birkmann, A., K. Mahr, A. Ensser, S. Yaguboglu, F. Titgemeyer, B. Fleckenstein, and F. Neipel.** 2001. Cell surface heparan sulfate is a receptor for human herpesvirus 8 and interacts with envelope glycoprotein K8.1. Journal of virology **75:**11583-11593.
18. **Blasig, C., C. Zietz, B. Haar, F. Neipel, S. Esser, N. H. Brockmeyer, E. Tschachler, S. Colombini, B. Ensoli, and M. Sturzl.** 1997. Monocytes in Kaposi's sarcoma lesions are productively infected by human herpesvirus 8. Journal of virology **71:**7963-7968.
19. **Boshoff, C., and Y. Chang.** 2001. Kaposi's sarcoma-associated herpesvirus: a new DNA tumor virus. Annual review of medicine **52:**453-470.
20. **Boshoff, C., Y. Endo, P. D. Collins, Y. Takeuchi, J. D. Reeves, V. L. Schweickart, M. A. Siani, T. Sasaki, T. J. Williams, P. W. Gray, P. S. Moore, Y. Chang, and R. A. Weiss.** 1997. Angiogenic and HIV-inhibitory functions of KSHV-encoded chemokines. Science **278:**290-294.
21. **Boulanger, E., L. Gerard, J. Gabarre, J. M. Molina, C. Rapp, J. F. Abino, J. Cadranel, S. Chevret, and E. Oksenhendler.** 2005. Prognostic factors and outcome of human herpesvirus 8-associated primary effusion lymphoma in patients with AIDS. Journal of clinical oncology : official journal of the American Society of Clinical Oncology **23:**4372-4380.
22. **Bubman, D., I. Guasparri, and E. Cesarman.** 2007. Deregulation of c-Myc in primary effusion lymphoma by Kaposi's sarcoma herpesvirus latency-associated nuclear antigen. Oncogene **26:**4979-4986.
23. **Cai, Q., S. Banerjee, A. Cervini, J. Lu, A. D. Hislop, R. Dzeng, and E. S. Robertson.** 2013. IRF-4-mediated CIITA transcription is blocked by KSHV encoded LANA to inhibit MHC II presentation. PLoS pathogens **9:**e1003751.
24. **Cai, Q., M. Murakami, H. Si, and E. S. Robertson.** 2007. A potential alpha-helix motif in the amino terminus of LANA encoded by Kaposi's sarcoma-associated herpesvirus is critical for nuclear accumulation of HIF-1alpha in normoxia. Journal of virology **81:**10413-10423.

25. **Cai, Q. L., J. S. Knight, S. C. Verma, P. Zald, and E. S. Robertson.** 2006. EC5S ubiquitin complex is recruited by KSHV latent antigen LANA for degradation of the VHL and p53 tumor suppressors. PLoS pathogens **2:**e116.
26. **Cai, X., S. Lu, Z. Zhang, C. M. Gonzalez, B. Damania, and B. R. Cullen.** 2005. Kaposi's sarcoma-associated herpesvirus expresses an array of viral microRNAs in latently infected cells. Proceedings of the National Academy of Sciences of the United States of America **102:**5570-5575.
27. **Campagnolo, L., A. Leahy, S. Chitnis, S. Koschnick, M. J. Fitch, J. T. Fallon, D. Loskutoff, M. B. Taubman, and H. Stuhlmann.** 2005. EGFL7 is a chemoattractant for endothelial cells and is up-regulated in angiogenesis and arterial injury. The American journal of pathology **167:**275-284.
28. **Campbell, M., P. C. Chang, S. Huerta, C. Izumiya, R. Davis, C. G. Tepper, K. Y. Kim, B. Shevchenko, D. H. Wang, J. U. Jung, P. A. Luciw, H. J. Kung, and Y. Izumiya.** 2012. Protein arginine methyltransferase 1-directed methylation of Kaposi sarcoma-associated herpesvirus latency-associated nuclear antigen. The Journal of biological chemistry **287:**5806-5818.
29. **Campbell, M., and Y. Izumiya.** 2012. Post-Translational Modifications of Kaposi's Sarcoma-Associated Herpesvirus Regulatory Proteins - SUMO and KSHV. Frontiers in microbiology **3:**31.
30. **Cannon, J. S., J. Nicholas, J. M. Orenstein, R. B. Mann, P. G. Murray, P. J. Browning, J. A. DiGiuseppe, E. Cesarman, G. S. Hayward, and R. F. Ambinder.** 1999. Heterogeneity of viral IL-6 expression in HHV-8-associated diseases. The Journal of infectious diseases **180:**824-828.
31. **Chandran, B.** 2010. Early events in Kaposi's sarcoma-associated herpesvirus infection of target cells. Journal of virology **84:**2188-2199.
32. **Chandriani, S., and D. Ganem.** 2010. Array-based transcript profiling and limiting-dilution reverse transcription-PCR analysis identify additional latent genes in Kaposi's sarcoma-associated herpesvirus. Journal of virology **84:**5565-5573.
33. **Chang, Y., E. Cesarman, M. S. Pessin, F. Lee, J. Culpepper, D. M. Knowles, and P. S. Moore.** 1994. Identification of herpesvirus-like DNA sequences in AIDS-associated Kaposi's sarcoma. Science **266:**1865-1869.
34. **Chang, Y., and P. Moore.** 2014. Twenty Years of KSHV. Viruses **6:**4258-4264.
35. **Chee, M. S., G. L. Lawrence, and B. G. Barrell.** 1989. Alpha-, beta- and gammaherpesviruses encode a putative phosphotransferase. The Journal of general virology **70 ( Pt 5):**1151-1160.
36. **Cheng, F., M. Weidner-Glunde, M. Varjosalo, E. M. Rainio, A. Lehtonen, T. F. Schulz, P. J. Koskinen, J. Taipale, and P. M. Ojala.** 2009. KSHV reactivation from latency requires Pim-1 and Pim-3 kinases to inactivate the latency-associated nuclear antigen LANA. PLoS pathogens **5:**e1000324.
37. **Cloutier, N., and L. Flamand.** 2010. Kaposi sarcoma-associated herpesvirus latency-associated nuclear antigen inhibits interferon (IFN) beta expression by competing with IFN regulatory factor-3 for binding to IFNB promoter. The Journal of biological chemistry **285:**7208-7221.

38. **Coscoy, L.** 2007. Immune evasion by Kaposi's sarcoma-associated herpesvirus. Nature reviews. Immunology **7:**391-401.
39. **Cotter, M. A., 2nd, C. Subramanian, and E. S. Robertson.** 2001. The Kaposi's sarcoma-associated herpesvirus latency-associated nuclear antigen binds to specific sequences at the left end of the viral genome through its carboxy-terminus. Virology **291:**241-259.
40. **Cunningham, C., S. Barnard, D. J. Blackbourn, and A. J. Davison.** 2003. Transcription mapping of human herpesvirus 8 genes encoding viral interferon regulatory factors. The Journal of general virology **84:**1471-1483.
41. **Davis, D. A., A. S. Rinderknecht, J. P. Zoeteweij, Y. Aoki, E. L. Read-Connole, G. Tosato, A. Blauvelt, and R. Yarchoan.** 2001. Hypoxia induces lytic replication of Kaposi sarcoma-associated herpesvirus. Blood **97:**3244-3250.
42. **Davison, A. J.** 2002. Evolution of the herpesviruses. Veterinary microbiology **86:**69-88.
43. **Davison, A. J.** 2007. Overview of classification. *In* A. Arvin, G. Campadelli-Fiume, E. Mocarski, P. S. Moore, B. Roizman, R. Whitley, and K. Yamanishi (ed.), Human Herpesviruses: Biology, Therapy, and Immunoprophylaxis, Cambridge.
44. **Diaz, R., J. Silva, J. M. Garcia, Y. Lorenzo, V. Garcia, C. Pena, R. Rodriguez, C. Munoz, F. Garcia, F. Bonilla, and G. Dominguez.** 2008. Deregulated expression of miR-106a predicts survival in human colon cancer patients. Genes, chromosomes & cancer **47:**794-802.
45. **DiGiovanna, J. J., and B. Safai.** 1981. Kaposi's sarcoma. Retrospective study of 90 cases with particular emphasis on the familial occurrence, ethnic background and prevalence of other diseases. The American journal of medicine **71:**779-783.
46. **Dimaio, T. A., and M. Lagunoff.** 2012. KSHV Induction of Angiogenic and Lymphangiogenic Phenotypes. Frontiers in microbiology **3:**102.
47. **Dittmer, D., M. Lagunoff, R. Renne, K. Staskus, A. Haase, and D. Ganem.** 1998. A cluster of latently expressed genes in Kaposi's sarcoma-associated herpesvirus. Journal of virology **72:**8309-8315.
48. **Emuss, V., D. Lagos, A. Pizzey, F. Gratrix, S. R. Henderson, and C. Boshoff.** 2009. KSHV manipulates Notch signaling by DLL4 and JAG1 to alter cell cycle genes in lymphatic endothelia. PLoS pathogens **5:**e1000616.
49. **Field, N., W. Low, M. Daniels, S. Howell, L. Daviet, C. Boshoff, and M. Collins.** 2003. KSHV vFLIP binds to IKK-gamma to activate IKK. Journal of cell science **116:**3721-3728.
50. **Fitch, M. J., L. Campagnolo, F. Kuhnert, and H. Stuhlmann.** 2004. Egfl7, a novel epidermal growth factor-domain gene expressed in endothelial cells. Developmental dynamics : an official publication of the American Association of Anatomists **230:**316-324.
51. **Fujimuro, M., J. Liu, J. Zhu, H. Yokosawa, and S. D. Hayward.** 2005. Regulation of the interaction between glycogen synthase kinase 3 and the

Kaposi's sarcoma-associated herpesvirus latency-associated nuclear antigen. Journal of virology **79:**10429-10441.

52. **Gao, S. J., C. Boshoff, S. Jayachandra, R. A. Weiss, Y. Chang, and P. S. Moore.** 1997. KSHV ORF K9 (vIRF) is an oncogene which inhibits the interferon signaling pathway. Oncogene **15:**1979-1985.
53. **Garber, A. C., M. A. Shu, J. Hu, and R. Renne.** 2001. DNA binding and modulation of gene expression by the latency-associated nuclear antigen of Kaposi's sarcoma-associated herpesvirus. Journal of virology **75:**7882-7892.
54. **Giffin, L., and B. Damania.** 2014. KSHV: pathways to tumorigenesis and persistent infection. Advances in virus research **88:**111-159.
55. **Grange, P. A., L. Gressier, J. F. Williams, O. F. Dyson, S. M. Akula, and N. Dupin.** 2012. Cloning a human saliva-derived peptide for preventing KSHV transmission. The Journal of investigative dermatology **132:**1733-1735.
56. **Greene, W., K. Kuhne, F. Ye, J. Chen, F. Zhou, X. Lei, and S. J. Gao.** 2007. Molecular biology of KSHV in relation to AIDS-associated oncogenesis. Cancer treatment and research **133:**69-127.
57. **Grundhoff, A., and D. Ganem.** 2004. Inefficient establishment of KSHV latency suggests an additional role for continued lytic replication in Kaposi sarcoma pathogenesis. The Journal of clinical investigation **113:**124-136.
58. **Grundhoff, A., and D. Ganem.** 2003. The latency-associated nuclear antigen of Kaposi's sarcoma-associated herpesvirus permits replication of terminal repeat-containing plasmids. Journal of virology **77:**2779-2783.
59. **Hahn, A., A. Birkmann, E. Wies, D. Dorer, K. Mahr, M. Sturzl, F. Titgemeyer, and F. Neipel.** 2009. Kaposi's sarcoma-associated herpesvirus gH/gL: glycoprotein export and interaction with cellular receptors. Journal of virology **83:**396-407.
60. **Hahn, A. S., J. K. Kaufmann, E. Wies, E. Naschberger, J. Panteleev-Ivlev, K. Schmidt, A. Holzer, M. Schmidt, J. Chen, S. Konig, A. Ensser, J. Myoung, N. H. Brockmeyer, M. Sturzl, B. Fleckenstein, and F. Neipel.** 2012. The ephrin receptor tyrosine kinase A2 is a cellular receptor for Kaposi's sarcoma-associated herpesvirus. Nature medicine **18:**961-966.
61. **Hayward, S. D., J. Liu, and M. Fujimuro.** 2006. Notch and Wnt signaling: mimicry and manipulation by gamma herpesviruses. Science's STKE : signal transduction knowledge environment **2006:**re4.
62. **Hu, J., A. C. Garber, and R. Renne.** 2002. The latency-associated nuclear antigen of Kaposi's sarcoma-associated herpesvirus supports latent DNA replication in dividing cells. Journal of virology **76:**11677-11687.
63. **Huang, C. H., X. J. Li, Y. Z. Zhou, Y. Luo, C. Li, and X. R. Yuan.** 2010. Expression and clinical significance of EGFL7 in malignant glioma. Journal of cancer research and clinical oncology **136:**1737-1743.
64. **Kaleeba, J. A., and E. A. Berger.** 2006. Kaposi's sarcoma-associated herpesvirus fusion-entry receptor: cystine transporter xCT. Science **311:**1921-1924.

65. **Kang, H., H. Cho, G. H. Sung, and P. M. Lieberman.** 2013. CTCF regulates Kaposi's sarcoma-associated herpesvirus latency transcription by nucleosome displacement and RNA polymerase programming. Journal of virology **87:**1789-1799.
66. **Kaul, R., S. C. Verma, and E. S. Robertson.** 2007. Protein complexes associated with the Kaposi's sarcoma-associated herpesvirus-encoded LANA. Virology **364:**317-329.
67. **Kedes, D. H., M. Lagunoff, R. Renne, and D. Ganem.** 1997. Identification of the gene encoding the major latency-associated nuclear antigen of the Kaposi's sarcoma-associated herpesvirus. The Journal of clinical investigation **100:**2606-2610.
68. **Kirshner, J. R., K. Staskus, A. Haase, M. Lagunoff, and D. Ganem.** 1999. Expression of the open reading frame 74 (G-protein-coupled receptor) gene of Kaposi's sarcoma (KS)-associated herpesvirus: implications for KS pathogenesis. Journal of virology **73:**6006-6014.
69. **Krishnan, H. H., P. P. Naranatt, M. S. Smith, L. Zeng, C. Bloomer, and B. Chandran.** 2004. Concurrent expression of latent and a limited number of lytic genes with immune modulation and antiapoptotic function by Kaposi's sarcoma-associated herpesvirus early during infection of primary endothelial and fibroblast cells and subsequent decline of lytic gene expression. Journal of virology **78:**3601-3620.
70. **Kumar, A., S. K. Sahu, S. Mohanty, S. Chakrabarti, S. Maji, R. R. Reddy, A. K. Jha, C. Goswami, C. N. Kundu, S. Rajasubramaniam, S. C. Verma, and T. Choudhuri.** 2014. Kaposi sarcoma herpes virus latency associated nuclear antigen protein release the G2/M cell cycle blocks by modulating ATM/ATR mediated checkpoint pathway. PloS one **9:**e100228.
71. **Kwun, H. J., S. R. da Silva, H. Qin, R. L. Ferris, R. Tan, Y. Chang, and P. S. Moore.** 2011. The central repeat domain 1 of Kaposi's sarcoma-associated herpesvirus (KSHV) latency associated-nuclear antigen 1 (LANA1) prevents cis MHC class I peptide presentation. Virology **412:**357-365.
72. **Lambert, P. J., A. Z. Shahrier, A. G. Whitman, O. F. Dyson, A. J. Reber, J. A. McCubrey, and S. M. Akula.** 2007. Targeting the PI3K and MAPK pathways to treat Kaposi's-sarcoma-associated herpes virus infection and pathogenesis. Expert opinion on therapeutic targets **11:**589-599.
73. **Lan, K., T. Choudhuri, M. Murakami, D. A. Kuppers, and E. S. Robertson.** 2006. Intracellular activated Notch1 is critical for proliferation of Kaposi's sarcoma-associated herpesvirus-associated B-lymphoma cell lines in vitro. Journal of virology **80:**6411-6419.
74. **Lan, K., D. A. Kuppers, and E. S. Robertson.** 2005. Kaposi's sarcoma-associated herpesvirus reactivation is regulated by interaction of latency-associated nuclear antigen with recombination signal sequence-binding protein Jkappa, the major downstream effector of the Notch signaling pathway. Journal of virology **79:**3468-3478.

75. **Lan, K., M. Murakami, T. Choudhuri, D. A. Kuppers, and E. S. Robertson.** 2006. Intracellular-activated Notch1 can reactivate Kaposi's sarcoma-associated herpesvirus from latency. Virology **351:**393-403.
76. **Lan, K., S. C. Verma, M. Murakami, B. Bajaj, R. Kaul, and E. S. Robertson.** 2007. Kaposi's sarcoma herpesvirus-encoded latency-associated nuclear antigen stabilizes intracellular activated Notch by targeting the Sel10 protein. Proceedings of the National Academy of Sciences of the United States of America **104:**16287-16292.
77. **Lee, H., J. Guo, M. Li, J. K. Choi, M. DeMaria, M. Rosenzweig, and J. U. Jung.** 1998. Identification of an immunoreceptor tyrosine-based activation motif of K1 transforming protein of Kaposi's sarcoma-associated herpesvirus. Molecular and cellular biology **18:**5219-5228.
78. **Lee, H. R., R. Amatya, and J. U. Jung.** 2015. Multi-Step Regulation of Innate Immune Signaling by Kaposi's Sarcoma-associated Herpesvirus. Virus research.
79. **Lee, H. R., K. Brulois, L. Wong, and J. U. Jung.** 2012. Modulation of Immune System by Kaposi's Sarcoma-Associated Herpesvirus: Lessons from Viral Evasion Strategies. Frontiers in microbiology **3:**44.
80. **Lee, H. R., S. Lee, P. M. Chaudhary, P. Gill, and J. U. Jung.** 2010. Immune evasion by Kaposi's sarcoma-associated herpesvirus. Future microbiology **5:**1349-1365.
81. **Lee, J. S., Q. Li, J. Y. Lee, S. H. Lee, J. H. Jeong, H. R. Lee, H. Chang, F. C. Zhou, S. J. Gao, C. Liang, and J. U. Jung.** 2009. FLIP-mediated autophagy regulation in cell death control. Nature cell biology **11:**1355-1362.
82. **Li, H., T. Komatsu, B. J. Dezube, and K. M. Kaye.** 2002. The Kaposi's sarcoma-associated herpesvirus K12 transcript from a primary effusion lymphoma contains complex repeat elements, is spliced, and initiates from a novel promoter. Journal of virology **76:**11880-11888.
83. **Li, X., D. Liang, X. Lin, E. S. Robertson, and K. Lan.** 2011. Kaposi's sarcoma-associated herpesvirus-encoded latency-associated nuclear antigen reduces interleukin-8 expression in endothelial cells and impairs neutrophil chemotaxis by degrading nuclear p65. Journal of virology **85:**8606-8615.
84. **Li, Z., C. F. Ni, J. Zhou, X. C. Shen, Y. Yin, P. Du, and C. Yang.** 2015. Expression of Epidermal Growth Factor-like Domain 7 is Increased by Transcatheter Arterial Embolization of Liver Tumors. Asian Pacific journal of cancer prevention : APJCP **16:**1191-1196.
85. **Liang, C., J. S. Lee, and J. U. Jung.** 2008. Immune evasion in Kaposi's sarcoma-associated herpes virus associated oncogenesis. Seminars in cancer biology **18:**423-436.
86. **Liang, Y., and D. Ganem.** 2003. Lytic but not latent infection by Kaposi's sarcoma-associated herpesvirus requires host CSL protein, the mediator of Notch signaling. Proceedings of the National Academy of Sciences of the United States of America **100:**8490-8495.

87. **Lim, C., H. Sohn, D. Lee, Y. Gwack, and J. Choe.** 2002. Functional dissection of latency-associated nuclear antigen 1 of Kaposi's sarcoma-associated herpesvirus involved in latent DNA replication and transcription of terminal repeats of the viral genome. Journal of virology **76:**10320-10331.
88. **Lin, X., X. Li, D. Liang, and K. Lan.** 2012. MicroRNAs and unusual small RNAs discovered in Kaposi's sarcoma-associated herpesvirus virions. Journal of virology **86:**12717-12730.
89. **Liu, F., and Z. H. Zhou.** 2007. Comparative virion structures of human herpesviruses. *In* A. Arvin, G. Campadelli-Fiume, E. Mocarski, P. S. Moore, B. Roizman, R. Whitley, and K. Yamanishi (ed.), Human Herpesviruses: Biology, Therapy, and Immunoprophylaxis, Cambridge.
90. **Liu, J., H. J. Martin, G. Liao, and S. D. Hayward.** 2007. The Kaposi's sarcoma-associated herpesvirus LANA protein stabilizes and activates c-Myc. Journal of virology **81:**10451-10459.
91. **Liu, L., M. T. Eby, N. Rathore, S. K. Sinha, A. Kumar, and P. M. Chaudhary.** 2002. The human herpes virus 8-encoded viral FLICE inhibitory protein physically associates with and persistently activates the Ikappa B kinase complex. The Journal of biological chemistry **277:**13745-13751.
92. **Liu, Y. S., Z. W. Huang, A. Q. Qin, Y. Huang, F. Giordano, Q. H. Lu, and W. D. Jiang.** 2015. The expression of epidermal growth factor-like domain 7 regulated by oxygen tension via hypoxia inducible factor (HIF)-1alpha activity. Postgraduate medicine **127:**144-149.
93. **Longnecker, R., and F. Neipel.** 2007. Introduction to the human gamma-herpesviruses. *In* A. Arvin, G. Campadelli-Fiume, E. Mocarski, P. S. Moore, B. Roizman, R. Whitley, and K. Yamanishi (ed.), Human Herpesviruses: Biology, Therapy, and Immunoprophylaxis, Cambridge.
94. **Lu, F., L. Day, S. J. Gao, and P. M. Lieberman.** 2006. Acetylation of the latency-associated nuclear antigen regulates repression of Kaposi's sarcoma-associated herpesvirus lytic transcription. Journal of virology **80:**5273-5282.
95. **Lu, J., H. C. Jha, S. C. Verma, Z. Sun, S. Banerjee, R. Dzeng, and E. S. Robertson.** 2014. Kaposi's sarcoma-associated herpesvirus-encoded LANA contributes to viral latent replication by activating phosphorylation of survivin. Journal of virology **88:**4204-4217.
96. **Lu, J., S. C. Verma, M. Murakami, Q. Cai, P. Kumar, B. Xiao, and E. S. Robertson.** 2009. Latency-associated nuclear antigen of Kaposi's sarcoma-associated herpesvirus (KSHV) upregulates survivin expression in KSHV-Associated B-lymphoma cells and contributes to their proliferation. Journal of virology **83:**7129-7141.
97. **Lukac, D. M., and Y. Yuan.** 2007. Reactivation and lytic replication of KSHV. *In* A. Arvin, G. Campadelli-Fiume, E. Mocarski, P. S. Moore, B. Roizman, R. Whitley, and K. Yamanishi (ed.), Human Herpesviruses: Biology, Therapy, and Immunoprophylaxis, Cambridge.
98. **Massimiani, M., L. Vecchione, D. Piccirilli, P. Spitalieri, F. Amati, S. Salvi, S. Ferrazzani, H. Stuhlmann, and L. Campagnolo.** 2015. Epidermal growth

factor-like domain 7 promotes migration and invasion of human trophoblast cells through activation of MAPK, PI3K and NOTCH signaling pathways. Molecular human reproduction.

99. **McCormick, C., and D. Ganem.** 2005. The kaposin B protein of KSHV activates the p38/MK2 pathway and stabilizes cytokine mRNAs. Science **307:**739-741.
100. **Mesri, E. A., E. Cesarman, and C. Boshoff.** 2010. Kaposi's sarcoma and its associated herpesvirus. Nature reviews. Cancer **10:**707-719.
101. **Moody, R., Y. Zhu, Y. Huang, X. Cui, T. Jones, R. Bedolla, X. Lei, Z. Bai, and S. J. Gao.** 2013. KSHV microRNAs mediate cellular transformation and tumorigenesis by redundantly targeting cell growth and survival pathways. PLoS pathogens **9:**e1003857.
102. **Moore, P. S., C. Boshoff, R. A. Weiss, and Y. Chang.** 1996. Molecular mimicry of human cytokine and cytokine response pathway genes by KSHV. Science **274:**1739-1744.
103. **Moore, P. S., and Y. Chang.** 2010. Why do viruses cause cancer? Highlights of the first century of human tumour virology. Nature reviews. Cancer **10:**878-889.
104. **Morales-Sanchez, A., and E. M. Fuentes-Panana.** 2014. Human Viruses and Cancer. Viruses **6:**4047-4079.
105. **Murakami, Y., S. Yamagoe, K. Noguchi, Y. Takebe, N. Takahashi, Y. Uehara, and H. Fukazawa.** 2006. Ets-1-dependent expression of vascular endothelial growth factor receptors is activated by latency-associated nuclear antigen of Kaposi's sarcoma-associated herpesvirus through interaction with Daxx. The Journal of biological chemistry **281:**28113-28121.
106. **Myoung, J., and D. Ganem.** 2011. Active lytic infection of human primary tonsillar B cells by KSHV and its noncytolytic control by activated CD4+ T cells. The Journal of clinical investigation **121:**1130-1140.
107. **Naranatt, P. P., H. H. Krishnan, S. R. Svojanovsky, C. Bloomer, S. Mathur, and B. Chandran.** 2004. Host gene induction and transcriptional reprogramming in Kaposi's sarcoma-associated herpesvirus (KSHV/HHV-8)-infected endothelial, fibroblast, and B cells: insights into modulation events early during infection. Cancer research **64:**72-84.
108. **Nealon, K., W. W. Newcomb, T. R. Pray, C. S. Craik, J. C. Brown, and D. H. Kedes.** 2001. Lytic replication of Kaposi's sarcoma-associated herpesvirus results in the formation of multiple capsid species: isolation and molecular characterization of A, B, and C capsids from a gammaherpesvirus. Journal of virology **75:**2866-2878.
109. **Nichol, D., and H. Stuhlmann.** 2012. EGFL7: a unique angiogenic signaling factor in vascular development and disease. Blood **119:**1345-1352.
110. **Ohsaki, E., and K. Ueda.** 2012. Kaposi's Sarcoma-Associated Herpesvirus Genome Replication, Partitioning, and Maintenance in Latency. Frontiers in microbiology **3:**7.

111. **Ohsaki, E., K. Ueda, S. Sakakibara, E. Do, K. Yada, and K. Yamanishi.** 2004. Poly(ADP-ribose) polymerase 1 binds to Kaposi's sarcoma-associated herpesvirus (KSHV) terminal repeat sequence and modulates KSHV replication in latency. Journal of virology **78:**9936-9946.
112. **Orenstein, J. M., S. Alkan, A. Blauvelt, K. T. Jeang, M. D. Weinstein, D. Ganem, and B. Herndier.** 1997. Visualization of human herpesvirus type 8 in Kaposi's sarcoma by light and transmission electron microscopy. Aids **11:**F35-45.
113. **Paludan, S. R., A. G. Bowie, K. A. Horan, and K. A. Fitzgerald.** 2011. Recognition of herpesviruses by the innate immune system. Nature reviews. Immunology **11:**143-154.
114. **Pan, H., J. Xie, F. Ye, and S. J. Gao.** 2006. Modulation of Kaposi's sarcoma-associated herpesvirus infection and replication by MEK/ERK, JNK, and p38 multiple mitogen-activated protein kinase pathways during primary infection. Journal of virology **80:**5371-5382.
115. **Parravicini, C., M. Corbellino, M. Paulli, U. Magrini, M. Lazzarino, P. S. Moore, and Y. Chang.** 1997. Expression of a virus-derived cytokine, KSHV vIL-6, in HIV-seronegative Castleman's disease. The American journal of pathology **151:**1517-1522.
116. **Parsons, C. H., B. Szomju, and D. H. Kedes.** 2004. Susceptibility of human fetal mesenchymal stem cells to Kaposi sarcoma-associated herpesvirus. Blood **104:**2736-2738.
117. **Paudel, N., S. Sadagopan, S. Balasubramanian, and B. Chandran.** 2012. Kaposi's sarcoma-associated herpesvirus latency-associated nuclear antigen and angiogenin interact with common host proteins, including annexin A2, which is essential for survival of latently infected cells. Journal of virology **86:**1589-1607.
118. **Paudel, N., S. Sadagopan, S. Chakraborty, G. Sarek, P. M. Ojala, and B. Chandran.** 2012. Kaposi's sarcoma-associated herpesvirus latency-associated nuclear antigen interacts with multifunctional angiogenin to utilize its antiapoptotic functions. Journal of virology **86:**5974-5991.
119. **Paul, A. G., B. Chandran, and N. Sharma-Walia.** 2013. Cyclooxygenase-2-prostaglandin E2-eicosanoid receptor inflammatory axis: a key player in Kaposi's sarcoma-associated herpes virus associated malignancies. Translational research : the journal of laboratory and clinical medicine **162:**77-92.
120. **Pekkonen, P., A. Jarviluoma, N. Zinovkina, A. Cvrljevic, S. Prakash, J. Westermarck, G. I. Evan, E. Cesarman, E. W. Verschuren, and P. M. Ojala.** 2014. KSHV viral cyclin interferes with T-cell development and induces lymphoma through Cdk6 and Notch activation in vivo. Cell cycle **13:**3670-3684.
121. **Pertel, P. E.** 2002. Human herpesvirus 8 glycoprotein B (gB), gH, and gL can mediate cell fusion. Journal of virology **76:**4390-4400.

122. **Pfeffer, S., A. Sewer, M. Lagos-Quintana, R. Sheridan, C. Sander, F. A. Grasser, L. F. van Dyk, C. K. Ho, S. Shuman, M. Chien, J. J. Russo, J. Ju, G. Randall, B. D. Lindenbach, C. M. Rice, V. Simon, D. D. Ho, M. Zavolan, and T. Tuschl.** 2005. Identification of microRNAs of the herpesvirus family. Nature methods **2:**269-276.
123. **Piolot, T., M. Tramier, M. Coppey, J. C. Nicolas, and V. Marechal.** 2001. Close but distinct regions of human herpesvirus 8 latency-associated nuclear antigen 1 are responsible for nuclear targeting and binding to human mitotic chromosomes. Journal of virology **75:**3948-3959.
124. **Plaisance-Bonstaff, K., H. S. Choi, T. Beals, B. J. Krueger, I. W. Boss, L. A. Gay, I. Haecker, J. Hu, and R. Renne.** 2014. KSHV miRNAs decrease expression of lytic genes in latently infected PEL and endothelial cells by targeting host transcription factors. Viruses **6:**4005-4023.
125. **Platt, G. M., G. R. Simpson, S. Mittnacht, and T. F. Schulz.** 1999. Latent nuclear antigen of Kaposi's sarcoma-associated herpesvirus interacts with RING3, a homolog of the Drosophila female sterile homeotic (fsh) gene. Journal of virology **73:**9789-9795.
126. **Prakash, O., Z. Y. Tang, X. Peng, R. Coleman, J. Gill, G. Farr, and F. Samaniego.** 2002. Tumorigenesis and aberrant signaling in transgenic mice expressing the human herpesvirus-8 K1 gene. Journal of the National Cancer Institute **94:**926-935.
127. **Prasad, A., M. Lu, D. M. Lukac, and S. L. Zeichner.** 2012. An alternative Kaposi's sarcoma-associated herpesvirus replication program triggered by host cell apoptosis. Journal of virology **86:**4404-4419.
128. **Prasad, A., J. Remick, and S. L. Zeichner.** 2013. Activation of human herpesvirus replication by apoptosis. Journal of virology **87:**10641-10650.
129. **Purushothaman, P., S. Thakker, and S. C. Verma.** 2014. Transcriptome Analysis of KSHV During De Novo Primary Infection of Human B and Endothelial Cells. Journal of virology.
130. **Purushothaman, P., T. Uppal, and S. C. Verma.** 2015. Molecular biology of KSHV lytic reactivation. Viruses **7:**116-153.
131. **Qin, Z., A. Jakymiw, V. Findlay, and C. Parsons.** 2012. KSHV-Encoded MicroRNAs: Lessons for Viral Cancer Pathogenesis and Emerging Concepts. International journal of cell biology **2012:**603961.
132. **Ray, A., V. Marshall, T. Uldrick, R. Leighty, N. Labo, K. Wyvill, K. Aleman, M. N. Polizzotto, R. F. Little, R. Yarchoan, and D. Whitby.** 2012. Sequence analysis of Kaposi sarcoma-associated herpesvirus (KSHV) microRNAs in patients with multicentric Castleman disease and KSHV-associated inflammatory cytokine syndrome. The Journal of infectious diseases **205:**1665-1676.
133. **Renne, R., C. Barry, D. Dittmer, N. Compitello, P. O. Brown, and D. Ganem.** 2001. Modulation of cellular and viral gene expression by the latency-associated nuclear antigen of Kaposi's sarcoma-associated herpesvirus. Journal of virology **75:**458-468.

134. **Renne, R., W. Zhong, B. Herndier, M. McGrath, N. Abbey, D. Kedes, and D. Ganem.** 1996. Lytic growth of Kaposi's sarcoma-associated herpesvirus (human herpesvirus 8) in culture. Nature medicine **2:**342-346.
135. **Rezaee, S. A., C. Cunningham, A. J. Davison, and D. J. Blackbourn.** 2006. Kaposi's sarcoma-associated herpesvirus immune modulation: an overview. The Journal of general virology **87:**1781-1804.
136. **Rivas, C., A. E. Thlick, C. Parravicini, P. S. Moore, and Y. Chang.** 2001. Kaposi's sarcoma-associated herpesvirus LANA2 is a B-cell-specific latent viral protein that inhibits p53. Journal of virology **75:**429-438.
137. **Rossetto, C. C., M. Tarrant-Elorza, S. Verma, P. Purushothaman, and G. S. Pari.** 2013. Regulation of viral and cellular gene expression by Kaposi's sarcoma-associated herpesvirus polyadenylated nuclear RNA. Journal of virology **87:**5540-5553.
138. **Sabbah, S., Y. J. Jagne, J. Zuo, T. de Silva, M. M. Ahasan, C. Brander, S. Rowland-Jones, K. L. Flanagan, and A. D. Hislop.** 2012. T-cell immunity to Kaposi sarcoma-associated herpesvirus: recognition of primary effusion lymphoma by LANA-specific CD4+ T cells. Blood **119:**2083-2092.
139. **Sadagopan, S., N. Sharma-Walia, M. V. Veettil, V. Bottero, R. Levine, R. J. Vart, and B. Chandran.** 2009. Kaposi's sarcoma-associated herpesvirus upregulates angiogenin during infection of human dermal microvascular endothelial cells, which induces 45S rRNA synthesis, antiapoptosis, cell proliferation, migration, and angiogenesis. Journal of virology **83:**3342-3364.
140. **Sadler, R., L. Wu, B. Forghani, R. Renne, W. Zhong, B. Herndier, and D. Ganem.** 1999. A complex translational program generates multiple novel proteins from the latently expressed kaposin (K12) locus of Kaposi's sarcoma-associated herpesvirus. Journal of virology **73:**5722-5730.
141. **Samols, M. A., J. Hu, R. L. Skalsky, and R. Renne.** 2005. Cloning and identification of a microRNA cluster within the latency-associated region of Kaposi's sarcoma-associated herpesvirus. Journal of virology **79:**9301-9305.
142. **Santag, S., W. Jager, C. B. Karsten, S. Kati, M. Pietrek, D. Steinemann, G. Sarek, P. M. Ojala, and T. F. Schulz.** 2013. Recruitment of the tumour suppressor protein p73 by Kaposi's Sarcoma Herpesvirus latent nuclear antigen contributes to the survival of primary effusion lymphoma cells. Oncogene **32:**3676-3685.
143. **Sarid, R., O. Flore, R. A. Bohenzky, Y. Chang, and P. S. Moore.** 1998. Transcription mapping of the Kaposi's sarcoma-associated herpesvirus (human herpesvirus 8) genome in a body cavity-based lymphoma cell line (BC-1). Journal of virology **72:**1005-1012.
144. **Sarid, R., T. Sato, R. A. Bohenzky, J. J. Russo, and Y. Chang.** 1997. Kaposi's sarcoma-associated herpesvirus encodes a functional bcl-2 homologue. Nature medicine **3:**293-298.
145. **Sathish, N., X. Wang, and Y. Yuan.** 2012. Tegument Proteins of Kaposi's Sarcoma-Associated Herpesvirus and Related Gamma-Herpesviruses. Frontiers in microbiology **3:**98.

146. **Schmidt, K., E. Wies, and F. Neipel.** 2011. Kaposi's sarcoma-associated herpesvirus viral interferon regulatory factor 3 inhibits gamma interferon and major histocompatibility complex class II expression. Journal of virology **85:**4530-4537.
147. **Seo, T., J. Park, C. Lim, and J. Choe.** 2004. Inhibition of nuclear factor kappaB activity by viral interferon regulatory factor 3 of Kaposi's sarcoma-associated herpesvirus. Oncogene **23:**6146-6155.
148. **Sharma-Walia, N., A. G. Paul, V. Bottero, S. Sadagopan, M. V. Veettil, N. Kerur, and B. Chandran.** 2010. Kaposi's sarcoma associated herpes virus (KSHV) induced COX-2: a key factor in latency, inflammation, angiogenesis, cell survival and invasion. PLoS pathogens **6:**e1000777.
149. **Sivakumar, R., N. Sharma-Walia, H. Raghu, M. V. Veettil, S. Sadagopan, V. Bottero, L. Varga, R. Levine, and B. Chandran.** 2008. Kaposi's sarcoma-associated herpesvirus induces sustained levels of vascular endothelial growth factors A and C early during in vitro infection of human microvascular dermal endothelial cells: biological implications. Journal of virology **82:**1759-1776.
150. **Sodhi, A., S. Montaner, V. Patel, M. Zohar, C. Bais, E. A. Mesri, and J. S. Gutkind.** 2000. The Kaposi's sarcoma-associated herpes virus G protein-coupled receptor up-regulates vascular endothelial growth factor expression and secretion through mitogen-activated protein kinase and p38 pathways acting on hypoxia-inducible factor 1alpha. Cancer research **60:**4873-4880.
151. **Staskus, K. A., R. Sun, G. Miller, P. Racz, A. Jaslowski, C. Metroka, H. Brett-Smith, and A. T. Haase.** 1999. Cellular tropism and viral interleukin-6 expression distinguish human herpesvirus 8 involvement in Kaposi's sarcoma, primary effusion lymphoma, and multicentric Castleman's disease. Journal of virology **73:**4181-4187.
152. **Sun, R., S. F. Lin, L. Gradoville, and G. Miller.** 1996. Polyadenylylated nuclear RNA encoded by Kaposi sarcoma-associated herpesvirus. Proceedings of the National Academy of Sciences of the United States of America **93:**11883-11888.
153. **Sun, R., S. F. Lin, L. Gradoville, Y. Yuan, F. Zhu, and G. Miller.** 1998. A viral gene that activates lytic cycle expression of Kaposi's sarcoma-associated herpesvirus. Proceedings of the National Academy of Sciences of the United States of America **95:**10866-10871.
154. **Tamburro, K. M., D. Yang, J. Poisson, Y. Fedoriw, D. Roy, A. Lucas, S. H. Sin, N. Malouf, V. Moylan, B. Damania, S. Moll, C. van der Horst, and D. P. Dittmer.** 2012. Vironome of Kaposi sarcoma associated herpesvirus-inflammatory cytokine syndrome in an AIDS patient reveals co-infection of human herpesvirus 8 and human herpesvirus 6A. Virology **433:**220-225.
155. **Thakker, S., P. Purushothaman, N. Gupta, S. Challa, Q. Cai, and S. C. Verma.** 2015. KSHV LANA inhibits MHC II expression by disrupting the enhanceosome assembly through binding with the RFX complex. Journal of virology.

156. **Uppal, T., S. Banerjee, Z. Sun, S. C. Verma, and E. S. Robertson.** 2014. KSHV LANA--the master regulator of KSHV latency. Viruses **6:**4961-4998.
157. **Veeranna, R. P., M. Haque, D. A. Davis, M. Yang, and R. Yarchoan.** 2012. Kaposi's sarcoma-associated herpesvirus latency-associated nuclear antigen induction by hypoxia and hypoxia-inducible factors. Journal of virology **86:**1097-1108.
158. **Veettil, M. V., C. Bandyopadhyay, D. Dutta, and B. Chandran.** 2014. Interaction of KSHV with host cell surface receptors and cell entry. Viruses **6:**4024-4046.
159. **Verma, S. C., T. Choudhuri, R. Kaul, and E. S. Robertson.** 2006. Latency-associated nuclear antigen (LANA) of Kaposi's sarcoma-associated herpesvirus interacts with origin recognition complexes at the LANA binding sequence within the terminal repeats. Journal of virology **80:**2243-2256.
160. **Verma, S. C., K. Lan, T. Choudhuri, and E. S. Robertson.** 2006. Kaposi's sarcoma-associated herpesvirus-encoded latency-associated nuclear antigen modulates K1 expression through its cis-acting elements within the terminal repeats. Journal of virology **80:**3445-3458.
161. **Verma, S. C., K. Lan, and E. Robertson.** 2007. Structure and function of latency-associated nuclear antigen. Current topics in microbiology and immunology **312:**101-136.
162. **Wang, F. Z., S. M. Akula, N. Sharma-Walia, L. Zeng, and B. Chandran.** 2003. Human herpesvirus 8 envelope glycoprotein B mediates cell adhesion via its RGD sequence. Journal of virology **77:**3131-3147.
163. **Wang, X., Z. He, T. Xia, X. Li, D. Liang, X. Lin, H. Wen, and K. Lan.** 2014. Latency-associated nuclear antigen of Kaposi sarcoma-associated herpesvirus promotes angiogenesis through targeting notch signaling effector Hey1. Cancer research **74:**2026-2037.
164. **Watanabe, T., M. Sugaya, A. M. Atkins, E. A. Aquilino, A. Yang, D. L. Borris, J. Brady, and A. Blauvelt.** 2003. Kaposi's sarcoma-associated herpesvirus latency-associated nuclear antigen prolongs the life span of primary human umbilical vein endothelial cells. Journal of virology **77:**6188-6196.
165. **Wen, K. W., and B. Damania.** 2010. Kaposi sarcoma-associated herpesvirus (KSHV): molecular biology and oncogenesis. Cancer letters **289:**140-150.
166. **Wies, E., Y. Mori, A. Hahn, E. Kremmer, M. Sturzl, B. Fleckenstein, and F. Neipel.** 2008. The viral interferon-regulatory factor-3 is required for the survival of KSHV-infected primary effusion lymphoma cells. Blood **111:**320-327.
167. **Wu, F., L. Y. Yang, Y. F. Li, D. P. Ou, D. P. Chen, and C. Fan.** 2009. Novel role for epidermal growth factor-like domain 7 in metastasis of human hepatocellular carcinoma. Hepatology **50:**1839-1850.
168. **Wu, L., P. Lo, X. Yu, J. K. Stoops, B. Forghani, and Z. H. Zhou.** 2000. Three-dimensional structure of the human herpesvirus 8 capsid. Journal of virology **74:**9646-9654.

169. **Wu, W., J. Vieira, N. Fiore, P. Banerjee, M. Sieburg, R. Rochford, W. Harrington, Jr., and G. Feuer.** 2006. KSHV/HHV-8 infection of human hematopoietic progenitor (CD34+) cells: persistence of infection during hematopoiesis in vitro and in vivo. Blood **108:**141-151.
170. **Xu, D., T. Coleman, J. Zhang, A. Fagot, C. Kotalik, L. Zhao, P. Trivedi, C. Jones, and L. Zhang.** 2007. Epstein-Barr virus inhibits Kaposi's sarcoma-associated herpesvirus lytic replication in primary effusion lymphomas. Journal of virology **81:**6068-6078.
171. **Xu, Y., A. Rodriguez-Huete, and G. S. Pari.** 2006. Evaluation of the lytic origins of replication of Kaposi's sarcoma-associated virus/human herpesvirus 8 in the context of the viral genome. Journal of virology **80:**9905-9909.
172. **Ye, F., X. Lei, and S. J. Gao.** 2011. Mechanisms of Kaposi's Sarcoma-Associated Herpesvirus Latency and Reactivation. Advances in virology **2011**.
173. **Ye, F. C., D. J. Blackbourn, M. Mengel, J. P. Xie, L. W. Qian, W. Greene, I. T. Yeh, D. Graham, and S. J. Gao.** 2007. Kaposi's sarcoma-associated herpesvirus promotes angiogenesis by inducing angiopoietin-2 expression via AP-1 and Ets1. Journal of virology **81:**3980-3991.
174. **Ye, F. C., F. C. Zhou, S. Nithianantham, B. Chandran, X. L. Yu, A. Weinberg, and S. J. Gao.** 2013. Kaposi's sarcoma-associated herpesvirus induces rapid release of angiopoietin-2 from endothelial cells. Journal of virology **87:**6326-6335.
175. **Ye, F. C., F. C. Zhou, S. M. Yoo, J. P. Xie, P. J. Browning, and S. J. Gao.** 2004. Disruption of Kaposi's sarcoma-associated herpesvirus latent nuclear antigen leads to abortive episome persistence. Journal of virology **78:**11121-11129.
176. **Zaldumbide, A., M. Ossevoort, E. J. Wiertz, and R. C. Hoeben.** 2007. In cis inhibition of antigen processing by the latency-associated nuclear antigen I of Kaposi sarcoma herpes virus. Molecular immunology **44:**1352-1360.
177. **Zhu, F. X., J. M. Chong, L. Wu, and Y. Yuan.** 2005. Virion proteins of Kaposi's sarcoma-associated herpesvirus. Journal of virology **79:**800-811.
178. **Zuo, J., A. D. Hislop, C. S. Leung, S. Sabbah, and M. Rowe.** 2013. Kaposi's sarcoma-associated herpesvirus-encoded viral IRF3 modulates major histocompatibility complex class II (MHC-II) antigen presentation through MHC-II transactivator-dependent and -independent mechanisms: implications for oncogenesis. Journal of virology **87:**5340-5350.

# Transcriptome Analysis of Kaposi's Sarcoma-Associated Herpesvirus during *De Novo* Primary Infection of Human B and Endothelial Cells

Journal of Virology, 2015 March 15; 89(6): 3093-111

PMID: 25552714

**Abstract:**

Kaposi's sarcoma-associated herpesvirus (KSHV) infects many target cells (e.g., endothelial, epithelial, and B cells, keratinocytes, and monocytes) to establish lifelong latent infections. Viral latent-protein expression is critical in inducing and maintaining KSHV latency. Infected cells are programmed to retain the incoming viral genomes during primary infection. KSHV transcribes many lytic genes immediately after infections that modulate various cellular pathways to establish successful infection. Analysis of the virion particle showed that the virions contain viral mRNAs, micro-RNAs, and other noncoding RNAs that are transduced into the target cells during infection, but their biological functions are largely unknown. We performed a comprehensive analysis of the KSHV virions packaged transcripts and the profiles of viral genes transcribed after *de novo* infections of various cell types (human PBMCs, $CD14^+$ monocytes, and TIVE cells), from viral entry until latency establishment. A next-generation sequence analysis of the total transcriptome showed that several viral RNAs (polyadenylated nuclear RNA, ORF58, ORF59, T0.7, and ORF17) were abundantly present in the KSHV virions and effectively transduced into the target cells. Analysis of the transcription profiles of each viral gene showed specific expression patterns in different cell lines with majority of the genes, other than latent genes, silencing after 24h post-infection. We differentiated the actively transcribing genes from the virions transduced transcripts using a nascent RNA capture approach (Click-It chemistry), which identified transcription of a number of viral genes during primary infection. Treating the infected cells with phosphonoacetic acid (PAA), to block the activity of viral DNA polymerase, confirmed the involvement of lytic DNA replication during primary infection. To further understand the role of DNA

replication during primary infection, we performed *de novo* PBMC infections with a recombinant ORF59 deleted KSHV virus, which showed significantly reduced viral copies in the latently infected cells. In summary, the transduced KSHV RNAs as well as the actively transcribed genes control critical processes of early infection to establish KSHV latency.

**Importance:**

Kaposi's sarcoma-associated herpesvirus (KSHV) is the causative agent of multiple human malignancies in immunocompromised individuals. KSHV establishes a lifelong latency in the infected host, during which only a limited number of viral genes are expressed. However, a fraction of latently infected cells undergo spontaneous reactivation to produce virions that infect the surrounding cells. These newly infected cells are primed early on to retain the incoming viral genome and induce cell growth. KSHV transcribes a variety of lytic proteins during *de novo* infections that modulate various cellular pathways to establish the latent infection. Interestingly, a large number of viral proteins and RNA are encapsidated in the infectious virions and transduced into the infected cells during a *de novo* infection. This study determined the kinetics of the viral gene expression during *de novo*-KSHV infections and the functional role of the incoming viral transcripts in establishing latency.

**Introduction:**

Kaposi's sarcoma-associated herpesvirus (KSHV), also called human herpesvirus 8 (HHV8), is a double-stranded DNA virus that causes Kaposi's sarcoma, primary effusion lymphomas, and multicentric Castleman's disease (1-3). Like other herpesviruses, KSHV

exhibits both latent and lytic modes of infection, persisting predominantly in the latent state in which only a subset of the viral proteins are expressed, including the latency-associated nuclear antigen (LANA) protein (4-8). Although the expression of latent proteins plays a critical role in inducing and maintaining KSHV latency, the infected cells are primed early on during the primary infection to retain the viral genomes and induce tumors (9). During the primary infection, KSHV undergoes a short lytic-replication cycle that transcribes an array of viral genes, which are shown to modulate various pathways for establishing the latent infection (9). In addition, a small fraction (1–5%) of the infected cells spontaneously undergo lytic reactivation to produce infectious virions, which is likely to be essential for increasing the population of infected cells and inducing viral pathogenesis (10-13).

The infection of target cells with KSHV is a complex multistep process involving a variety of host-cell surface receptors and multiple viral glycoproteins. Irrespective of its mechanism of entry, for a successful infection, KSHV must overcome the obstacles it encounters during the transportation of viral capsids from the plasma membrane into the nucleus. The main obstacles include apoptosis triggered by the virus's binding and entry, autophagy, and the induction of various intrinsic, innate, and adaptive immune responses (14, 15). The mechanisms by which KSHV successfully circumvents these obstacles are beginning to be resolved. During *de novo* infections, KSHV generally establishes latency by 24 h post-inoculation (hpi) in cell culture systems (14, 16-20). However, very early on, immediately after a *de novo* infection, KSHV undergoes a limited initial burst of lytic transcript accumulation (14). At this point, the viral gene expression shows a more complex pattern, wherein the latent and lytic genes are expressed concurrently, with an

initial moderate proportion of lytic transcripts followed by the onset of accumulating more latent transcripts (14).

It has been shown that another gamma herpesvirus, Epstein-Barr virus (EBV), exhibits a similar pattern during early infection. The primary infection of B cells by EBV shows an expression of lytic genes (21-23). The expression in the lytic genes before the latent genes during early infection suggests that this initial expression of lyitc gene are important for the successful establishment of EBV latency (21, 22). It has also been shown that EBV viral particles contain mRNAs and other nonstructural RNAs that are transduced into the target cells early during infection (22). These mRNAs play crucial roles during infection to establish the EBV latency (22). The detection of lytic transcripts early on during *de novo*-KSHV infections followed by the latent transcripts suggests that a mechanism similar to that of EBV may be occurring during the primary infection of KSHV. Additionally, the concurrent expression of ORF73 and ORF50 transcripts, detected early during KSHV infection at 2 and 4 hpi (9), respectively, indicates that these transcripts might be transported into the newly infected cell during the virus entry and are involved in altering the cellular environment prior to transcription from the incoming viral genome.

Indeed, several recent studies have shown that herpesviruses, including KSHV virus particles, contain a variety of viral proteins (24, 25) and diverse RNA species such as viral mRNA, non-coding RNA, viral and cellular micro-RNA (miRNA), and unusual small RNA (usRNA) (26, 27). These RNAs are selectively packaged during virion budding and released into the target cells during *de novo* infection, and they have been shown to be biologically functional (27). The KSHV ORF59 transcript is also present in

the virions and translated very early during primary infection (27). Recent studies have similarly shown that several of the viral and cellular miRNAs are selectively packaged into the virions and released into the target cells during infection (26). However, the exact composition of the virion transcripts in the KSHV particles and their functions remain unclear (27). A recent study reported a higher transient expression of lytic genes at 24 hpi in comparison to the latently infected cells. Moreover, the KSHV genome undergoes rapid chromatinization following infection, indicating that the initial burst of lytic gene transcription likely originates from transcriptionally permissive chromatin rather than from incoming naked DNA (28).

This study aimed to analyze the viral genes transcribed early on during the primary infection of PBMCs, CD14+ and TIVE cells. To differentiate the RNAs present in the virion and transcribed early during primary infection, non-internalized virions were removed from the cell surface by treating the cells with trypsin at 2 hpi, followed by capturing the nascently transcribing RNA after 4 and 24hpi. Also, the cells were collected at 0, 4, 24, 48, 72, 96, and 120 hpi to extract total RNA for the transcriptomic profiling and real-time quantitative PCR (qPCR) analysis. The encapsulated RNA in the virions was determined by an RNA-sequencing (RNA-seq) analysis as well as by reverse transcription quantitative real-time PCR (RT-qPCR) for all of the viral genes. We captured newly synthesized RNA with a Click-iT technology during the *de novo*-PBMC infections to identify the actively transcribing gens. The treatment of KSHV infected human PBMCs with phosphonoacetic acid (PAA), to block the viral DNA polymerase activity, determined the involvement of lytic DNA replication during primary infection. To understand the functional significance of the lytic genes transcription during KSHV

infection and the establishment of latency, we investigated the role of ORF59, an abundantly packaged mRNA in the virions that is transcribed during primary infection. The infectious recombinant KSHV BAC36WT and its ORF59-deletion mutant (BAC36ΔORF59) were used for *de novo*-PBMC infections. The infected cells showed that virions from the ΔORF59 cells were not able to attain latent genomic copies as high as the wild-type BAC36 virus, suggesting a defect in the lytic DNA replication. Overall, our data shows that a large number of virion transcripts are transduced into the host cells along with the viral genome during the infection of the target cells, which helps in amplifying the viral genome copies and latency establishment.

**Materials and Methods:**

**Cell culture, plasmids, and antibodies**

The KSHV-positive cell line TRExBCBL1-RTA, provided by Dr. Jae Jung (University of Southern California), was cultured in RPMI 1640 medium supplemented with 10% fetal bovine serum (FBS), 2 mM L-glutamine, 5 U/mL penicillin, 5 μg/mL streptomycin, and 20 μg/mL hygromycin B. Cells (293L) harboring either BAC36WT or BAC36ΔORF59 were cultured in Dulbecco modified Eagle medium supplemented with 10% FBS, 2 mM L-glutamine, 5 U/mL penicillin, 5 μg/mL streptomycin, and 50 μg/mL hygromycin B. Telomerase-immortalized vascular endothelial (TIVE) cells, kindly provided by Dr. Erle S. Robertson, were cultured in endothelial basal medium-2 (Lonza) supplemented with endothelial growth factor supplements (Lonza). Human PBMCs (ReachBio, WA) were cultured in RPMI 1640 medium (Hyclone) supplemented with 10% FBS, 2 mM L-glutamine, and penicillin/streptomycin (5 U/mL and 5 μg/mL,

respectively). Human $CD14^+$ cells were isolated from cord blood received from the Colorado Cord Blood Bank (University of Colorado). Cells were maintained in Iscove Modified Dulbecco Medium (Hyclone), supplemented with 20% heat-inactivated FBS (Hyclone), 50 ng/mL macrophage colony-stimulating factor (M-CSF), 50 ng/mL stem cell factor, 50 ng/mL granulocyte CSF (G-CSF), 50 ng/mL GM-CSF, and 50 ng/mL interleukin-3 (R&D Systems), at a density of $1 \times 10^6$ cells/mL on a low cell-binding plate (Nunc Hydrocell). Protocols to obtain blood-associated cells were approved by the Institutional Review Board and Office of Human Research Protection at the University of Nevada, Reno. The plasmid pA3F-LANA, carrying a flag-tagged ORF73, has been previously described (29, 30). Commercially available antibodies mouse anti-K8.1 and rat anti-LANA (Advanced Biotechnologies, Inc.), were used in this study.

**KSHV virion purification**

KSHV virions were purified as previously described (26, 27). Approximately 100 million TRExBCBL1-RTA cells were induced with doxycycline (1 μg/mL) for 5 days, after which the culture supernatant was collected, centrifuged at 4000 rpm for 10 minutes, and filtered through a 0.45 μM filter to remove cellular debris before concentrating the virus by centrifugation at 25,000 rpm for 2 h at 4°C. The concentrated virions were resuspended in 1 mL phosphate-buffered saline (PBS), layered onto a 30–50% sucrose gradient, and centrifuged at 70,000 × *g* for 2 h. The purified virions formed a white opaque ring, which was collected in a syringe by puncturing the tube with the needle at the band site. The collected band was diluted with PBS before centrifuging for 2 h at 25,000 × *g* to pellet the virions.

**Western blot**

The purified virus particles were resuspended in 100 μL of lysis buffer [50 mM Tris-HCl (pH 7.5), 150 mM NaCl, 1 mM EDTA, 0.25% sodium deoxycholate, and 1% NP40] supplemented with protease inhibitors (1 mM phenylmethylsulfonyl fluoride, 10 μg/mL pepstatin, 10 μg/mL leupeptin, and 10 μg/mL aprotinin). The lysates were centrifuged at high speed, mixed with protein sample buffer, resolved the protein on a 4-15% SDS-PAGE, and Western blotted using standard protocols (Bio-Rad Laboratories). The KSHV-encoded structural glycoprotein K8.1 was detected using mouse anti-K8.1 antibody followed by incubation with infrared dye-tagged (IR680, IR800) secondary antibodies and scanning with an Odyssey infrared scanner (LI-COR Biosciences, Lincoln, NE).

**KSHV *de novo* infection**

Approximately 8 × 107 human PBMCs were infected with KSHV purified from the induced TRExBCBL1-RTA cells. Two hours after infection at 37°C in the presence of 8 μg/mL polybrene, the cells were washed once with 0.005% trypsin in PBS and three times with PBS to remove the loosely bound virions, after which they were resuspended and maintained in RPMI 1680 medium until harvesting. The de novo KSHV-infected PBMCs (~5 × 106) were collected at different time points, washed twice with PBS, and processed separately to isolate the DNA and RNA.

**Indirect immunofluorescence microscopy**

At 120 hpi, KSHV-infected PBMCs were washed with PBS, spread evenly on cover slips, and air-dried. The cells were fixed for 10 min at room temperature with 4% paraformaldehyde and permeabilized with 0.2% Triton X-100 in PBS for 10 min, also at

room temperature. The cells were blocked by incubating in PBS containing 0.4% fish skin gelatin and 0.05% Triton X-100. The fixed cells were then incubated with primary rat anti-LANA antibody for 1 h at room temperature, washed with PBS, incubated with Alexa Fluor 488 secondary antibody (Molecular Probes) for 45 min at room temperature, and washed with PBS. The nuclear stain TO-PRO-3 (Molecular Probes) was used for counterstaining the nucleus. Images were obtained using a laser scanning confocal microscope (Carl Zeiss, Inc.).

**Flow cytometry**

PBMCs de novo-infected with KSHV were harvested 120 hpi and fixed in Streck tissue fixative (STF, Streck Laboratories) for 30 min. The fixed cells were washed twice in 1× PBS, permeabilized with 0.2% Triton X-100, blocked with 0.4% fish skin gelatin, and incubated with fluorescently tagged mouse anti-CD19 (Alexa Fluor 488), mouse anti-CD3 (Alexa Fluor 488; Rockland Immunochemicals, Inc.), and rat anti-LANA (Advanced Biotechnologies, Inc.), which was detected with a secondary antibody conjugated to Alexa Fluor 555 (Rockland Immunochemicals, Inc.). The data were acquired on a FACSCalibur flow cytometer equipped with CellQuest Pro software and analyzed using FlowJo software.

**Viral genome extraction and quantification**

De novo-infected cells were collected by centrifugation (~2 × $10^6$ cells per sample) and washed twice with PBS before extracting the total DNA using a modified Hirt lysis method (31). The PCR primers used for the KSHV genome quantification were selected from the ORF73 gene as previously described (9, 32). Two-fold serial dilutions of the pA3F-LANA plasmid were used as template in qPCR reactions to produce a

standard curve for the quantifications. The extracted total DNA was resuspended in 50μL sterile water, and a 5μL aliquot of the DNA was used for the qPCR amplification of the KSHV-ORF73-specific sequence. The viral DNA copy numbers were calculated with reference to the standard curve

**RNA preparation and sequencing**

The RNA-seq of the KSHV virions and de novo-infected PBMCs was performed on a HiSeq next-generation sequencer (Illumina, Inc.). Total RNA was isolated from the purified KSHV virions after treating them with micrococcal nuclease (NEB) for 30 min at 37°C and terminating the reaction with EGTA. The total RNA was isolated with TRIzol reagent per the manufacturer instructions (Life Technologies), and viral DNA was eliminated by treating with DNase I (GE Health Care Life Sciences), which was subsequently inactivated. The total RNA from the de novo-infected PBMCs was prepared using an Illustra RNAspin Mini kit with an in-column DNase treatment per the manufacturer instructions (GE Health Care Life Sciences). The concentration and purity of the extracted RNA was determined with a NanoDrop 2000c spectrophotometer (NanoDrop Technologies). A TrueSeq RNA sample preparation kit v2 (Illumina, Inc.) was used to prepare cDNA libraries for the RNA-seq according to the manufacturer instructions. The fragment sizes and purity of the mature libraries were confirmed by analyzing on a Bioanalyzer 2100 (Agilent Technologies). The quantities of the libraries required for RNA-seq were determined by real-time qPCR using a KAPA library quantification kit for the Illumina platform (Kapa Biosystems). The libraries were sequenced using HiSeq (Illumina), and the sequences were mapped to the KSHV reference genome (accession number NC_009333) using the RNA-Seq Analysis tool in

the CLC Genomic Workbench 7 (CLC Bio) software. The relative expression of the viral genes at different time points was determined based on RPKM (reads per kilobase of exon per million mapped reads) values, which were also similarly used to generate heat maps showing the relative expression of those genes at different time points utilizing the hierarchical-clustering feature of the CLC Genomic Workbench 7 software.

**Nascent RNA capture by Click-iT technology**

To identify the newly synthesized RNA during the de novo infections, a Click-iT RNA capture technology was used as described by the manufacturer (Life technologies, Inc.). Briefly, 8 × 107 human PBMCs were infected with KSHV purified from the induced TRExBCBL1-RTA cells as described above. Four hours post-infection, the cells were incubated for 1 h with ethylene uridine (33) ribonucleotide homologs containing an alkyne-reactive group. Additionally, a de novo infection of KSHV was performed in the presence of phosphonoacetic acid (PAA), an inhibitor of viral DNA polymerase and lytic DNA replication. The PBMCs were pretreated with 0.5mM PAA for 1 h prior to the infection, with the treatment continuing until harvesting at 24 hpi, similarly to a previously described method (34, 35). The de novo-infected PBMCs were collected 4 and 24 hpi and washed twice with PBS before isolating total RNA with an Illustra RNAspin Mini kit per the manufacturer instructions (GE Health Care). Biotin azide was 'clicked on' to the isolated RNA, and the newly synthesized RNA was captured using streptavidin magnetic beads. DMSO instead of biotin azide was added as control for the click reaction. The captured RNAs were further utilized for preparing cDNA libraries with a TrueSeq RNA sample preparation kit v2 (Illumina, Inc.) and for the RNA-seq analysis on a Hi-seq Illumina sequencer. Relative copies of the newly synthesized transcripts were determined

by the ratios of the biotin enriched (clicked) versus control, DMSO enriched (non-clicked) copies of the transcripts identified by RNA-sequence analysis.

**Quantitative real-time PCR**

The real-time qPCR reactions were performed in a 96-well plate in a total volume of 20 μL that included 10 μL of SYBR green PCR 2× master mix (Applied Biosystems) and 0.5 μM of each KSHV ORF-specific primer. Primers for the human housekeeping genes β-actin and GAPDH were included for normalizing the Ct values. Purified genomic DNA samples or the virion cDNA samples and KSHV-infected PBMCs were amplified on an ABI StepOnePlusTM Real-Time PCR machine (Applied Biosystems). As a standard practice, a no reverse-transcription (no-RT) control reaction was included for all of the prepared RNA samples to ensure their purity.

**Accession numbers**

The RNA-seq data was deposited in the NCBI Gene Expression Omnibus (GEO) database, and the accession number for the complete data set is GSE62344.

**Results:**

**Purification of the KSHV virions**

We isolated the KSHV particles from doxycycline-induced (1μg/mL) TRExBCBL1-RTA cells and purified them on a 20–50% sucrose gradient. The three white bands observed on the sucrose gradient (Fig. 1A) were consistent with previous reports (26, 36), representing the A-type (empty virus particles), B-type (intermediate virus particles), and C-type KSHV particles (mature virions). The lower band representing the mature C-type KSHV virion particles was collected with a syringe and

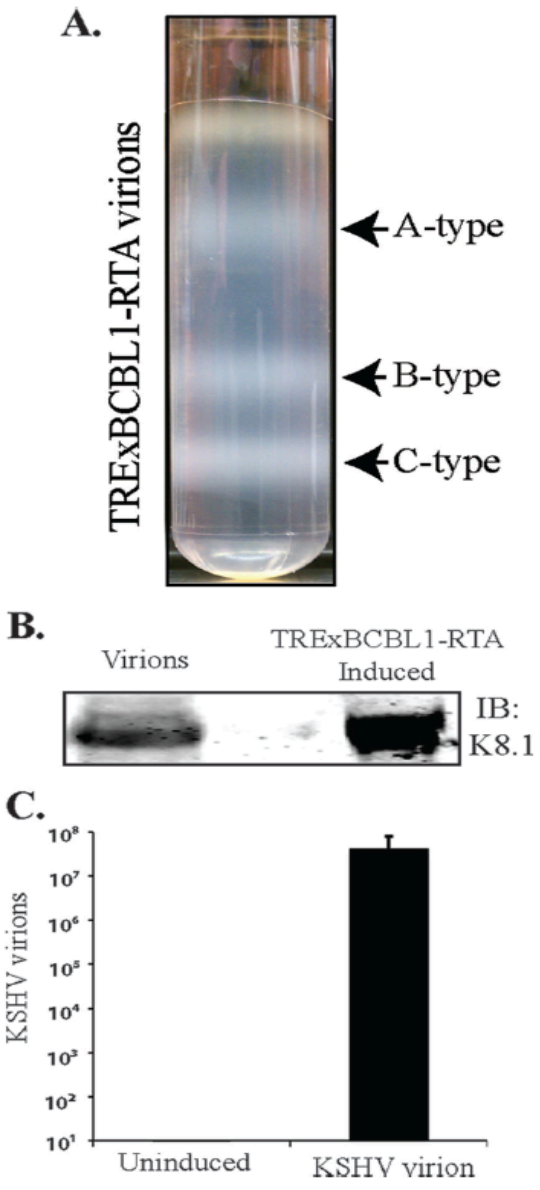


**FIG 1** Purification of KSHV virions. (A) Virions were purified from the culture supernatant of approximately $9 \times 10^8$ reactivated TRExBCBL1-RTA cells by a20 to 50% sucrose gradient ultracentrifugation. The three white bands as indicated represent A-type (empty), B-type (intermediate), and C-type (mature) KSHV virus particles. (B) Western blotting of purified virions for the presence of KSHV envelope glycoprotein K8.1 by immunoblotting with anti-K8.1 antibody. Total lysate from induced TRExBCBL1-RTA cells was used as a positive control. (C) Supernatants of uninduced or induced TRExBCBL1-RTA cells were used for real-time qPCR quantification of viral genome copy using ORF73-specific primers along with ORF73 plasmid standards. Approximately $8.06 \times 10^7$ copies of viral DNA representing C-type virions were detected.

diluted before pelleting the virions by ultracentrifugation. These purified virions were tested for the presence of the KSHV envelope glycoprotein K8.1 by immunoblotting with anti-K8.1 antibody (Fig. 1B). The virion DNA was extracted to quantify the number of viral copies in a real-time qPCR assay using ORF73-specific primers (Fig. 1C), which showed approximately $8.0 \times 10^7$ virions/ml. This fraction of mature virions, which was confirmed by both analyses, was further used for *de novo* infections of the indicated target cells.

**KSHV viral transcripts were abundantly present during the primary infection of human PBMCs, CD14+ and TIVE cells**

To determine the profiles of the viral transcripts expressed during the primary infection of B and endothelial cells (natural target cells of KSHV), purified virions were used for the de novo infection of human PBMCs, CD14+ monocytes, and endothelial (TIVE) cells. An RNA-seq analysis was performed on total RNA extracted from these

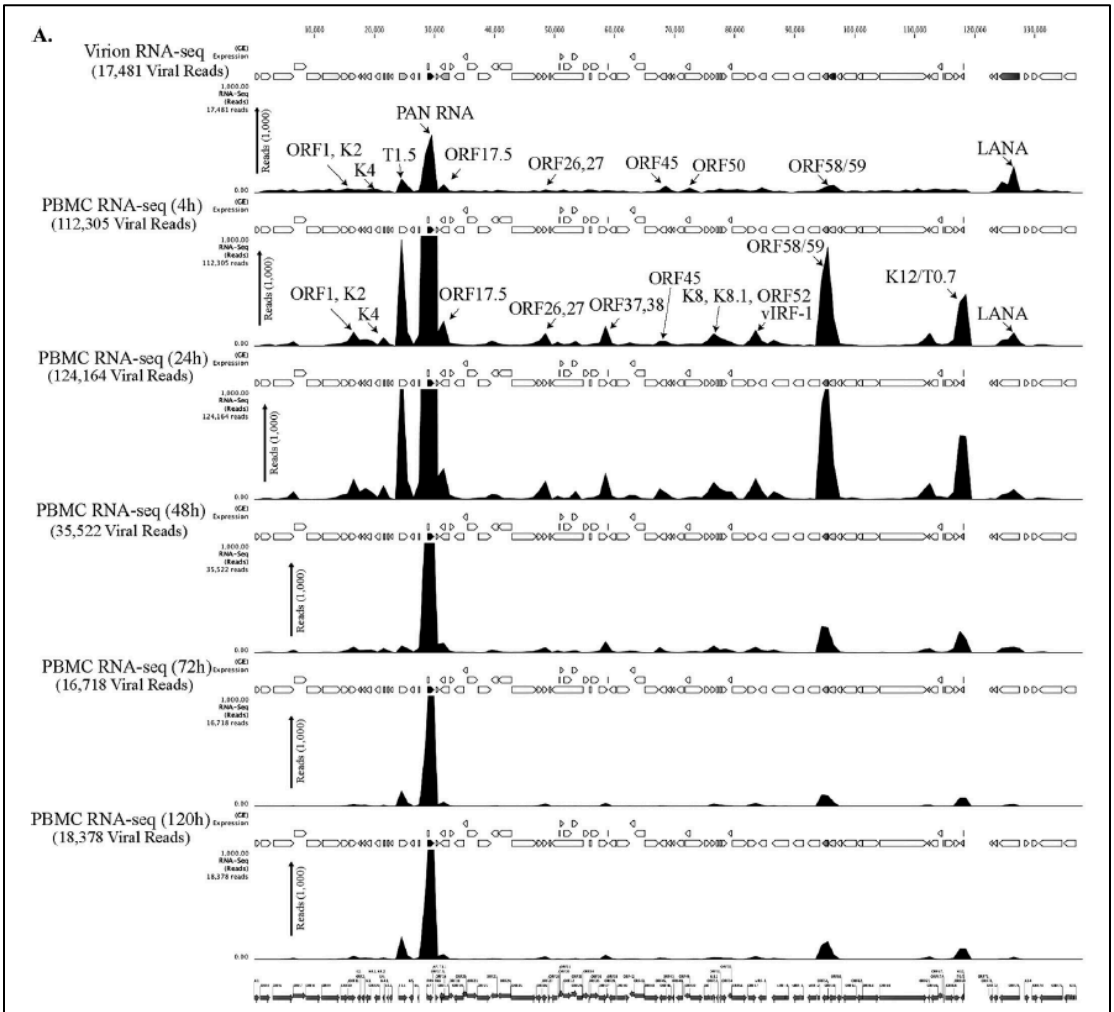


**FIG 2** (A) Transcriptome analysis of KSHV during *de novo* infection of human PBMCs. Total RNAs extracted from *de novo*-infected PBMCs harvested at 4 h, 24 h, 48 h, 72 h, and 120 h postinfection were subjected to cDNA library preparation using a TrueSeq RNA-seq library kit. The libraries were sequenced using HiSeq, and the sequences were mapped to the reference KSHV genome to determine the relative abundance of viral transcripts. Purified virions treated with micrococcal nuclease to eliminate nucleic acid contamination were subjected to total RNA extraction. RNA treated with DNase was used for sequencing after cDNA library preparation. The number of transcripts mapping to the viral genome is shown in parentheses in each panel. The peak height represents the number of reads for the indicated genes, and the predominant peaks are marked in virion RNA-seq and 4-h-postinfection samples. PAN RNA showed the highest peak in virions as well as KSHV-infected PBMCs. The bottom panel shows the locations of KSHV genes on the coordinates. (B) Transcriptome analysis of *de novo*-infected $CD14^+$ cells. Total RNAs extracted from *de novo*-infected $CD14^+$ cells harvested at 4 h, 24 h, 48 h, 72 h, and 96 h postinfection were subjected to cDNA library preparation using a TrueSeq RNA-seq library kit. The libraries were sequenced using HiSeq, and the sequences were mapped to the reference KSHV genome to determine the relative abundance of viral transcripts. The number of transcripts mapping to the viral genome is shown in parentheses in each panel. The peak heights representing the number of reads for the indicated genes are marked in 4-h-postinfection and 24-h-postinfection samples. PAN RNA showed the highest peak until 48 h postinfection, followed by a decline to very low levels. LANA expression progressively increased, showing establishment of latency. The bottom panel shows the locations of KSHV genes on the coordinates. (C) Transcriptome analysis of *de novo*-infected TIVE cells. Total RNAs extracted from *de novo*-infected TIVE cells harvested at 4 h, 24 h, 48 h, 72 h, and 120 h postinfection were subjected to cDNA library preparation using a TrueSeq RNA-seq library kit. The libraries were sequenced using HiSeq, and the sequences were mapped to the reference KSHV genome to determine the relative abundance of viral mRNA. The numbers of transcripts mapping to the viral genome are shown in parenthesis on each panel. The peak heights representing the number of reads for the indicated genes are marked in 4-h-postinfection and 24-h-postinfection samples. The sample from 72 h postinfection showed lower peaks because of the lower number of total reads, which were normalized by calculating the RPKM values in the heat maps. The bottom panel shows the locations of KSHV genes on the coordinates.

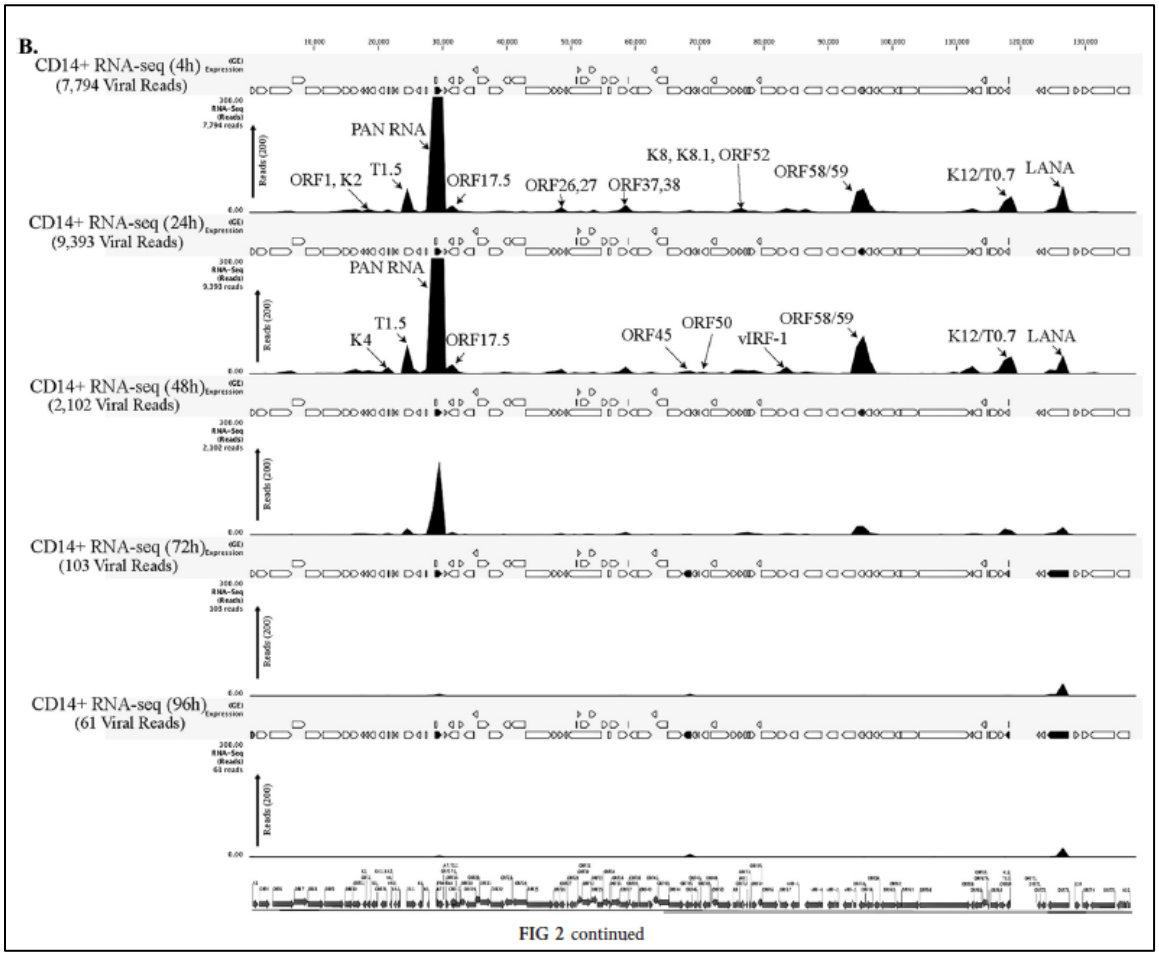


FIG 2 continued

infected cells at different time points (4, 24, 48, 72, and 120 hpi). Furthermore, 10pM of the quantified libraries were sequenced and mapped to the reference KSHV genome (NC_009333). The transcriptome analysis revealed that several of the KSHV lytic and latent transcripts accumulated as early as 4hpi (Figs. 2A–C and 3).

Apart from the ORF50 replication and trans-activator protein (RTA), a number of other lytic transcripts involved in immune modulation, lytic-DNA replication, and nucleic acid processing/synthesis were detected in significant amounts early during the infection. These included polyadenylated nuclear (PAN) RNA, ORF58/59, kaposin B, K2, K4, K6, ORF11, ORF17, ORF45, ORF27, ORF37, ORF57, ORF64, ORF65, ORF73, and the recently identified T0.7. Among these, PAN RNA was the most abundant as determined

by the relative peak height (Figs. 2A–C) and RPKM values (Fig. 3) in all the three tested cell types. Although the overall patterns of the viral gene expressions were similar, i.e. majority of the genes expressing at 24hpi in all the three tested cells, CD14+ monocytes showed complete silencing of viral gene expressions, other than LANA, after 24hpi (Figs. 2A–C and 3). However, the human PBMCs and TIVE showed detectable levels of PAN RNA and ORF58/59 transcripts along with LANA after 48hpi (Figs. 2A–C and 3).

This suggests a cell type specific viral gene expression patterns during primary *de novo* infection and latency establishment. Relative abundance of many of the viral transcripts including ORF1, K2, K4, T1.5, PAN RNA, ORF17.5, ORF26, ORF27, ORF37 ORF38, ORF45, K8, K8.1, ORF52, vIRF-1, ORF58/59, K12/T0.7 and LANA showed an increase in their abundance in PBMCs at 4hpi and 24hpi when compared with their abundance in the virions (Fig. 2A). However, the CD14+ monocytes cells showed

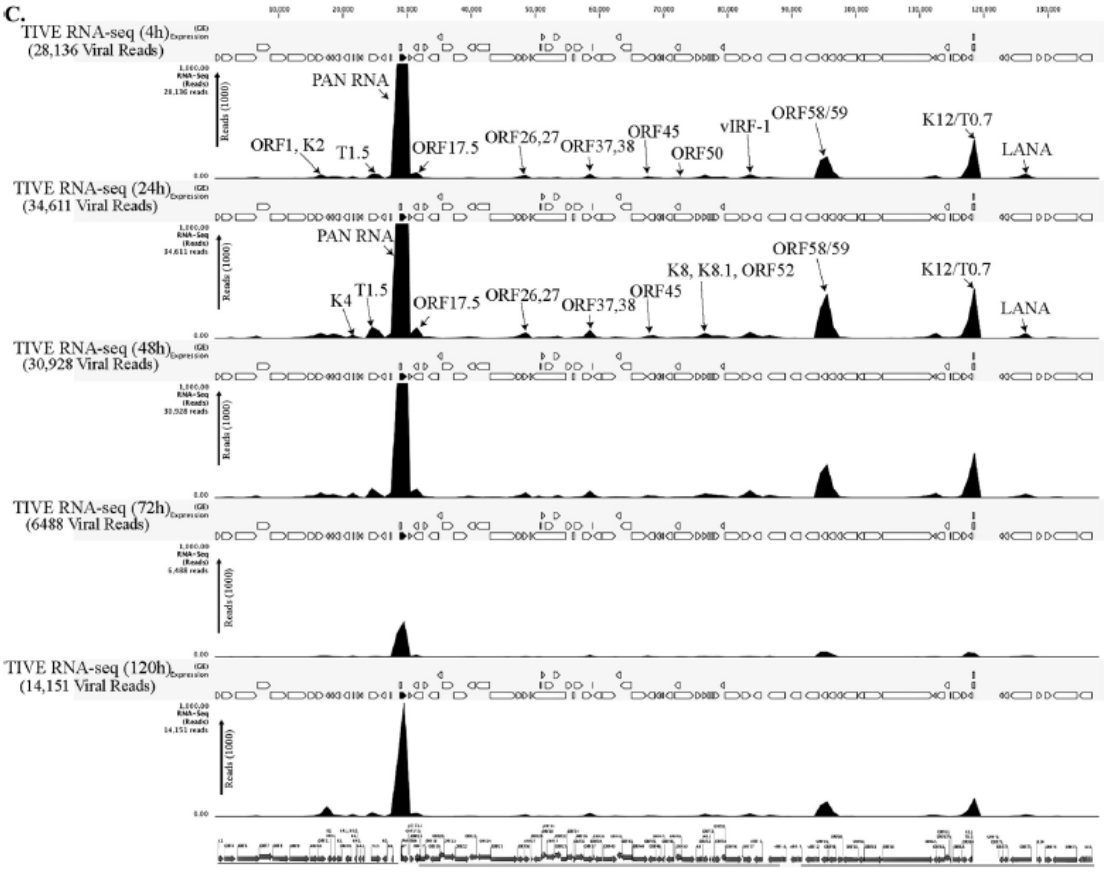


FIG 2 continued

increases in the abundance of only fewer genes as compared to the PBMCs (Fig. 2B). Importantly, LANA was the only gene abundantly detected after 72hpi in these CD14+ cells representing a true latency model of KSHV infection. The endothelial cells (TIVE) showed detectable levels of viral transcripts but their relative abundance increased only slightly at 24hpi (Fig. 2C). The heat-maps generated based on the RPKM values showed an increase in their copies from 4hpi to 24hpi, suggesting an active transcription and these included, PAN RNA, ORF73, ORF45, ORF58, T0.7, Kaposin B, ORF59, K4, K6, ORF17, ORF65, ORF27, K8.1, ORF11, ORF37, ORF38, ORF57, ORF69, ORF52, ORF54 and T1.5 (Fig. 3). The viral DNA polymerase, ORF9 along with other lytic DNA replication proteins were detected but their expression level did not increase (Fig. 3). Also, there were several other detectable transcripts (K1, ORF4, ORF10, K6, ORF43, ORF44, ORF67, ORF68, and K14) but their abundance did not increase and the RPKM values remained unchanged during the time course tested, suggested that these genes did not transcribe but were present due to their transduction through the virion particles during infection.

Earlier studies reported that immediately after *de novo* infection, the herpesviruses express genes involved in lytic DNA replication (28, 37, 38). Our RNA-seq analysis detected the transcripts of proteins involved in viral DNA replication as early as 4 hpi, and these included ORF59 (processivity factor), ORF9 (DNA polymerase), ORF6 (single-stranded DNA binding protein), ORF56 (DNA replication protein), ORF40 (primase-associated factor), ORF54 (dUTPase) along with ORFs 60 and 61 (ribonucleoprotein reductase), ORF70 (thymidylate synthase), and ORF 37 (alkaline exonuclease). Apart from these transcripts, several other transcripts encoding the viral

structural proteins ORF8 (glycoprotein B), K8.1 (glycoprotein), and ORFs 64 and 75 (tegument protein) were also detected in our transcription profiling data. Moreover, many of the noncoding RNAs, including PAN RNA, T0.7, and T1.5 (OriLyt transcript), were abundantly detected in the RNA-seq analysis. RNA-seq profiling of the virion encapsidated RNA, as relative abundance, showed packaging of a large number of viral transcripts, which are brought into the target cells by the KSHV virion during the *de novo* infection (Fig. 2 and Table 1).

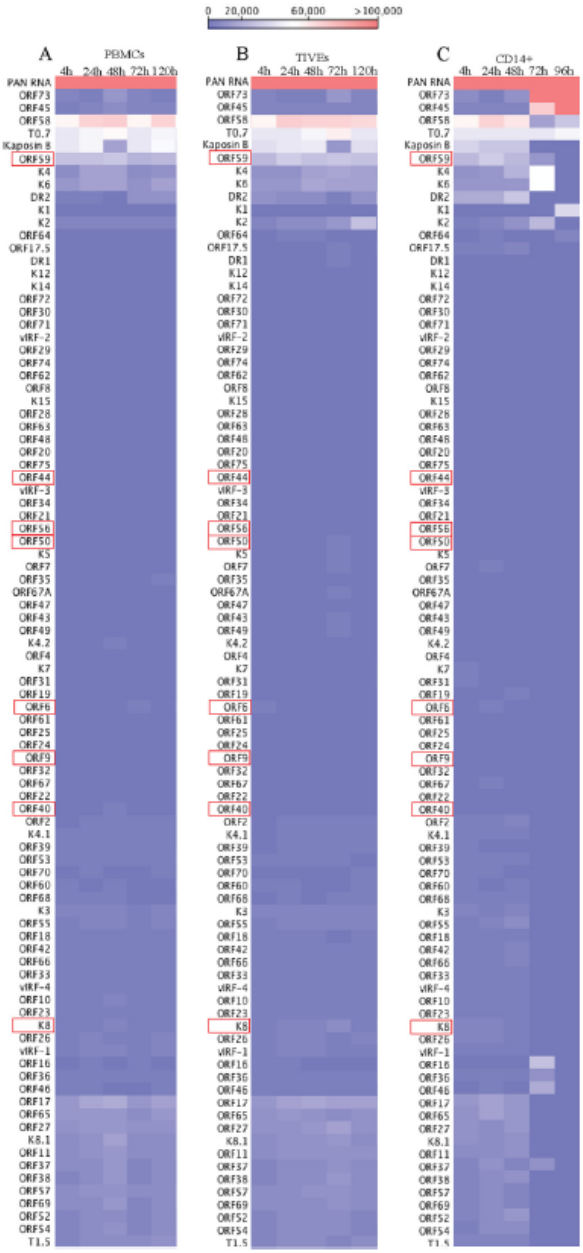


**FIG 3** Transcriptome analysis of KSHV in *de novo*-infected PBMCs, TIVE cells, and CD14$^+$ cells. RPKM values, calculated based the number of reads for each gene, were used for analyzing relative expression of KSHV genes as heat maps. Hierarchal clustering of genes was performed using CLC Workbench 7.0. Increasing RPKM values are represented from blue to red. (A) KSHV transcriptome from *de novo*-infected human PBMCs. (B) KSHV transcriptome from *de novo*-infected human TIVE cells. (C) KSHV transcriptome from *de novo*-infected human CD14$^+$ cells.

In agreement with the previous report, our results showed the concurrent expression of ORF50 and ORF73 transcripts during early primary infection (Figs. 2A–C and 3). However, the expression of ORF50 decreased after 24 h, whereas the expression of ORF73 increased exponentially (Fig. 3, heat maps). The KSHV latency-associated protein ORF73 is the predominant protein expressed during

latency and is responsible for immune evasion, latent DNA replication, and genome maintenance, whereas the ORF50-encoded protein RTA activates lytic cycle-specific KSHV genes in a cascaded manner to facilitate the lytic replication process (39-43).

**TABLE 1** mRNAs detected in purified TRExBCBL1-RTA virions by RNA-seq analysis[a]

| No. | mRNA | RPKM value | Total gene reads | Function | Transcription 4 h after *de novo* infection of human PBMCs | Source or reference |
|---|---|---|---|---|---|---|
| 1 | ORF4 | 2,633.55 | 101 | Complement control protein (KCP), regulates complement activation | | This study |
| 2 | ORF6 | 3,804.2 | 300 | Single-stranded DNA binding protein essential for lytic DNA replication | | This study |
| 3 | ORF7 | 2,332.60 | 113 | Probably DNA packaging | | This study |
| 4 | ORF8 | 4,432.43 | 261 | Virion envelope-associated glycoprotein | | This study |
| 5 | ORF9 | 5,318.55 | 375 | KSHV DNA polymerase | | This study |
| 6 | ORF10 | 6,446.37 | 188 | Specific suppressor of interferon signaling | | This study |
| 7 | ORF11 | 6,275.82 | 191 | Viral lytic protein | Yes | This study |
| 8 | K2 | 7,218.64 | 103 | K2 (viral interleukin-6), regulates cellular proliferation | Yes | 27 |
| 9 | K3 | 6,004.86 | 135 | E3 ubiquitin ligases that reduce surface expression in infected cells | | This study |
| 10 | ORF70 | 5,568.35 | 131 | Homolog of viral thymidylate synthase | | This study |
| 11 | K4.2 | 4,632.04 | 59 | | | This study |
| 12 | T1.5 | 10,245.93 | 358 | | | This study |
| 13 | K6 | 10,027.11 | 67 | vMIP-IA | | 27 |
| 14 | PAN RNA | 159,519.90 | 3,986 | Late gene expression, lytic DNA replication, immune modulation | | 27 |
| 15 | ORF17 | 13,534.71 | 504 | | Yes | 27 |
| 16 | ORF18 | 2,840.02 | 51 | Late gene regulation | | This study |
| 17 | ORF19 | 3,134.66 | 120 | | | This study |
| 18 | ORF21 | 3,140.50 | 127 | Thymidine kinase | | This study |
| 19 | ORF22 | 1,729.56 | 88 | Glycoprotein H | | This study |
| 20 | ORF23 | 2,305.84 | 65 | Predicted glycoprotein | | This study |
| 21 | ORF24 | 2,823.83 | 148 | Essential for DNA replication | | This study |
| 22 | ORF25 | 3,338.78 | 320 | Major capsid protein | | This study |
| 23 | ORF26 | 3,239.66 | 69 | Minor capsid protein | | This study |
| 24 | ORF27 | 6,270.22 | 127 | Glycoprotein | Yes | This study |
| 25 | ORF29 | 3,163.27 | 390 | Packaging protein | | This study |
| 26 | ORF34 | 2,233.92 | 51 | | | This study |
| 27 | ORF35 | 5,613.67 | 59 | | | This study |
| 28 | ORF36 | 4,907.44 | 152 | Serine protein kinase | Yes | This study |
| 29 | ORF37 | 2,625.62 | 89 | Alkaline exonuclease Sox protein | Yes | This study |
| 30 | ORF39 | 2,149.70 | 60 | Glycoprotein M | | This study |
| 31 | ORF40 | 2,904.36 | 144 | Helicase/primase | | This study |
| 32 | ORF44 | 2,676.778 | 147 | Helicase | | This study |
| 33 | ORF45 | 6,972.31 | 198 | Virion-associated tegument protein regulating IFN function | Yes | This study |
| 34 | ORF46 | 7,969.30 | 142 | Uracil deglycosylase | | This study |
| 35 | ORF48 | 3,101.60 | 87 | Activates JNK/p38 | | This study |
| 36 | ORF50 | 4,389.71 | 309 | Replication transcriptional activator protein | | This study |
| 37 | K8 | 4,072.23 | 89 | bZIP | Yes | 27 |
| 38 | K8.1 | 3,918.32 | 71 | Glycoprotein | Yes | This study |
| 39 | ORF52 | 6,095.17 | 56 | Tegument protein | Yes | This study |
| 40 | ORF54 | 9,659.02 | 199 | dUTPase/immune modulation | | 27 |
| 41 | ORF55 | 6,364.41 | 101 | Tegument protein | | This study |
| 42 | ORF56 | 3,830.11 | 225 | DNA replication | | This study |
| 43 | ORF57 | 3,533.39 | 121 | Lytic replication protein homologous to EBV SM protein, mRNA splicing | Yes | This study |
| 44 | vIRF-1 | 7,407.08 | 232 | Immune modulation | Yes | This study |
| 45 | vIRF-4 | 2,324.47 | 153 | Facilitates lytic replication by targeting cellular IRF4 and Myc gene | Yes | This study |
| 46 | vIRF-3 | 2,302.58 | 96 | Immune modulation | | This study |
| 47 | vIRF-2 | 2,429.94 | 122 | Type I interferon signaling | | This study |
| 48 | ORF58 | 16,775.11 | 418 | | Yes | 27 |
| 49 | ORF59 | 26,201.13 | 724 | Processivity factor | Yes | 27 |
| 50 | ORF60 | 4,601.25 | 98 | Ribonucleoprotein reductase | | This study |
| 51 | ORF61 | 3,659.74 | 202 | Ribonucleoprotein reductase | | This study |
| 52 | ORF63 | 2,891.99 | 187 | NLR homolog | | This study |
| 53 | ORF64 | 3,897.02 | 715 | Deubiquitinase | Yes | This study |
| 54 | ORF65 | 5,629.25 | 67 | Capsid protein | | This study |
| 55 | ORF66 | 5,646.64 | 169 | Capsid protein | | This study |
| 56 | ORF67 | 4,753.85 | 90 | Nuclear egress complex | | This study |
| 57 | ORF68 | 5,372.34 | 175 | Glycoprotein | | This study |
| 58 | ORF69 | 6,353.81 | 134 | BRLF2 nuclear egress | Yes | This study |

(Continued on following page)

**TABLE 1** mRNAs detected in purified TRExBCBL1-RTA virions by RNA-seq analysis[a]

| No. | mRNA | RPKM value | Total gene reads | Function | Transcription 4 h after *de novo* infection of human PBMCs | Source or reference |
|---|---|---|---|---|---|---|
| 59 | T0.7 | 9,310.93 | 151 | | | This study |
| 60 | ORF72 | 3,118.46 | 56 | vCyclin | | This study |
| 61 | ORF73 | 23,623.23 | 1,858 | Latency-associated nuclear antigen | | This study |
| 62 | K14 | 3,116.41 | 59 | vOX2 | | This study |
| 63 | ORF74 | 4,481.89 | 107 | vGPCR | | This study |
| 64 | ORF75 | 3,810.57 | 344 | Tegument protein vFGARAT | Yes | This study |

[a] Total gene reads above 50 and a qPCR relative fold change above 10 were considered significant.

In a cell culture system, the over-expression of RTA is capable of triggering the lytic DNA replication (39, 43). Our data detected the transcripts of ORF50 and other lytic genes along with ORF73 during early infection suggest that KSHV may enter into a DNA replicative phase before establishing latent infection.

**Quantitative real-time PCR validation of the RNA sequencing analysis**

To further confirm the results of the transcriptome analysis by an independent method, we performed a real-time qPCR analysis on *de novo*-infected PBMCs harvested at different time points (4, 24, 48, 96, and 120 hpi). A custom qPCR array of the KSHV genes in a 96-well format (Bar Harbor Biotechnology) was used for the quantification of the viral mRNA levels. The fold-changes of the individual KSHV genes were calculated for the various times post-infection using the ΔΔCt method and plotted separately (Fig. 4). The viral genes showed expression kinetics similar to those seen with the RNA-seq analysis. As first shown by the RNA-seq analysis, even at 4 hpi, several lytic transcripts (ORF58/59, ORF11, ORF8, K8, K8.1, ORF17, ORF22, ORF57, ORF 45, ORF27, ORF 37, and ORF64) were detected at high levels, and the expression of these transcripts was gradually depleted after 24 hpi (Fig. 4). In addition, latent transcripts (ORF73, K12, and ORF72) were consistently detected at significant levels during early infection (Fig. 4).

As reported previously (9), the real-time qPCR analysis showed the concurrent expression of ORF50 and ORF73 at 4 hpi, and ORF50 showed a much higher fold-increase during early infection than ORF 73. However, the expression of the ORF73

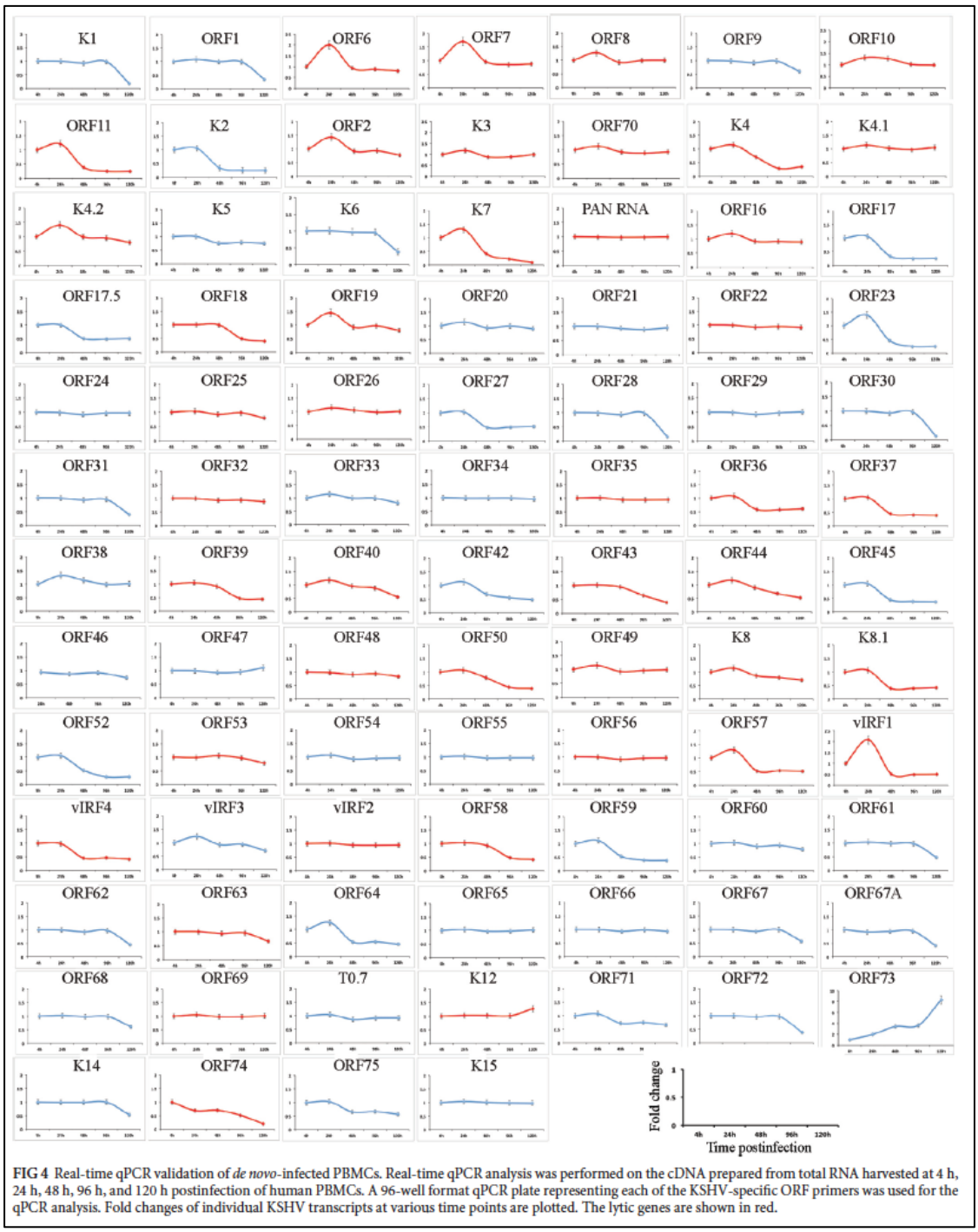


**FIG 4** Real-time qPCR validation of *de novo*-infected PBMCs. Real-time qPCR analysis was performed on the cDNA prepared from total RNA harvested at 4 h, 24 h, 48 h, 96 h, and 120 h postinfection of human PBMCs. A 96-well format qPCR plate representing each of the KSHV-specific ORF primers was used for the qPCR analysis. Fold changes of individual KSHV transcripts at various time points are plotted. The lytic genes are shown in red.

transcript increased exponentially until 96 hpi. Additionally, the non-coding PAN RNA and recently identified T0.7 transcripts were also detected abundantly at 4 hpi (Fig. 4). The qPCR validation of the RNA-seq analysis suggested that the limited lytic-gene accumulation observed during primary infection might have been influenced by the RTA mediated gene expression as well as by the transduction of viral transcripts with the virions during the *de novo* infection.

**Detection of actively transcribing genes during *de novo* infection**

The transcriptome analysis of *de novo*-infected cells during early infection revealed a significantly higher expression of several genes, which are expressed during lytic replication cycle including ORF50, ORF6, ORF9, ORF8, ORF7, ORF10, ORF11, ORF22, ORF27, ORF31, ORF37, ORF40/41, ORF45, ORF54, ORF55, ORF56, ORF58, ORF59, and ORF69 (Figs. 2A–C and 3). In addition, many of the immediate-early KSHV unique genes such as K7, K8, K3, K5, K9, and K12, as well as late K8.1, were also detected. Many of these transcripts have crucial regulatory roles in immune evasion and nucleic acid processing and synthesis, which are associated with lytic-DNA replication. The real-time qPCR analysis of the viral transcripts fully corroborated the RNA-seq analysis (Fig. 4).

To further identify the actively transcribing genes during *de novo* infection, we used an approach to capture the nascent transcribed RNA from the KSHV infected PBMCs by labeling them with EdU and isolating them by Click-It approach. The sequencing of newly synthesized RNA captured from the KSHV infected PBMCs showed peaks of many viral genes at 4hpi and these included ORF2, K3, T1.5, PAN RNA, ORF26, ORF29, ORF36, ORF37, ORF40, ORF50, K8.1, ORF55, vIRF-2,

ORF58/59, ORF60, ORF63, ORF64, ORF67, T0.7, ORF72, ORF73 and ORF74 (Fig. 5A). Importantly, majority of these were showing increased expression in relative abundance graph as well as in the heat maps (Figs. 2, 3 and 5). Interestingly, majority of the active transcription were limited to the ORF73, detected by the sequence reads, at 24hpi suggested for the beginning of a latency establishment (Fig. 5, 24h panel). We also confirmed the transcription during *de novo* infection by treating the cells with actinomycin D to block active transcription. Comparison of the transcript levels at 4 hpi

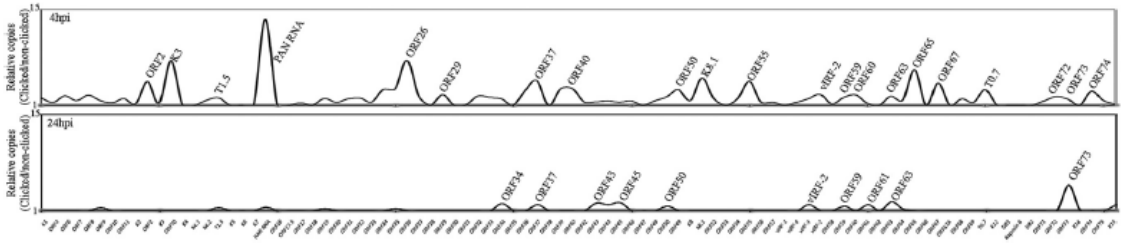


**FIG 5** Viral genes transcribed at 4 hpi and 24 hpi, identified by a nascent RNA capture approach. Human PBMCs infected with KSHV virions were incubated with EdU (alkyne) at 4 hpi and 24 hpi to label the newly transcribing RNA. Total RNA extracted from these cells was subjected to click reaction with biotin-azide (Invitrogen, Inc.). DMSO instead of biotin-azide was used in control click reactions. Newly synthesized, biotin-labeled RNA was enriched by streptavidin magnetic beads as per the manufacturer's instructions. These enriched RNAs were subjected to RNA-seq analysis by HiSeq, and the sequences were mapped to the KSHV reference genome (NC_009333) using CLC Bio Workbench 7.5. The relative numbers of copies of the newly synthesized viral RNA were determined by ratios of specific (biotin-labeled) to nonspecific (DMSO) sequence reads.

in the untreated with actinomycin D treated cells revealed almost similar profiles to the nascent RNA capture data of gene transcription at 4hpi (data not shown). As expected, the ORF50 gene showed a moderate level of *de novo* transcription within 4 hpi (Fig. 5). Interestingly, not all the genes required for lytic DNA replication showed an active transcription during de novo infection, but were detected in RNA-seq analysis suggesting that those genes were transduced with the virions. Not surprisingly, the ORF50 gene transcripts and those of genes regulated by ORF50 decreased after 24 hpi. Also, a gradual increase in ORF73 transcripts by 24 hpi may aid in suppressing the expression of other viral genes to promote the establishment of latency.

**KSHV genome copy numbers increased exponentially after *de novo* infection**

To investigate whether the detection of lytic-reactivation genes leads to lytic-DNA replication and genome amplification, we analyzed the KSHV genome copy number during the *de novo* infection of PBMCs. Total DNA from different time points (0, 4, 24, 48, 72, 96, and 120 hpi) were subjected to a real-time qPCR analysis to analyze the relative viral copies in the infected cells. We used ORF73-specific primers and ORF73-plasmid standards to obtain the copy numbers of the KSHV genome. The relative number of KSHV genome copies was calculated in the real-time qPCR assay by amplifying the ORF73 gene and normalizing it against GAPDH. KSHV viral DNA was detected as early as 4 hpi, which increased exponentially up to 48 hpi, and then slightly decreased over time after establishing latency (Fig. 6A). This exponential increase in the genome copies confirms for a genome replication during early infection till the establishment of latency.

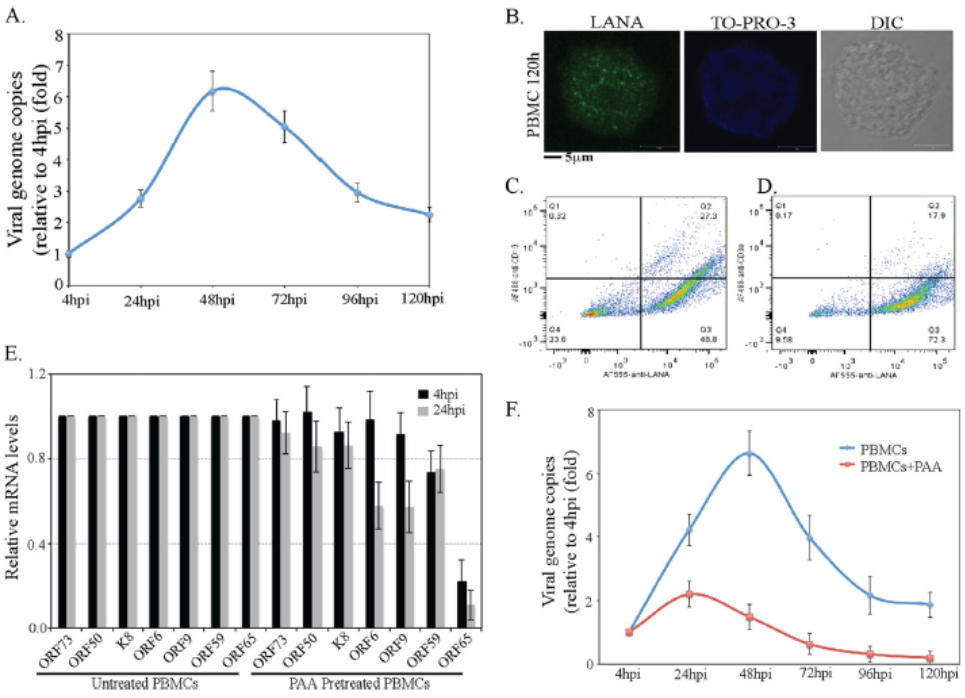


**FIG 6** KSHV genome copies exponentially increase after infection. (A) Approximately $8 \times 10^7$ human PBMCs were infected with KSHV isolated from reactivated TRExBCBL1-RTA, with a multiplicity of infection (MOI) of 10. *De novo*-infected PBMCs were harvested at 4 h, 24 h, 48 h, 72 h, 96 h, and 120 h postinfection, followed by extraction of total DNA using a modified Hirt lysis method. This DNA was used to analyze the genome copy number by real-time qPCR using ORF73-specific primers and ORF73 plasmid as a standard. (B) Indirect immunofluorescence assay (IFA) for LANA on *de novo*-infected PBMCs. KSHV-infected PBMCs at 120 h postinfection were subjected to IFA with rat anti-LANA antibody followed by detection with Alexa Fluor 488 secondary antibody. Nuclear stain TO-PRO-3 was used for staining the nuclei. LANA is shown in green, and nuclear stain TO-PRO 3 is shown in blue. (C and D) Flow cytometry analysis of *de novo*-infected PBMCs. KSHV-infected PBMCs at 120 h postinfection were subjected to flow cytometry analysis to detect the percentages of B and T lymphocytes infected with KSHV. Mouse anti-CD19 was used for the detection of B lymphocytes, and mouse anti-CD3 was used for the detection of T lymphocytes. Rat anti-LANA was used to gate KSHV-positive cells. Data were acquired on a FACSCalibur equipped with CellQuest Pro software and analyzed using FlowJo software. (E) PAA treatment reduces the expression of late genes. Untreated or PAA-pretreated human PBMCs were infected with KSHV virions (MOI of 10) for 4 h or 24 h. Total RNAs extracted at 4 hpi and 24 hpi were subjected to detection of selected viral transcripts by real-time qPCR, which showed significant reduction in ORF65 (late gene) expression with PAA treatment. (F) PAA treatment reduces viral genome copies in KSHV-infected human PBMCs. Untreated or PAA-treated human PBMCs infected with KSHV virions (MOI of 10) were subjected to genome copy analysis. Viral genome copies at different time postinfection were determined relative to the copies at 4 hpi.

The punctate immunolocalization of LANA in the *de novo*-infected PBMCs (120 hpi) clearly demonstrated the establishment of latency in these cells (Fig. 6B). A flow cytometry analysis of *de novo*-infected PBMCs using anti-LANA and B- and T-lymphocyte markers gated for LANA expression showed that the populations of both the B- (~55.94%) and T-lymphocytes (~24.75%) were successfully infected with KSHV (Fig. 6C and D). Since the viral genome copies increased about 6 fold at 48 hpi from the 4 hpi (the non-internalized virions were removed at 2 hpi by treating the cells with trypsin), we wanted to determine whether the virus has undergone to latent or lytic modes of DNA synthesis to amplify the genome copies. To this end, we treated the cells with a viral DNA polymerase inhibitor, phosphonoacetic acid (PAA) to block the lytic DNA replication. The cells pretreated with PAA or untreated were infected with KSHV virions for 4h and 24h for the transcriptome analysis. Analysis of the selected genes of latent, immediate early and early genes showed almost no effect of PAA on the transcription of latent (ORF73) and immediate early genes (ORF50) at 4 hpi (Fig. 6E). However, the expression of late gene (ORF65) was significantly reduced with PAA at both, 4 and 24 hpi (Fig. 6D). We also determined the genome copies during *de-novo* infection of PBMCs in the presence of PAA. The relative genome copies showed a significant reduction in viral genome amplification in cells treated with PAA (Fig. 6F). Since there was still slight increase in the viral genome copies at 24 hpi, we speculate that other mechanism; besides the lytic DNA replication, takes place during *de novo* infection of PBMCs.

**KSHV virions packaged the viral transcripts**

To analyze the RNA composition in the encapsidated virions, total RNA extracted from the purified C-type KSHV virions was used for the RNA-seq analysis. After confirming the purity of the RNA, the total RNA from two independent virus purifications was used to construct cDNA libraries. After quantifying, 10 pM of the mature library samples were used for the RNA-seq analysis. In comparison with previous reports (26, 27), the transcriptome analysis with the CLC Genomic Workbench 7 software using KSHV as the reference genome detected a larger number of KSHV mRNAs in the virions. A previous DNA microarray study identified 11 KSHV mRNAs in the virions (27), but in this study, we identified more than 60 KSHV-specific transcripts, including mRNAs for latent genes (Table 1). The mRNAs with 50 or more specific-gene reads and a 10-fold higher abundance in the qPCR assays were considered significant (Fig. 7A and Table 1). The most abundant transcripts detected in the virions included PAN RNA, K7, K14, K12, ORF58/59, and the recently identified T0.7, with PAN RNA being the most abundant (Fig. 7A). In addition, many lytic-specific mRNAs were also present in the virions, such as ORF50, ORF8, ORF9, ORF21, ORF22, ORF31, ORF40/41, ORF45, ORF54, ORF55, ORF69, and ORF75. Moreover, many of the immediate-early and early KSHV-unique K genes (K7, K8, K3, K5, K9) and the late K8.1 gene were also detected. Interestingly, in contrast to the previous report (27), a significant amount of latent-specific ORF73 mRNA was detected in the virions (Fig. 7A). Both this and the previous studies suggest that virion transcripts are released into the target cells immediately after *de novo* infection (26, 27). This may be the reason for the immediate concurrent expression of ORF50 and ORF73 in the target cells (9). It has been

shown that proteins encoded by these transcripts have significant regulatory roles in various cellular pathways, including cell signaling, immune modulation, and apoptosis, that could critically affect the phenotype of the newly infected cell and its microenvironment (14, 15, 44, 45) to provide the necessary factors required for a successful infection.

**Virion-packaged transcript specificity**

To further clarify the RNA-Seq results, we performed a real-time qPCR analysis on cDNA prepared from the same source of total RNA (extracted from purified C-type KSHV virions) used in the sequencing analysis. A custom qPCR array representing each of the KSHV-specific ORF primers was used for the analysis. The uninfected PBMCs used as a reference control did not amplify, and a no-RT control was used to ensure the quality of the RNA. The qPCR data showed results similar to those of the RNA-seq analysis, confirming the presence of viral transcripts in the virions.

To determine whether there is a specific mechanism of RNA encapsidation during

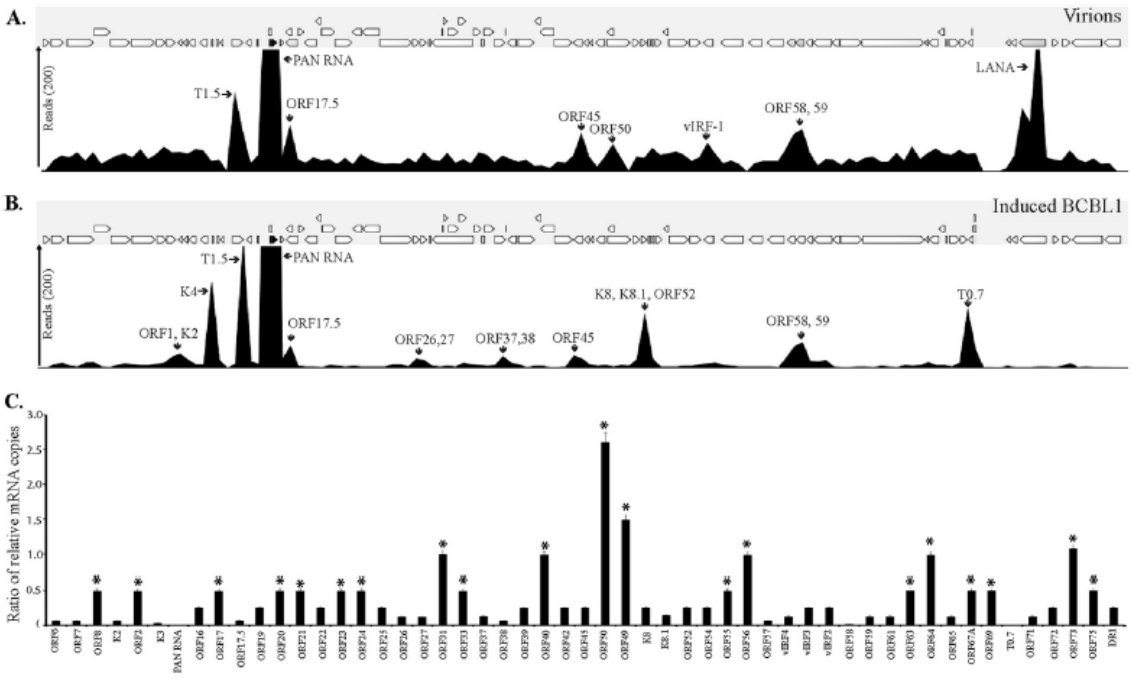


**FIG 7** RNA-seq and real-time qPCR validation of the KSHV virion transcriptome. (A) RNA-seq analysis of virions purified from induced TRExBCBL1-RTA. (B) RNA-seq analysis of induced TRExBCBL1-RTA. Arrows indicate the most abundantly expressed KSHV genes. (C) Specificity of RNA encapsidation by KSHV virion. Graphs show the ratio of virion-encapsidated mRNA to that in induced TRExBCBL1-RTA cells. The ratio was calculated by dividing the number of virion-packaged transcripts copies by the number of copies expressed during lytic reactivation.

virion assembly, we compared the abundance of viral transcripts in the virions with the amounts present during the lytic reactivation of the cells. An earlier study indicated that RNA encapsidation by the KSHV virion could be a specific event (27), and a recent report on KSHV virion miRNA also suggested that transcript encapsidation might be a specific process (26). To confirm this, we performed transcriptome (Fig. 7B) and real-time qPCR analyses of the viral genes in the cDNA extracted from induced BCBL1 cells for comparison with the transcripts present in the purified virions (Fig. 7A and B). Many of the transcripts present in the virions were expressed in abundance during lytic reactivation in the TRExBCBL1-RTA cells. To understand the specificity of RNA encapsidation in the virion, we calculated the ratio of virion transcripts to the transcript expression levels present during reactivation in the induced TRExBCBL1-RTA cells. Several of the transcripts, including PAN RNA, T0.7, DR1, ORF58, and ORF59, that were detected in high abundance in the virions were highly expressed during reactivation, and thus the ratios of encapsidated to mRNA transcripts in the induced cells were lower. We therefore concluded that they were packaged simply due to their abundance, not because of any specificity. However, some of the transcripts, including ORF73, ORF31, ORF40, ORF50, ORF56, ORF49, and ORF64, showed significantly higher ratios ($\geq$0.5) of virion transcripts in comparison to their abundance during reactivation, suggesting the involvement of a specific mechanism in their encapsidation. The viral genes with the ratio of virion packaged to the induced cells above 0.5 were considered significant and are marked by asterisks in Fig. 7C. Many of the virion-encapsidated latent- and lytic-specific transcripts that were detected early during *de novo* infection showed a significantly higher ratio; the ratio for the latent transcript ORF73 was 1.0843, whereas

the ratio for the lytic transcript ORF50 was 2.6103. Taken together, this suggests that KSHV may selectively encapsidate the latent and lytic transcripts required during early infection for priming the cells to successfully establish latency.

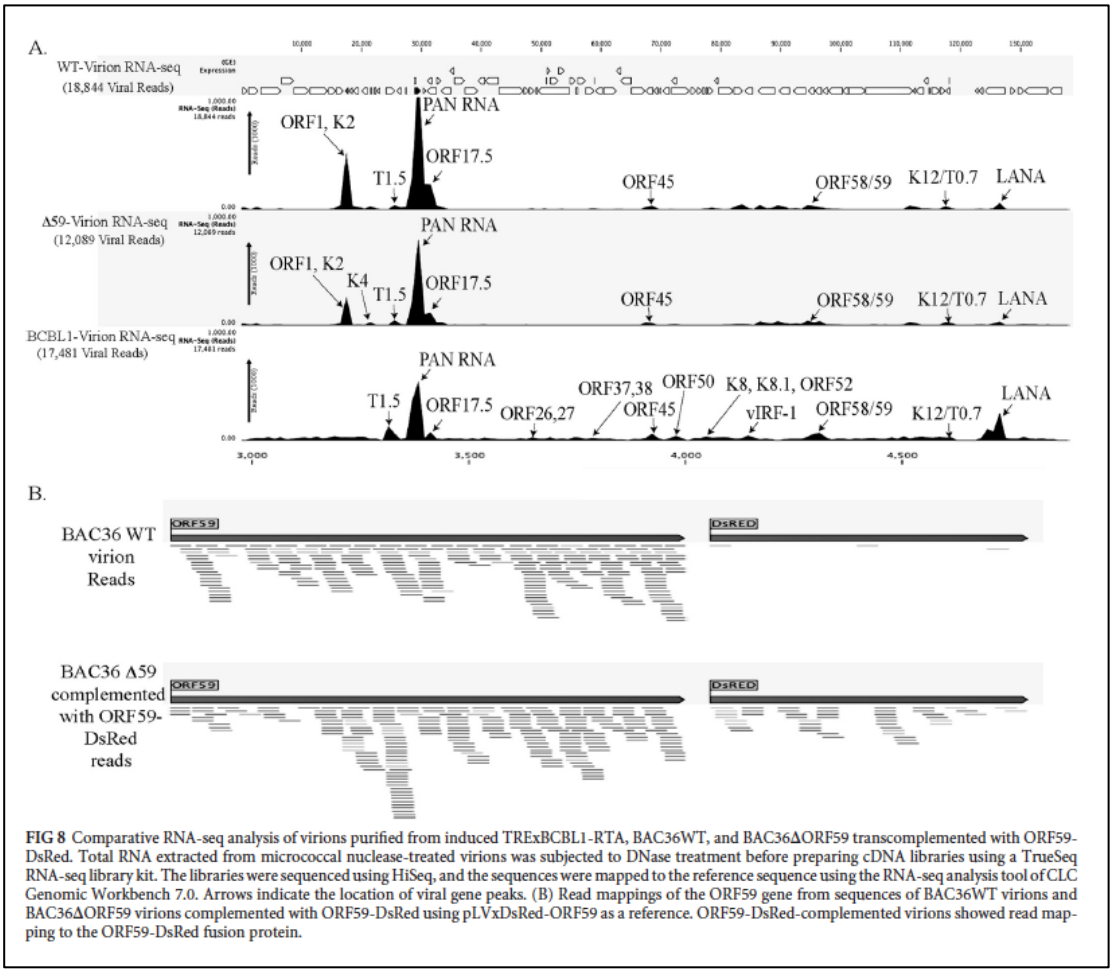


**FIG 8** Comparative RNA-seq analysis of virions purified from induced TRExBCBL1-RTA, BAC36WT, and BAC36ΔORF59 transcomplemented with ORF59-DsRed. Total RNA extracted from micrococcal nuclease-treated virions was subjected to DNase treatment before preparing cDNA libraries using a TrueSeq RNA-seq library kit. The libraries were sequenced using HiSeq, and the sequences were mapped to the reference sequence using the RNA-seq analysis tool of CLC Genomic Workbench 7.0. Arrows indicate the location of viral gene peaks. (B) Read mappings of the ORF59 gene from sequences of BAC36WT virions and BAC36ΔORF59 virions complemented with ORF59-DsRed using pLVxDsRed-ORF59 as a reference. ORF59-DsRed-complemented virions showed read mapping to the ORF59-DsRed fusion protein.

**Early ORF59 expression is required for KSHV *de novo* infection and genome amplification**

Our transcriptome data showed a high expression of ORF59 during the primary early infection of both B and endothelial cells, which led us to believe that ORF59 may be required during the early events of KSHV infection and latency establishment. To this end, we used a recombinant KSHV with a stop codon in the ORF59 gene

(BAC36ΔORF59) (46) for *de novo* infection. Knowing that the ORF59-deleted BAC36 cannot produce virion particles, we generated a 293L-cell line stably expressing the ORF59 gene fused with DsRed to complement the ORF59 in BAC36ΔORF59. These bacterial artificial chromosomes (BACs), WT in 293L and BAC36ΔORF59 in ORF59-DsRed-complemented 293L, were transfected and selected with hygromycin to obtain pure cell populations maintaining the BACs. These stable cells were induced with sodium butyrate (NaB) and tetradecanoyl phorbol acetate to produce virion particles, and the C-type virions were purified by sucrose density-gradient centrifugation for DNA extraction and the infection studies.

**TABLE 2** RPKM and gene reads of viral genes packaged in BAC36WT and ΔORF59-BAC36 virions

| | | BAC36WT virion | | BAC36Δ59 virion | | |
|---|---|---|---|---|---|---|
| No. | mRNA | RPKM | Gene reads | RPKM | Gene reads | Function |
| 1 | K1 | 4,106.397 | 65 | 3,545.13 | 36 | Glycoprotein |
| 2 | ORF11 | 9,104.682 | 210 | 5,136.19 | 76 | Viral lytic protein |
| 3 | K2 | 264,559.9 | 3,066 | 1800,100.6 | 1,339 | K2 (viral interleukin-6), regulates cellular proliferation |
| 4 | K3 | 13,800.78 | 252 | 1,621.957 | 19 | E3 ubiquitin ligases that reduce surface expression in infected cells |
| 5 | K4 | 14,151.28 | 76 | 17,124.46 | 59 | vMIP-II |
| 6 | T1.5 | 2,572.319 | 73 | 3,735.02 | 68 | |
| 7 | K5 | 9,016.62 | 131 | 4,291.56 | 40 | E3 ubiquitin ligase |
| 8 | K6 | 10,134.38 | 55 | 2,010.55 | 7 | vMIP-IA |
| 9 | PAN RNA | 456,221 | 9,259 | 554,384.1 | 7,218 | Late gene expression, lytic DNA replication, immune modulation |
| 10 | ORF16 | 5,125.818 | 51 | 2,506.66 | 16 | Bcl2 homolog |
| 11 | ORF17 | 61,895.31 | 1,872 | 40,406.45 | 784 | Protease |
| 12 | ORF18 | 12,752.6 | 186 | 13,786.64 | 129 | Late gene regulation |
| 13 | ORF45 | 5,332.74 | 123 | 4,798.29 | 71 | Virion-associated tegument protein regulating interferon function |
| 14 | ORF54 | 4,601.55 | 77 | 94.15 | 1 | dUTPase/immune modulation |
| 15 | ORF57 | 16,862.17 | 469 | 4,203.24 | 75 | Lytic replication protein homologous to EBV SM protein, mRNA splicing |
| 16 | vIRF-4 | 6,565.60 | 351 | 10,321.76 | 354 | Facilitates lytic replication by targeting cellular IRF4 and Myc gene |
| 17 | vIRF-3 | 8,888.84 | 301 | 11,738.21 | 255 | Immune modulation |
| 18 | vIRF-2 | 2,305.14 | 94 | 2,493.35 | 77 | Type I interferon signaling |
| 19 | ORF58 | 167,550.29 | 339 | 17,252.55 | 224 | |
| 20 | ORF59 | 9,980.75 | 224 | 14,863.18 | 214 | Processivity factor |
| 21 | ORF60 | 3,005.99 | 52 | 2,793.37 | 31 | Ribonucleoprotein reductase |
| 22 | ORF61 | 1,672.91 | 75 | 1,599.45 | 46 | Ribonucleoprotein reductase |
| 23 | ORF64 | 899.21 | 134 | 1,234.312 | 118 | Deubiquitinase |
| 24 | ORF65 | 8,585.93 | 83 | 8,384.85 | 52 | Capsid protein |
| 25 | ORF66 | 3,085.30 | 75 | 3,077.94 | 48 | Capsid protein |
| 26 | T0.7 | 10,097.21 | 125 | 18,224.4 | 154 | |
| 27 | ORF73 | 2,081.99 | 133 | 1,445.63 | 68 | Latency-associated nuclear antigen |
| 28 | ORF50 | 192.39 | 11 | 545.28 | 20 | Replication and transcription activator |

To determine the composition of the KSHV virion-encapsidated RNA in BAC36WT and BAC36ΔORF59, we performed an RNA-seq analysis on the virions from these two cell lines. Unsurprisingly, the patterns of the viral mRNA transcripts were similar (Fig. 8A and Table 2). We also compared the virion mRNA patterns from the

BACs with those of the TRExBCBL1-RTA virions, which showed a slightly different packaging of the viral mRNA, but similar levels of PAN RNA (Fig. 8A). Interestingly, the virions produced in the 293L cells complemented with ORF59-DsRed and containing BAC36ΔORF59 also encapsidated ORF59, which was confirmed by mapping the sequence reads with ORF59-DsRed (Fig. 8B). The sequence reads from BAC36WT mapped only to the ORF59 regions, confirming that BAC36WT packaged the parental ORF59 gene (Fig. 8B), as expected. Interestingly, the total number of virions produced by BAC36ΔORF59 was three logs lower than that produced by BAC36WT (Fig. 9B), even with the ORF59-DsRed complementation, which is reflected in the C-type band intensity in the BAC36ΔORF59 tube (Fig. 9A).

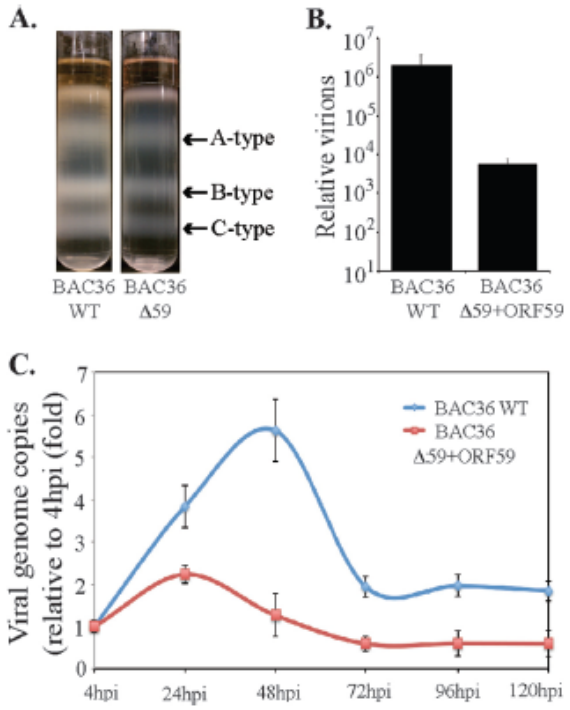


**FIG 9** *De novo* infection of PBMCs with BAC36WT and BAC36ΔORF59 virions. (A) Virions were purified from culture supernatant of approximately $9 \times 10^8$ reactivated 293L cells harboring either BAC36WT or BAC36ΔORF59 on a 20 to 50% sucrose gradient. The three white bands as indicated represent A-type (empty), B-type (intermediate), and C-type (mature) KSHV virus particles, respectively. (B) Supernatants from 293L cells containing BAC36WT or BAC36ΔORF59 were used for real-time qPCR quantification of viral genome copies using ORF73-specific primers along with ORF73 plasmid standards. (C) Human PBMCs were infected with KSHV isolated from reactivated 293L cells containing BAC36WT or BAC36ΔORF59, with a multiplicity of infection (MOI) of 10. *De novo*-infected PBMCs were harvested at 4 h, 24 h, 48 h, 72 h, 96 h, and 120 h postinfection, followed by extraction of total DNA using a modified Hirt lysis method. This DNA was used for analyzing the genome copy number by real-time qPCR using ORF73-specific primers and ORF73 plasmid as a standard.

We normalized the number of virions used for the infection of human PBMCs by extracting the virion DNA and quantifying it in a real-time qPCR assay. Cells were

collected at 4, 24, 48, 72, 96, and 120 hpi and analyzed for viral gene expression and the number of KSHV genome copies during early infection. Our results showed that both BAC36WT and BAC36ΔORF59 trans-complemented with ORF59-DsRed produced infectious virions and infected PBMCs (Fig. 9C). However, the KSHV genome copy analysis of the PBMCs infected with the trans-complemented BAC36ΔORF59 showed a reduced number of KSHV genome copies in comparison to BAC36WT (Fig. 9C). This suggested that the lytic-cycle gene ORF59 is required for amplifying the viral genome during primary infection, probably by allowing DNA replication through lytic origins.

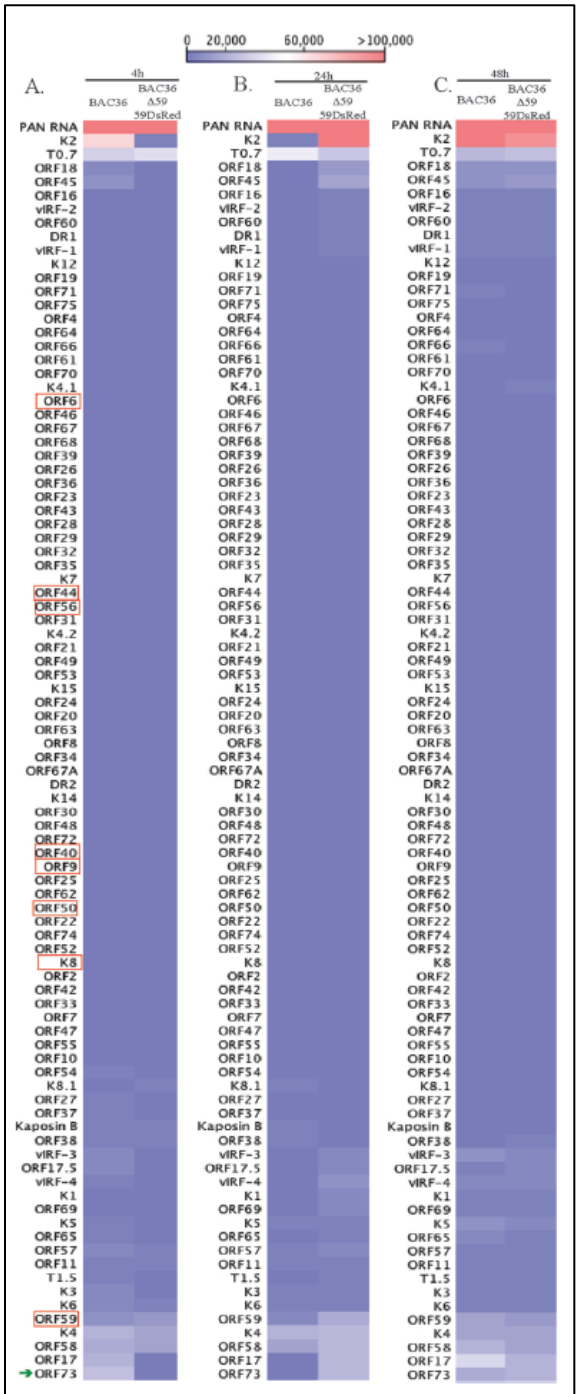


**FIG 10** Expression profiles of viral genes in BAC36WT and BAC36ΔORF59 at different times postinfection. Normalized expression (RPKM values) of viral genes in BAC36WT and BAC36ΔORF59 at different times postinfection was used for generating hierarchal clustering. (A) Relative expression of KSHV

The total RNA extracted from the *de novo*-infected PBMCs at different time points (4, 24, and 48 hpi) were used for a transcriptome analysis to determine whether there were differences in the viral gene expression profiles in the ORF59-deleted virus. The expression profiles of the viral genes were determined based on RPKM

values and compared with the wild-type virus at each of the time points. The heat map generated based on the RPKM values showed subtle differences in the viral gene expression profiles (Fig. 10). The genes required for lytic-DNA replication (ORF9, ORF6, ORF40/41, ORF44, ORF56, ORF50, and K8), encircled by red boxes showed almost no difference in their expression profiles (Fig. 10). ORF59 showed a gradual decrease in virion-released ORF59 transcripts for the ORF59-deleted virus. However, BAC36WT showed a slight increase in the number of ORF59 transcripts. The PAN RNA levels were comparable in the wild type and ORF59-deleted viruses at the time points analyzed. The K2 and ORF17 expression was distinctly different in the ORF59-deleted virus, being expressed earlier than in the PBMCs with the BAC36WT virus (Fig. 10). Interestingly, the ORF59-deleted virus showed a higher expression of the ORF73 gene (LANA) at earlier time points than did BAC36WT, suggesting an early onset of latency in the virus lacking ORF59. Overall, these data suggest that ORF59 is required for replicating the DNA and amplifying the viral genome during primary infection of human PBMCs.

**Discussion:**

KSHV infection is a complex multi-step process involving the regulation of various cellular pathways. KSHV infects a variety of cellular targets and establishes a latent infection, generally by 24 hpi (14, 16-20). To understand the differential expression of viral transcripts early during infection, PBMCs, CD14+, and TIVE cells were *de novo* infected with KSHV for different lengths of time (0, 4, 24, 48, 72, and 120 h). The transcriptome and real-time qPCR analyses on the *de novo*-infected PBMCs revealed that several lytic- and latent-specific mRNAs were concurrently expressed very early on

following the *de novo* infections. Previous reports have shown that immediately after *de novo* infection with herpesviruses such as EBV and herpes simplex virus, the virus undergoes a short lytic DNA replication phase (37, 38). Our data also showed the presence of the lytic DNA replication-associated transcripts, suggesting the activation of a lytic cycle. Many of the lytic-cycle replication-associated transcripts were detected as early as 4 hpi, including ORF59 (processivity factor), ORF9 (DNA polymerase), ORF6 (single-stranded DNA binding protein), ORF56 (DNA replication protein), ORF40 (primase associated factor), ORF54 (dUTPase), ORFs 60 and 61 (Ribonucleoprotein reductase), ORF70 (thymidylate synthase), ORF37 (alkaline exonuclease). In addition, the ORF50, ORF2, K3, PAN RNA, ORF26, ORF29, ORF37, ORF55, ORF60 ORF63, ORF73 and ORF74 transcripts were found to be actively transcribing at 4 hpi detected by capturing the nascent RNA and the actinomycin D treatment.

Apart from these lytic transcripts, the expression of several other transcripts encoding structural proteins such as K8.1 (glycoprotein), and ORFs 65 (tegument protein) were also detected early during infection. Moreover, many of the noncoding RNAs, including PAN RNA, T0.7, and T1.5 (OriLyt transcript), were also expressed during early infection. PAN RNA has been shown to modulate viral and cellular transcription as well as activate KSHV lytic cycle by interacting with the ORF50 promoter and viral genome (47, 48). Furthermore, there were a large number of viral transcripts, whose expression did not increase from their levels at 4 hpi suggesting that those were transduced with the virions.

The detection of PAN RNA in the virion and during infection suggests that PAN RNA could be playing major role in triggering lytic cycle cascade. The KSHV ORF50-

encoded immediate-early protein RTA is known to activate the cascade of lytic genes for facilitating the lytic replication process (39-43). Studies on the primary infection of B cells by EBV showed an accumulation of lytic transcripts during infection, indicating the requirement of a short lytic replication prior to the establishment of latency (21, 23). Earlier studies have shown that the KSHV virion also contains several KSHV lytic proteins, including ORF50, ORF8, ORF25, ORF26, K12, ORF62, ORF63, and ORF75, that are brought into the target cells during *de novo* infection (24). The ORF50 protein accompanying the virion may also be important for orchestrating the activation of RTA-responsive genes early on during infection to induce a short lytic cycle. A significant amount of the concurrent expression of ORF50 and the KSHV latent protein, ORF73 was detected as early as 4 hpi. Similar observations were reported in a previous study based on microarray and real-time qPCR analyses, but the possibility of lytic DNA replication was not proposed due to the lack of detecting all of the proteins required for lytic-DNA replication (9).

A recent study on histone modifications of the KSHV genome during *de novo* infection demonstrated that there is a distinct pattern of activating the histone H3K4me3 mark across the KSHV genome, which is gradually replaced by the repressive H3K27me3 mark by the LANA-mediated displacement of soluble sp100 (49). Additionally, in comparison to the repressive H3K27me3 mark and the rest of the genome, a LANA ChIP-seq analysis of TRExBCBL1-RTA and TIVE-LTC showed a clear association of H3K4me3 mark and RNA pol II activation on the latent gene promoters (50). Our results showed that immediately after the *de novo* infection of PBMCs, the viral genome increased exponentially up to 48 hpi, followed by a slight

decrease at 72 hpi. The accumulation of ORF50 and other RTA-regulated lytic-cycle genes during early infection is suggestive of the involvement of lytic-DNA replication for genome amplification. Treating the cells with a late gene expression inhibitor, PAA showed significantly reduced viral genome copies further substantiated the involvement of lytic DNA replication for genome copies amplification in human PBMCs.

Discriminating whether the transcripts detected at 4 hpi were due to the virion-transduced mRNA or active transcription, RNA-seq analysis of the newly synthesized transcripts at 4 hpi of human PBMCs showed transcription of only a limited number of genes during primary infection. However, a large number of viral transcripts are detected at 4 hpi as well as in the virions particles, which confirms that those transcripts are introduced into the infected cells along with the virions. Detection of actively synthesizing mRNA in KSHV infected PBMCs at 24 hpi showed transcription of primarily the ORF73 gene, which confirmed that the viral genome gets chromatinized and epigenetically modified for restricted gene expression by 24 hpi. An earlier study reported the viral gene transcription of ORF59 during primary infection (27), and here we provide a comprehensive list of the genes transcribed during a *de novo* infection. The transcription of the viral genes as early as 4 hpi suggests that the viral DNAs entering the targets cells are capable of transcribing genes before the assembly of the epigenetic histone marks. Not surprisingly, the latent protein ORF73 gene showed active transcription at 4 hpi, suggesting that LANA begins transcription as early as 4 hpi and accumulates over time to help establish latency. The immediate-early protein ORF50 undergoes a moderate level of transcription immediately after infection, which may contribute in triggering the transcription of the lytic cascade to complete the DNA

replication. The KSHV virions have also been shown to encapsidate a small quantity of the RTA protein, which may also be important in triggering the lytic-gene expression cascade (24, 27).

It has been shown that both KSHV and EBV encapsidate biologically functional virion transcripts that are transported into the target cells during *de novo* infections (22, 26, 27). A previous study using a DNA microarray and real-time qPCR identified 11 of the virus transcripts packaged into the virion (27). In this study, using RNA-seq and transcriptome analyses, we detected additional KSHV latent- and lytic-cycle transcripts encapsidated in the virions that were also transported into the targets cells. This data was validated by a real-time qPCR analysis using KSHV gene-specific primer arrays, which showed consistent results. The transcriptome analysis identified a variety of virion transcripts in high abundance, including PAN RNA, K7, K14, K12, ORF 58/59, and the recently identified T1.5 and T0.7. Additionally, many lytic-specific mRNAs (ORF50, ORF8, ORF9, ORF21, ORF22, ORF31, ORF 40/41, ORF45, ORF54, ORF55, ORF 69, and ORF75) were present in the virion in moderate amounts. A number of immediate-early and early KSHV-unique K genes (K7, K8, K3, K5, K9, and late K8.1) were also detected in the virion, in addition to a significant amount of latent-specific mRNAs (ORF73, ORF72, and K2).

The mechanism of RNA encapsidation by KSHV is currently unknown. Reports show that, similarly to the herpes simplex virus, the RNA packaging and encapsidation by KSHV could be a specific event (26, 27). In addition, the specific encapsidation of miRNA by the KSHV virion has recently been demonstrated (26). However, both the previous study and this study determined that the majority of mRNAs detected in the

KSHV virions were present at very high levels during lytic reactivation (9, 27). This suggests that these transcripts might have been randomly packaged into the virions simply due to their higher abundance. Nonetheless, the qPCR analysis to determine the specificity of the virion versus the reactivated TRExBCBL1-RTA showed that the ORF31, ORF40, ORF50, ORF56, ORF49, ORF64, and ORF73 transcripts had significantly higher proportions of encapsidated mRNA than did the PAN RNA, ORF58, ORF59, T0.7, and DR1 transcripts, suggesting a specific packaging mechanism for those transcripts.

Several of these highly expressed KSHV lytic genes have been shown to have regulatory roles in immune modulation, anti-apoptosis, and lytic DNA replication, indicating that their expression may be priming the host cell for retaining the incoming viral DNA during the initial infection. This is evident from the *de novo* infection of PBMCs with virions produced from the BAC36ΔORF59 virus. Although significantly fewer virions were produced from BAC36ΔORF59 than from BAC36WT, a similar number of virions were used to compare the viral genome copy numbers and expression profiles. The lower number of virion copies in BAC36ΔORF59 complemented with ORF59-DsRed may have been due to a comparably lower expression of ORF59 in those cells. The transcriptome analysis of the *de novo*-infected PBMCs showed the differential expression of only a few latent- and lytic-specific genes (PAN RNA, T0.7, K2, K4, ORF17, ORF18, ORF58, ORF45, and ORF73), confirming that the incoming DNA is transcription competent.

The virions from both the BAC36WT and ORF59-complemented cells showed the packaging of ORF59 transcripts. However, the BAC36ΔORF59 virus genome in *de*

*novo*-infected PBMCs failed to show an appreciable increase of copy number in comparison to BAC36WT. This indicates that the extended expression of ORF59 during early infection is probably required for synthesizing viral DNA through lytic DNA replication to increase the copy number. The exact mechanism requiring the initial transient accumulation of lytic-specific transcripts for the establishment of latency currently remains elusive. To fully understand the early events of KSHV infection:- latency establishment and genome amplification, further experiments identifying the viral proteins expressed and the mechanism of viral DNA replication during primary infection in various cells are currently ongoing.

**Acknowledgments:**

We thank Prof. Erle S. Robertson at the University of Pennsylvania for providing the cell lines and LANA expression plasmids. This work was supported by public health grants from the NIH (CA174459 and AI105000) to SCV. STT was supported by Mick Hitchcock Fellowship at the University of Nevada, Reno.

**References:**

1. **Chang PSMaY.** 2010. Why do viruses cause cancer? Highlights of the first century of human tumour virology. Nature Reviews Cancer **10:**878-889.
2. **Moore PS, Chang Y.** 2003. Kaposi's sarcoma-associated herpesvirus immunoevasion and tumorigenesis: two sides of the same coin? Annu Rev Microbiol **57:**609-639.
3. **Verma SC, Robertson ES.** 2003. Molecular biology and pathogenesis of Kaposi sarcoma-associated herpesvirus. FEMS Microbiol Lett **222:**155-163.
4. **Fakhari FD, Dittmer DP.** 2002. Charting latency transcripts in Kaposi's sarcoma-associated herpesvirus by whole-genome real-time quantitative PCR. J Virol **76:**6213-6223.
5. **Jenner RG, Alba MM, Boshoff C, Kellam P.** 2001. Kaposi's sarcoma-associated herpesvirus latent and lytic gene expression as revealed by DNA arrays. J Virol **75:**891-902.

6. **Verma SC, Lan K, Robertson E.** 2007. Structure and function of latency-associated nuclear antigen. Curr Top Microbiol Immunol **312:**101-136.
7. **Zhong W, Wang H, Herndier B, Ganem D.** 1996. Restricted expression of Kaposi sarcoma-associated herpesvirus (human herpesvirus 8) genes in Kaposi sarcoma. Proc Natl Acad Sci U S A **93:**6641-6646.
8. **Ballestas ME, Chatis PA, Kaye KM.** 1999. Efficient persistence of extrachromosomal KSHV DNA mediated by latency-associated nuclear antigen. Science **284:**641-644.
9. **Krishnan HH, Naranatt PP, Smith MS, Zeng L, Bloomer C, Chandran B.** 2004. Concurrent expression of latent and a limited number of lytic genes with immune modulation and antiapoptotic function by Kaposi's sarcoma-associated herpesvirus early during infection of primary endothelial and fibroblast cells and subsequent decline of lytic gene expression. J Virol **78:**3601-3620.
10. **Cannon JS, Ciufo D, Hawkins AL, Griffin CA, Borowitz MJ, Hayward GS, Ambinder RF.** 2000. A new primary effusion lymphoma-derived cell line yields a highly infectious Kaposi's sarcoma herpesvirus-containing supernatant. J Virol **74:**10187-10193.
11. **Grundhoff A, Ganem D.** 2004. Inefficient establishment of KSHV latency suggests an additional role for continued lytic replication in Kaposi sarcoma pathogenesis. J Clin Invest **113:**124-136.
12. **Renne R, Zhong W, Herndier B, McGrath M, Abbey N, Kedes D, Ganem D.** 1996. Lytic growth of Kaposi's sarcoma-associated herpesvirus (human herpesvirus 8) in culture. Nat Med **2:**342-346.
13. **Wang CY, Sugden B.** 2004. New viruses shake old paradigms. J Clin Invest **113:**21-23.
14. **Chandran B.** 2010. Early events in Kaposi's sarcoma-associated herpesvirus infection of target cells. J Virol **84:**2188-2199.
15. **Chakraborty S, Veettil MV, Chandran B.** 2012. Kaposi's Sarcoma Associated Herpesvirus Entry into Target Cells. Frontiers in microbiology **3:**6.
16. **Akula SM, Naranatt PP, Walia NS, Wang FZ, Fegley B, Chandran B.** 2003. Kaposi's sarcoma-associated herpesvirus (human herpesvirus 8) infection of human fibroblast cells occurs through endocytosis. J Virol **77:**7978-7990.
17. **Akula SM, Pramod NP, Wang FZ, Chandran B.** 2002. Integrin alpha3beta1 (CD 49c/29) is a cellular receptor for Kaposi's sarcoma-associated herpesvirus (KSHV/HHV-8) entry into the target cells. Cell **108:**407-419.
18. **Bechtel JT, Liang Y, Hvidding J, Ganem D.** 2003. Host range of Kaposi's sarcoma-associated herpesvirus in cultured cells. J Virol **77:**6474-6481.
19. **Lagunoff M, Bechtel J, Venetsanakos E, Roy AM, Abbey N, Herndier B, McMahon M, Ganem D.** 2002. De novo infection and serial transmission of Kaposi's sarcoma-associated herpesvirus in cultured endothelial cells. J Virol **76:**2440-2448.
20. **Chakraborty S, Veettil MV, Bottero V, Chandran B.** 2012. Kaposi's sarcoma-associated herpesvirus interacts with EphrinA2 receptor to amplify signaling essential for productive infection. Proceedings of the National Academy of Sciences of the United States of America **109:**E1163-1172.

21. **Halder S MM, Verma SC, Kumar P, Yi F, Robertson ES.** 2009. Early events associated with infection of Epstein-Barr virus infection of primary B-cells. PloS one **4**.
22. **Jochum S RR, Moosmann A, Hammerschmidt W, Zeidler R.** 2012. RNAs in Epstein-Barr virions control early steps of infection. Proceedings of the National Academy of Sciences of the United States of America **109:**1396-1404.
23. **Wangrong Wen DI, Koji Yamamoto, Seiji Maruo, Teru Kanda, and Kenzo Takada.** 2007. Epstein-Barr Virus BZLF1 Gene, a Switch from Latency to Lytic Infection, Is Expressed as an Immediate-Early Gene after Primary Infection of B Lymphocytes. Journal of virology **81**.
24. **Bechtel JT, Winant RC, Ganem D.** 2005. Host and viral proteins in the virion of Kaposi's sarcoma-associated herpesvirus. J Virol **79:**4952-4964.
25. **Zhu FX, Chong JM, Wu L, Yuan Y.** 2005. Virion proteins of Kaposi's sarcoma-associated herpesvirus. J Virol **79:**800-811.
26. **Lin X, Li X, Liang D, Lan K.** 2012. MicroRNAs and unusual small RNAs discovered in Kaposi's sarcoma-associated herpesvirus virions. Journal of virology **86:**12717-12730.
27. **Bechtel J, Grundhoff A, Ganem D.** 2005. RNAs in the virion of Kaposi's sarcoma-associated herpesvirus. J Virol **79:**10138-10146.
28. **Toth Z, Brulois K, Lee HR, Izumiya Y, Tepper C, Kung HJ, Jung JU.** 2013. Biphasic euchromatin-to-heterochromatin transition on the KSHV genome following de novo infection. PLoS pathogens **9:**e1003813.
29. **Verma SC, Bajaj BG, Cai Q, Si H, Seelhammer T, Robertson ES.** 2006. Latency-associated nuclear antigen of Kaposi's sarcoma-associated herpesvirus recruits uracil DNA glycosylase 2 at the terminal repeats and is important for latent persistence of the virus. J Virol **80:**11178-11190.
30. **Verma SC, Choudhuri T, Kaul R, Robertson ES.** 2006. Latency-associated nuclear antigen (LANA) of Kaposi's sarcoma-associated herpesvirus interacts with origin recognition complexes at the LANA binding sequence within the terminal repeats. J Virol **80:**2243-2256.
31. **Hirt B.** 1967. Selective extraction of polyoma DNA from infected mouse cell cultures. . J. Mol. Biol. **26:**365-369.
32. **Lallemand F, Desire N, Rozenbaum W, Nicolas JC, Marechal V.** 2000. Quantitative analysis of human herpesvirus 8 viral load using a real-time PCR assay. J Clin Microbiol **38:**1404-1408.
33. **Bates I, Bedu-Addo G, Jarrett RF, Schulz T, Wallace S, Armstrong A, Sheldon J, Rutherford T.** 2001. B-lymphotropic viruses in a novel tropical splenic lymphoma. Br J Haematol **112:**161-166.
34. **Medveczky MM, Horvath E, Lund T, Medveczky PG.** 1997. In vitro antiviral drug sensitivity of the Kaposi's sarcoma-associated herpesvirus. AIDS **11:**1327-1332.
35. **Chang PJ, Boonsiri J, Wang SS, Chen LY, Miller G.** 2010. Binding of RBP-Jkappa (CSL) protein to the promoter of the Kaposi's sarcoma-associated herpesvirus ORF47 (gL) gene is a critical but not sufficient determinant of transactivation by ORF50 protein. Virology **398:**38-48.

36. **Nealon K, Newcomb WW, Pray TR, Craik CS, Brown JC, Kedes DH.** 2001. Lytic replication of Kaposi's sarcoma-associated herpesvirus results in the formation of multiple capsid species: isolation and molecular characterization of A, B, and C capsids from a gammaherpesvirus. J Virol **75:**2866-2878.
37. **Sabyasachi Halder MM, Subhash C. Verma, Pankaj Kumar, Fuming Yi, Erle S. Robertson.** 2009. Early Events Associated with Infection of Epstein-Barr Virus Infection of Primary B-Cells. PloS one **4**.
38. **Roizman BaDMK.** 2001. Herpes Simplex Viruses and Their Replication. Chapter 72. In: Fields Virology, Fourth Edition, D.M. Knipe, P.M. Howley et al., eds., **Lippincott, Williams & Wilkins, Philadelphia, PA. :**pp. 2399-2459.
39. **Guito J, Lukac DM.** 2012. KSHV Rta Promoter Specification and Viral Reactivation. Frontiers in microbiology **3:**30.
40. **Dourmishev LA, Dourmishev AL, Palmeri D, Schwartz RA, Lukac DM.** 2003. Molecular genetics of Kaposi's sarcoma-associated herpesvirus (human herpesvirus-8) epidemiology and pathogenesis. Microbiol Mol Biol Rev **67:**175-212, table of contents.
41. **Sun R, Lin SF, Staskus K, Gradoville L, Grogan E, Haase A, Miller G.** 1999. Kinetics of Kaposi's sarcoma-associated herpesvirus gene expression. J Virol **73:**2232-2242.
42. **West JT, Wood C.** 2003. The role of Kaposi's sarcoma-associated herpesvirus/human herpesvirus-8 regulator of transcription activation (RTA) in control of gene expression. Oncogene **22:**5150-5163.
43. **Nakamura H, Lu M, Gwack Y, Souvlis J, Zeichner SL, Jung JU.** 2003. Global changes in Kaposi's sarcoma-associated virus gene expression patterns following expression of a tetracycline-inducible Rta transactivator. J Virol **77:**4205-4220.
44. **Chan SR, Bloomer C, Chandran B.** 1998. Identification and characterization of human herpesvirus-8 lytic cycle-associated ORF 59 protein and the encoding cDNA by monoclonal antibody. Virology **240:**118-126.
45. **Unal A, Pray TR, Lagunoff M, Pennington MW, Ganem D, Craik CS.** 1997. The protease and the assembly protein of Kaposi's sarcoma-associated herpesvirus (human herpesvirus 8). J Virol **71:**7030-7038.
46. **McDowell ME, Purushothaman P, Rossetto CC, Pari GS, Verma SC.** 2013. Phosphorylation of Kaposi's sarcoma-associated herpesvirus processivity factor ORF59 by a viral kinase modulates its ability to associate with RTA and oriLyt. J Virol **87:**8038-8052.
47. **Rossetto CC, Pari G.** 2012. KSHV PAN RNA associates with demethylases UTX and JMJD3 to activate lytic replication through a physical interaction with the virus genome. PLoS pathogens **8:**e1002680.
48. **Rossetto CC, Pari GS.** 2011. Kaposi's sarcoma-associated herpesvirus noncoding polyadenylated nuclear RNA interacts with virus- and host cell-encoded proteins and suppresses expression of genes involved in immune modulation. J Virol **85:**13290-13297.
49. **Gunther T, Schreiner S, Dobner T, Tessmer U, Grundhoff A.** 2014. Influence of ND10 components on epigenetic determinants of early KSHV latency establishment. PLoS pathogens **10:**e1004274.

50. **Hu J, Yang Y, Turner PC, Jain V, McIntyre LM, Renne R.** 2014. LANA binds to multiple active viral and cellular promoters and associates with the H3K4methyltransferase hSET1 complex. PLoS Pathog **10:**e1004240.

# Kaposi's Sarocma-Associated Herpesvirus Latency-Associated Nuclear Antigen Inhibits Major Histocompatibility Complex Class II Expression by Disrupting Enhanceosome Assembly through binding with the Regulatory Factor X Complex

Journal of Virology, 2015 March 4. Pii JVI.03713-14

PMID: 25740990

**Abstract:**

Major histocompatibility class II (MHC II) molecules play central role in adaptive antiviral immunity by presenting viral peptides to the CD4+ T cells. Due to their key role in adaptive immunity, many viruses including Kaposi's sarcoma associated herpesvirus (KSHV) have evolved multiple strategies to inhibit MHC II antigen presentation pathway. Expression of MHC II, which is mainly controlled at the levels of transcription, is strictly dependent upon the binding of class II transactivator (CIITA) to the highly conserved promoters of all MHC II genes. Recruitment of CIITA to MHC II promoters requires its direct interactions with pre-assembled MHC II enhanceosome consisting of cyclic AMP response element-binding protein (CREB), nuclear factor Y complex (NF-Y) and regulatory factor X complex (RFX) proteins. Here, we show that KSHV encoded latency associated nuclear antigen (LANA) disrupts the association of CIITA to MHC II enhanceosome by binding to the components of RFX complex. Our data show that LANA is capable of binding with all the three components of RFX complex: RFXAP, RFX5 and RFXANK *in vivo*, however, more strongly with the RFXAP component in an *in vitro* binding assay. Levels of MHC II proteins were significantly reduced in KSHV infected as well as LANA expressing B-cells. Additionally, an expression of LANA in luciferase promoter reporter assay showed reduced HLA-DRA promoter activity in a dose dependent manner. Chromatin immunoprecipitation assay showed LANA binding to MHC II promoter along with RFX proteins and an over expression of LANA disrupted the association of CIITA to the MHC II promoter. These assays conclude that the interaction of LANA with RFX proteins interferes the recruitment of CIITA to MHC II promoters, resulting into an inhibition of MHC II genes expression. Thus, the data

presented here identifies a novel mechanism used by KSHV to downregulate the expressions of MHC II genes.

**Importance:**

Kaposi's sarcoma associated herpesvirus is the causative agent of multiple human malignancies. It establishes a life-long latent infection and persists in the infected cells without being detected by the host's immune surveillance system. Only a limited number of viral proteins are expressed during latency and these proteins play a significant role in suppressing both the innate and adaptive immunities of the host. Latency Associated Nuclear Antigen (LANA) is one of the major proteins expressed during latent infection. Here, we show that LANA blocks MHC II gene expression to subvert host immune system by disrupting the MHC II enhanceosome through binding with RFX transcription factors. Therefore, this study identifies a novel mechanism utilized by KSHV LANA to deregulate MHC II gene expression, which is critical for CD4+ T cell response in order to escape the host immune surveillance.

**Introduction:**

Kaposi's sarcoma associated herpes virus (KSHV) is an oncogenic γ-herpesvirus that causes several malignancies such as Kaposi's sarcoma (KS), Primary Effusion Lymphomas (PELs) and Multicentric Castleman's Disease (MCD) in immunocompromised individuals (1, 2). The life cycle of KSHV consists of a predominant latent phase marked by restricted gene expression and a transient lytic replication phase characterized by the production of functional virions. KSHV maintains a life long persistent infection in susceptible hosts after primary infection (3, 4). One of the main factors contributing to a successful life-long persistence of KSHV is its

astounding ability to hide from the surveillance of host immunity. During the course of evolution, KSHV has evolved multiple mechanisms to evade and modulate nearly all aspects of both the innate and adaptive immunities of the infected hosts (5-7).

Latency associated nuclear antigen (LANA or LANA-1) is the most abundantly expressed proteins in all the KSHV infected cells (8-10). LANA is a large multifunctional protein that plays diverse roles in maintaining successful KSHV latency such as maintenance of viral episomes, transcriptional regulation of many viral and cellular genes and the progression of cell cycle (1, 11, 12). Since latency is the immunologically silent stage of KSHV life cycle and LANA is the major latent protein, it is speculated to play active roles in the modulation of host immune response. Indeed, LANA has been shown to inhibit many aspects of host's innate and adaptive immune pathways including interference with neutrophil recruitment and TNF-α signaling (13), interference with interferon signaling (14) and inhibition of MHC I peptide presentation (15, 16). Recently, LANA was also shown to inhibit MHC II antigen presentation pathway by inhibiting the transcription of class II trans activator (CIITA) (17).

Effectiveness of adaptive immunity, which is a critical arm of the antiviral host defense, relies primarily on the activation of CD4+ T cells. Activation of CD4+ T cells seems to be particularly important for anti-KSHV immunity (18, 19). Major histocompatibility class II (MHC II) molecules play a central role in the activation of CD4+ T cells by presenting antigenic peptides to these cells (20, 21). Since peptide presentation in conjunction with MHC II molecules is indispensable for the activation of CD4+ T cells, down-regulation of MHC II molecules is a frequently employed strategy by many viruses (22). Reports published in the past couple of years established that

KSHV has the ability to downregulate MHC II molecules (17, 23-25). Since KSHV's ability to persist in the infected hosts critically depends on being invisible to CD4+ T cells, KSHV most likely uses multiple simultaneous strategies for efficient blocking of MHC II antigen presentation pathway.

MHC II molecules are highly polymorphic cell surface glycoproteins consisting of an alpha and a beta chain that are constitutively expressed in professional antigen presenting cells (26, 27). In humans, there are three "classical" isotypes, HLA-DR, HLA-DP and HLA-DQ that are present on cell surface. MHC II gene family also includes "non-classical" cytoplasmic molecules HLA-DM and HLA-DO, and the invariant chain (Ii) involved in peptide loading. Expressions of all the members of MHC II gene family are highly coordinated and predominantly regulated at the levels of transcription (28-30). Promoters of all MHC II genes contain a highly conserved *cis*-acting DNA sequences consisting of S-X-X2-Y boxes, which is bound by various nuclear proteins. These proteins include regulatory factor X (RFX), nuclear factor Y (NF-Y) and cAMP response element binding (CREB) (29, 31). RFX complex is a hetero-trimeric complex composed of RFX5, RFXAP and RFXANK, which binds to the S and X boxes and the Nuclear Factor Y (NF-Y) and CREB binds to the Y and X2 boxes, respectively (32-39). Coordinated binding of these protein complexes to the conserved sequences of MHC II promoter makes a functional MHC II enhanceosome (reviewed in (22, 40). Among these proteins, RFX complex is the core DNA binding component of the MHC II enhanceosome. It facilitates the assembly of other enhanceosome proteins onto the MHC II promoters (30, 41-43). All three components of the RFX complex are indispensible for constitutive and induced expression of MHC II genes. Once assembled on MHC II

promoters, the enhanceosome complex recruits a transcriptional co-activator, CIITA (class II transactivator), a master regulator of MHC II expression. All the components of MHC II enhanceosome except CIITA are constitutively expressed in almost every cell types in humans (44). However, the expression of CIITA is constitutive only in antigen presenting cells but can be induced in most other cell types in response to IFN-γ (44). Binding of CIITA to the MHC II promoters is absolutely critical for the transcription of MHC II genes. However, CIITA does not possess any DNA binding domain to bind directly to MHC II promoter. Instead, it is recruited through the proteins of enhanceosome complex especially through direct association with RFX5. Once bound to MHC II enhanceosome, CIITA orchestrates transcription of MHC II genes by recruiting the remaining transcriptional machinery to the promoters (40, 45-47).

So far, two KHSV latent proteins, vIRF3 and LANA have been reported to down-regulate MHC II antigen presentation pathway (17, 18, 23, 25). The report by *Cai et al* demonstrated that LANA down-regulates MHC II through an inhibition of CIITA transcription by suppressing pIII and PIV promoter activities (17). In this study, we identified an additional mechanism used by KSHV LANA to inhibit the expression of MHC II genes. We show that LANA interferes with the assembly of functional MHC II enhanceosome by reducing the binding of CIITA to the HLA-DRA promoter. The immunoprecipitation (IP) experiments showed that LANA binds with all the three components of RFX complex *in vivo* but preferentially binds to RFXAP in the *in vitro* assays. Similarly, chromatin immunoprecipitation (ChIP) assays determined that LANA associates with the chromatin of HLA-DRA promoter. Electrophoretic mobility shift assays further supported that LANA associates with HLA-DRA promoter through its

interactions with the components of RFX complex. Additionally, expression of LANA reduced the activity of HLA-DRA core promoter in a dose dependent manner even when CIITA was expressed through a constitutive CMV promoter confirming that the presence of LANA prevents the binding of CIITA to HLA-DRA promoter. Disruption of CIITA binding to enhanceosome was further supported by a chromatin immunoprecipitation assay, which showed decreased association of CIITA at HLA-DRA promoter in presence of LANA. Taken together, these data identifies a novel mechanism used by KSHV LANA to deregulate the expression of MHC II genes.

**Materials and Methods:**

**Cell culture**

The KSHV and EBV-negative Burkitt lymphoma cell line, BJAB; KSHV-negative monocytic leukemia cell line, THP-1; KSHV-positive but EBV negative PEL cell lines, BCBL-1 and BC-3 were cultured in RPMI 1640 medium supplemented with 10% fetal bovine serum, 2mM L-glutamine, and penicillin-streptomycin (5U/ml and 5g/ml, respectively). Human Embryonic Kidney (HEK) cell lines, 293T cells and 293L were cultured in Dulbecco's modified Eagle's medium (DMEM) supplemented with 10% fetal bovine serum, 2mM L-glutamine, and penicillin-streptomycin (5U/ml and 5g/ml, respectively). All cell lines were grown at 37°C in a humidified environment supplemented with 5% $CO_2$.

**Antibodies**

The following commercial antibodies were used for this study: rat anti-LANA (Advanced Biotechnologies, Inc.), mouse anti-GAPDH (US Biological), mouse anti-Flag M2 (Sigma-Aldrich), mouse anti-Myc 9E10 (Sigma-Aldrich), rabbit polyclonal anti MHC class II (Abcam), rabbit polyclonal anti-RFXANK (Abcam), mouse monoclonal anti-RFX5 (Santa Cruz Biotechnology) and mouse monoclonal anti-RFXAP (Santa Cruz Biotechnology). Mouse monoclonal anti-LANA antibody was a gift from Ke Lan (Institute Pasteur of Shanghai, China).

**Plasmids**

To construct mammalian expression plasmids, RFXANK was PCR amplified from Myc-DDK tagged RFXANK clone (cat#RC220744) obtained from Origene USA, and cloned into a Flag tagged, pA3F or Myc tagged, pA3M vectors at BamHI and EcoRI restriction sites. RFXAP was PCR amplified from BJAB cDNA to clone into pA3F and pA3M vectors at BamHI and EcoRI sites. RFX5 was PCR amplified from RFX5-GFP construct received from Dr. Jeremy Boss, (EMORY School of Medicine), and was subcloned into pA3M or pA3F vectors at HindIII and EcoRV restriction sites. All the truncation mutants of RFXAP were PCR amplified from full-length RFXAP to subclone into pA3M or pA3F vectors at BamHI and EcoRI restriction sites. CIITA was similarly PCR amplified from CIITA plasmid, received as a gift from Dr. Jenny Ting, (UNC) to clone into pA3F vector using BglII and EcoRI restriction sites. In-frame positions of all the clones with the respective tags were confirmed by DNA sequencing done at the Nevada Genomics Center, University of Nevada, Reno. HLA-DRA-Luc plasmid was a generous gift from Dr. Jenny Ting (UNC,). Myc tagged full length LANA (pA3M-

LANA), Flag tagged full length LANA (pA3F-LANA) and their deletion mutants containing LANA N-terminal domain (1 to 340aa) or C-terminal domain (940-1162aa), GFP-NLS Myc, GFP LANA-N Myc (1-340aa) and its truncations: GFP LANA-N 250 Myc (1-250aa), GFP LANA-N 150 Myc (1-150aa), GFP LANA N32 Myc (1-32aa), lentiviral constructs pLVX-LANA-YFP-Flag and its control construct pLVX-YFP-Flag have been described previously (48). shRNA expressing plasmids, Ctrl shRNA and LANA shRNA, are described previously (49). LANA-N GST and LANA-C GST also have been described previously (50).

**DNA transfections**

HEK 293T cells were seeded at the density of $5\times10^6$ cells per 100-mm dish the day before transfection. Plasmids of interest were transfected using polyethylenimine (PEI) (Polysciences, Inc). Approximately 60 μg of total plasmid DNA was mixed with 150mM NaCl and 70μl of PEI solution (1mg/ml, pH 7.0). The resulting transfection mix was incubated at room temperature for 15 minutes and then added drop-wise onto the cells. For reporter assays, transfections were done using metafectene (Biontex Laboratories, GmbH) according to the manufacturer's protocol. B cells were transfected using electroporation as described previously (51).

**Co-immunoprecipitation assays and western blot analysis**

Approximately 20 million cells expressing the proteins of interest were washed with PBS (phosphate buffered saline, 10mM $NaPO_4$, 137mM NaCl, 2.5mM KCl, pH 7.5) and lysed in RIPA cell lysis buffer (50mM Tris-HCl, pH 7.5, 150mM NaCl, 1mM EDTA and 1% NP-40) supplemented with protease inhibitors (1mM phenylmethylsulfonyl fluoride, 10mg/ml pepstatin, 10mg/ml leupeptin and 10mg/ml aprotinin). Cellular lysates

were then sonicated to shear DNA and centrifuged at 12,000 rpm for 10 minutes at $4^0$C to remove cellular debris. The supernatants were pre-cleared with protein A+G sepharose beads (GE Healthcare) for 30 minutes at $4^0$C and gently rotated overnight at $4^0$C with specific antibodies. Resulting immunocomplexes were captured by the addition of protein A and G conjugated sepharose beads and rotating the lysates for 2 hours at $4^0$C. The immunocomplexes were collected by centrifuging at 2000 rpm for 2 minutes at $4^0$C. The beads were washed three times with ice-cold RIPA buffer supplemented with protease inhibitors and boiled in 50µl of SDS PAGE sample loading buffer for 5 minutes. The immunoprecipitated proteins and respective total cell lysates were resolved on 9% SDS-polyacrylamide gel and transferred onto 0.45-µm nitrocellulose membranes (GE Healthcare) at 100 V for 75 minutes. The blots were blocked with 5% non-fat milk in TBST buffer (10mM Tris-HCl, pH 7.5, 150mM NaCl, 0.05% Tween 20) and washed three times with TBST buffer before incubating overnight at $4^0$C with specific primary antibodies. The blots were washed three times with TBST followed by incubating with appropriate secondary antibodies conjugated with Alexa Fluor 680 or Alexa Fluor 800 (Molecular Probes, Carlsbad, CA) secondary antibodies at 1:10,000 dilutions. The membranes were scanned with the Odyssey scanner (LI-COR, Lincoln, NE).

**Yeast-two-hybrid assay**

LANA-N (1-340aa) was cloned in-frame with the DNA binding domain of GAL4 (GAL4-DBD) of a pAS1 vector (Clontech, Mountain View, CA) to use as bait. This plasmid was transformed into *S. cerevesiae* strain Y190 (Clontech, Mountain View, CA) and selected on a DOBA-Trp dropout medium (Clontech, Mountain View, CA). Expression of LANA-N with DBD fusion protein was determined by anti-GAL4 DBD

antibody (Santa Cruz Biotechnology Inc.) on a Western blot. Yeast, Y190 containing LANA-N-DBD was transformed with cDNA library (generous gift from Dr. Erle S. Robertson, University of Pennsylvania) cloned into pACT vector and selected on BOBA-Trp, His, Leu dropout medium (Clontech, Mountain View, CA) in presence of 30mM 3-aminotriazole as described previously (52). Selected colonies were subjected for plasmid isolation, which was further electroporated into *E. coli* DH5a for their amplification. Plasmid DNA from individual bacterial colonies were isolated and subjected for sequencing at Nevada Genomics Center after determining their restriction pattern. Identities of the cDNA clones were determined by matching with the database sequence (NCBI).

**Immunofluorescence assay**

KSHV positive BCBL-1 and BC-3 cells were washed with phosphate-buffered saline (PBS) before spreading on coverslips. The cells were allowed to air-dry for 10 minutes, fixed them with 4% paraformaldehyde for 10 minutes at room temperature followed by permeabilization with 0.2% Triton X-100 in PBS for 10 minutes at room temperature. Cells were blocked with PBS containing 0.4% fish skin gelatin and 0.05% Triton X-100 for 30 minutes at room temperature. The cells were then incubated with specific primary antibodies for 1 hour at room temperature, washed with PBS before incubating them with Alexa Fluor conjugated secondary antibodies (Molecular Probes) for 45 minutes at room temperature. The cells were washed three times with PBS to remove non-specifically bound antibodies before staining with nuclear stain, TO-PRO3 (Molecular Probes). Images were captured using a confocal laser-scanning microscope (Carl Zeiss, Inc.).

**Chromatin immunoprecipitation assay (ChIP)**

Chromatin immunoprecipitation was performed as described previously (53). Briefly, 15 to 20 million cells were fixed with a final concentration of 1% formaldehyde for 10 minutes at room temperature followed by adding glycine at a final concentration of 125mM for 5 minutes to block cross-linking. The cells were rinsed three times with ice-cold PBS and lysed in cell lysis buffer (5mM PIPES (pH 8.0), 85mM KCl, and 0.5mM NP-40) supplemented with protease inhibitors for 10 minutes on ice. The nuclei were enriched by low speed centrifugation and resuspended in protease inhibitors supplemented nuclear lysis buffer containing 50mM Tris-HCl, pH 8.1, 10mM EDTA and 1% SDS. Chromatin was sonicated to an average length of 500 to 800 bp, centrifuged for 10 minutes at 13,000rpm to remove the cell debris. The resulting supernatant was diluted 5-fold with ChIP dilution buffer containing 16.7mM Tris-HCl, pH 8.1, 167mM NaCl, 1.2mM EDTA, 0.01% SDS, 1.1% Triton X-100, and protease inhibitors. The diluted chromatin was pre-cleared with Protein A+G sepharose beads pretreated with 1mg/ml BSA and 1mg/ml sheared salmon sperm DNA for 30 minutes at $4^0$C with rotation followed by incubating overnight with either control or specific antibodies at $4^0$C with rotation. Immune complexes were collected by incubating with Protein A+G sepharose beads for 1–2h at 4°C. The beads were collected and washed subsequently with a low-salt buffer (0.1% SDS, 1.0% Triton X-100, 2mM EDTA, 20mM Tris [pH 8.1], 150mM NaCl), a high-salt buffer (0.1% SDS, 1.0% Triton X-100, 2mM EDTA, 20mM Tris [pH 8.1], 500mM NaCl), and a LiCl wash buffer (0.25M LiCl, 1.0% NP-40, 1% deoxycholate, 1mM EDTA, 10mM Tris [pH 8.0]). The beads were then washed twice with Tris-EDTA buffer and chromatin was eluted using an elution buffer (1% SDS, 0.1M

NaHCO3) and reverse cross-linked by adding 0.3M NaCl at 65°C overnight. Eluted DNA was precipitated, treated with RNAse and proteinase K at $45^0$C for 2h, and purified using Min-Elute PCR purification kit (Qiagen, USA). The purified DNA was analyzed by PCR for the presence of HLA-DRA promoter region.

Primers used for HLA-DRA promoter amplification were described earlier.

Forward: 5'-GTTGTCCTGTTTGTTTAAGAAC-3',

Reverse: 5'-GCTCTTTTGGGAGTCAG-3' (44).

KSHV TR primers have also been described earlier.

Forward: 5′-GGGGGACCCCGGGCAGCGAG-3',

Reverse: 5'-GGCTCCCCCAAACAGGCTCA-3' (51).

**Dual luciferase reporter assay**

Nearly $5\times10^5$ HEK293 L cells were seeded into 6-well plates the day before transfection. The cells were co-transfected with 0.5μg of DRA-Luc reporter plasmid, 0.2μg of CIITA-Flag plasmid and increasing amounts of LANA expression vector (1, 2, and 3 μg). pA3F empty vector was used as filler DNA. Transfection efficiencies were monitored by transfecting green fluorescent protein (GFP) containing vector, pEGFP. Renilla luciferase-expressing plasmid (pRRLSV40) was transfected at 40ng/well for data normalization. All the transfections for reporter assays were done using metafectene (Biontex Laboratories GmbH) according to the manufacturer's protocol. 36 hours post transfection cells were lysed in cell lysis buffer (Promega) and 50μl of the cell lysate was used for the reporter assay using dual luciferase reporter assay kit (Promega, USA). Relative luciferase units (RLU) were calculated after normalizing the HLA-DRA luciferase readings with Renilla luciferase to account for the transfection efficiencies. A

portion of the cell lysates was used for Western blotting to detect LANA, CIITA and GAPDH. All experiments were repeated multiple times and the data shown is mean of three independent experiments.

***In vitro* translation and GST pull-down assay**

For the GST pull-down assays, GST fusion proteins were expressed in *E. coli* BL21 cells. Briefly, the cells were induced with 1mM IPTG (isopropyl-B-d-thiogalactopyranoside) for 4 hours at $37^0$C and the GST fusion proteins were extracted from the bacterial cell lysates using glutathione-Sepharose beads (GE Healthcare, USA). Components of RFX complex and its truncation mutants RFXAP Δ1-70aa, RFXAP Δ1-150aa and RFXAP Δ1-240aa, were translated *in vitro* using TNT T7 Quick coupled transcription-translation system (Promega, Madison, WI). Nearly 3μg of expression plasmids were translated per 50μl reaction containing 1mM (32μCi) $^{35}$S methionine according to the manufacturer's protocol. The translated proteins were rotated overnight at $4^0$C with either control-GST, LANA-N GST or LANA-C GST in NETN binding buffer (0.1% NP-40, 20mM Tris, 1mM EDTA and 100mM NaCl) supplemented with protease inhibitors. Control-GST, LANA-N GST and LANA-C GST proteins have been described earlier (54). Next day, GST bound proteins were gently washed three times in ice-cold NETN binding buffer supplemented with protease inhibitors and the precipitated protein complexes were resolved on SDS-PAGE and detected by autoradiography.

**Electrophoretic mobility shift assay (EMSA)**

EMSA was performed using a double-stranded oligonucleotide containing the HLA-DRA X box sequence as a probe. This sequence is known to bind with the RFX complex previously in gel shift assays (55). The probe was end labeled with α-$^{32}$P and

purified on a GE Illustra ProbeQuant G-50 micro column (GE Healthcare, USA). RFX complex proteins and LANA-N (1-340aa) proteins were translated *in vitro* using a TNT Quick coupled transcription-translation rabbit reticulocyte lysate system (Promega, USA). A 40µl DNA-protein binding assay contained 12mM HEPES (pH 7.9), 12% glycerol, 60mM KCl, 5mM MgCl2, 0.12mM EDTA, 0.3mM DTT, 0.1µg poly (dI/dC) and 0.05µg of denatured salmon sperm DNA as carrier (55). *In vitro* translated proteins were pre-incubated on ice for 10 minutes before adding 1µl of end-labeled DNA probe. The reaction was incubated on ice for 30 minutes and the bound complexes were resolved on 5% non-denaturing polyacrylamide gel in 0.5X TBE buffer (0.045M Tris Borate, pH 8.2, 1.0mM EDTA). The gel was run at $4^0$C at 100V for 10 to 12 hours. The signals were detected by autoradiography.

**Quantitative Real-time PCR (qRT-PCR) assays**

For quantitative Reverse-Transcriptase PCR assays, total mRNA from the cells was extracted using illustra RNAspin Mini kit (GE Healthcare) according to the manufacturer's instruction and cDNA was made using High Capacity cDNA reverse transcription kit (Applied Biosystems, USA). Each PCR reaction consisted of 10µl of 2X PCR master mix (Applied Biosystems, USA), 1µM of each forward and reverse primers and 2µl of the cDNA. The cDNA was amplified on an ABI StepOne plus real-time PCR machine (Applied Biosystems, USA) and relative gene copies or the transcripts were calculated by the $\Delta\Delta C_T$ method. Each experiment included duplicate samples and the data shown represents the mean of three independent experiments. P values were calculated by two-tailed t-tests using Graphpad (Prism 6) software. The primer sequences

used for the amplification of different HLA genes were taken from previously published article, which are listed in table 1 (23).

TABLE 1 Primers used in real-time PCR assays

| Gene | Forward primer | Reverse primer |
|---|---|---|
| β-Actin | 5′-ACAATGTGGCCGAGGACTTTGA-3′ | 5′-TGTGTGGACTTGGGAGAGGACT-3′ |
| LANA | 5′-TTGCCTATACCAGGAAGTCCCACA-3′ | 5′-GGAGGAAGACGTGGTTACGGG-3′ |
| HLA-DRA | 5′-TTTGAGGCTCAAGGTGCATTG-3′ | 5′-TGGAGGTACATTGGTGATCGG-3′ |
| HLA-DRB | 5′-CCGAGTACTGGAACAGCCAGAA-3′ | 5′-TGCACTGTGAAGCTCTCACCAA-3′ |
| HLA-DPA | 5′GCCCTGAAGACAGAATGTTCCA-3′ | 5′-GCGGCATAAGTTGACACATGG-3′ |
| HLA-DPB | 5′-ACAGTCTGATTCTGCCCGGAGT-3′ | 5′-CTTGCTCCTCCTGTGCATGAAG-3′ |
| HLA-DQA | 5′-ATCATCCAAGGCCTGCGTT-3′ | 5′-TCTTCTGCTCCTGTAGATGGCG-3′ |
| HLA-DQB | 5′-GCAGAGACTCTCCCGAGGATTT-3′ | 5′-CGCACGATCTCTTCTCGGTTAT-3′ |

**Results:**

**LANA interacts with the components of RFX complex**

Since LANA is a major latent protein, expresses ubiquitously in all KSHV infected cells and modulates various cellular pathways; we sought to identify LANA interacting proteins. Our yeast-two hybrid screen with amino terminal domain of LANA fused to Gal4-DNA binding domain (as bait), identified a number of cellular proteins, which are listed in Table 2. The clones of these identified proteins were detected at least twice in the screen. With the aim of determining LANA's role in immune modulation, we focused further studies on RFXAP; a component of the RFX complex, critical for the transcription of HLA genes. RFX complex proteins are absolutely essential for the expression of MHC class II molecules. In order to determine whether RFX complex proteins interacted with LANA in KSHV infected cells, we performed co-immunoprecipitation assays from KSHV infected primary effusion lymphoma (PEL) cell lines, BCBL-1 and BC-3. The results of these co-immunoprecipitation experiments showed that all the three components of RFX complex: RFX5, RFXAP and RFXANK co-immunoprecipitated with LANA from KSHV positive PEL cell lines, BCBL-1 and

TABLE 2 LANA-interacting proteins identified by the yeast two-hybrid assay

| Protein identification[a] | GenBank accession no. |
|---|---|
| TNF receptor-associated protein 1 variant | AK223205.1 |
| Inorganic pyrophosphatase | AAD34643 |
| RFXAP | NM_000538.3 |
| Gamma interferon-inducible lysosomal thiol reductase | AF097362_1 |
| PCNA | NP_002583.1 |
| MCM6 | NM_005915.4 |
| POTE ankyrin domain family, member F | NM_001099771.2 |
| PDLIM1 | NM_020992.2 |
| HLA class I histocompatibility antigen, A-69 alpha chain-like | NT_167245.1 |
| WDR47 | NM_001142551.1 |
| High-mobility-group AT hook 2 | NP_001287847 |
| WD repeat domain 34 | EAW87814.1 |
| SNX10 | NM_013322.2 |
| *Homo sapiens* guanine nucleotide-binding protein beta polypeptide 2-like 1 | NM_006098.4 |
| Ran-specific GTPase-activating protein isoform 2 | NP_002873 |
| *Homo sapiens* chromodomain helicase DNA-binding protein 4 | BC038596.1 |
| MPP1 | Q96Q89.2 |
| DTX3 | NM_178502.2 |
| Ornithine decarboxylase antizyme 1 | AAA82155.1 |
| Elongation factor 1 gamma | NP_001395 |
| NOP58 ribonucleoprotein | NP_057018 |

[a] PCNA, proliferating cell nuclear antigen; MCM6, minichromosome maintenance complex component 6; PDLIM1, PDZ and LIM domain 1; WDR47, WD repeat domain 47; SNX10, *Homo sapiens* sorting nexin 10; MPP1, M-phase phosphoprotein 1; DTX3, *Homo sapiens* deltex homolog 3 (*Drosophila*).

BC-3 (Fig. 1A, lanes 3 and 6). Lack of RFX proteins precipitation with control antibody (CoAb) confirmed the specificity of LANA association with these proteins (Fig. 1A, lanes 2 and 5). In order to further validate the interactions between LANA and the components of RFX complex, we examined co-localization of LANA with RFX proteins

using immunofluorescence assay in BC-3 and BCBL-1 cells. As expected, LANA showed the typical punctate staining in the nucleus (Fig. 1B, LANA panel in red). The components of the RFX complex, RFX5, RFXAP and RFXANK showed distinct staining pattern in the nucleus (Fig. 1B, panels in green). As seen in the merged panels, all the

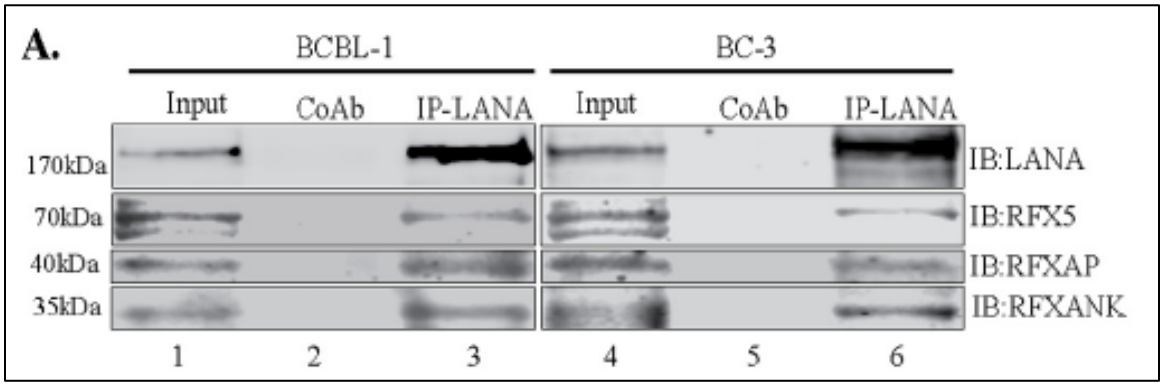


three proteins of RFX complex showed varying degree of co-localization with LANA in the nuclear compartments of both the PEL cells, BC-3 and BCBL-1 (Fig. 1B, yellow dots in RFXs+LANA panels), suggesting that some fraction of LANA is in the same vicinity to the RFX proteins in the nucleus of KSHV infected cells. To assess whether KSHV/LANA altered the normal localization patterns of RFX proteins, we examined the staining patterns of RFX proteins in a KSHV negative, BJAB cells. Not surprisingly, BJAB also showed distinct staining patterns of RFX proteins, which was very much similar to the patterns seen in KSHV positive PEL cells (Fig. 1B, BJAB panels). LANA was not detected in these BJAB cells as expected. Nuclei of these PELs and BJAB cells were stained with TO-PRO-3 and the integrity of these cells were confirmed in DIC panels (Fig. 1B, DIC panels).

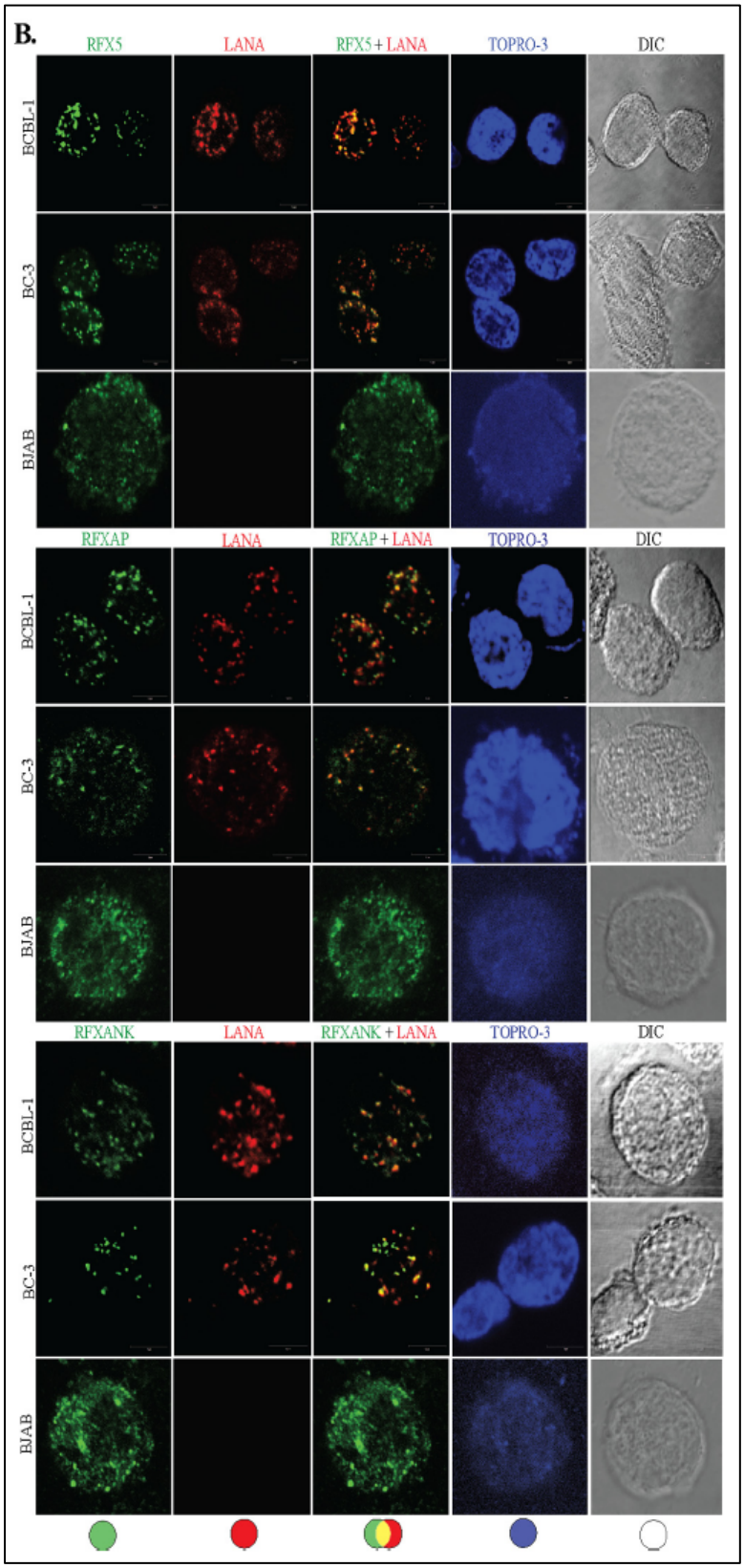


In an attempt to determine whether all the components of RFX complex were in the same nuclear compartment as LANA, we determined co-localization of LANA with two RFX proteins (RFXAP and RFX5) in a triple immunofluorescence assay. Co-localization of RFXAP with LANA in KSHV positive PEL cells, BCBL-1 and BC-3 (Fig. 1C, red panels) showed almost similar co-localization (based on the number of yellow dots from multiple cells) as RFX5 with LANA (sky blue dots in LANA and RFX5 panel from multiple cells). This

suggested that LANA binds to the components of RFX complex in KSHV infected cells. BJAB cells showed perfect co-localization of RFXAP (red) and RFX5 (blue), which was also seen in KSHV positive PEL cells (Fig. 1C, merge all panel) confirming that these RFX proteins are in the same nuclear compartments. We expect RFXANK to be in the same loci but were unable to perform co-localization of all three RFX proteins with LANA because of a lack of host specific antibody for all three RFX proteins.

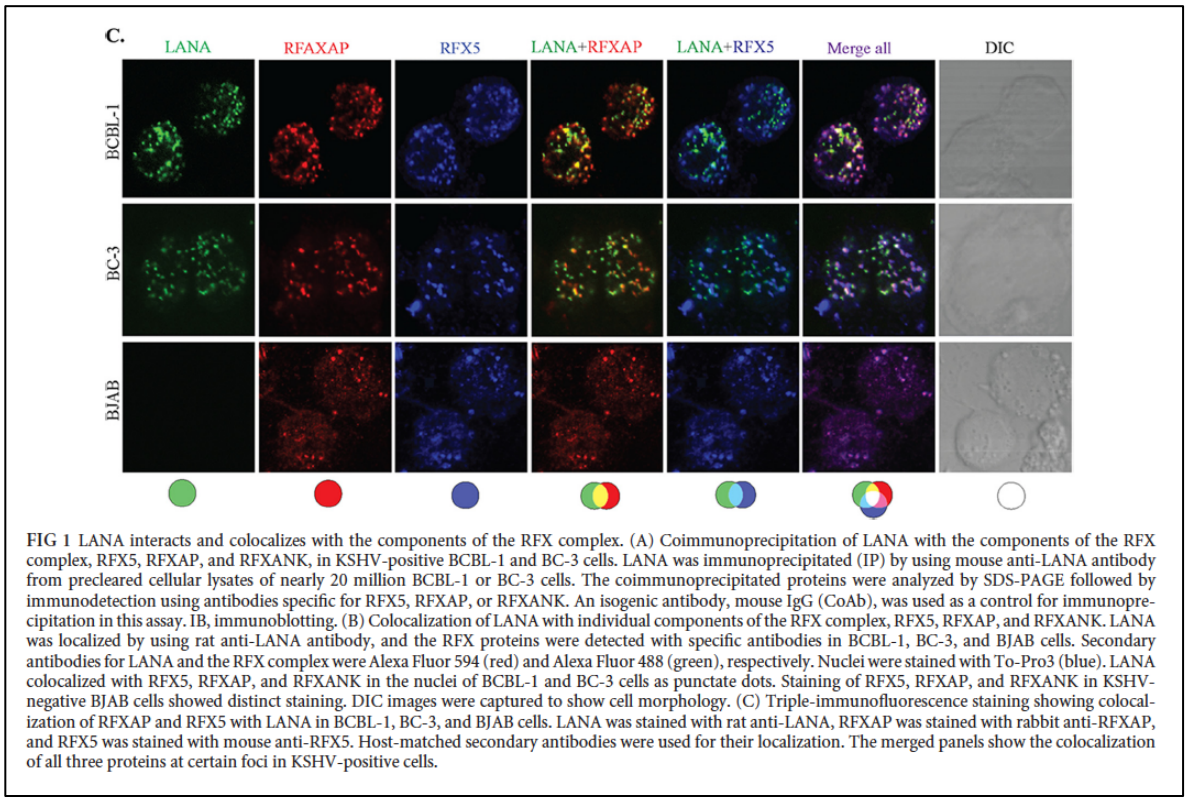


FIG 1 LANA interacts and colocalizes with the components of the RFX complex. (A) Coimmunoprecipitation of LANA with the components of the RFX complex, RFX5, RFXAP, and RFXANK, in KSHV-positive BCBL-1 and BC-3 cells. LANA was immunoprecipitated (IP) by using mouse anti-LANA antibody from precleared cellular lysates of nearly 20 million BCBL-1 or BC-3 cells. The coimmunoprecipitated proteins were analyzed by SDS-PAGE followed by immunodetection using antibodies specific for RFX5, RFXAP, or RFXANK. An isogenic antibody, mouse IgG (CoAb), was used as a control for immunoprecipitation in this assay. IB, immunoblotting. (B) Colocalization of LANA with individual components of the RFX complex, RFX5, RFXAP, and RFXANK. LANA was localized by using rat anti-LANA antibody, and the RFX proteins were detected with specific antibodies in BCBL-1, BC-3, and BJAB cells. Secondary antibodies for LANA and the RFX complex were Alexa Fluor 594 (red) and Alexa Fluor 488 (green), respectively. Nuclei were stained with To-Pro3 (blue). LANA colocalized with RFX5, RFXAP, and RFXANK in the nuclei of BCBL-1 and BC-3 cells as punctate dots. Staining of RFX5, RFXAP, and RFXANK in KSHV-negative BJAB cells showed distinct staining. DIC images were captured to show cell morphology. (C) Triple-immunofluorescence staining showing colocalization of RFXAP and RFX5 with LANA in BCBL-1, BC-3, and BJAB cells. LANA was stained with rat anti-LANA, RFXAP was stained with rabbit anti-RFXAP, and RFX5 was stained with mouse anti-RFX5. Host-matched secondary antibodies were used for their localization. The merged panels show the colocalization of all three proteins at certain foci in KSHV-positive cells.

**LANA associates with RFX complex independent of other viral components**

Next, we wanted to determine whether LANA alone is sufficient for its association with the components of RFX complex, or it requires any other viral latent proteins to associate with the components of RFX complex.

To this end, we performed co-immunoprecipitation assays of individual RFX proteins with LANA in an over-expression system in HEK293T cells. Lysates from the cells co-transfected with plasmids expressing either control-Flag or LANA-Flag and Myc tagged RFX5, RFXAP or RFXANK were subjected to immunoprecipitation with anti-Flag antibody. Detection of co-precipitating RFX proteins showed efficient binding of all three proteins of the RFX complex with LANA (Fig. 2A, 2B and 2C, IB:Myc panel).

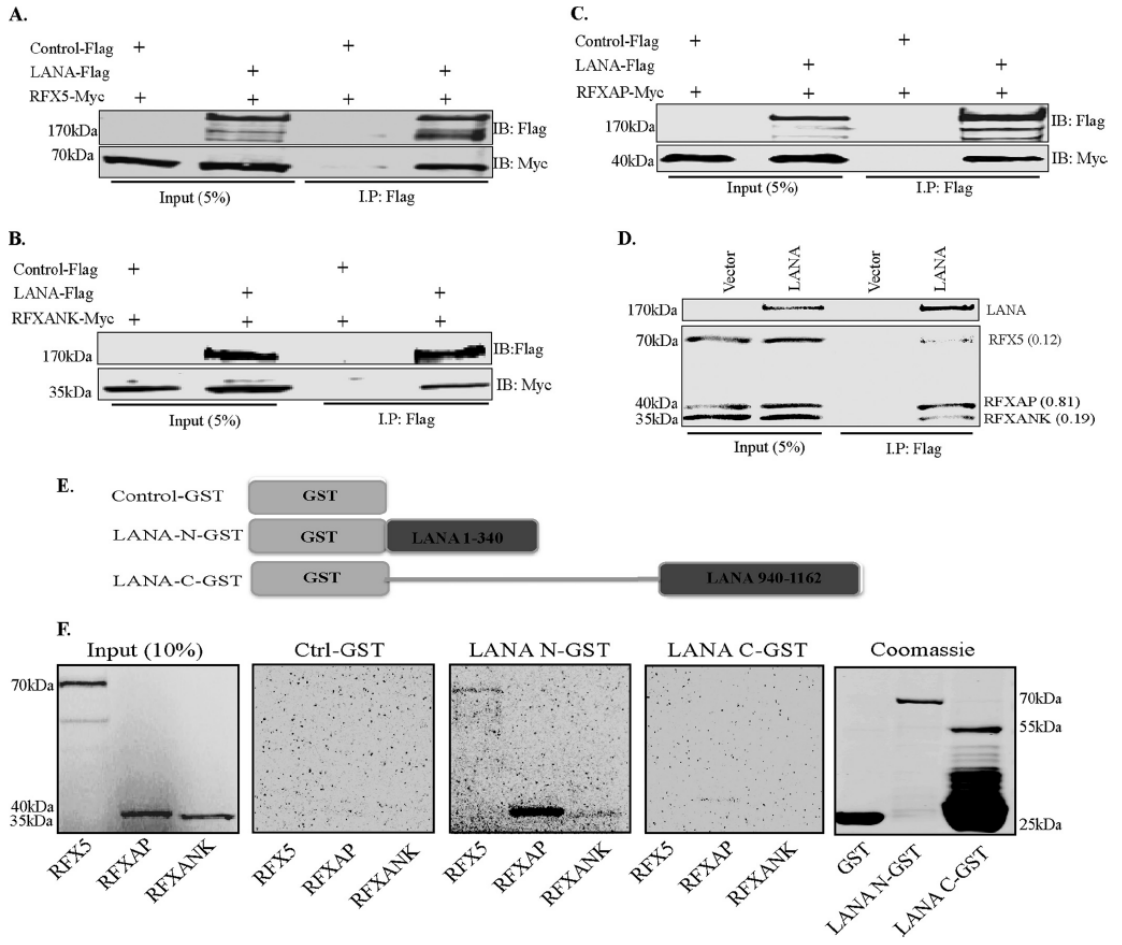


FIG 2 LANA does not require other KSHV factors to associate with the components of the RFX complex. (A to C) Assays of protein-protein interactions of LANA with all three components of the RFX complex were performed with HEK293T cells by transiently cotransfecting cells with Flag-tagged wild-type LANA and Myc-tagged RFX5 (A), Myc-tagged RFXANK (B), or Myc-tagged RFXAP (C). The pA3F empty vector was used as a control. The cells were lysed 48 h after transfection, and LANA was immunoprecipitated by using anti-Flag antibody, followed by immunodetection with anti-Flag and anti-Myc antibodies. Overexpressed LANA efficiently coimmunoprecipitated RFX5, RFXAP, and RFXANK. (D) *In vitro*-translated full-length LANA-Flag protein was combined with *in vitro*-translated RFX5-Myc, RFXAP-Myc, and RFXANK-Myc and rotated overnight at 4°C after preclearing with protein A and G beads. LANA was immunoprecipitated with anti-Flag antibody, and the bound complexes were resolved on SDS-PAGE gels, followed by autoradiography to detect the coimmunoprecipitated proteins. Relative binding values (shown in parentheses) of RFX components were determined by taking the respective inputs as 1. (E) Schematic of LANA domains fused with GST used in pulldown assays. (F) GST pulldown assay showing binding of amino- and carboxy-terminal domains of LANA with the components of the RFX complex. Full-length *in vitro*-translated RFX5, RFXAP, and RFXANK proteins were rotated with either GST alone (Ctrl), LANA-N–GST, or LANA-C–GST after preclearing with GST beads. The bound proteins were resolved on SDS-PAGE gels and visualized by autoradiography. Expressions of GST and the GST fusion proteins were confirmed by SDS-PAGE and Coomassie staining (right).

Lack of co-precipitating RFX proteins in control-Flag lane confirmed the specificity of the assay. These results demonstrate that presence of LANA is sufficient to associated with the components of RFX complex.

Since all the three components of RFX complex-RFX5, RFXAP and RFXANK associated with LANA in PEL cell lines as well in the overexpression systems, we wanted to determine whether any of these three RFX proteins of the trimeric complex is the main interacting partner of LANA. To answer this, we performed an *in vitro* binding assay by using *in vitro* translated and $S^{35}$ methionine labeled proteins. The sizes of these *in vitro* translated proteins were confirmed by specific antibody in a Western blot. The radiolabeled proteins of RFX complex were incubated with *in vitro* translated Flag-LANA of empty vector (Vector) to immunoprecipitate with anti-Flag antibody. The proteins resolved on SDS-PAGE and followed by autoradiography detected co-immunoprecipitating RFX proteins, which were also confirmed by specific antibodies. Consistent with the results of our endogenous and expressed proteins immunoprecipitation assays, all the three components of the RFX complex co-immunoprecipitated with LANA (Fig. 2D, IP-Flag LANA lane). Although all the three components of RFX bound with LANA, the level of RFXAP binding was higher when normalized to their respective inputs. The binding efficiencies calculated by taking input as 1 are presented in parenthesis (Fig. 2D, IP-Flag LANA lane, RFXAP at 0.81). These results again confirmed that LANA associates with the components of RFX complex independent of other KSHV components.

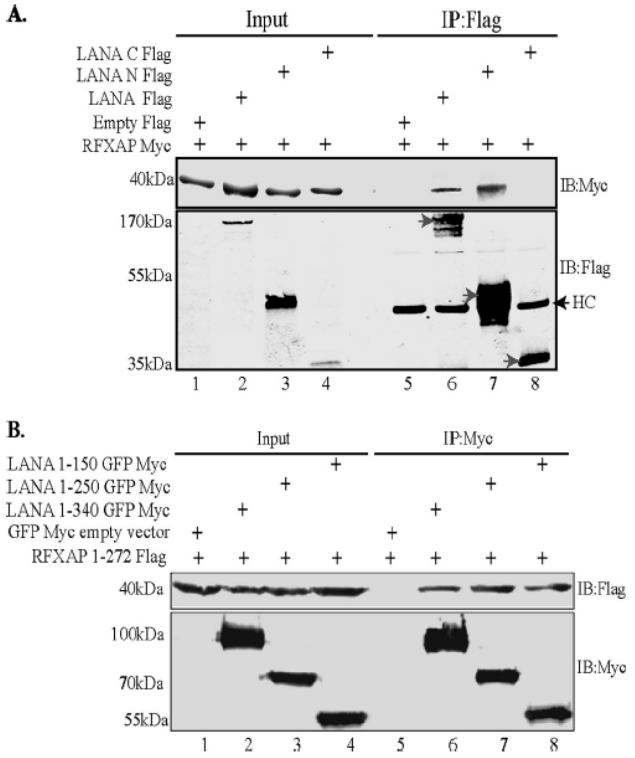


**FIG 3** Coimmunoprecipitation of RFXAP with the LANA truncation spanning aa 1 to 150. (A) HEK293T cells were transiently transfected with the Flag-tagged pA3F vector (control), LANA-Flag, LANA-N–Flag, or LANA-C–Flag along with RFXAP-Myc. Cell lysates were subjected to immunoprecipitation with anti-Flag antibody, and the immunoprecipitated proteins were detected with anti-Flag and anti-Myc antibodies after resolving proteins on SDS-PAGE gels and Western blotting. HC represents the heavy chain of the antibody. (B) HEK293T cells were cotransfected with RFXAP-Flag and either NLS-GFP-Myc (vector control), the LANA truncation spanning aa 1 to 340 (LANA 1-340)-GFP-Myc, LANA 1-250–GFP–Myc, or LANA 1-150–GFP–Myc. Cell lysates were subjected to IP using rabbit anti-Myc antibody, and the immunoprecipitated proteins were resolved on SDS-PAGE gels, followed by detection with mouse anti-Myc and anti-Flag antibodies, in order to avoid detection of the heavy chain that comigrates with the LANA region spanning aa 1 to 150.

To validate these results by another experimental approach, we performed glutathione-S-transferase (GST) fusion-protein pull-down experiments. In this assay, *in vitro* translated and $S^{35}$ methionine labeled RFX5, RFXAP or RFXANK proteins was individually incubated with GST fused LANA-N (1-340aa), LANA-C (940-1162aa) or control-GST (Fig. 2E). GST pull-down assay showed that while LANA-N GST very strongly associated with RFXAP; it also showed weaker interactions with other RFX components, RFX5 and RFXANK (Fig. 2F, LANA-N GST panel). Interestingly, LANA-C GST showed very weak interaction with RFXAP (Fig. 2F, LANA-C GST panel). Lack of any binding with control GST confirmed the specificity of the binding assay (Fig. 2F, Ctrl-GST panel). A representative image of coomassie stained gel for GST-fusion proteins is shown in figure 2F (coomassie panel). Binding of RFXAP to the N-terminus of LANA was consistent with our yeast two-hybrid data where the N-terminus of LANA (bait) identified RFXAP as potential LANA interacting protein (Table 2). Since, RFXAP

was identified in the yeast-two-hybrid assay and it also bound most strongly to LANA in GST pull-down assay, we focused the domain-mapping experiments on RFXAP component of the RFX complex.

**LANA 1-150aa interacts with RFXAP**

To further ensure that amino terminus of LANA (1-340aa) is responsible for binding with RFXAP, a co-immunoprecipitation experiment were performed in HEK293T cells with RFXAP transiently co-expressed with either vector control, full length LANA, LANA-N (1-340aa), or LANA-C (940-1162aa). The immune detection with anti-Myc antibody for RFXAP showed co-immunoprecipitation of RFXAP with both, the full length as well as N terminus of LANA (1-340aa) but not with LANA-C (940-1162aa) (Fig. 3A, IB:Myc panel). Immunoprecipitated LANA and its truncations are indicated with an arrow (Fig. 3A, IB:Flag panel). In line with yeast-two-hybrid data and the GST pull-down results, this co-immunoprecipitation assay confirmed that RFXAP binds strongly to the amino terminal domain of LANA. We were further interested in determining the regions in amino terminal domain of LANA sufficient to interact with RFXAP. To do this, LANA truncation regions, 1-340aa (as control of binding), 1-250aa or 1-150aa were transiently co-expressed with full-length RFXAP in HEK293T cells and a co-immunoprecipitation assay was performed. Detection of co-precipitating RFXAP showed efficient binding with all three LANA truncations suggested that LANA 1-150aa is sufficient for interaction with RFXAP (Fig. 3B, IB:Flag panel). LANA truncations were detected by anti-Myc antibody (Fig. 3B, IB:Myc panel).

**RFXAP interacts with LANA through its C-terminus**

RFXAP component of the RFX complex has distinct N-terminal acidic, C-terminal glutamine-rich and a middle basic domain. Previous studies have shown that the last 43 amino acid region at the C-terminal glutamine-rich domain of RFXAP is sufficient for the expression of HLA-DRA gene however, the expression of other HLA genes (HLA-DQ and HLA-DP) requires a larger C-terminal segment of RFXAP (last 130aa) (56). The last 43aa in the C-terminal domain of RFXAP have been reported to

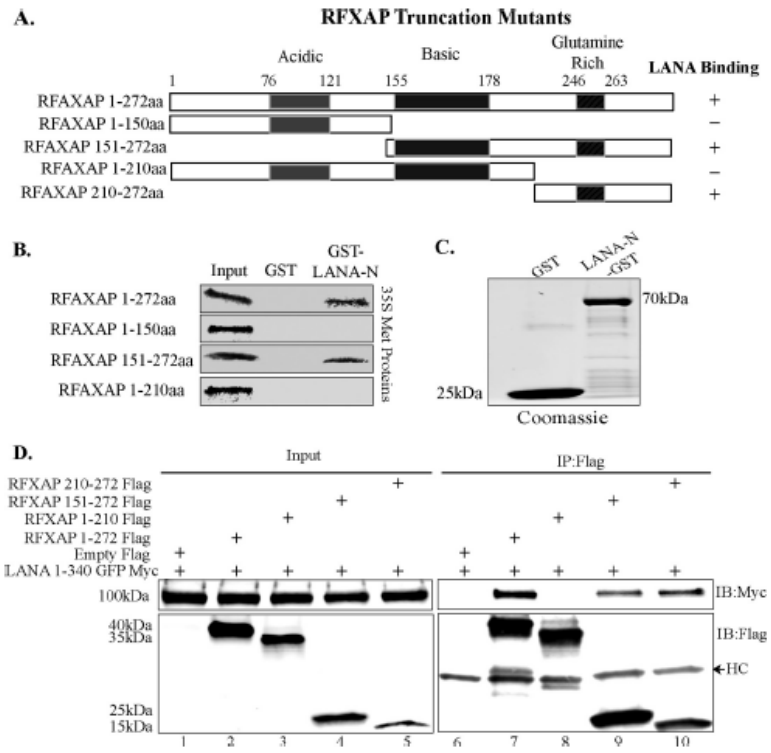


**FIG 4** The C terminus of RFXAP interacts with LANA. (A) Schematic showing RFXAP domains used for coimmunoprecipitation and GST pulldown assays. (B) *In vitro*-translated full-length RFXAP (aa 1 to 172) or the truncated RFXAP mutant spanning aa 1 to 150, aa 151 to 272, or aa 1 to 210 was pulled down with GST or LANA-N–GST and resolved on SDS-PAGE gels, followed by detection by autoradiography. (C) Expression of control GST and LANA-N–GST proteins that were used for GST pulldown of RFXAP truncation mutants. (D) Coimmunoprecipitation assay of the N terminus of LANA and different truncation mutants of RFXAP. HEK293T cells were transiently cotransfected with LANA-N–GFP–Myc and either the empty control vector pA3F, full-length Flag-tagged RFXAP (aa 1 to 272) or the truncated RFXAP protein spanning aa 1 to 210, aa 150 to 272, or aa 210 to 272. The cell lysates were immunoprecipitated with anti-Flag antibody, and immunoprecipitated proteins were immunoblotted with anti-Flag (mouse) and anti-Myc antibodies. HC represents the heavy chain detected because mouse anti-Flag was used for the detection of Flag-tagged proteins.

interact with the other two components of RFX complex- RFX5 and RFXANK (56-60). Hence, in order to understand the mechanism of how LANA's binding may affect the

RFX complex formation and also the assembly of a functional enhanceosome to alter the expression of MHC II genes, we sought to determine whether LANA binds to RFXAP in the C-terminus or to the functionally dispensable N-terminal region of RFXAP. To this end, we constructed Flag tagged deletion mutants of RFXAP as shown in the schematic (Fig. 4A) and performed *in vitro* GST binding and co-immunoprecipitation assays to determine the RFXAP binding domain with LANA. RFXAP full length (1-272aa) and its truncations, 1-150aa, 151-272aa and 1-210aa efficiently translated *in vitro* detected as a distinct band by autoradiography. Binding assay with LANA-N-GST showed interactions with full length (1-272aa) RFXAP, as expected and the domains with C-terminus (151-272aa) but not with N-terminal domains (1-150aa or 1-210aa) (Fig. 4B). The GST fusion proteins (control GST or LANA-N GST) used in this *in vitro* binding assay was detected by coomassie staining (Fig. 4C). These results suggested that LANA binds with RFXAP in the C-terminus region of 210 to 272aa, which is also the region that mediates the interaction with the other two components of RFX complex-RFXANK and RFX5. These binding results were further confirmed is a co-immunoprecipitation assay by co-expressing LANA-N terminus fused to GFP-Myc with either empty Flag vector of Flag tagged RFXAP (1-272aa) and its truncations (1-172aa, 1-210aa, 150-272aa and 210-272aa). The results of this co-immunoprecipitation assay also confirmed that the N-terminal domain of RFXAP (1-210aa) was dispensable for its interaction with LANA. These binding assays determined that LANA binds in the C-terminal domain of RFXAP (210-272aa), which is also the interaction domain for other components of the RFX complex. We were unable to *in vitro* translate the smallest truncation of RFXAP (210-

272aa), despite of repeated attempts, therefore was used only in over expression immunoprecipitation assay.

**LANA associates with HLA-DRA promoter**

The components of RFX complex bind, to the promoters of MHC class II molecules in order to promote the assembly of multi-protein enhanceosome complex for the recruitment of CIITA (61). Since LANA bound with RFX complex, we wanted to determine whether LANA associates with the promoters of MHC II genes. In order to test this, we performed chromatin immunoprecipitation (ChIP) assays with anti-LANA antibody from KSHV infected PEL cell lines, BCBL-1 and BC-3. The results determined by qPCR showed the copies of HLA-DRA promoter from the chromatin precipitated with LANA antibody but not in the chromatin with control antibody in both the, BC-3 and BCBL-1 cells, indicating specific association of LANA with the promoter of HLA-DRA gene (Fig. 5A, panel a). Since LANA associates with the terminal repeats (TR) sequence of KSHV genome, we used the LANA bound chromatin for the detection of TR as a positive control of anti-LANA ChIP. As expected, TR sequence amplified from the chromatin immunoprecipitated with anti-LANA antibody but not from the control antibody, confirming the specificity of anti-LANA ChIP (Fig. 5A, panel b). The western blot showing the efficiency of anti-LANA antibody immunoprecipitation is presented in Fig. 5A panel c).

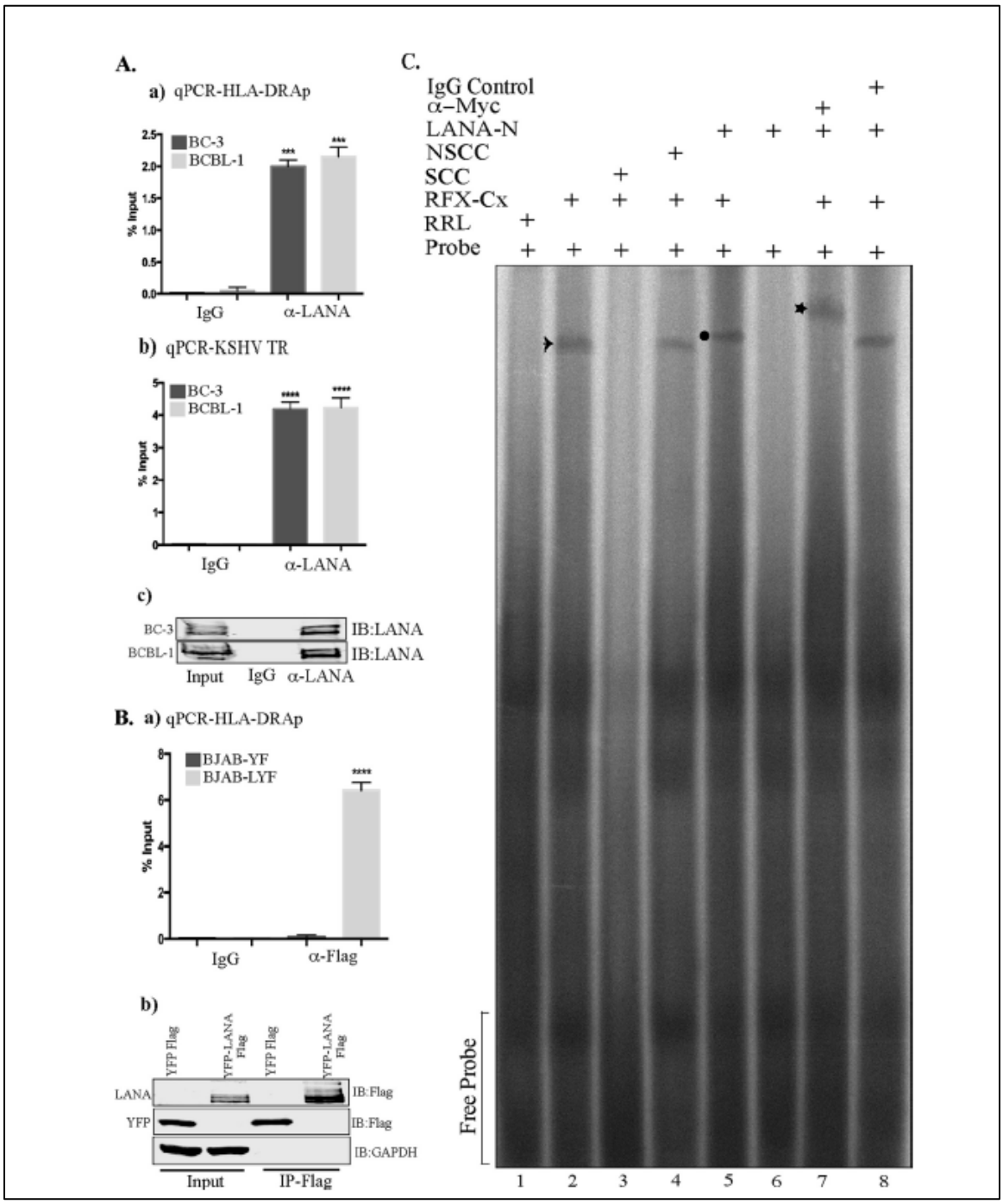
A.
a) qPCR-HLA-DRAp
BC-3
BCBL-1
% Input
IgG
α-LANA
b) qPCR-KSHV TR
BC-3
BCBL-1
% Input
IgG
α-LANA
c)
BC-3
BCBL-1
IB:LANA
IB:LANA
Input
IgG
α-LANA
B. a) qPCR-HLA-DRAp
BJAB-YF
BJAB-LYF
% Input
IgG
α-Flag
b)
YFP Flag
YFP-LANA Flag
YFP Flag
YFP-LANA Flag
LANA
YFP
IB:Flag
IB:Flag
IB:GAPDH
Input
IP-Flag
C.
IgG Control
α–Myc
LANA-N
NSCC
SCC
RFX-Cx
RRL
Probe
Free Probe
1 2 3 4 5 6 7 8

FIG 5 LANA associates with HLA-DRA promoter. **A.** Chromatin Immunoprecipitation (ChIP) assay was done with anti-LANA antibody on the chromatins PEL cells, BC-3 and BCBL-1. Sonicated chromatin was immunoprecipitated with a) anti-LANA or control antibodies (IgG) and the chromatin bound DNA was subjected for the quantitation of HLA-DRA promoter by qPCR. b) Amplification of KSHV terminal region (TR), binding site of LANA, was included as a positive control for LANA-ChIP. c) Immune-blot showing specificity and efficiency of anti-LANA antibody in immunoprecipitation. **B.** b) Chromatin immunoprecipitation with anti-Flag antibody from the sonicated chromatin of BJAB cells stably expressing YFP-LANA-Flag tagged (BJAB-LYF) or control YFP (BJAB-YF). Presence of HLA-DRA promoter sequence in the immunoprecipitated chromatin was detected by qPCR. The error bars represents standard deviations from the mean of at least three experimental replicates. Relative binding (% Input) was determined by copies of the target sequence in the immunoprecipitated chromatin respective to the copies in the inputs. The *P* values were calculated by two-tailed *t* tests comparing the LANA ChIP with control antibody. *, $P < 0.05$; **, $P < 0.01$; ***, $P < 0.001$; and ****, $P < 0.0001$. (b) A western-blot showing specificity and efficiency of anti-Flag antibody. **C.** Electrophoretic mobility shift assay (EMSA) showing LANA's binding to the HLA-DRA promoter bound with RFX complex proteins. EMSA was performed with p32 labeled double stranded X-box sequence of HLA-DRA probe and *in vitro* translated Flag tagged RFX5, RFXAP, RFXANK and Myc tagged LANA-N. Lane 1, X-box probe with rabbit reticulocyte lysate (RRL); lane 2, X-box probe with RFX complex (RFX-Cx Flag) showing binding of RFX-Cx Flag complex to the probe (arrow); lane 3, X-box probe with RFX-Cx Flag and 200x specific cold competitor probe (SCC), which competed with the binding of radiolabeled probe to RFX-Cx Flag; lane 4, X-box probe with RFX-Cx Flag and 200x non-specific cold competitor probe (NSCC) was not able to compete the binding; lane 5, X-box probe with RFX-Cx Flag and LANA-N Myc showing reduced mobility of the probe due to the binding of LANA-N Myc with RFX-Cx Flag (circle); lane 6, HLA-DRA probe with LANA-N Myc without RFX-Cx Flag showed no direct binding of LANA-N to the probe; lane 7, HLA-DRA probe with RFX-Cx Flag, LANA-N Myc, and α-Myc antibody (asterisk). α-Myc antibody further retarded the mobility of the probe bound to RFX-Cx: LANA-N protein by binding to the Myc epitope tag of LANA-N. The asterisk shows super-shifted complex; lane 8, HLA-DRA probe with RFX-Cx Flag, LANA-N Myc, and IgG control antibody. IgG control antibody failed to super-shift the mobility of the probe bound with RFX-Cx: LANA N protein complex.

The presence of LANA at the chromatin of HLA-DRA promoter was also detected in cells stably expressing LANA as the only KSHV protein. A KSHV negative B cell line, BJAB was stably transduce d with lentivirus vector expressing LANA-YFP-Flag or control YFP-Flag and selected to obtain an enriched population of cells expressing yellow fluorescing protein (YFP). Chromatin immunoprecipitation (ChIP) was performed with anti-Flag antibody from both; control YFP-Flag (BJAB-YF) and YFP-LANA-Flag expressing BJAB cells (BJAB LYF). DNA purified from the immunoprecipitated chromatin was subjected qPCR to detect the HLA-DRA promoter sequence. Detection of HLA-DRA promoter in the chromatin from BJAB with YFP-

LANA-Flag but not in YFP-Flag (Fig. 5B, panel a), confirmed specific association of LANA with HLA-DRA promoter. Immunoprecipitating YFP-LANA-Flag and YFP-Flag were detected with anti-Flag antibody (Fig. 5B, panel b). Since LANA bound to the chromatin of HLA-DRA promoter in BJAB cells expressing LANA as the sole KSHV protein, it confirmed that LANA associates with HLA-DRA promoter without the aid of any other KSHV episome. This data further confirmed our findings that LANA can associate with RFX proteins independent of the involvement of other viral components.

Binding of LANA to the HLA-DRA promoter was further established by an electrophoretic mobility shift assay (EMSA). For EMSA, radiolabelled double stranded RFX complex binding sequence (X-Box sequence) of HLA-DRA promoter was used as a probe (55). RFX complex proteins- RFX5, RFXAP and RFXANK, as well as LANA-N were translated with cold methionine *in vitro* to ensure that these proteins were free of other cellular proteins. Radiolabeled X-box sequence (probe) showed binding with RFX complex (RFX-Cx) as detected by a specific band (Fig. 5C, lane 2, arrow). The binding of RFX-Cx with radiolabeled probe was eliminated by an addition of 200 fold excess of specific cold competitor, SCC (Fig. 5C, compare lanes 2 with 3), but not with a similar fold excess of non-specific (scrambled) probe (non-specific cold competitor, NSCC) (Fig. 5C, compare lanes 2 with 4). This confirmed that RFX-Cx specifically binds with X-box sequence of the probe. Addition of *in vitro* translated RFX binding domain of LANA (LANA-N; 1-340aa) to the RFX-Cx bound probe further retarded the mobility of the complex (Fig. 5C, lane 5, circle), confirming the association of LANA-N with RFX-Cx bound to the X-box sequence of the HLA-DRA promoter. Since LANA-N, without the RFX complex, was unable to alter the mobility of free probes (Fig. 5C, lane 6) it

confirmed that LANA-N can not bind directly to the X-box sequence of HLA-DRA promoter but through its association with the components of RFX complex. Specificity of LANA-N's association with the RFX-Cx bound to the radiolabelled probe was determined by adding α-Myc antibody to the myc epitope tag of LANA-N (Fig. 5C, lane 7). The mobility of the complex was further retarded (super shifted) in the presence of α-Myc antibody but not with mouse IgG (control antibody) (Fig. 5C, asterisk, compare lane 7 with 8). This confirmed that LANA-N forms a complex with the components of RFX complex at the HLA-DRA promoter.

**LANA reduces the transcriptional activity of HLA-DRA promoter**

Expression of MHC II genes is mainly controlled at the transcriptional level by binding of the MHC II regulatory proteins including the proteins of RFX complex at the MHC II promoters (62). Since LANA interacted with the RFX complex bound to the HLA-DRA promoter, we wanted to investigate whether the presence of LANA affects the activity of HLA-DRA promoter to alter the expression of MHC II molecules. To determine LANA's affect, a dual luciferase reporter assays were performed using core HLA-DRA promoter that contained the essential *cis*-elements required for the transcription of HLA-DRA gene (63, 64). HLA-DRA reporter assay was performed in two different cell lines: 293L cells, a non antigen-presenting cells chosen because of the ease of transfection; and DG-75 cells, an antigen presenting B cells. The results of promoter reporter assay revealed that CIITA was able to activate the HLA-DRA promoter activity in both the cell lines, as expected (Fig. 6A and B, lane 2). Co-expression of LANA in the cells expressing CIITA reduced the luciferase activity, determined by the relative luciferase units in both 293L and DG75 cell lines. An

increasing amount of LANA expression vector subsequently reduced the HLA-DRA promoter activity in a dose dependent manner (Fig. 6A and B, lanes 3, 4 and 5). Importantly, the highest concentrations of LANA, used in this assay completely

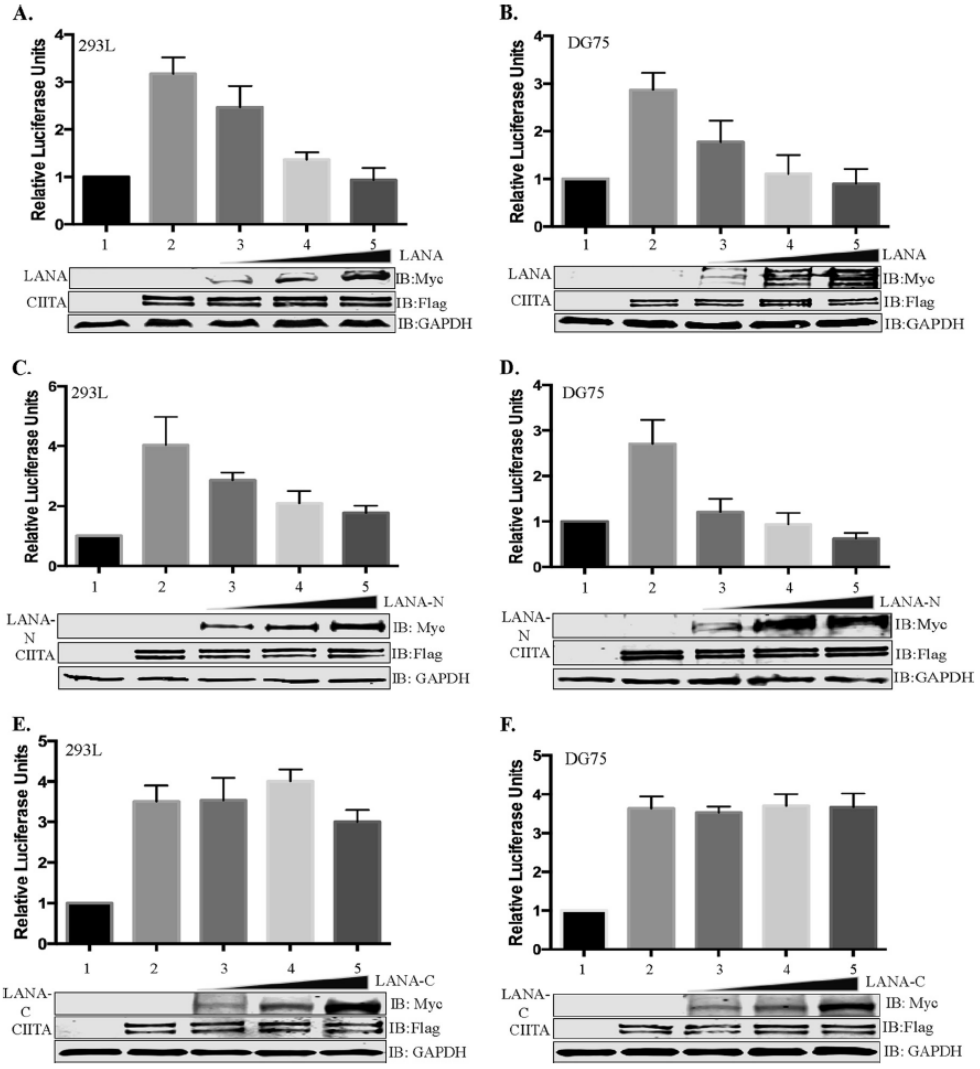


FIG 6 LANA inhibits transcriptional activity of the HLA-DRA promoter. Luciferase reporter assays show a dose-dependent reduction of the luciferase activity mediated by the HLA-DRA promoter when CIITA-expressing cells were cotransfected with full-length LANA or the amino-terminal region of LANA but not with the carboxy-terminal region of LANA. For the reporter assay, the HLA-DRA promoter fused with the luciferase reporter was transiently transfected into HEK293L cells (A, C, and E) or DG75 cells (B, D, and F). The cells were cotransfected with CIITA to stimulate the HLA-DRA promoter along with either full-length LANA (A and B), the RFXAP-interacting domain of LANA, the amino-terminal domain of LANA (C and D), or the carboxy-terminal domain of LANA (LANA-C) (E and F). The cell lysates were used for measuring luciferase activities using a dual-luciferase assay kit. Relative luciferase units were calculated relative to the basal promoter activity. Lane 1, basal DRA-luciferase activity; lane 2, CIITA-stimulated DRA-luciferase activity; lane 3, CIITA-stimulated DRA-luciferase activity with 1 μg of LANA or a truncation (LANA-N or LANA-C); lane 4, CIITA-stimulated DRA-luciferase activity with 2 μg of LANA or a truncation (LANA-N or LANA-C); lane 5, CIITA-stimulated DRA-luciferase activity with 3 μg of LANA or a truncation (LANA-N or LANA-C). The error bars represent standard deviations of the means from at least three experimental replicates. Equal amounts of cell lysates from each experimental set were used for the detection of overexpressed CIITA and LANA proteins. The GAPDH immunoblot shows equal loading of the cell lysates.

abrogated the CIITA stimulated HLA-DRA promoter activity bringing the activity comparable to basal levels (Fig. 6 A and B, compare lanes 1 with 5). The amounts of over

expressed CIITA (by CMV promoter) was comparable among those samples with increasing LANA amounts confirmed that inhibition in HLA-DRA promoter was not due to a reduced levels of CIITA in those cells (Fig. 6A and B, IB: Flag). Detection of LANA by anti-Myc immune-blot showed increasing amounts of LANA in the lysate. Since the amino-terminal domain of LANA was able to bind with RFX complex, we wanted to determine whether would be sufficient to inhibit the HLA-DRA promoter activity similar to LANA full-length. To test this, we expressed increasing amounts of LANA-N in both 293L and DG75 cells, which showed similar effect on reducing the HLA-DRA promoter activity as full length LANA (Fig. 6C and D, lanes 3, 4 and 5). In contrast, the C-terminal domain of LANA, which did not bind to CIITA complex, was unable to appreciably reduce the HLA-DRA promoter activity even high levels of LANA-C expression (Fig. 6E and F). Since comparable amounts of CIITA were overexpressed in all the test samples, abrogation of promoter activity by full-length LANA and LANA-N is most likely due to the inhibition of CIITA's recruitment to the enhanceosome because of LANA binding with RFX complex. Dose dependent inhibition of the HLA-DRA promoter activity may suggest a competition between LANA and CIITA to bind with the RFX complex.

**LANA downregulates the expression of MHC II molecules**

Since RFX proteins are crucial for the expression of MHC II molecules and the expression of LANA inhibited the activity of one of the promoter (HLA-DRA) encoding MHC II gene, we hypothesized that binding of LANA with the components of RFX complex may have downstream effect on the transcription of MHC II molecules. We therefore analyzed the levels of MHC II transcripts in two antigen-presenting cells, BJAB and THP-1 stably expressing LANA through a lentiviral vector. Total RNA extracted

from the control (YFP-Flag, YFP) and LANA (LANA-YFP-Flag, LYF) cells were subjected for the analysis of MHC II genes using quantitative real-time PCR (qRT-PCR) assay. Since LANA also down regulates the expression of CIITA to consequently repress the expression of MHC II molecules (17), we took that lower levels of CIITA into account for determining the levels of HLA genes by normalizing the levels of CIITA in LANA expressing cells with the control cells. While it was intricate to distinguish the percentages of MHC II down-regulation due to LANA's binding with RFX complex from the reduced expression of CIITA (LANA mediated down regulation of CIITA promoter) (17), we presumed that normalized levels of CIITA would yield comparable levels of MHC II genes, if no other mechanism involved. Therefore, we calculated the levels of MHC II genes by determining the ratios of CIITA in LANA expressing cells, which was $0.6^{\pm}0.1$ as compared to the control cells. To compensate for the reduced levels of CIITA in LANA expressing cells, the levels of MHC II genes were determined by multiplying the ratios of MHC II genes with 1.66 (CIITA levels were reduced to 0.6 fold, therefore, the multiplication factor was 1/0.6=1.66). Importantly, the transcripts levels of all the classical MHC II genes (HLA-DRA, HLA-DRB, HLA-DPA, HLA-DPB, HLA-DQA and HLA-DQB) were down regulated significantly, even after normalizing the CIITA levels, in LANA expressing BJAB as well as THP-1 cells (BJAB-LYF and THP-LYF) compared to the respective control cells, BJAB-YFP and THP-YFP (Fig. 7 A and C). The results of the reporter assays, where CIITA was expressed through a CMV promoter (the levels of CIITA was unaltered with LANA), showing reduction in HLA promoter activity as well as the above CIITA levels normalized MHC II expression strongly advocates for an involvement of additional mechanisms in down regulation of MHC II genes by LANA

along with reduction of CIITA expression. Prevention of binding of CIITA to HLA promoters is one such plausible mechanism. The western blot analysis of MHC II levels in these LANA expressing, BJAB and THP-1 cells showed reduced levels of MHC II expression as compared to the control, YFP expressing cells (Fig. 7B and D). Immune blot for the detection of LANA-YFP-Flag and YFP-Flag in these BJAB and THP-1 cells confirmed the expression of LANA (Fig. 7B and 7D). Furthermore, the expressions of MHC II genes in KSHV infected PEL cells, BC-3 and BCBL-1, showed significantly reduced levels as compared to a KSHV negative, BJAB cells, analyzed by normalizing the levels of CIITA (Fig. 7E). We were unable to detect the mRNA of HLA-DQB in KSHV infected cells, even after multiple attempts, therefore are excluded from the relative mRNA calculation in this figure. Immune detection of MHCII expression in KSHV infected cells showed very low levels as compared to the KSHV negative cells, BJAB (Fig. 7F). These results are in corroboration with the results published by Cai et al (17), which showed reduced expression of MHC II proteins during KSHV infection.

**LANA interferes with the association of CIITA to RFXAP**

Since LANA interacted with RFX complex at the HLA-DRA promoter and down regulated the expression of MHC II molecules through mechanisms in addition to CIITA downregulation, we hypothesized that LANA might interfere with the binding of CIITA to RFXAP to disrupt the formation of a functional enhanceosome. To test this hypothesis, we immunoprecipitated CIITA and analyzed co-immunoprecipitating RFXAP in presence or absence of RFXAP binding region of LANA (LANA-N) in an overexpression system using HEK293T cells (Fig. 8A). As expected, RFXAP efficiently co-immunoprecipitated with CIITA in absence of LANA-N, but not with the control (Fig.

8A, IB: Myc panel, lanes 5 and 6). However, the amounts of co-immunoprecipitating RFXAP were significantly reduced in the presence of LANA-N (Fig. 8A, IB: Myc panel, lanes 7 and 8). The binding of RFXAP to CIITA was very weak at increased amounts of LANA-N (Fig. 8A, IB: Myc panel, lane 8) confirming that LANA's binding to RFXAP blocked the binding of CIITA to RFXAP. Furthermore, LANA did not co-immunoprecipitate with CIITA indicating that LANA does not directly interact with CIITA (Fig. 8A, IB: Myc panel, lanes 7 and 8).

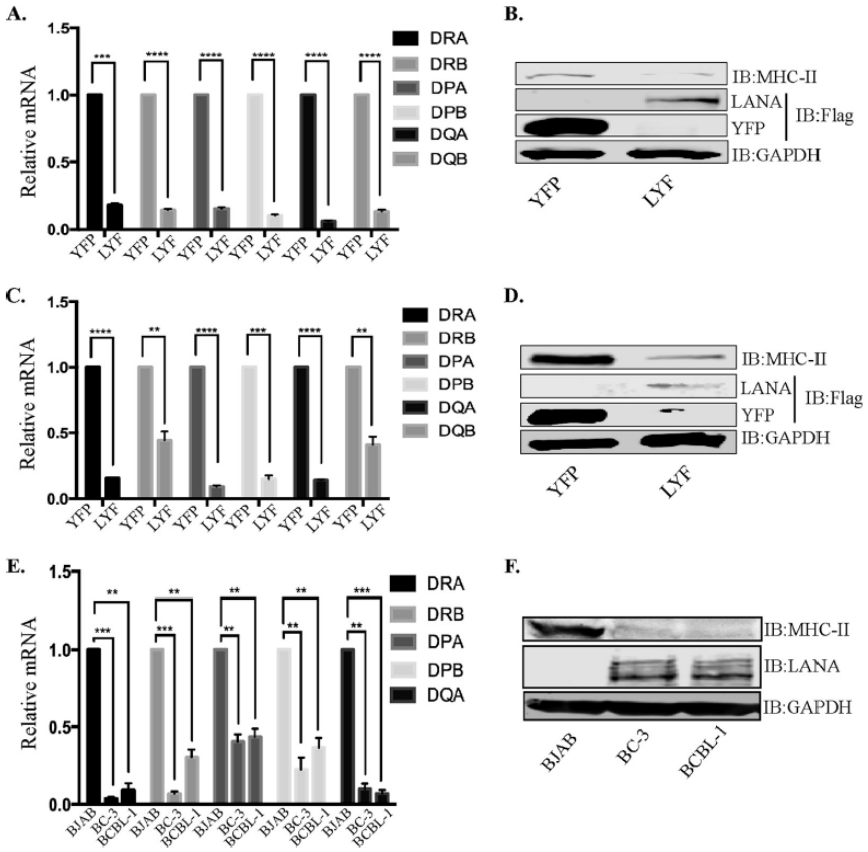


FIG 7 LANA downregulates the expression of MHC-II molecules. (A, C, and E) Relative mRNA levels of different HLA genes in LANA-expressing BJAB (LYF) cells compared to control BJAB cells with YFP (YFP) (A), in LANA-expressing THP-1 (LYF) cells compared to control THP-1 cells with YFP (C), and in KSHV-infected BC-3 and BCBL-1 PEL cells compared to BJAB cells (E). The mRNA levels were quantified by using qRT-PCR, and the expression levels of HLA genes were normalized to CIITA levels, as explained in Results. The errors bars represent standard deviations of the means from at least three experimental replicates. *P* values were calculated by two-tailed *t* tests comparing LYF cells with control YFP cells. **, $P < 0.01$; ***, $P < 0.001$; ****, $P < 0.0001$. (B, D, and F) Immune detection of MHC-II expression in BJAB-LYF and BJAB-YFP cells (B), in THP-1 LYF and YFP cells (D), and in BJAB, BC3, and BCBL1 cells (F). Flag-tagged LANA (YFP-LANA-Flag) and YFP were detected with an anti-Flag antibody, GAPDH, to show equal loading of the cell lysates. LANA in PEL cells was detected by using a rat anti-LANA antibody.

A similar immunoprecipitation assay was also performed using cell-free system where CIITA, components of RFX complex and LANA-N terminus (1-340aa) were translated *in vitro*, for a co-immunoprecipitation assay with CIITA in presence of LANA-N (1-340aa). Immunoprecipitation of CIITA with anti-Flag antibody co-precipitated RFX5 (component of RFX complex) (Fig. 8B, lane 6, RFX5 panel). The other components of RFX complex did not co-precipitate with CIITA in this cell-free system indicating that direct interaction between CIITA and RFXAP/RFXANK is very weak when these proteins are translated in *vitro*. Interestingly, co-immunoprecipitation of RFX5 was significantly reduced in the presence of LANA-N (Fig. 8B, lanes 7 and 8, RFX5 panel), confirming that LANA's binding with the components of RFX complex results into a reduced binding of CIITA to the RFX complex.

CIITA does not posses any direct DNA binding domain but is recruited to the MHC II promoters via interactions with the proteins of MHC II enhanceosome complex including the proteins of RFX complex (44). We speculated that a reduction in the binding of CIITA to the components of RFX complex would result into a reduced binding of CIITA to the enhanceosome of MHC II promoter. To confirm this, we performed anti-CIITA ChIP from BJAB cells stably expressing LANA (BJAB-LYF) and compared the binding of CIITA onto MHC II promoter in cells without LANA (BJAB-YF). qPCR analysis of the ChIP assay revealed that association of CIITA with HLA-DRA promoter was significantly reduced in LANA expressing BJAB cells as compared to the cells without LANA (Fig. 8C, panel a).

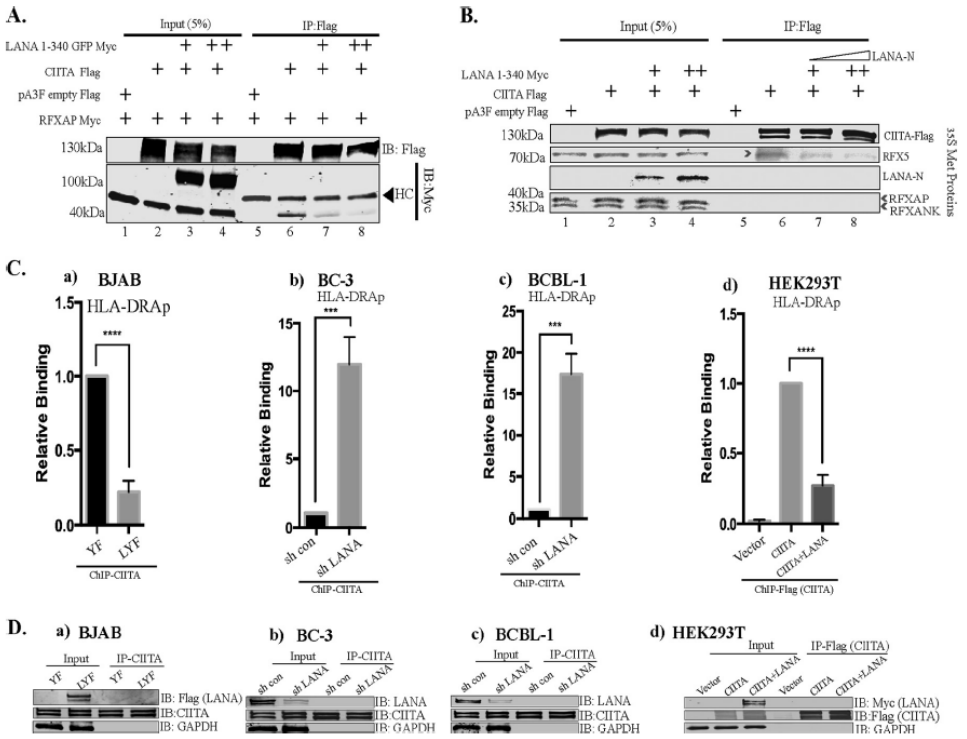


**FIG 8** LANA interferes with the association of CIITA and RFXAP. (A) Coimmunoprecipitation assay showing reduced associations of RFXAP with CIITA in the presence of LANA. Flag-tagged CIITA, Myc-tagged RFXAP, and Myc-tagged LANA-N (aa 1 to 340) were used in this competitive coimmunoprecipitation assays after transfection into HEK293T cells. CIITA was immunoprecipitated from the cellular lysates by using an anti-Flag antibody. The proteins were resolved on SDS-PAGE gels, and coimmunoprecipitated proteins were detected by using anti-Myc and anti-Flag antibodies. HC, heavy chain. (B) Coimmunoprecipitation assay showing reduced association of RFX5 with CIITA in an *in vitro* binding assay. *In vitro*-translated and [$^{35}$S]methionine-labeled LANA-N (aa 1 to 340)–Myc, RFXAP-Myc, RFX5-Myc, RFXANK-Myc, and CIITA-Flag were used for *in vitro* binding assays. The proteins were allowed to interact overnight at 4°C, followed by immunoprecipitation with anti-Flag antibody (CIITA). The bound protein complexes were resolved on SDS-PAGE gels, followed by detection by autoradiography. (Ca) ChIP assays showing reduced binding of CIITA to the HLA-DRA promoter in LANA-expressing BJAB cells compared to control YFP-expressing cells. (b and c) Relative binding of CIITA in LANA-depleted and control KSHV-infected BC-3 (b) and BCBL-1 (c) PEL cells. (d) Relative binding of CIITA on the chromatin HLA-DRA promoters in the expression system. The HLA-DRA-Luc vector and RFX components (Myc tagged) were transfected with the Flag vector (control), CIITA-Flag, or CIITA-Flag with LANA-Myc in HEK293L cells, followed by a ChIP assay with anti-Flag (CIITA) antibody. The amount of CIITA-bound HLA-DR was reduced in LANA-expressing cells. The error bars represent standard deviations of the means from at least three experimental replicates. *P* values were calculated by two-tailed *t* tests comparing treated to control cells. ***, $P < 0.001$; ****, $P < 0.0001$. (D) Immunoblot showing the expression of LANA and CIITA and the immunoprecipitation efficiency of anti-CIITA antibody used for ChIP assays. (b and c) LANA depletion in KSHV-infected BC-3 (b) and BCBL-1 (c) PEL cells by the lentiviral vector showing efficient knockdown of LANA compared to shControl cells. (d) Immune detection of LANA and CIITA in inputs and immunoprecipitated cells with anti-Myc and anti-Flag antibodies, respectively.

The efficiency of anti-CIITA antibody for immune precipitation were analyzed from BJAB cells expressing LANA-YFP-Flag and YFP-Flag, which showed comparable levels of CIITA in both the cells (Fig. 8D, IB: CIITA, panel a). LANA was detected with anti-Flag antibody in BJAB-LYF cells, as expected (Fig. 8D, IB: Flag, panel a). Furthermore, in PEL cell lines, BC-3 and BCBL-1, shRNA mediated reduction of LANA resulted into an increased association of CIITA to the chromatin of HLA-DRA (Fig. 8C, panels b and c), confirming a direct role of LANA in CIITA binding to the HLA-DRA

promoter. shRNA for LANA significantly reduced the levels of LANA confirmed by anti-LANA immune blot (Fig. 8D, panel b and c). Anti-CIITA antibody precipitated comparable amounts of CIITA from sh control (sh con) or sh LANA cells (Fig. 8D, panels b and c), confirming that reduced levels of HLA-DRA promoter was not due to reduced amounts of immunoprecipitated CIITA. While these results showed that the presence of LANA abrogates and depletion of LANA facilitates CIITA binding to the promoter to regulate MHC II expression, we performed a ChIP assay by expressing CIITA driven by CMV promoter (to obtain equal expressions of CIITA in all the samples) to rule out the possibility that reduction in CIITA binding to the HLA-DRA promoter was not due to a reduced expression of CIITA by LANA. We overexpressed Flag tagged CIITA along with or without LANA in cells transfected with HLA-DRA promoter plasmid and the components of the RFX complex in HEK293T cells by transient transfections. qPCR analysis of the HLA-DRA promoter from the chromatin immunoprecipitated with anti-Flag (CIITA) showed reduced levels of CIITA bound HLA-DRA promoter in cells expressing LANA confirmed that LANA directly reduced the binding of CIITA to HLA-DRA chromatin (Fig. 8C, panel d). Expression and immunoprecipitation of LANA and CIITA were detected by anti-Myc and anti-Flag immunoblots, respectively (Fig. 8D, panel d).

Finally, to gain a better understanding of the mechanism by which LANA could be interfering with the recruitment of CIITA and the assembly of functional enhanceosome, we investigated whether binding of the components of RFX complex to the enhanceosome is affected in presence of LANA.

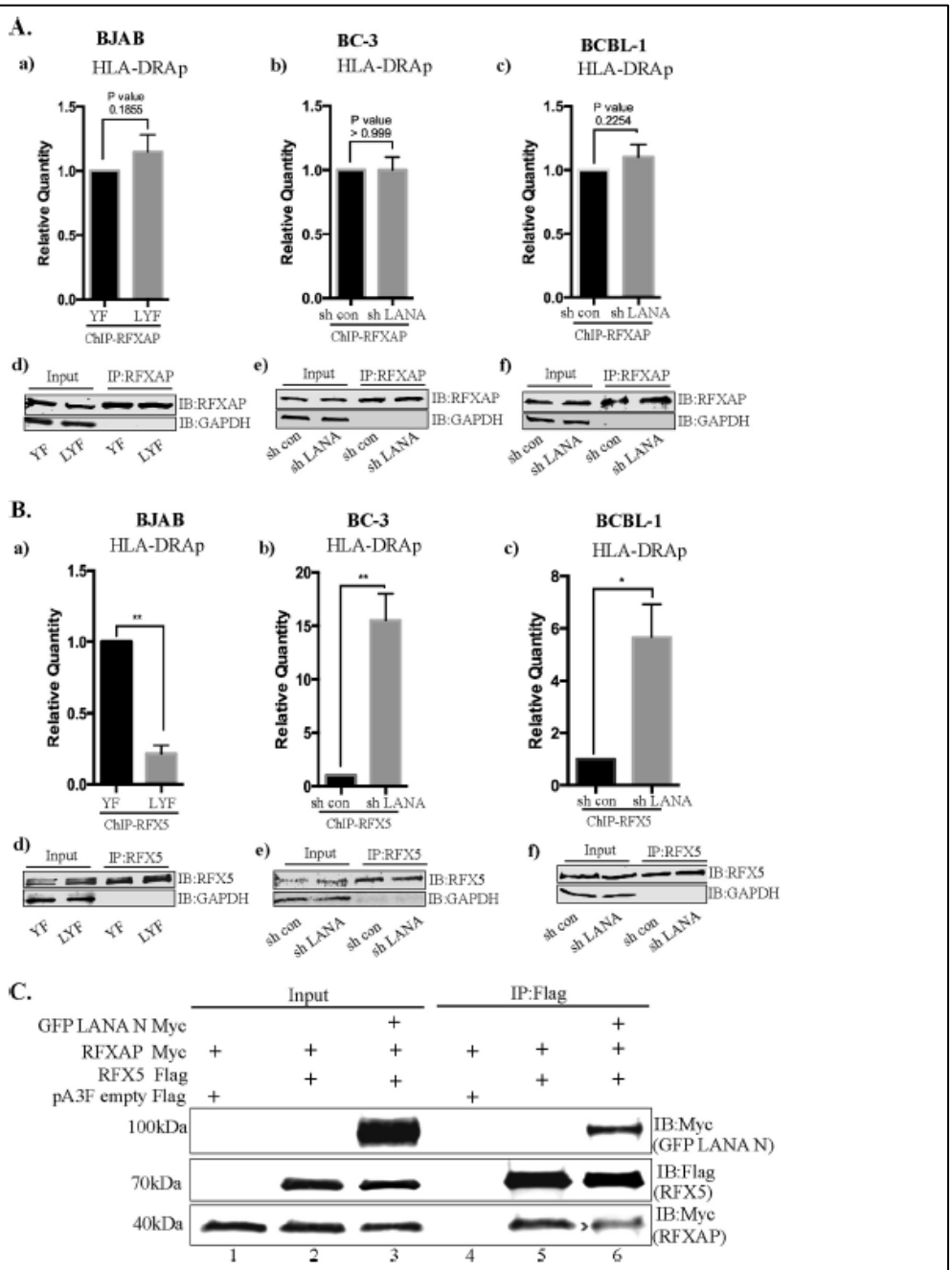


**FIG 9** Binding of RFXAP and RFX5 to the HLA-DRA promoter in the presence of LANA. (Aa) ChIP assays coupled with qPCR analysis showing binding of RFXAP to the HLA-DRA promoter in the presence of LANA in KSHV-negative BJAB cells stably expressing LANA (LYF) or control cells with YFP expression (YFP). (b and c) LANA depletion in KSHV-infected BC3 (b) and BCBL1 (c) PEL cells by a lentiviral vector. RFXAP ChIP in BJAB-YFP and LYF cells as well as with or without LANA knockdown in BC-3 and BCBL-1 cells showed similar binding of RFXAP. The error bars represents standard deviations of the means from at least three experimental replicates. *P* values calculated by two-tailed *t* tests showed no significant difference between analyzed samples. (d to f) Efficient immunoprecipitation with anti-RFXAP antibody. (Ba) ChIP assay with anti-RFX5 antibody showing reduced copy numbers of the HLA-DRA promoter bound to RFX5 in LANA-expressing BJAB cells. (b and c) The association of RFX5 with the HLA-DRA promoter was increased when LANA was knocked down in BC-3 (b) and BCBL1 (c) cells compared to cells without LANA knockdown. The error bars represent standard deviations of the means from at least three experimental replicates. *P* values were calculated by two-tailed *t* tests. *, $P < 0.05$; **, $P < 0.01$. (d to f) Efficient immunoprecipitation with anti-RFX5 antibody. (C) LANA-N disrupts the association of RFX5 with RFXANK. Immunoprecipitation of RFX5 (Flag tagged) in the presence of LANA-N (GFP–LANA-N–Myc) reduced the amounts of coprecipitating RFXANK compared to those in the cells without LANA-N (middle, compare lane 6 to lane 5).

To address this, we analyzed the binding of RFXAP and RFX5 on HLA-DRA promoter by performing ChIP assays on cells stably expressing LANA and also from PEL cells depleted with LANA. We did not observe any significant difference in the association of RFXAP to the HLA-DRA promoter in BJAB cells without or with LANA expression, as BJAB-YF and LYF showed almost similar levels of chromatin bound HLA-DRA promoter (Fig. 9A, panel a). Depletion of LANA by shRNA did not significantly change the association of RFXAP to HLA-DRA in both the PEL cell lines, BC-3 and BCBL-1, as shControl (sh con) and shLANA cells showed similar levels of chromatin bound HLA-DRA promoter (Fig. 9A, panels b and c). Efficiencies of RFXAP immunoprecipitations from BJAB and PEL cells showed comparable levels of RFXAP in respective set of cells (Fig. 9A, panels d, e and f). These results suggest that LANA interacts with RFXAP bound to the HLA-DRA promoter and does not interfere with the binding of RFXAP to HLA-DRA promoter.

Since, the interaction of RFX5 with RFXAP is necessary for the binding of RFX5 to the MHC II promoters (65), and LANA binds to the same domain of RFXAP that is required for RFXAP's interaction with RFX5; we speculated that LANA's association with RFXAP may result into a reduced binding of RFX5 to HLA-DRA promoter. Interestingly, the association of RFX5 to the chromatin of HLA-DRA promoter was significantly reduced in BJAB cells expressing LANA (BJAB-LYF) as compared to control (BJAB-YF) cells (Fig. 9B, panel a). Additionally, RFX5 binding to chromatin of HLA-DRA promoter was enhanced in LANA depleted KSHV positive, BC-3 and BCBL-1 cells (Fig. 9B, panels c and d). Immunoprecipitation with anti-RFX5 antibody showed comparable levels of RFX5 proteins in respective sets of cells (Fig. 9B, panels d, e and f).

Disrupted binding of RFX5 with RFXAP component was further confirmed in a co-immunoprecipitation assay expressing LANA-N (RFXAP binding domain of LANA). While RFX5 but not the control vector efficiently co-immunoprecipitated RFXAP (Fig. 9C, lanes 4 and 5), co-immunoprecipitation of RFXAP with RFX5 was reduced in the presence of LANA-N (Fig. 9C, RFXAP panel, compare lane 6 with lane 5). A detectable level of co-immunoprecipitating LANA-N with RFX5 (Fig. 9C, GFP LANA-N panel, lane 6) further supported that LANA's binding with RFX components. Collectively, these data show that binding of LANA with the components of RFX complex inhibits binding of RFX5 and CIITA without affecting the binding of RFXAP to the HLA-DRA promoter.

**Discussion:**

KSHV has evolved excellent immune evasion and immune modulation strategies that allow it to establish a life long latency. Some of these strategies are identified but KSHV most likely have many more strategies up its sleeve that can sabotage host immunity. Of these, targeting MHC II antigen presentation pathway seems to be very crucial because MHCII molecules can present virally derived antigens to CD4+ T lymphocytes (66) and turn-on the adaptive antiviral immune responses. In addition to coordinating adaptive immune responses, activated CD4+ T cells also play a direct cytolytic role in killing the infected cells displaying viral antigens in conjugation with MHC II molecules (67). So far, two KSHV latent proteins vIRF3 and LANA have been shown to inhibit MHC II antigen presenting pathway (17, 23, 25). LANA was previously reported to inhibit the expression of MHC II molecules via suppression of CIITA transcripts (17). The data presented here establishes a yet another mechanism used by LANA for evading the host immune system. Here, we show that LANA disrupts the assembly of functional MHC II

enhanceosome by interacting with the components of RFX complex and thereby contributes to the inhibition of MHC II pathway. To the best of our knowledge, this is the first study that shows a disruption of functional MHC enhanceosome by any virus to subvert the host immunity.

Expression of MHC II molecules is primarily controlled at the level of transcription by a set of highly conserved transcription factors (29). Of these, the transcription factors of notable importance are CIITA and the three components of RFX complex, RFX5, RFXAP and RFXANK. The fact that defects in any of these four genes can result into a bare lymphocyte syndrome (BLS) characterized by severely reduced expression of MHC II genes, highlights the significance of these four proteins in regulation of MHC II genes (66, 68, 69). Transcription of all MHC II genes is highly coordinated and is strictly contingent upon binding of CIITA to the promoters of MHC II. CIITA is a non-DNA binding MHC II transactivator that is recruited to the promoters of MHC II genes via protein-protein interactions with the transcriptional factors pre-assembled at the promoters of MHC II genes, termed as MHC II enhanceosome (29). RFX proteins are very important components of MHC II enhanceosome and binding of CIITA to the promoters of MHC II requires its interactions with the components of the RFX complex. Binding of CIITA to MHC II promoters is conceived to be absolutely essential for the expression of MHC II genes, as so far alternate pathways for MHC II expression are not known to exist. Targeting the RFX proteins and CIITA is therefore a very effective strategy for escaping the host adaptive immunity. *Cai et al* have previously reported that LANA deregulates CIITA transcription resulting into down regulate MHC II expression (17). In this study, we have identified a novel mechanism by which KSHV

LANA disrupts the association of functional enhanceosome to suppress the transcription of MHC II genes. Our report shows that LANA binds to the components of RFX complex, which prevents the recruitment of trans-activator, CIITA onto the promoters of MHC II genes to form a functional enhanceosome for down regulating the expression of MHC II genes.

We identified RFX transcription factors as LANA interacting protein in a yeast-two-hybrid screen. We further validated the interactions between LANA and RFX proteins using *in-vivo* and *in vitro* assays. Our data shows that LANA directly interacts with all the three components of RFX complex-RFX5, RFXAP and RFXANK and prevents binding of CIITA to the promoters of MHC II genes. While LANA can bind to all the three components of RFX complex, it has higher affinity to RFXAP.

We demonstrated that the domain responsible for LANA's interactions with RFX transcription factors is in the N terminal domain of LANA. Cai et al have reported that LANA's C terminal domain is involved in the downregulation of MHC II by binding with IRF-4 (17). Involvement of multiple domains of LANA in the downregulation of MHC II emphasizes the importance of inhibiting MHC II pathway during KSHV latency. Since the amino terminal domain of LANA is known to associate with host chromatin (51, 70) it raised the possibility that LANA might be interacting with the RFX proteins indirectly through chromatin binding factors. However, the interactions between the N terminus of LANA and RFX proteins was verified in cell free system, by using *in vitro* translated LANA and RFX proteins, which confirmed that these interactions are direct and independent of any cellular or viral factors.

RFXAP contains three biochemically distinct regions in its primary sequence including an acidic region, a basic region and a glutamine rich region. Of these regions, the C-terminal region, which includes the basic and the glutamine rich regions, is a highly conserved region (71). This region is both necessary and sufficient for its interactions with other components of RFX complex, RFX5 and RFXANK (32, 41, 59, 60, 72). Since LANA bound to the C-terminal region of RFXAP, we hypothesized that binding of LANA to the C- terminus of RFXAP may disrupt the assembly of functional RFX complex by reducing its association with either RFX5 or RFXANK or both. In support of this hypothesis, when we pulled down *in vitro* translated components of RFX complex through LANA, we observed a distorted stoichiometry of the RFX complex marked by a noticeably reduced association of RFX5 in the immunoprecipitated complex. This suggests that binding of RFXAP to LANA partially excludes RFX5 from the RFX complex, which have important implications on recruiting CIITA to the MHC II promoters because RFX5 and RFXANK, but not RFXAP, are known to directly interact with CIITA (43, 59, 71, 73). Indeed, the association of CIITA at HLA-DRA promoter was reduced in the presence of LANA in ChIP assays. We also demonstrated that co-precipitation of RFX5 was reduced in presence of LANA when *in vitro* translated components of the RFX complex were co-immunoprecipitated with CIITA. RFXAP did not directly co-immunoprecipitate with CIITA in a cell-free system, probably due to the lack of direct interactions between CIITA and RFXAP in a cell-free system, or due to lack of proper post-translational modifications of these two proteins. However, when tested *in vivo*, co-immunoprecipitation of RFXAP with CIITA was reduced in a co-

immunoprecipitation assay, affirming that the association of CIITA with RFX proteins was reduced in the presence of LANA.

We further showed that LANA associates with MHC II promoters in order to disrupt the binding of CIITA with RFX complex using anti-LANA ChIP assay. However, LANA does not directly associate with the X box DNA sequence, a conserved *cis* acting RFX complex binding domain on MHC II promoters. Instead, LANA is recruited to the MHC II promoters by binding with the RFX proteins as evident by the results of electrophoretic mobility shift assays performed using *in vitro* translated RFX proteins and the amino terminal domain of LANA. We anticipated that association of LANA at MHC II promoters inhibits MHC II promoter activity, which subsequently results in reduced transcription and expression of MHC II genes. As expected, presence of full length as well as the N-terminus of LANA, which binds to RFX complex proteins, efficiently and dose dependently reduced the HLA-DRA promoter activity in luciferase reporter assays. While all the necessary component of MHC II transcription machinery is constitutively expressed in all cell types, expression of CIITA is restricted only to professional antigen presenting cells. However, the expression of CIITA can be induced in most cell types by IFN-ϒ treatment. Hence, in order to induce HLA-DRA promoter activity, we treated the cells with IFN-ϒ, which induced CIITA expression and HLA-DRA promoter activity but was suppressed in the presence of LANA (data not shown). While we observed an efficient inhibition of the HLA-DRA activity induced by IFN-ϒ treatment in presence of LANA, the report by Cai et al (17) raised the possibility that this inhibition could be because of reduced expression of CIITA, as LANA inhibits the activity of CIITA promoters pIII and PIV. In order to alleviate the effect of LANA on CIITA repression

and subsequent reduction of HLA promoter, we modified our luciferase reporter assays and expressed the CIITA from a constitutively active CMV promoter, which showed comparable expression in presence or absence of LANA. Our data showed that even when the CIITA was expressed through CMV promoter, the activity of HLA-DRA promoter was efficiently and dose dependently downregulated by the full length as well as amino-terminal domain of LANA. These results confirm that in order to ensure efficient inhibition of MHC II transcription, LANA interferes with the binding of existing CIITA to the HLA promoters and disrupts the formation of functional enhanceosome. In our co-immunoprecipitation experiments, we did not find CIITA interacting with LANA suggesting that LANA does not directly associate with CIITA. Taken together, these data confirm that LANA binds with RFX proteins, and thereby interferes with the recruitment of CIITA to MHC II promoters. The eventual effect of LANA mediated interference of CIITA binding to MHC II promoters is reduced transcription and expression of MHC II genes.

In an attempt to identify the mechanism by which LANA disrupts MHC II enhanceosome, we discovered that LANA's association with RFXAP did not prevent the association of RFXAP with HLA-DRA promoter but it reduced the binding of RFX5 with RFXAP, as demonstrated by ChIP assay. Reduced binding of RFX5 to HLA-DRA promoter in presence of LANA was most likely due to LANA's binding to RFXAP in the same region as RFX5 binding, thus disrupting RFXAP's association with RFX complex. Notably, association of RFXAP with RFX5 is required for relieving the auto-inhibition of RFX5 that prevents the DNA binding activity of RFX5 (65). Our ChIP data supported this hypothesis as association of RFX5 with HLA-DRA promoter was reduced in the

presence of LANA. Based on the overall results of this study, we propose a model (Fig. 10) in which LANA disrupts the assembly of functional enhanceosome necessary for the expression of MHC II genes.

Our findings about LANA's association with the components of RFX complex have implications on the expression of MHC I molecules as well. Transcription of MHC I genes is regulated by the binding of NLRC5 transcriptional co-activator to MHC I promoter in a fashion similar to the regulation of MHC II genes by CIITA (74). NLRC5 mediated expression of MHC I requires its association with RFX proteins for optimal transcription of MHC I genes (74). Hence, disruption of RFX complex by LANA may result into a reduced binding of NLRC5 to MHC I enhanceosome thus leading to a reduced expression of MHC I genes as well. MHC I antigen presentation is critical for activation of CD8+ T cells which has also been shown to play an important role in controlling KSHV infections (75, 76). The role of LANA in inhibiting MHC I through this mechanism remains to be explored but targeting RFX complex by KSHV appears to help the virus in dodging both MHC I and MHC II antigen presenting pathways and consequently evading the CD4+ T and CD8+ T cell immunities simultaneously. Given that collective T cell immunity is very critical in mounting anti-viral host response (18, 77, 78), targeting RFX complex gives an edge to KSHV in establishing life-long persistence in the infected host.

In summary, we identified a new mechanism used by LANA to inhibit the expression of MHC II molecules. LANA disrupts the functional MHC II enhanceosome by binding with the RFX transcription factors and thus reduces the binding of master

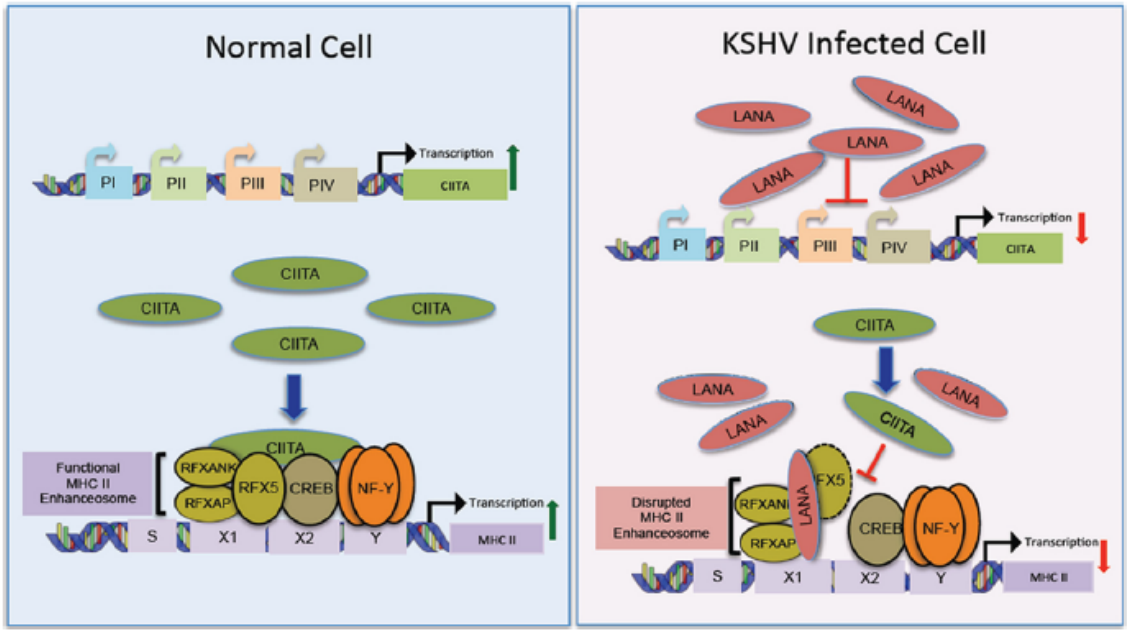


**FIG 10** Proposed model of MHC-II transcriptional downregulation through interactions of LANA with RFX proteins. MHC-II expression is regulated predominantly at the transcriptional level, and transcription of MCH-II genes is strictly contingent upon the binding of a non-DNA-binding transactivator, CIITA, to the promoters of MHC-II genes. The promoters of all the MHC-II genes contain a highly conserved *cis*-acting module that consists of the S-, X1-, X2-, and Y-box sequences. A heterotrimeric RFX complex consisting of RFX5, RFXAP, and RFXANK occupies the X1 box. The X2 and Y boxes are occupied by CREB protein and trimeric NF-Y complexes, respectively. Proper assembly of these proteins on MHC-II promoters makes a functional MHC-II enhanceosome. In normal cells, the assembled MHC-II enhanceosome initiates the transcription of MHC-II genes by recruiting CIITA to the promoters of MHC-II genes. However, in KSHV-infected cells, the KSHV latent protein LANA, as shown previously, reduces the transcriptional activity of CIITA promoters PIII and PIV, resulting in reduced expression of CIITA, which in turn contributes to an inhibition of MHC-II genes. There is an additional mechanism to inhibit the binding of residual CIITA to the promoters of MHC-II. The results of the present study show that LANA binds to the components of the RFX complex at MHC-II promoters and disrupts the assembly of these factors. The disrupted RFX complex is unable to recruit CIITA and thus mitigates the efficiency of residual CIITA in stimulating MHC-II transcription. The culminating effect of these pathways leads to a reduction in the transcription of MHC-II genes.

regulator, CIITA to the MHC II promoters. The overall effect of the disruption of functional enhanceosome is reduction in the transcription of MHC II genes leading to a lower level of MHC II expression. There may be involvement of multiple strategies by KSHV to completely block the expression of MHC II molecules on the cell surface as demonstrated previously (25). Inhibition of MHC II antigen presentation pathway is very crucial for the establishment of effective lifelong KSHV latency and hence LANA as

well as other latent proteins of KSHV are likely to target multiple immune pathways at multiple steps in order to efficiently block MHC II expression.

**Acknowledgments:**

We thank Dr. Erle S. Robertson, University of Pennsylvania, USA, for providing the cell lines and LANA expression plasmids, Dr. Jeremy Boss, Emory University School of Medicine, USA for providing RFX5-GFP plasmid, and Dr. Jenny Ting, University of North Carolina, Chapel Hill, for providing HLA-DRA-Luc promoter reporter and CIITA-Flag plasmids. This work was supported by the public health grants from NIH (CA174459 and AI105000) and American Heart Association (13BGIA14520036) to SCV. STT was partially supported by Reno Cancer Foundation and Mick Hitchcock Fellowship, University of Nevada, Reno.

**References:**

1. **Cai Q, Verma SC, Lu J, Robertson ES.** 2010. Molecular biology of Kaposi's sarcoma-associated herpesvirus and related oncogenesis. Adv Virus Res **78:**87-142.
2. **Cesarman E.** 2013. Gammaherpesviruses and Lymphoproliferative Disorders. Annu Rev Pathol.
3. **Toth Z, Brulois K, Jung JU.** 2013. The chromatin landscape of Kaposi's sarcoma-associated herpesvirus. Viruses **5:**1346-1373.
4. **Verma SC, Robertson ES.** 2003. Molecular biology and pathogenesis of Kaposi sarcoma-associated herpesvirus. FEMS Microbiol Lett **222:**155-163.
5. **Coscoy L.** 2007. Immune evasion by Kaposi's sarcoma-associated herpesvirus. Nat Rev Immunol **7:**391-401.
6. **Lee HR, Brulois K, Wong L, Jung JU.** 2012. Modulation of Immune System by Kaposi's Sarcoma-Associated Herpesvirus: Lessons from Viral Evasion Strategies. Front Microbiol **3:**44.
7. **Alibek K, Baiken Y, Kakpenova A, Mussabekova A, Zhussupbekova S, Akan M, Sultankulov B.** 2014. Implication of human herpesviruses in oncogenesis through immune evasion and supression. Infect Agent Cancer **9:**3.
8. **Dupin N, Fisher C, Kellam P, Ariad S, Tulliez M, Franck N, van Marck E, Salmon D, Gorin I, Escande JP, Weiss RA, Alitalo K, Boshoff C.** 1999. Distribution of human herpesvirus-8 latently infected cells in Kaposi's sarcoma, multicentric Castleman's disease, and primary effusion lymphoma. Proc Natl Acad Sci U S A **96:**4546-4551.

9. **Parravicini C, Chandran B, Corbellino M, Berti E, Paulli M, Moore PS, Chang Y.** 2000. Differential viral protein expression in Kaposi's sarcoma-associated herpesvirus-infected diseases: Kaposi's sarcoma, primary effusion lymphoma, and multicentric Castleman's disease. Am J Pathol **156:**743-749.
10. **Kellam P, Bourboulia D, Dupin N, Shotton C, Fisher C, Talbot S, Boshoff C, Weiss RA.** 1999. Characterization of monoclonal antibodies raised against the latent nuclear antigen of human herpesvirus 8. J Virol **73:**5149-5155.
11. **Mesri EA, Cesarman E, Boshoff C.** 2010. Kaposi's sarcoma and its associated herpesvirus. Nat Rev Cancer **10:**707-719.
12. **Verma SC, Lan K, Robertson E.** 2007. Structure and function of latency-associated nuclear antigen. Curr Top Microbiol Immunol **312:**101-136.
13. **Li X, Liang D, Lin X, Robertson ES, Lan K.** 2011. Kaposi's sarcoma-associated herpesvirus-encoded latency-associated nuclear antigen reduces interleukin-8 expression in endothelial cells and impairs neutrophil chemotaxis by degrading nuclear p65. J Virol **85:**8606-8615.
14. **Cloutier N, Flamand L.** 2010. Kaposi sarcoma-associated herpesvirus latency-associated nuclear antigen inhibits interferon (IFN) beta expression by competing with IFN regulatory factor-3 for binding to IFNB promoter. J Biol Chem **285:**7208-7221.
15. **Zaldumbide A, Ossevoort M, Wiertz EJ, Hoeben RC.** 2007. In cis inhibition of antigen processing by the latency-associated nuclear antigen I of Kaposi sarcoma herpes virus. Mol Immunol **44:**1352-1360.
16. **Kwun HJ, da Silva SR, Qin H, Ferris RL, Tan R, Chang Y, Moore PS.** 2011. The central repeat domain 1 of Kaposi's sarcoma-associated herpesvirus (KSHV) latency associated-nuclear antigen 1 (LANA1) prevents cis MHC class I peptide presentation. Virology **412:**357-365.
17. **Cai Q, Banerjee S, Cervini A, Lu J, Hislop AD, Dzeng R, Robertson ES.** 2013. IRF-4-mediated CIITA transcription is blocked by KSHV encoded LANA to inhibit MHC II presentation. PLoS Pathog **9:**e1003751.
18. **Sabbah S, Jagne YJ, Zuo J, de Silva T, Ahasan MM, Brander C, Rowland-Jones S, Flanagan KL, Hislop AD.** 2012. T-cell immunity to Kaposi sarcoma-associated herpesvirus: recognition of primary effusion lymphoma by LANA-specific CD4+ T cells. Blood **119:**2083-2092.
19. **Zuo J, Rowe M.** 2012. Herpesviruses placating the unwilling host: manipulation of the MHC class II antigen presentation pathway. Viruses **4:**1335-1353.
20. **Cresswell P.** 1994. Assembly, transport, and function of MHC class II molecules. Annu Rev Immunol **12:**259-293.
21. **Ting JP, Zhu XS.** 1999. Class II MHC genes: a model gene regulatory system with great biologic consequences. Microbes Infect **1:**855-861.
22. **Hegde NR, Chevalier MS, Johnson DC.** 2003. Viral inhibition of MHC class II antigen presentation. Trends Immunol **24:**278-285.
23. **Schmidt K, Wies E, Neipel F.** 2011. Kaposi's sarcoma-associated herpesvirus viral interferon regulatory factor 3 inhibits gamma interferon and major histocompatibility complex class II expression. J Virol **85:**4530-4537.

24. **Butler LM, Jeffery HC, Wheat RL, Long HM, Rae PC, Nash GB, Blackbourn DJ.** 2012. Kaposi's sarcoma-associated herpesvirus inhibits expression and function of endothelial cell major histocompatibility complex class II via suppressor of cytokine signaling 3. J Virol **86:**7158-7166.
25. **Zuo J, Hislop AD, Leung CS, Sabbah S, Rowe M.** 2013. Kaposi's sarcoma-associated herpesvirus-encoded viral IRF3 modulates major histocompatibility complex class II (MHC-II) antigen presentation through MHC-II transactivator-dependent and -independent mechanisms: implications for oncogenesis. J Virol **87:**5340-5350.
26. **Siegrist CA, Martinez-Soria E, Kern I, Mach B.** 1995. A novel antigen-processing-defective phenotype in major histocompatibility complex class II-positive CIITA transfectants is corrected by interferon-gamma. The Journal of experimental medicine **182:**1793-1799.
27. **van den Elsen PJ, van der Stoep N, Vietor HE, Wilson L, van Zutphen M, Gobin SJ.** 2000. Lack of CIITA expression is central to the absence of antigen presentation functions of trophoblast cells and is caused by methylation of the IFN-gamma inducible promoter (PIV) of CIITA. Human immunology **61:**850-862.
28. **Boss JM.** 1997. Regulation of transcription of MHC class II genes. Current opinion in immunology **9:**107-113.
29. **Krawczyk M, Reith W.** 2006. Regulation of MHC class II expression, a unique regulatory system identified by the study of a primary immunodeficiency disease. Tissue Antigens **67:**183-197.
30. **Reith W, Mach B.** 2001. The bare lymphocyte syndrome and the regulation of MHC expression. Annu Rev Immunol **19:**331-373.
31. **Jabrane-Ferrat N, Nekrep N, Tosi G, Esserman LJ, Peterlin BM.** 2002. Major histocompatibility complex class II transcriptional platform: assembly of nuclear factor Y and regulatory factor X (RFX) on DNA requires RFX5 dimers. Molecular and cellular biology **22:**5616-5625.
32. **Durand B, Sperisen P, Emery P, Barras E, Zufferey M, Mach B, Reith W.** 1997. RFXAP, a novel subunit of the RFX DNA binding complex is mutated in MHC class II deficiency. EMBO J **16:**1045-1055.
33. **Hasegawa SL, Boss JM.** 1991. Two B cell factors bind the HLA-DRA X box region and recognize different subsets of HLA class II promoters. Nucleic acids research **19:**6269-6276.
34. **Masternak K, Barras E, Zufferey M, Conrad B, Corthals G, Aebersold R, Sanchez JC, Hochstrasser DF, Mach B, Reith W.** 1998. A gene encoding a novel RFX-associated transactivator is mutated in the majority of MHC class II deficiency patients. Nature genetics **20:**273-277.
35. **Moreno CS, Beresford GW, Louis-Plence P, Morris AC, Boss JM.** 1999. CREB regulates MHC class II expression in a CIITA-dependent manner. Immunity **10:**143-151.
36. **Moreno CS, Emery P, West JE, Durand B, Reith W, Mach B, Boss JM.** 1995. Purified X2 binding protein (X2BP) cooperatively binds the class II MHC X box

region in the presence of purified RFX, the X box factor deficient in the bare lymphocyte syndrome. Journal of immunology **155:**4313-4321.

37. **Nagarajan UM, Louis-Plence P, DeSandro A, Nilsen R, Bushey A, Boss JM.** 1999. RFX-B is the gene responsible for the most common cause of the bare lymphocyte syndrome, an MHC class II immunodeficiency. Immunity **10:**153-162.
38. **Reith W, Siegrist CA, Durand B, Barras E, Mach B.** 1994. Function of major histocompatibility complex class II promoters requires cooperative binding between factors RFX and NF-Y. Proceedings of the National Academy of Sciences of the United States of America **91:**554-558.
39. **Steimle V, Durand B, Barras E, Zufferey M, Hadam MR, Mach B, Reith W.** 1995. A novel DNA-binding regulatory factor is mutated in primary MHC class II deficiency (bare lymphocyte syndrome). Genes & development **9:**1021-1032.
40. **Ting JP, Trowsdale J.** 2002. Genetic control of MHC class II expression. Cell **109 Suppl:**S21-33.
41. **Laird KM, Briggs LL, Boss JM, Summers MF, Garvie CW.** 2010. Solution structure of the heterotrimeric complex between the interaction domains of RFX5 and RFXAP from the RFX gene regulatory complex. J Mol Biol **403:**40-51.
42. **Emery P, Durand B, Mach B, Reith W.** 1996. RFX proteins, a novel family of DNA binding proteins conserved in the eukaryotic kingdom. Nucleic Acids Res **24:**803-807.
43. **Hake SB, Masternak K, Kammerbauer C, Janzen C, Reith W, Steimle V.** 2000. CIITA leucine-rich repeats control nuclear localization, in vivo recruitment to the major histocompatibility complex (MHC) class II enhanceosome, and MHC class II gene transactivation. Mol Cell Biol **20:**7716-7725.
44. **Masternak K, Muhlethaler-Mottet A, Villard J, Zufferey M, Steimle V, Reith W.** 2000. CIITA is a transcriptional coactivator that is recruited to MHC class II promoters by multiple synergistic interactions with an enhanceosome complex. Genes Dev **14:**1156-1166.
45. **LeibundGut-Landmann S, Waldburger JM, Krawczyk M, Otten LA, Suter T, Fontana A, Acha-Orbea H, Reith W.** 2004. Mini-review: Specificity and expression of CIITA, the master regulator of MHC class II genes. Eur J Immunol **34:**1513-1525.
46. **Devaiah BN, Singer DS.** 2013. CIITA and Its Dual Roles in MHC Gene Transcription. Front Immunol **4:**476.
47. **Harton JA, Ting JP.** 2000. Class II transactivator: mastering the art of major histocompatibility complex expression. Mol Cell Biol **20:**6185-6194.
48. **Verma SC, Cai Q, Kreider E, Lu J, Robertson ES.** 2013. Comprehensive analysis of LANA interacting proteins essential for viral genome tethering and persistence. PLoS One **8:**e74662.
49. **Cai QL, Knight JS, Verma SC, Zald P, Robertson ES.** 2006. EC5S ubiquitin complex is recruited by KSHV latent antigen LANA for degradation of the VHL and p53 tumor suppressors. PLoS Pathog **2:**e116.
50. **Kaul R, Verma SC, Robertson ES.** 2007. Protein complexes associated with the Kaposi's sarcoma-associated herpesvirus-encoded LANA. Virology **364:**317-329.

51. **Purushothaman P, McDowell ME, McGuinness J, Salas R, Rumjahn SM, Verma SC.** 2012. Kaposi's sarcoma-associated herpesvirus-encoded LANA recruits topoisomerase IIbeta for latent DNA replication of the terminal repeats. J Virol **86:**9983-9994.
52. **Izumi KM.** 2001. The yeast two-hybrid assay to identify interacting proteins. Methods Mol Biol **174:**249-258.
53. **Gao J, Cai Q, Lu J, Jha HC, Robertson ES.** 2011. Upregulation of cellular Bcl-2 by the KSHV encoded RTA promotes virion production. PLoS One **6:**e23892.
54. **Krithivas A, Young DB, Liao G, Greene D, Hayward SD.** 2000. Human herpesvirus 8 LANA interacts with proteins of the mSin3 corepressor complex and negatively regulates Epstein-Barr virus gene expression in dually infected PEL cells. J Virol **74:**9637-9645.
55. **Hasegawa SL, Sloan JH, Reith W, Mach B, Boss JM.** 1991. Regulatory factor-X binding to mutant HLA-DRA promoter sequences. Nucleic Acids Res **19:**1243-1249.
56. **Peretti M, Villard J, Barras E, Zufferey M, Reith W.** 2001. Expression of the three human major histocompatibility complex class II isotypes exhibits a differential dependence on the transcription factor RFXAP. Mol Cell Biol **21:**5699-5709.
57. **Nekrep N, Jabrane-Ferrat N, Peterlin BM.** 2000. Mutations in the bare lymphocyte syndrome define critical steps in the assembly of the regulatory factor X complex. Mol Cell Biol **20:**4455-4461.
58. **Caretti G, Cocchiarella F, Sidoli C, Villard J, Peretti M, Reith W, Mantovani R.** 2000. Dissection of functional NF-Y-RFX cooperative interactions on the MHC class II Ea promoter. J Mol Biol **302:**539-552.
59. **DeSandro AM, Nagarajan UM, Boss JM.** 2000. Associations and interactions between bare lymphocyte syndrome factors. Mol Cell Biol **20:**6587-6599.
60. **Garvie CW, Stagno JR, Reid S, Singh A, Harrington E, Boss JM.** 2007. Characterization of the RFX complex and the RFX5(L66A) mutant: implications for the regulation of MHC class II gene expression. Biochemistry **46:**1597-1611.
61. **Seguin-Estevez Q, De Palma R, Krawczyk M, Leimgruber E, Villard J, Picard C, Tagliamacco A, Abbate G, Gorski J, Nocera A, Reith W.** 2009. The transcription factor RFX protects MHC class II genes against epigenetic silencing by DNA methylation. J Immunol **183:**2545-2553.
62. **Chang CH, Gourley TS, Sisk TJ.** 2002. Function and regulation of class II transactivator in the immune system. Immunologic research **25:**131-142.
63. **Cressman DE, Chin KC, Taxman DJ, Ting JP.** 1999. A defect in the nuclear translocation of CIITA causes a form of type II bare lymphocyte syndrome. Immunity **10:**163-171.
64. **Radosevich M, Song Z, Gorga JC, Ksander B, Ono SJ.** 2004. Epigenetic silencing of the CIITA gene and posttranscriptional regulation of class II MHC genes in ocular melanoma cells. Invest Ophthalmol Vis Sci **45:**3185-3195.
65. **Garvie CW, Boss JM.** 2008. Assembly of the RFX complex on the MHCII promoter: role of RFXAP and RFXB in relieving autoinhibition of RFX5. Biochim Biophys Acta **1779:**797-804.

66. **Schmid D, Pypaert M, Munz C.** 2007. Antigen-loading compartments for major histocompatibility complex class II molecules continuously receive input from autophagosomes. Immunity **26:**79-92.
67. **Brown DM.** 2010. Cytolytic CD4 cells: Direct mediators in infectious disease and malignancy. Cell Immunol **262:**89-95.
68. **Glimcher LH, Kara CJ.** 1992. Sequences and factors: a guide to MHC class-II transcription. Annu Rev Immunol **10:**13-49.
69. **Long AB, Boss JM.** 2005. Evolutionary conservation and characterization of the bare lymphocyte syndrome transcription factor RFX-B and its paralogue ANKRA2. Immunogenetics **56:**788-797.
70. **Barbera AJ, Chodaparambil JV, Kelley-Clarke B, Joukov V, Walter JC, Luger K, Kaye KM.** 2006. The nucleosomal surface as a docking station for Kaposi's sarcoma herpesvirus LANA. Science **311:**856-861.
71. **Long AB, Ferguson AM, Majumder P, Nagarajan UM, Boss JM.** 2006. Conserved residues of the bare lymphocyte syndrome transcription factor RFXAP determine coordinate MHC class II expression. Mol Immunol **43:**395-409.
72. **Briggs L, Laird K, Boss JM, Garvie CW.** 2009. Formation of the RFX gene regulatory complex induces folding of the interaction domain of RFXAP. Proteins **76:**655-664.
73. **Zhu XS, Linhoff MW, Li G, Chin KC, Maity SN, Ting JP.** 2000. Transcriptional scaffold: CIITA interacts with NF-Y, RFX, and CREB to cause stereospecific regulation of the class II major histocompatibility complex promoter. Mol Cell Biol **20:**6051-6061.
74. **Meissner TB, Liu YJ, Lee KH, Li A, Biswas A, van Eggermond MC, van den Elsen PJ, Kobayashi KS.** 2012. NLRC5 cooperates with the RFX transcription factor complex to induce MHC class I gene expression. J Immunol **188:**4951-4958.
75. **Bihl F, Berger C, Chisholm JV, 3rd, Henry LM, Bertisch B, Trojan A, Nadal D, Speck RF, Flepp M, Brander C, Mueller NJ, Swiss HIVCS.** 2009. Cellular immune responses and disease control in acute AIDS-associated Kaposi's sarcoma. AIDS **23:**1918-1922.
76. **Lepone L, Rappocciolo G, Knowlton E, Jais M, Piazza P, Jenkins FJ, Rinaldo CR.** 2010. Monofunctional and polyfunctional CD8+ T cell responses to human herpesvirus 8 lytic and latency proteins. Clin Vaccine Immunol **17:**1507-1516.
77. **Duman S, Toz H, Asci G, Alper S, Ozkahya M, Unal I, Celik A, Ok E, Basci A.** 2002. Successful treatment of post-transplant Kaposi's sarcoma by reduction of immunosuppression. Nephrol Dial Transplant **17:**892-896.
78. **Kwun HJ, da Silva SR, Shah IM, Blake N, Moore PS, Chang Y.** 2007. Kaposi's sarcoma-associated herpesvirus latency-associated nuclear antigen 1 mimics Epstein-Barr virus EBNA1 immune evasion through central repeat domain effects on protein processing. J Virol **81:**8225-8235.

**KSHV LANA induces expression of EGFL7 to promote angiogenesis**

Unpublished Data

**Abstract:**

Kaposi's sarcoma (KS) is a highly vascularized tumor characterized by inflammation and extensive neo-angiogenesis. The tumor microenvironment is rich in inflammatory and pro-angiogenic cytokines. Epidermal growth factor-like domain 7 (EGFL7) is a secreted pro-angiogenic cytokine that has been implicated in angiogenesis and the proliferation of endothelial cells during many physiological and pathological conditions. Here, we report that the expression of EGFL7 is upregulated in Kaposi's sarcoma-associated herpes virus (KSHV) infected cells. Our data show that primary effusion lymphoma cells have increased levels of EGFL7 at mRNA and protein amounts compared with uninfected cells. We furthermore show that the KSHV latent protein, latency-associated nuclear antigen (LANA), is the viral factor responsible for this upregulation. The mechanism of EGFL7 expression by LANA seems to involve sequestration of death domain-associated protein 6 (Daxx), which is a suppressor of avian erythroblastosis virus E26 oncogene homolog 1 (Ets-1) activity, one of the core transcription factors required for the expression of EGFL7. We additionally show that the upregulation of EGFL7 contributes to the promotion of angiogenesis by LANA since siRNA-mediated knockdown of EGFL7 reduced *in vitro* tubulogenesis in LANA-expressing HUVEC cells. EGFL7 appears to promote angiogenesis through autocrine as well paracrine mechanisms. We establish EGFL7 as one of the important angiogenic molecules secreted during KSHV infection that may be an important therapeutic target in conjugation with other anti-angiogenic therapies.

**Importance:**

Kaposi's sarcoma (KS) is the second most common malignancy associated with AIDS worldwide and remains a significant cause of morbidity and mortality in AIDS patients. The fact that KS tumors are characterized by extensive neo-angiogenesis, even in early stages of development, highlights the significance of angiogenesis in the progression of KS tumors. Inhibiting angiogenesis is therefore an attractive therapeutic strategy for the treatment of KS. While many angiogenic mechanisms used by KSHV are known, the need for an effective anti-angiogenic therapy with long-term efficacy and a potent inhibition of tumor specific angiogenesis still prevails. This need calls for a deeper understanding of the host mechanisms manipulated by KSHV in order to promote angiogenesis. The present study explores one such mechanism involving a relatively newly identified host angiogenic cytokine EGFL7 that contributes to KSHV-induced angiogenesis.

**Introduction:**

Kaposi's sarcoma-associated herpes virus (KSHV) is an oncogenic virus responsible for multiple human malignancies including Kaposi's sarcoma (KS) and two-lymphoproliferative diseases- primary effusion lymphoma (PEL or BCBL) and multicentric Castleman's disease (3, 10, 22). KS is the most common cancer associated with HIV infection and remains a leading cause of morbidity and mortality in AIDS patients. It is a highly vascular tumor of endothelial origin involving a complex interplay of immune evasion, inflammation and angiogenesis. Angiogenesis, the process of growing new blood vessels from preexisting ones, is a hallmark of KS tumors. The significance of angiogenesis in KS tumors is highlighted by the fact that KS tumors are

highly vascularized, even in early stages of development (7). Multiple angiogenic cytokines, including vascular endothelial growth factor (VEGF), basic fibroblast growth factor (b-FGF), angiopoietin-2, angiogenin and cycloxigenase-2 (COX-2), are known to be induced during KSHV infection (25, 30, 32, 34, 35, 37, 38, 47, 48).

EGFL7 (also known as a vascular endothelial (VE) statin) belongs to the epidermal growth factor-like domain family of growth factor. It is an angiogenic factor secreted by the endothelial cells that also acts on endothelial cells (26). In addition to its role in physiological angiogenesis, EGFL7 has also been implicated in the growth and metastasis of many solid tumors (6, 11, 14, 15, 20, 45, 46). Normally, EGFL7 expression is restricted to endothelial cells or its expression is very weak in most human tissues. Under pathological conditions such as cancers, many tumors cells are known to secrete EGFL7 in order to promote angiogenesis (6, 15, 45). Interestingly, hypoxic conditions are known to induce expression of EGFL7 indicating that EGFL7 may play important roles in hypoxic conditions (such as are found in KS tumors) (5, 26). Since KS tumors exhibit extensive neo-angiogenesis, KSHV infection is likely to induce the expression of EGFL7. Here, we have explored the role of EGFL7 and its mechanism in KSHV-induced angiogenesis. Our data show that EGFL7 expression is upregulated during KSHV infection and potentially contributes to the angiogenesis associated with KS.

Latency-associated nuclear antigen (LANA) is a latent KSHV protein that is highly expressed in all latently infected cells (8, 16, 27). LANA is a multifunctional protein that is essential for establishing and maintaining a successful latency. LANA has been previously shown to promote angiogenesis and endothelial cell proliferation through manipulation of multiple signaling pathways (4, 29, 44). For example, LANA can

promote angiogenesis by inducing the expression of VEGF A, an important angiogenic cytokine by stabilizing hypoxia-induced factor 1α (HIF 1α), a transcription factor that upregulates VEGF A expression (2, 7, 36, 38). LANA also promotes angiogenesis by inhibiting the degradation of Hey1, a key component of the Notch signaling pathway with pronounced angiogenic activities (43). LANA regulates expression of many viral and cellular genes through its interactions with multiple host and viral proteins (3, 23, 41). One such host protein that LANA interacts with is death domain-associated protein 6 (Daxx), a repressor of avian erythroblastosis virus E26 oncogene homolog 1 (Ets-1) (24). Ets-1 is a transcription factor that positively regulates expression of EGFL7 (26, 42). Daxx is known to inhibit the transcriptional activity of several Ets-1 responsive promoters through direct protein-protein interactions (18, 24). Here, we show that LANA induces the expression of EGFL7. This outcome can be partly attributed to the ability of LANA to sequester Daxx and the subsequent removal of inhibition posed on Ets-1 bound to EGFL7 promoter. Furthermore, when EGFL7 expression is inhibited with anti-EGFL7 siRNA, the *in vitro* tubulogenic effect of LANA is also reduced.

**Materials and Methods:**

**Cell culture**

The EBV- and KSHV-negative Burkitt lymphoma cell line BJAB and the KSHV-positive but EBV-negative primary effusion lymphoma cell lines BC3 and BCBL1 were cultured in RPMI 1640 medium supplemented with 10% bovine growth serum, 2mM L-glutamine and penicillin-streptomycin (5 U/ml and 5 g/ml, respectively). The HUVEC cells were cultured in Medium 200 supplemented (Gibco, USA) with low serum-growth supplement (Gibco), 5 U/ml penicillin and 5 g/ml streptomycin. HUVECs with fewer

than 8 passages were used. Human embryonic kidney cells HEK293L were cultured in Dulbecco's modified Eagle's medium (DMEM) supplemented with 10% fetal bovine serum, 2mM L-glutamine and penicillin-streptomycin (5 U/ml and 5 g/ml, respectively). All cell lines were grown at 37°C in a humidified environment supplemented with 5% $CO_2$.

**Plasmids**

Myc-tagged full-length LANA (pA3M-LANA), or Flag-tagged full-length LANA (pA3F-LANA), lentiviral-construct pLVX-LANA-YFP-Flag and its control construct pLVX-YFP-Flag, shRNA-expressing plasmids Ctrl shRNA and LANA shRNA, have been described previously in the literature (40). Flag-Daxx/PRK5 was obtained from Addgene (USA) (Cat#. 27974). For lentiviral-construct LANA-Flag-Puro, the full-length, Flag-tagged LANA sequence was transferred from pA3F-LANA into pLVxPuro-cloning vector (Ctrl Puro) between the EcoRI and XbaI restriction sites. Full-length (-1670 to +100) EGFL7 promoter-luciferase reporter construct was purchased from Addgene (Cat# 32244). Its truncations (-150 to +100 and -71 to +100) were further subcloned into PGL3basic vector using an In-Fusion cloning kit (Takara/Clontech, USA) according to the manufacturer's instructions. The primers sequences used for this cloning were:

*(-71 to +100) EGFL7 promoter-luciferase Forward:*

5'-AGCTCTTACGCGTGCTAGCATCCCAATCCCGATTACCCA-3',

*(-150 to +100) EGFL7 promoter-luciferase Forward:*

5'-AGCTCTTACGCGTGCTAGCCTCAGCCTCCTGTTTGTCCGA-3',

*(+100) EGFL7 promoter-luciferase Reverse:*

5'-AGTACCGGAATGCCAAGCTTTGGACCCTAGCCCTTGCTGG-3'.

**Antibodies**

The following commercial antibodies were used: Mouse anti-EGFL7 (sc-373898, Santa Cruz, USA), mouse anti-Daxx (sc-8043, Santa Cruz), rabbit anti-Ets1 (sc-350, Santa Cruz), mouse anti-GAPDH (US Biological, USA), mouse anti-Flag M2 (Sigma Aldrich, USA) and mouse anti-Myc 9E10 (Sigma-Aldrich). Mouse anti-LANA monoclonal antibody was generated at Genscript (USA).

**Chromatin immunoprecipitation assays**

Chromatin immunoprecipitation (ChIP) was performed as described previously in the literature (9). Nearly 20 million cells were fixed with a final concentration of 1% formaldehyde for 10 minutes at room temperature followed by the addition of glycine at a final concentration of 125mM for 5 minutes to block cross-linking. The cells were rinsed three times with ice-cold phosphate buffered saline (PBS) and lysed in cell lysis buffer (5mM PIPES (pH 8.0), 85mM KCl and 0.5mM NP-40) supplemented with protease inhibitors for 10 minutes on ice. The nuclei were enriched by low-speed centrifugation and resuspended in protease inhibitor-supplemented nuclear lysis buffer containing 50mM Tris-HCl, pH 8.1, 10 mM EDTA and 1% SDS. Chromatin was sonicated to an average length of 500–800 bp and centrifuged for 10 minutes at 13,000 rpm to remove cell debris. The resulting supernatant was diluted 5-fold with a ChIP dilution buffer containing 16.7mM Tris-HCl, pH 8.1, 167mM NaCl, 1.2mM EDTA, 0.01% SDS, 1.1% Triton X-100 and protease inhibitors. The diluted chromatin was pre-cleared with Protein A and G sepharose beads pretreated with 1 mg/ml BSA and 1 mg/ml sheared salmon sperm DNA for 30 minutes at 4°C with rotation followed by incubation overnight with either control or specific antibodies at 4°C with rotation. The immune complexes were

collected via incubation with Protein A and G sepharose beads for 1–2 h at 4°C. The beads were collected and washed subsequently with a low-salt buffer (0.1% SDS, 1.0% Triton X-100, 2mM EDTA, 20mM Tris [pH 8.1], 150mM NaCl), a high-salt buffer (0.1% SDS, 1.0% Triton X-100, 2mM EDTA, 20mM Tris [pH 8.1], 500mM NaCl), and a LiCl wash buffer (0.25M LiCl, 1.0% NP-40, 1% deoxycholate, 1mM EDTA, 10mM Tris [pH 8.0]). The beads were then washed twice with Tris-EDTA buffer and the chromatin was eluted using an elution buffer (1% SDS, 0.1M NaHCO3) and reverse cross-linked by adding 0.3M NaCl at 65°C overnight. The eluted DNA was precipitated, treated with RNAse and proteinase K at 45°C for 2h and purified using a Min-Elute PCR purification kit (Qiagen, USA). The purified DNA was analyzed by RT-PCR for the presence of the EGFL7 promoter region. We used the following primers for the detection of EGFL7 promoter during RT-PCR:

Forward: 5'-CCA GCA GGG TCC AGC CCT GGT-3'

Reverse: 5'-TGG GTA ATC GGG ATT GGG ATG-3'

**Dual luciferase reporter assays**

$5\times10^5$ HEK293 L cells or $0.5\times10^5$ HUVEC cells were seeded into 6-well plates the day before transfection. 0.5 μg of either wild-type EGFL7 promoter, (-150 to +100) EGFL7 promoter-luciferase, or (-71 to +100) EGFL7 promoter-luciferase plasmids were co-transfected with either the variable amounts of either Flag-Daxx or pA3F-LANA or both, as specified in the experiments. Empty-vector plasmid pA3F was used as a filler plasmid. The transfection efficiencies were monitored by a transfecting green fluorescent protein (GFP)-containing vector, pEGFP. Renilla luciferase-expressing plasmid (pRRLSV40) was transfected at 40 ng/well for data normalization. All of the

transfections were done using Metafectene (Biontex Laboratories GmbH, Germany) according to the manufacturer's protocol. Twenty-four h after transfection the cells were lysed in cell lysis buffer (Promega) and 50 µl of the cell lysate was used for the reporter assay using a dual luciferase reporter assay kit (Promega, USA). The EGFL7 promoter-luciferase readings were normalized against Renilla luciferase to account for the transfection efficiencies and were reported as relative luciferase units (RLU). A portion of the cell lysates was used for Western blotting to detect LANA, Daxx and GAPDH. All of the experiments were repeated multiple times and the data shown are the mean of three independent experiments.

**Co-immunoprecipitation assays and Western blotting analysis**

Approximately 10 million cells expressing the proteins of interest were washed with PBS (10mM $NaPO_4$, 137mM NaCl, 2.5mM KCl, pH 7.5) and lysed in RIPA cell lysis buffer (50mM Tris-HCl, pH 7.5, 150mM NaCl, 1mM EDTA and 1% NP-40) supplemented with protease inhibitors (1mM phenylmethylsulfonyl fluoride, 10mg/ml pepstatin, 10mg/ml leupeptin and 10mg/ml aprotinin). The cellular lysates were then sonicated to shear the DNA and centrifuged at 12,000 rpm for 10 minutes at 4°C to remove cellular debris. The supernatants were pre-cleared with protein A and G sepharose beads (GE Healthcare, USA) for 30 minutes at 4°C and gently rotated overnight at 4°C with specific antibodies. The resulting immune complexes were captured by the addition of protein A and G conjugated sepharose beads and rotating the lysates for 2 h at 4°C. The immune complexes were collected by centrifuging at 2000 rpm for 2 minutes at 4°C. The beads were washed three times with ice-cold RIPA buffer supplemented with protease inhibitors and boiled in 50 µl of SDS PAGE sample loading

buffer for 5 minutes. The cellular lysates and immunoprecipitated proteins were separated on SDS-PAGE gels and transferred onto 0.45 μm nitrocellulose membranes (GE Healthcare, USA) at 100 V for 75 minutes. The blots were then blocked with 5% non-fat milk in TBST buffer (10mM Tris-HCl, pH 7.5, 150mM NaCl, 0.05% Tween 20) and washed three times with TBST buffer before being incubated overnight at 4°C with specific primary antibodies. The blots were washed three times with TBST and were then incubated with appropriate secondary antibodies conjugated with Alexa Fluor 680 or Alexa Fluor 800 (Molecular Probes, USA) secondary antibodies at 1:10,000 dilutions. The membranes were scanned with an Odyssey scanner (LI-COR, USA).

**Quantitative real-time PCR**

For quantitative Reverse-Transcriptase PCR assays, we extracted the total mRNA from the cells using an illustra RNAspin Mini kit (GE Healthcare) according to the manufacturer's instructions. The cDNA was made from the extracted mRNA using a High-Capacity cDNA reverse transcription kit (Applied Biosystems, USA). Each PCR reaction consisted of 10 μl of 2X SYBR PCR master mix (Applied Biosystems), 1μM of each forward and reverse primers and 2μl of the cDNA. The cDNA was amplified on an ABI StepOne plus real-time PCR machine (Applied Biosystems), and the relative gene copies or the transcripts were calculated with the $\Delta\Delta C_T$ method. Each experiment included duplicate samples and the data shown represent the mean of three independent experiments. We calculated P values using two-tailed *t*-tests with Graphpad (Prism 6, USA) software.

**RNA sequencing**

The RNA-seq of BJAB cells stably expressing LANA (BJAB-LYF) and the control cells BJAB-YFP was performed on a HiSeq next-generation sequencer (Illumina, Inc., USA) as described previously in the literature (33). The total RNA was isolated with TRIzol reagent following the manufacturer's instructions (Life Technologies, USA). The concentration and purity of the extracted RNA was determined using a Nano Drop 2000c spectrophotometer (Nano Drop Technologies, USA). A TrueSeq RNA sample preparation kit v2 (Illumina, Inc.) was used to prepare the cDNA libraries for RNA-seq according to the manufacturer's instructions. The fragment sizes and purity of the mature libraries were confirmed using a Bioanalyzer 2100 (Agilent Technologies, USA). The quantities of the libraries required for RNA-seq were determined by real-time qPCR using a KAPA library quantification kit for the Illumina platform (Kapa Biosystems, Location). We sequenced the libraries using HiSeq (Illumina, Inc.), and the sequences were mapped to a human reference genome using the RNA-Seq Analysis tool in CLC Genomic Workbench 7 (CLC Bio, Denmark) software.

**Lentivirus production**

Control YFP and LANA-expressing LYF lentivirus particles were produced using Vesicular stomatitis virus-G envelope-pseudotyped lentiviral virions by co-transfecting 20 μg lentiviral construct (LANA-expressing pLVx-Ac-YFP-C1-LANA-Flag or control pLVx-AcYFP-C1-Flag), along with pseudotyped lentiviral packaging vectors 6.0 μg REV, 10.0 μg GP and 3.0 μg VSV-G into a 10 cm dish of ~85% confluent HEK293T cells using polyethylenimine as described previously in the literature (40). Eight h after transfection, the medium was changed and the cells were induced using 10 mM Sodium

Butyrate in DMEM supplemented with 10% fetal bovine serum, 2 mM L-glutamine and penicillin-streptomycin (5 U/ml and 5 g/ml, respectively) buffered with 10 mM HEPES (4-(2-hydroxyethyl)-1-piperazineethanesulfonic acid). The media was changed 24 h after transfection to remove the Sodium Butyrate. The medium containing the lentiviral particles was collected, passed through a 0.45 μm filter and concentrated to 1/120 of its original volume. The cells to be transduced were pre-incubated with polybrene (Hexadimethrine bromide) at the final concentration of 8 μg/ml for 30 minutes before adding the concentrated lentiviral particles. The infections of the target cells were carried out by incubating the concentrated lentiviral particles for 12–18 h, after which the medium was changed. The expression of the constructs was confirmed with RT-PCR analysis.

**Endothelial tube formation assay**

We performed the endothelial tube formation assay using an angiogenesis starter kit (Life Technologies, USA) according to the manufacturer's instructions. Briefly, the assay was performed using a 24-well micro-titer plate coated with 100 μl of Geltrex Matrix and incubated at 37°C for 30 minutes. The HUVEC cells were re-suspended in supplemented Medium 200 and plated on the Geltrex Matrix coated wells at a density of approximately $0.8 \times 10^5$ cells per well. Photographs were taken with a digital camera attached to an inverted fluorescence microscope 24 h after plating.

**Results:**

**Identification of EGFL7 as a LANA responsive gene**

Considering the pleiotropic effects of LANA during KSHV latency, we wished to identify the host genes that were directly or indirectly regulated by LANA using a sensitive and unbiased approach of next-generation RNA sequencing. In order to identify the genes that were differentially regulated in response to LANA expression, we generated a LANA-expressing stable cell line (BJAB-LYF) and its matching control cell line (BJAB-YFP) by transducing a KSHV-negative B cell line, BJAB with the lentivirus particles expressing the constructs of interest (Fig 1). The expression of LANA in BJAB-LYF was confirmed with RT-PCR (data not shown) and Western blotting (Fig 2B). The total mRNA was isolated from these cells to prepare the cDNA libraries for RNA sequencing using Illumina HiSeq. The results of this screen identified more than a thousand cellular genes that were differentially regulated in LANA-expressing B cells. Some of the interesting genes identified during this screen are listed in Table 1. Among

Table 1: A few of the interesting cellular genes differentially regulated in LANA expressing B cells compared to control cells

| ID | Gene name | GenBank accession no. | Fold change |
|---|---|---|---|
| IL17B | Interleukin 17B | NM_014443 | -3.5 |
| IFNG | Interferon, gamma | NG_015840 | -11.8 |
| NOTCH3 | Notch3 | U97669.1 | +3.4 |
| FLT1 | Fms related tyrosine kinase 1 | NM_002019 | +3.6 |
| FGFR2 | Fibroblast growth factor receptor 2 | Z71929.1 | +5.34 |
| JAG2 | Jagged 2 | AF029778.1 | +6.1 |
| EGFL7 | EGF-like-domain, multiple7 | NR_046367 | +12.0 |
| ERBB3 | v-erb-b2 avian erythroblastic leukemia viral oncogene homolog 3 | NM_001982 | +579.3 |

these genes, the EGFL7 gene was selected for further study considering the feasibility of the study and the gene's potential significance to promote angiogenesis in KS tumors.

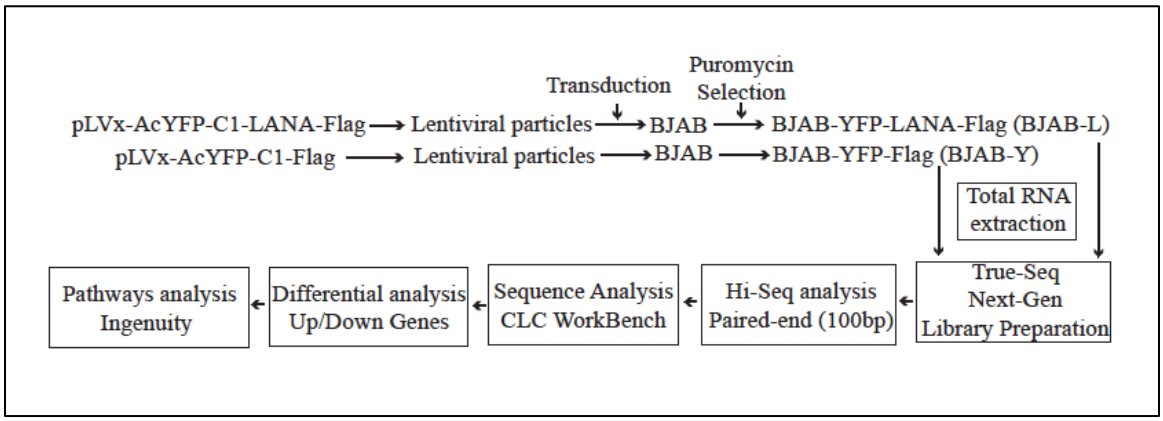


Figure 1 Experimental design for the transcriptome analysis of LANA-expressing B cells. The lentivirus particles were concentrated from the supernatant of HEK293T cells transfected with either LANA-expressing pLVx-Ac-YFP-C1-LANA-Flag or control pLVx-AcYFP-C1-Flag along with the packaging vectors and were used to transduce KSHV-negative BJAB cells. The total mRNA was extracted from the BJAB cells stably expressing LANA-YFP-Flag (BJAB-LYF) or the control cells expressing YFP-Flag (BJAB-YFP). The cDNA libraries were prepared using the TrueSeq RNA-seq library Kit. The libraries were sequenced using HiSeq and the sequences were mapped to the reference human genome to analyze the differential expression of up or down regulated cellular genes.

**EGFL7 is upregulated during KSHV infection**

Following the identification of EGFL7 as a gene induced in response to LANA expression, an increase in the transcription of EGFL7 by LANA was further confirmed using an independent approach of RT-PCR in the BJAB-LYF and BJAB-YFP cells (Fig 2A). The relative mRNA expression of EGFL7 was considerably higher in the LANA-expressing cells compared with the control cells (Fig 2A). The expression of the EGFL7 protein in these cells was confirmed by Western blotting the cellular lysates of these cells for EGFL7 (anti-EGFL7 antibody) and LANA (anti-Flag antibody). GAPDH served as a control for equal loading. Consistent with the observed increase of the EGFL7 transcript

level, increased expression of the EGFL7 protein was also observed in LANA-expressing cells compared with the control cells (Fig 2B).

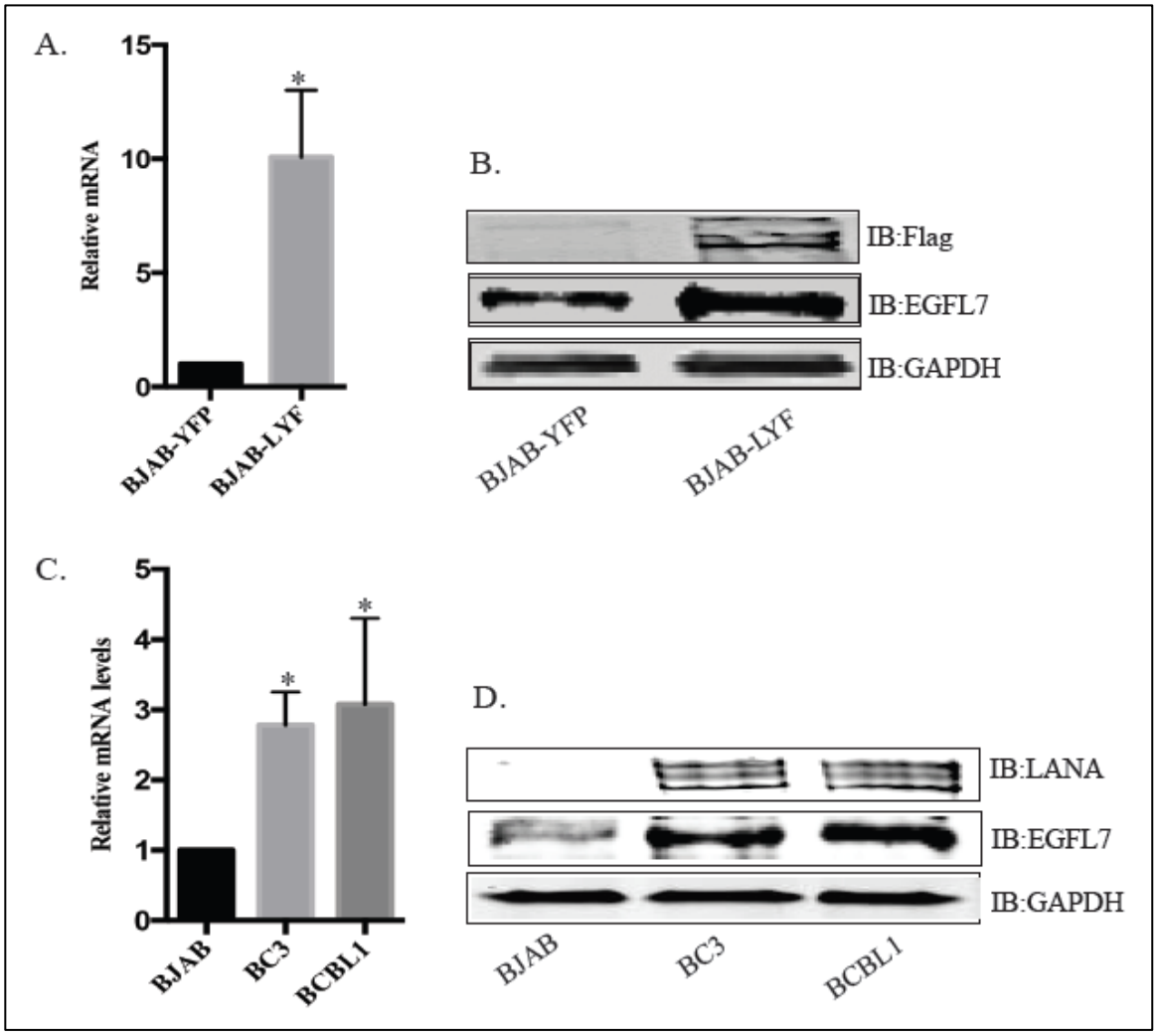


Figure 2 LANA induces expression of EGFL7. Relative mRNA levels of EGFL7 gene in **A.** BJAB (LYF) cells compared with the control BJAB with YFP (YFP) and **B.** KSHV-infected PEL cells BC3 and BCBL1 compared with the BJAB cells. The mRNA levels were quantified using RT-PCR and the expression levels were normalized against the GAPDH gene. The error bars represent standard deviations from the mean of at least three experimental replicates. * indicates $P < 0.05$. The immune detection of EGFL7 expression in **C.** BJAB-YFP and BJAB-LYF **D**. BJAB, BC3 and BCBL1 cells. GAPDH shows equal loading of the lysates.

The results of these experiments confirmed that LANA expression was sufficient to induce the expression of EGFL7 at both the mRNA and the protein levels. In order to

determine whether LANA-mediated upregulation of EGFL7 was also relevant in the context of long-term KSHV infection, we analyzed the relative mRNA expression of EGFL7 using RT-PCR (Fig 2C) and EGFL7 protein expression using Western blotting (Fig 2D) in latently KSHV-infected primary effusion lymphoma cell lines (BC3 and BCBL1). The relative abundance of the EGFL7 transcript was significantly higher in both the KSHV-positive cell lines (BC3 and BCBL1) compared with the KSHV-negative BJAB cells at the mRNA (Figs 1A and C). This result was also reflected in the observed higher protein expression of EGFL7 in the corresponding cells (Fig 1D). Significant upregulation of EGFL7 in primary effusion lymphoma cell lines suggests that that EGFL7 likely plays an important role in KSHV infection.

**LANA upregulates EGFL7 promoter activity**

LANA has been shown to modulate the activities of many cellular and viral promoters. Hence, we examined whether LANA expression enhances EGFL7 expression by activating EGFL7 promoter. To this end, we performed promoter reporter assays using a full-length EGFL7 promoter luciferase construct that has been described previously in the literature (12). The reporter assays performed in two different cell lines HEK293T cells (Fig 3B) and endothelial HUVEC cells (Fig 3C) revealed that LANA expression in both of these two cell lines transactivated full-length EGFL7 promoter (-1670 to +100) in a dose-dependent manner (Fig 3C). These results confirmed that LANA induces the expression of EGFL7 by activating EGFL7 promoter activity.

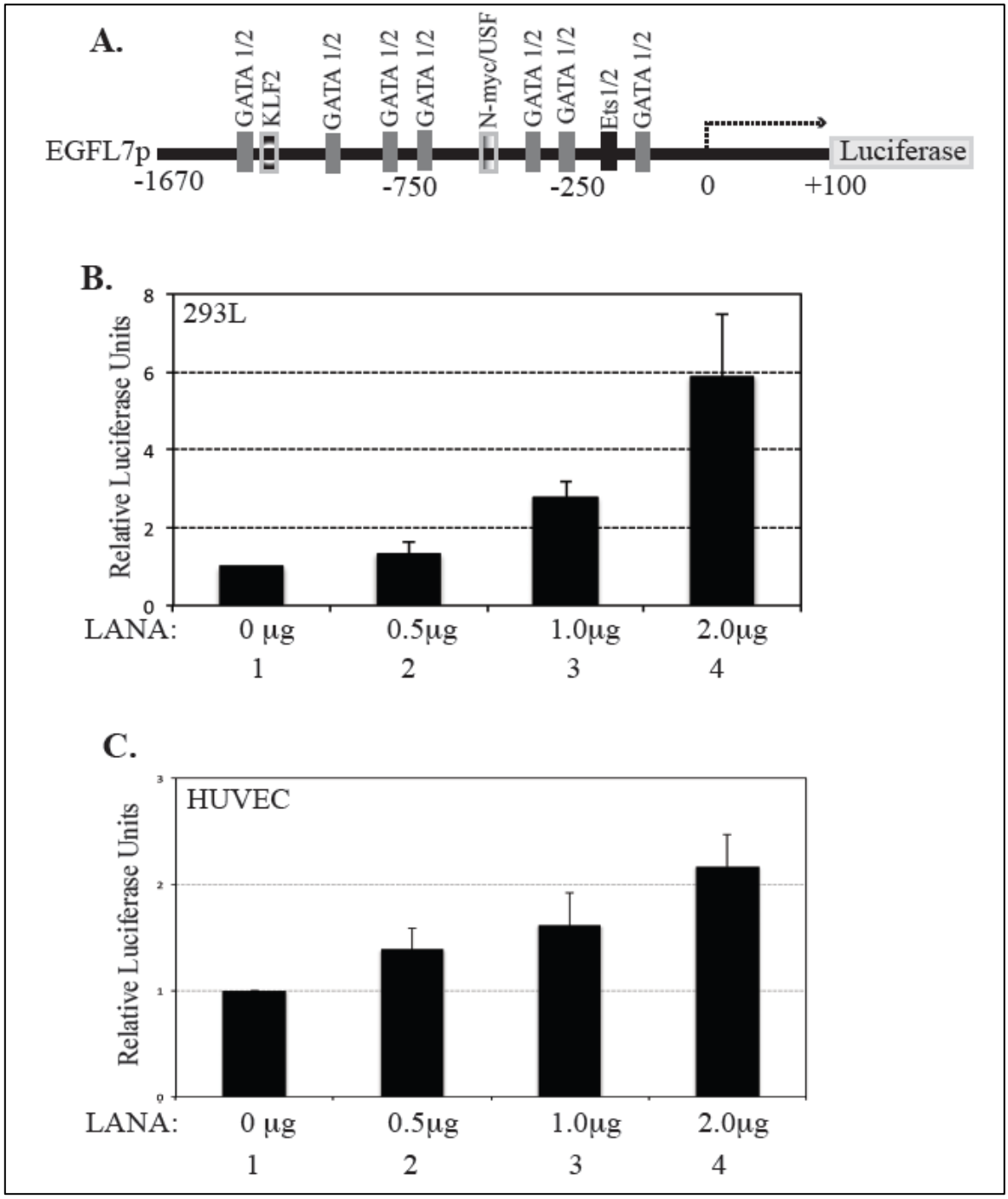


Figure 3 LANA activates EGFL7 promoter by sequestering Daxx. **A.** Schematic full-length EGFL7 promoter-luciferase construct showing a map of the transcription factor binding sites. This figure has been adopted from the paper 'Ets-1 and Ets-2 regulate the expression of miR-126 in endothelial cell' by Harris et al. (2010). The dual luciferase reporter assay results show a dose-dependent increase in EGFL7 luciferase activity in response to the increasing expression of LANA. **B.** HEK293T cells and **C.** HUVEC cells. The cells were transfected with 0.5 µg (lane 2), 1.0 µg (lane 3) or 2.0 µg (lane 4) of Flag-tagged LANA-expressing plasmid pA3F-LANA. RLU were calculated relative to the basal (mock transfected, lane 1) promoter activity. The error bars represent standard deviations from the mean of at least three experimental replicates.

**LANA upregulates EGFL7 expression by sequestering Daxx**

LANA could activate the EGFL7 promoter in multiple potential ways such as the activation of one or more transcription factors necessary for EGFL7 expression, recruitment of activators, or the removal of repressors of the EGFL7 promoter. Since previous studies have demonstrated that LANA sequesters Daxx, which acts as a repressor of EGFL7 promoter by inhibiting Ets-1, one of the important transcription factors regulating the activity of EGFL7, we speculated that this mechanism might contribute to the activation of EGFL7 promoter by LANA. In order to test this hypothesis, we performed a series of reporter assays in HUVEC cells transfected with Daxx and/or LANA (Fig 4A). As expected, the overexpression of Daxx reduced the activity of the EGFL7 promoter (compare lanes 1 with lanes 2 and 3), confirming that Daxx represses the EGFL7 promoter. However, this repression of the promoter activity was not very significant. This effect may be explained by the nearly saturated levels of endogenous Daxx suppressing EGFL7 promoter activity. In support of this speculation, we failed to observe a dose-dependent effect of EGFL7 promoter inhibition by Daxx (lanes 2 and 3). Importantly, consistent with our hypothesis, when LANA was co-expressed with Daxx it increased the activity of EGFL7 promoter in a dose-dependent manner (lanes 4, 5 and 6). The increase in the promoter activity was significant, suggesting that the overexpression of LANA not only sequesters overexpressed Daxx but also sequesters endogenous Daxx (given that sequestration of Daxx is the primary mechanism responsible for the upregulation of EGFL7 promoter activity by LANA). Western blotting of the cellular lysates confirmed the expression of Daxx and LANA (Fig 4B).

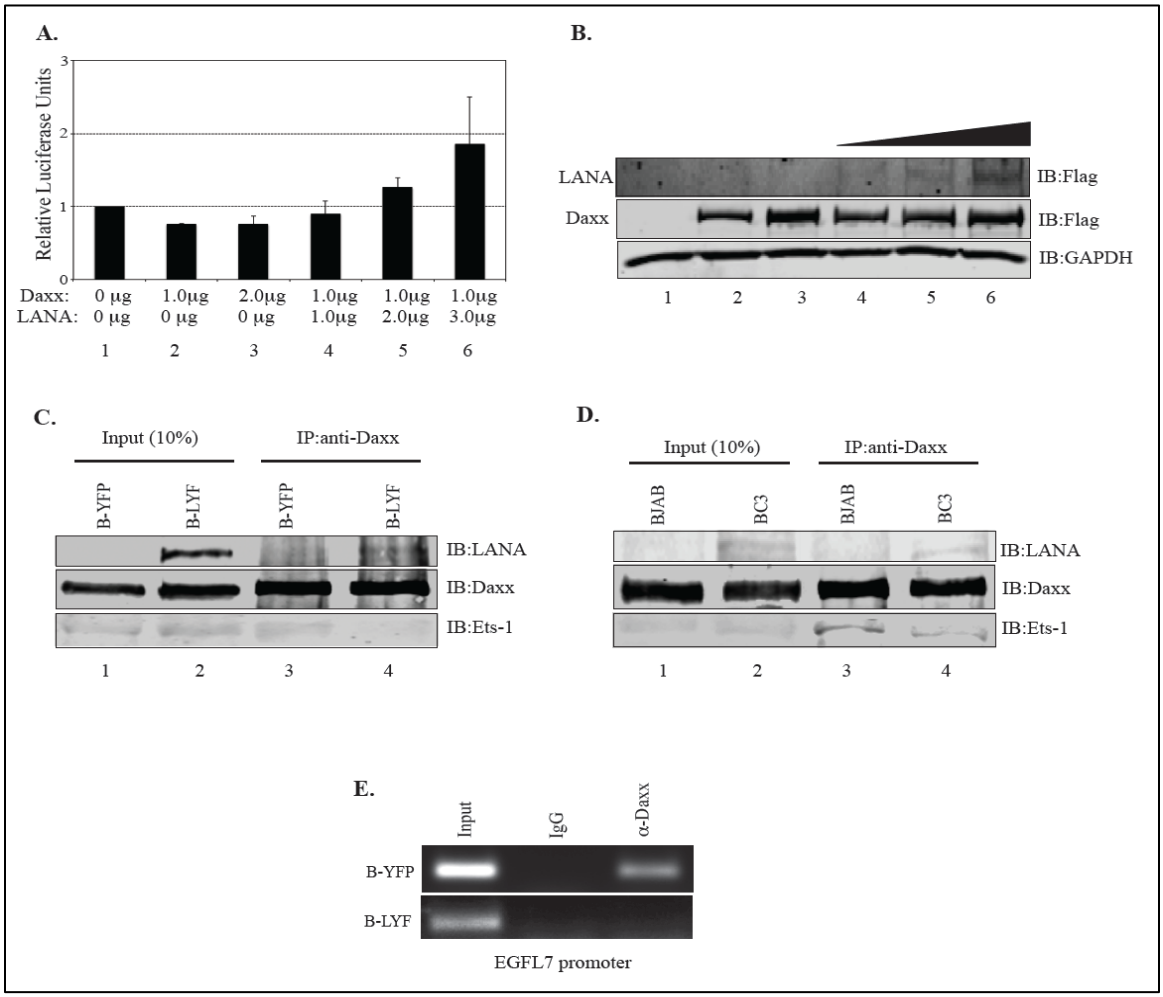


Figure 4 LANA upregulates EGFL7 promoter activity by sequestering DAXX. **A.** Dual luciferase reporter assay in HUVEC cells with overexpressed DAXX and overexpressed LANA. The cells were transfected with DAXX and LANA as indicated. RLU were calculated relative to the basal (mock transfected, lane 1) promoter activity. The error bars represent standard deviations from the mean of at least three experimental replicates. **B.** Corresponding Western blotting showing the expression of DAXX and LANA. An immunoprecipitation assay showing reduced association of DAXX with Ets-1 in **C.** LANA-expressing BJAB cells (B-LYF) compared with the control cells (B-YFP) and **D.** Latently KSHV-infected B cells BC3. A ChIP assay showing the reduced association of EGFL7 promoter with DAXX in the presence of LANA in BJAB cells.

In the absence of LANA, Daxx associates with Ets-1 in order to repress its activity. However, LANA's sequestering of Daxx disrupts its association with Ets-1 (24). Using co-immunoprecipitation assays, we confirmed that association of Ets-1 with Daxx was indeed reduced in the presence of LANA. Considerably less Ets-1 co-

immunoprecipitated with Daxx in the presence of LANA in BJAB cells expressing LANA as a sole KSHV protein (Fig 4C; compare lanes 3 and 4). Similar results were obtained in latently KSHV-infected BC3 cells (Fig 4D; compare lanes 3 and 4).

Finally, LANA-mediated removal of Daxx from the EGFL7 promoter was confirmed by a ChIP assay in LANA-expressing BJAB (B-LYF) and the control cells (B-YFP) (Fig 4E). The Daxx antibody, but not the control IgG antibody, efficiently precipitated the EGFL7 promoter DNA in control cells, confirming the specificity of the Daxx antibody in precipitating the EGFL7 promoter. However, this association was significantly reduced in LANA-expressing B-LYF cells, suggesting that LANA efficiently removes Daxx from the EGFL7 promoter. Collectively, these results point toward the sequestration of Daxx by LANA as a primary mechanism behind LANA-mediated transactivation of the EGFL7 promoter.

**The Ets-1 binding region of the EGFL7 promoter is responsible for LANA-mediated induction of EGFL7**

To further confirm that Daxx sequestration is a primary mechanism behind the transactivation of the EGFL7 promoter by LANA, we studied the regulation of the EGFL7 promoter in response to LANA using deletion analysis of the EGFL7 promoter (Fig 5). The EGFL7 promoter contains potential binding sites for several transcription factors including the binding sites for GATA1, GATA2, Ets-1 and Ets-2 (Fig 3A) (12). Of these, the EGFL7 promoter region -150 to + 100 contains binding sites for Ets-1 and 2, as well as for GATA 1 and 2; and the region -71 to + 100 contains binding sites for GATA 1 and 2 only. We cloned these two deletion constructs of the EGFL7 promoter (-

150 to +100 and -71 to +100) in the PGL3 basic vector in order to fuse these regions with the luciferase reporter (Fig 5A). We studied the responsiveness of these two constructs to LANA using reporter assays. The results of these experiments revealed that the region -150 to +100 was transactivated in a dose-dependent manner by LANA (black bars, Fig 5B and C) but the region -71 to +100 (white bars, Fig 5B and C) was not responsive to LANA expression in HEK293L (Fig 5B) and HUVEC cells (Fig 5C). These results suggest that the LANA-responsive region of the EGFL7 promoter contains Ets binding sites but not GATA binding sites. The specificity of Daxx at repressing the EGFL7

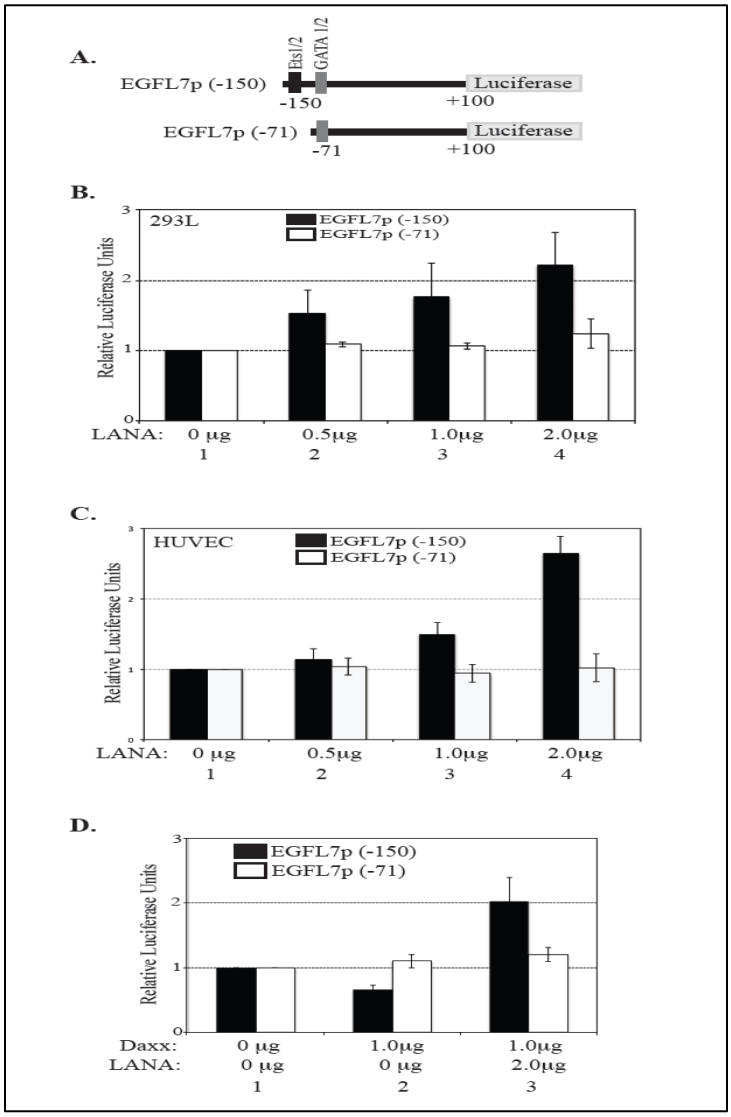


Figure 5 The Ets binding site is important for the transactivation of the EGFL7 promoter by LANA. **A.** Schematic showing the deletion constructs used in the reporter assays and dual luciferase assays in response to increasing concentrations of LANA **B.** HEK293L cells and **C.** HUVEC cells. The concentration of LANA expression plasmid transfected in the cells is indicated below each of the bars. **D.** Dual luciferase activity in HUVEC cells transfected with a variable amount of DAXX and LANA expression plasmids, as indicated below the bars. The black bars represent relative luciferase activities of the (-150 to +100) construct and the white bars represent relative luciferase activities of the (-71 to +100) construct. RLU were calculated relative to the basal (mock transfected, lane 1) promoter activity. The error bars represent standard deviations from the mean of at least three experimental replicates.

promoter through Ets-1 binding was demonstrated by studying the responsiveness of the -150 to +100 and -71 to +100 promoter luciferase constructs by overexpressing Daxx and LANA (Fig 5D). Expression of Daxx inhibited the activity of the -150 to +100 reporter construct containing the Ets-1 binding site (Fig 5D, lane 2, black bar) but not the -71 to +100 construct lacking the Ets-1 binding site (Fig 5D, lane 2, white bar). Furthermore, LANA expression significantly increased activity of the -150 to +100 construct but not the -71 to 100 construct, indicating that LANA cannot activate the EGFL7 promoter if the Ets-1 binding site is not present. Taken together, these results clearly demonstrate that the sequestration of Daxx is the primary mechanism by which LANA upregulates EGFL7.

**EGFL7 contributes to LANA-induced angiogenic phenotype *in vitro***

LANA has been demonstrated to promote angiogenesis through a variety of mechanisms (13, 24, 28, 43, 44). EGFL7 also has been shown to promote angiogenesis in a variety of cancers. We therefore investigated whether EGFL7 contributes to LANA-induced angiogenesis. To this end, we studied the effect of EGFL7 knockdown on the angiogenic potential of LANA-expressing HUVEC cells using an *in vitro* endothelial tube formation assay. EGFL7 was depleted using EGFL7 siRNA in the HUVEC cells stably expressing LANA. As expected, the LANA-expressing cells demonstrated increased endothelial tube formation compared with the control cells (Fig 6A, a and b). However, when EGFL7 was knocked down using siRNA, tubule formation was reduced in LANA-expressing cells compared with the same cells transfected with control siRNA (Fig 6A, b and c). Western blotting analysis of the transfected cells used in the *in vitro* angiogenesis assay showed that EGFL7 expression was efficiently reduced by EGF7

siRNA (Fig 6B). These results demonstrated that EGFL7 is an important mediator of LANA-induced angiogenesis.

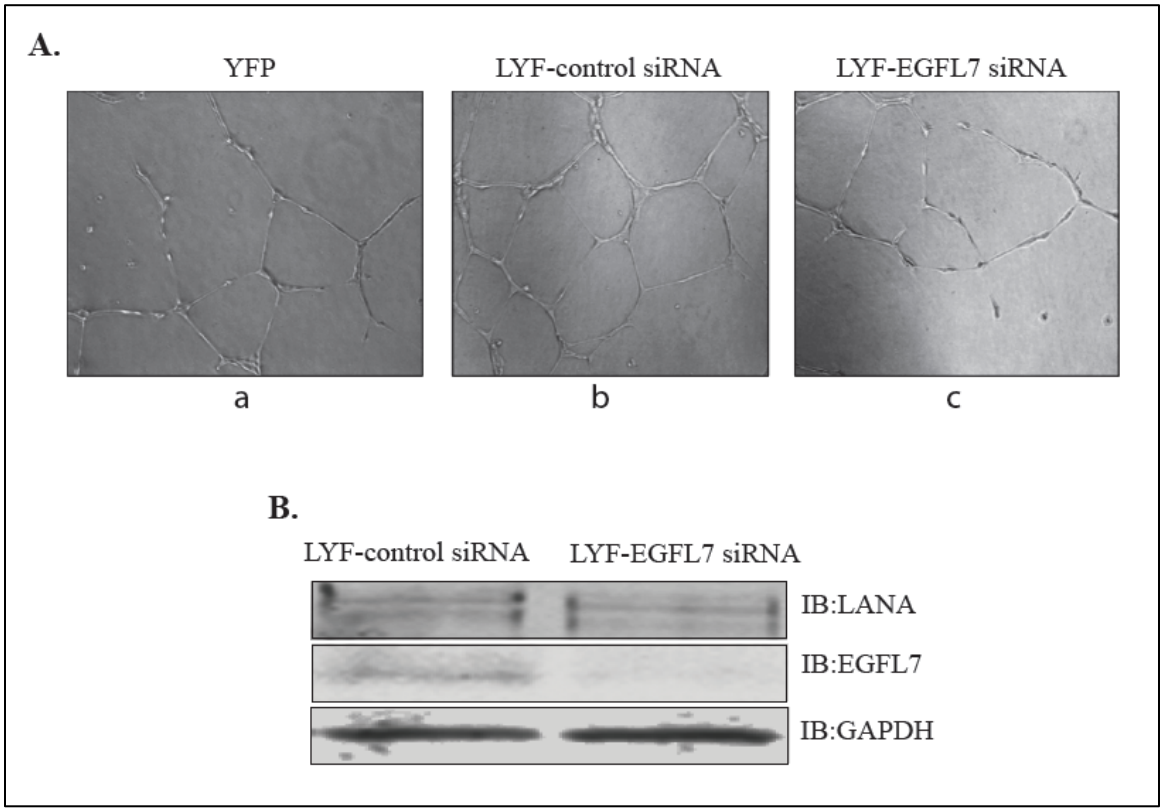


Figure 6 EGFL7 contributes to LANA-induced *in vitro* endothelial tubule formation. **A.** Representative images of tube formation in **(a)** control HUVEC cells (YFP), **(b)** HUVEC cells stably expressing LANA transfected with control siRNA (LYF-control siRNA) and **(c)** HUVEC cells stably expressing LANA transfected with EGFL7 siRNA (LYF- EGFL7 siRNA). The cells were plated on Geltrex Matrix-coated plates 24 h after transfection and the images were taken 24 h after plating. Ten percent of the transfected cells were reserved for Western blotting analysis. **B.** Western blotting showing the expression of EGFL7 and LANA in the cells used for the *in vitro* tubulogenesis assay. GAPDH expression was used as a control of equal loading.

**Discussion:**

Angiogenesis is a critical process for the survival of tumor cells since it fulfills the increased demands of oxygen and nutrients required by the rapidly dividing tumor cells. As a result, many solid tumors induce the expression of pro-angiogenic cytokines. EGFL7 is one such angiogenic cytokine overexpressed in multiple malignancies such as

malignant glioma, colorectal cancer, renal cell carcinoma and hepatocellular carcinoma (6, 11, 14, 15, 20, 45, 46). In these tumors, EGFL7 has been found to be positively associated with angiogenesis, growth and invasiveness. Extensive angiogenesis is an important feature of KS tumors. Comparable to the role of EGFL7 in other tumors that require extensive angiogenesis, it most likely plays important roles in the progression of KS tumors as well.

We initially identified EGFL7 as one of the genes induced in response to LANA in a screen designed to identify differentially regulated LANA responsive cellular genes using next-generation RNA sequencing. Also, hypoxia has been recently shown to induce expression of EGFL7 (19). The KS tumor environment is also highly hypoxic; KS tumors frequently arise in locations with low oxygen levels such as the lower extremities (5, 21, 49). Based on these findings, we further investigated the reactivation of EGFL7 expression during KSHV infection and the underlying mechanism in the present study. Our results revealed that EGFL7 transcript and protein expression were significantly elevated in latently KSHV-infected primary effusion lymphoma cells (BC3 and BCBL1) compared with KSHV-negative B cells (BJAB). The fact that LANA is responsible for this upregulation was highlighted by the fact that EGFL7 expression was also significantly elevated in B cells expressing LANA as a sole KSHV protein. An intriguing aspect of these findings is the elevated expression of EGFL7 in B cells. Normally, B cells do not participate in angiogenesis. Hence, the significance of EGFL7 overexpression in B cells during KSHV infection points toward the possible involvement of the paracrine mechanism inducing angiogenesis in the spindle cells of KS lesions, the cells that are thought to be of endothelial origin and serve as perpetual reservoirs of the virus.

Normally, EGFL7 expression is highly restricted to endothelial cells. Under physiological conditions, EGFL7 is only expressed under conditions that require angiogenesis such as embryogenesis and wound healing. This restricted pattern of EGFL7 expression could be at least part due to the inhibitory effects of Daxx protein on the Ets-1-dependent transactivation of the EGFL7 promoter (18). The interaction of Daxx with Ets-1 has been previously reported to repress transcriptional activation of at least three genes involved in the promotion of angiogenic phenotypes (MMP1, Bcl2 and Flt-1/VEGF receptor 1) (18, 24). Interestingly, LANA has been shown to sequester Daxx and consequently relieve Daxx-mediated inhibition on Ets-1-dependent VEGF receptor 1 promoter (24). Because the EGFL7 promoter also contains binding sites for Ets-1 we investigated whether LANA could activate the EGFL7 promoter by sequestering Daxx in a similar fashion. Our results showed that indeed LANA could activate EGFL7 promoter activity even when Daxx was overexpressed. This finding suggested that LANA transactivates the EGFL7 promoter by sequestering Daxx (Fig 4A). A deletion analysis of the EGFL7 promoter revealed that LANA could activate EGFL7 promoter only when an Ets-1 biding site was present. Irrespective of Daxx overexpression, LANA had no effect on the EGFL7 promoter when there was no Ets-1 binding site. Additionally, the association of Daxx protein with Ets-1 protein and the association of Daxx protein with the EGFL7 promoter were also reduced in the presence of LANA. Collectively, these results suggest that the sequestration of Daxx is the primary mechanism behind the LANA-mediated transactivation of the EGFL7 promoter. Further evidence in support of this hypothesis arose by comparing the ability of LANA to transactivate the full-length EGFL7 promoter construct that contains binding sites for all of the transcription factors (-1670 to +100) versus a promoter

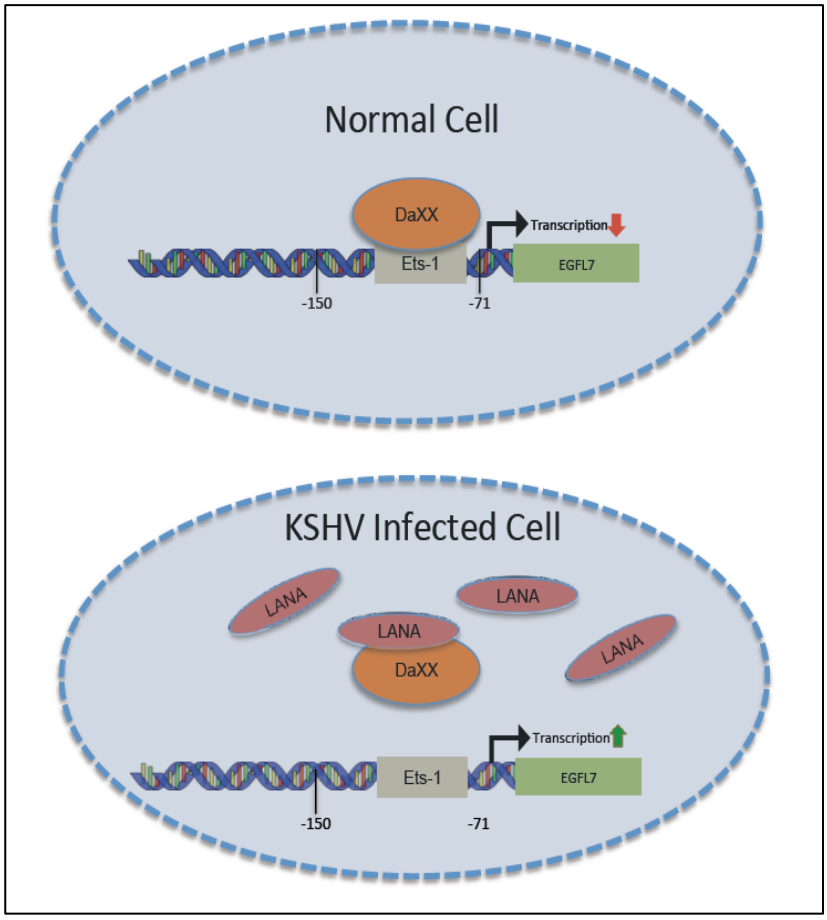


Figure 7 A model depicting the possible mechanism behind LANA-mediated upregulation of EGFL7. This figure has been adapted and modified from Murakami et al, (2006) (PMID: PMID: 16861237).

construct that contains Ets and GATA binding sites (-150 to +100) versus a promoter construct that contains GATA binding sites but not Ets-1 binding sites (-71 to +100). The magnitude of the LANA-mediated transactivation of the full-length EGFL7 promoter construct and the construct containing Ets/GATA binding sites was similar (compare Fig 3C, lane 4 and Fig 5D, lane 3, black bar). LANA failed to transactivate the (-71 to +100) promoter construct from which the Ets binding sites were deleted but the GATA binding sites were intact, suggesting that LANA-mediated upregulation of the EGFL7 promoter was indeed dependent on Ets1. Figure 7 shows a schematic summary of these results.

While the sequestration of Daxx appears to be the primary mechanism behind the upregulation of the EGFL7 promoter by LANA, the possibility of LANA transactivating the EGFL7 promoter through additional mechanisms remains. LANA has been

previously shown to activate hypoxia inducible factor (HIF)-α (1, 2, 4, 49). Recently, EGFL7 has been identified as a gene induced in response to HIF-1α. Several studies have suggested that the expression of HIF-1α potentiates the expression of Ets-1, although the underlying mechanism is not clear (17, 31, 39). While not explored in this study, the possibility exists that LANA could induce Ets-1 expression through HIF-α in addition to relieving inhibition on existing Ets-1 bound to the EGFL7 promoter.

The functional significance of EGFL7 upregulation by LANA was demonstrated by comparing the *in vitro* tubulogenic potential of HUVEC cells that did not express LANA, the cells that expressed LANA and the cells that expressed LANA but in which EGFL7 expression was knocked down using RNA interference. LANA-expressing cells showed higher tubulogenesis compared with control cells. However, when EGFL7 expression was knocked down in these LANA-expressing cells, tubulogenesis was compromised. When expressed in isolation, LANA has been demonstrated to induce angiogenesis through multiple mechanisms (4, 13, 34, 44). Even so, the fact that knockdown of EGFL7 in LANA-expressing cells compromises tubulogenesis highlights the significant contribution of EGFL7 in LANA-mediated angiogenesis.

In summary, we have identified EGFL7 as an angiogenic cytokine induced during KSHV infection and have explored the mechanism behind its upregulation during KSHV infection. Anti-angiogenic therapy is a promising avenue for the treatment of KS. Targeting EGFL7 in combination with the other currently available anti-angiogenic therapies may increase the efficacy of the currently available anti-angiogenic regimen available for KS treatment. Furthermore, because of the highly restricted pattern of EGFL7 expression during normal physiological conditions, one can expect anti-EGFL7

therapy to be relatively safer than other anti-angiogenic therapies that target molecules with broader expression profiles and pleiotropic effects. This study lays the foundation for future research focusing on the evaluation of EGFL7 as a potential anti-angiogenic target for the treatment of KS.

**References:**


1. **Cai, Q., K. Lan, S. C. Verma, H. Si, D. Lin, and E. S. Robertson.** 2006. Kaposi's sarcoma-associated herpesvirus latent protein LANA interacts with HIF-1 alpha to upregulate RTA expression during hypoxia: Latency control under low oxygen conditions. Journal of virology **80:**7965-7975.
2. **Cai, Q., M. Murakami, H. Si, and E. S. Robertson.** 2007. A potential alpha-helix motif in the amino terminus of LANA encoded by Kaposi's sarcoma-associated herpesvirus is critical for nuclear accumulation of HIF-1alpha in normoxia. Journal of virology **81:**10413-10423.
3. **Cai, Q., S. C. Verma, J. Lu, and E. S. Robertson.** 2010. Molecular biology of Kaposi's sarcoma-associated herpesvirus and related oncogenesis. Advances in virus research **78:**87-142.
4. **Cai, Q. L., J. S. Knight, S. C. Verma, P. Zald, and E. S. Robertson.** 2006. EC5S ubiquitin complex is recruited by KSHV latent antigen LANA for degradation of the VHL and p53 tumor suppressors. PLoS pathogens **2:**e116.
5. **Davis, D. A., A. S. Rinderknecht, J. P. Zoeteweij, Y. Aoki, E. L. Read-Connole, G. Tosato, A. Blauvelt, and R. Yarchoan.** 2001. Hypoxia induces lytic replication of Kaposi sarcoma-associated herpesvirus. Blood **97:**3244-3250.
6. **Diaz, R., J. Silva, J. M. Garcia, Y. Lorenzo, V. Garcia, C. Pena, R. Rodriguez, C. Munoz, F. Garcia, F. Bonilla, and G. Dominguez.** 2008. Deregulated expression of miR-106a predicts survival in human colon cancer patients. Genes, chromosomes & cancer **47:**794-802.
7. **Dimaio, T. A., and M. Lagunoff.** 2012. KSHV Induction of Angiogenic and Lymphangiogenic Phenotypes. Frontiers in microbiology **3:**102.
8. **Dupin, N., C. Fisher, P. Kellam, S. Ariad, M. Tulliez, N. Franck, E. van Marck, D. Salmon, I. Gorin, J. P. Escande, R. A. Weiss, K. Alitalo, and C. Boshoff.** 1999. Distribution of human herpesvirus-8 latently infected cells in Kaposi's sarcoma, multicentric Castleman's disease, and primary effusion lymphoma. Proc Natl Acad Sci U S A **96:**4546-4551.
9. **Gao, J., Q. Cai, J. Lu, H. C. Jha, and E. S. Robertson.** 2011. Upregulation of cellular Bcl-2 by the KSHV encoded RTA promotes virion production. PloS one **6:**e23892.
10. **Giffin, L., and B. Damania.** 2014. KSHV: pathways to tumorigenesis and persistent infection. Advances in virus research **88:**111-159.
11. **Hansen, T. F., R. Christensen, R. F. Andersen, F. B. Sorensen, A. Johnsson, and A. Jakobsen.** 2013. MicroRNA-126 and epidermal growth factor-like

domain 7-an angiogenic couple of importance in metastatic colorectal cancer. Results from the Nordic ACT trial. British journal of cancer **109:**1243-1251.

12. **Harris, T. A., M. Yamakuchi, M. Kondo, P. Oettgen, and C. J. Lowenstein.** 2010. Ets-1 and Ets-2 regulate the expression of microRNA-126 in endothelial cells. Arteriosclerosis, thrombosis, and vascular biology **30:**1990-1997.
13. **He, M., W. Zhang, T. Bakken, M. Schutten, Z. Toth, J. U. Jung, P. Gill, M. Cannon, and S. J. Gao.** 2012. Cancer angiogenesis induced by Kaposi sarcoma-associated herpesvirus is mediated by EZH2. Cancer research **72:**3582-3592.
14. **Huang, C., X. Yuan, Z. Li, Z. Tian, X. Zhan, J. Zhang, and X. Li.** 2014. VE-statin/Egfl7 siRNA inhibits angiogenesis in malignant glioma in vitro. International journal of clinical and experimental pathology **7:**1077-1084.
15. **Huang, C. H., X. J. Li, Y. Z. Zhou, Y. Luo, C. Li, and X. R. Yuan.** 2010. Expression and clinical significance of EGFL7 in malignant glioma. Journal of cancer research and clinical oncology **136:**1737-1743.
16. **Kellam, P., D. Bourboulia, N. Dupin, C. Shotton, C. Fisher, S. Talbot, C. Boshoff, and R. A. Weiss.** 1999. Characterization of monoclonal antibodies raised against the latent nuclear antigen of human herpesvirus 8. J Virol **73:**5149-5155.
17. **Kosaka, T., A. Miyajima, S. Shirotake, E. Kikuchi, M. Hasegawa, S. Mikami, and M. Oya.** 2010. Ets-1 and hypoxia inducible factor-1alpha inhibition by angiotensin II type-1 receptor blockade in hormone-refractory prostate cancer. The Prostate **70:**162-169.
18. **Li, R., H. Pei, D. K. Watson, and T. S. Papas.** 2000. EAP1/Daxx interacts with ETS1 and represses transcriptional activation of ETS1 target genes. Oncogene **19:**745-753.
19. **Liu, Y. S., Z. W. Huang, A. Q. Qin, Y. Huang, F. Giordano, Q. H. Lu, and W. D. Jiang.** 2015. The expression of epidermal growth factor-like domain 7 regulated by oxygen tension via hypoxia inducible factor (HIF)-1alpha activity. Postgraduate medicine **127:**144-149.
20. **Luo, B. H., F. Xiong, J. P. Wang, J. H. Li, M. Zhong, Q. L. Liu, G. Q. Luo, X. J. Yang, N. Xiao, B. Xie, H. Xiao, R. J. Liu, C. S. Dong, K. S. Wang, and J. F. Wen.** 2014. Epidermal growth factor-like domain-containing protein 7 (EGFL7) enhances EGF receptor-AKT signaling, epithelial-mesenchymal transition, and metastasis of gastric cancer cells. PloS one **9:**e99922.
21. **Ma, Q., L. E. Cavallin, B. Yan, S. Zhu, E. M. Duran, H. Wang, L. P. Hale, C. Dong, E. Cesarman, E. A. Mesri, and P. J. Goldschmidt-Clermont.** 2009. Antitumorigenesis of antioxidants in a transgenic Rac1 model of Kaposi's sarcoma. Proceedings of the National Academy of Sciences of the United States of America **106:**8683-8688.
22. **Mesri, E. A., L. E. Cavallin, B. M. Ashlock, H. J. Leung, Q. Ma, and P. J. Goldschmidt-Clermont.** 2013. Molecular studies and therapeutic targeting of Kaposi's sarcoma herpesvirus (KSHV/HHV-8) oncogenesis. Immunologic research **57:**159-165.
23. **Mesri, E. A., E. Cesarman, and C. Boshoff.** 2010. Kaposi's sarcoma and its associated herpesvirus. Nat Rev Cancer **10:**707-719.

24. **Murakami, Y., S. Yamagoe, K. Noguchi, Y. Takebe, N. Takahashi, Y. Uehara, and H. Fukazawa.** 2006. Ets-1-dependent expression of vascular endothelial growth factor receptors is activated by latency-associated nuclear antigen of Kaposi's sarcoma-associated herpesvirus through interaction with Daxx. The Journal of biological chemistry **281:**28113-28121.
25. **Naranatt, P. P., H. H. Krishnan, S. R. Svojanovsky, C. Bloomer, S. Mathur, and B. Chandran.** 2004. Host gene induction and transcriptional reprogramming in Kaposi's sarcoma-associated herpesvirus (KSHV/HHV-8)-infected endothelial, fibroblast, and B cells: insights into modulation events early during infection. Cancer research **64:**72-84.
26. **Nichol, D., and H. Stuhlmann.** 2012. EGFL7: a unique angiogenic signaling factor in vascular development and disease. Blood **119:**1345-1352.
27. **Parravicini, C., B. Chandran, M. Corbellino, E. Berti, M. Paulli, P. S. Moore, and Y. Chang.** 2000. Differential viral protein expression in Kaposi's sarcoma-associated herpesvirus-infected diseases: Kaposi's sarcoma, primary effusion lymphoma, and multicentric Castleman's disease. Am J Pathol **156:**743-749.
28. **Paudel, N., S. Sadagopan, S. Balasubramanian, and B. Chandran.** 2012. Kaposi's sarcoma-associated herpesvirus latency-associated nuclear antigen and angiogenin interact with common host proteins, including annexin A2, which is essential for survival of latently infected cells. Journal of virology **86:**1589-1607.
29. **Paudel, N., S. Sadagopan, S. Chakraborty, G. Sarek, P. M. Ojala, and B. Chandran.** 2012. Kaposi's sarcoma-associated herpesvirus latency-associated nuclear antigen interacts with multifunctional angiogenin to utilize its antiapoptotic functions. Journal of virology **86:**5974-5991.
30. **Paul, A. G., B. Chandran, and N. Sharma-Walia.** 2013. Cyclooxygenase-2-prostaglandin E2-eicosanoid receptor inflammatory axis: a key player in Kaposi's sarcoma-associated herpes virus associated malignancies. Translational research : the journal of laboratory and clinical medicine **162:**77-92.
31. **Peters, C. L., C. J. Morris, P. I. Mapp, D. R. Blake, C. E. Lewis, and V. R. Winrow.** 2004. The transcription factors hypoxia-inducible factor 1alpha and Ets-1 colocalize in the hypoxic synovium of inflamed joints in adjuvant-induced arthritis. Arthritis and rheumatism **50:**291-296.
32. **Prakash, O., Z. Y. Tang, X. Peng, R. Coleman, J. Gill, G. Farr, and F. Samaniego.** 2002. Tumorigenesis and aberrant signaling in transgenic mice expressing the human herpesvirus-8 K1 gene. Journal of the National Cancer Institute **94:**926-935.
33. **Purushothaman, P., S. Thakker, and S. C. Verma.** 2015. Transcriptome Analysis of Kaposi's Sarcoma-Associated Herpesvirus during De Novo Primary Infection of Human B and Endothelial Cells. Journal of virology **89:**3093-3111.
34. **Sadagopan, S., N. Sharma-Walia, M. V. Veettil, V. Bottero, R. Levine, R. J. Vart, and B. Chandran.** 2009. Kaposi's sarcoma-associated herpesvirus upregulates angiogenin during infection of human dermal microvascular endothelial cells, which induces 45S rRNA synthesis, antiapoptosis, cell proliferation, migration, and angiogenesis. Journal of virology **83:**3342-3364.

35. **Sharma-Walia, N., A. G. Paul, V. Bottero, S. Sadagopan, M. V. Veettil, N. Kerur, and B. Chandran.** 2010. Kaposi's sarcoma associated herpes virus (KSHV) induced COX-2: a key factor in latency, inflammation, angiogenesis, cell survival and invasion. PLoS pathogens **6:**e1000777.
36. **Shin, Y. C., C. H. Joo, M. U. Gack, H. R. Lee, and J. U. Jung.** 2008. Kaposi's sarcoma-associated herpesvirus viral IFN regulatory factor 3 stabilizes hypoxia-inducible factor-1 alpha to induce vascular endothelial growth factor expression. Cancer research **68:**1751-1759.
37. **Sivakumar, R., N. Sharma-Walia, H. Raghu, M. V. Veettil, S. Sadagopan, V. Bottero, L. Varga, R. Levine, and B. Chandran.** 2008. Kaposi's sarcoma-associated herpesvirus induces sustained levels of vascular endothelial growth factors A and C early during in vitro infection of human microvascular dermal endothelial cells: biological implications. Journal of virology **82:**1759-1776.
38. **Sodhi, A., S. Montaner, V. Patel, M. Zohar, C. Bais, E. A. Mesri, and J. S. Gutkind.** 2000. The Kaposi's sarcoma-associated herpes virus G protein-coupled receptor up-regulates vascular endothelial growth factor expression and secretion through mitogen-activated protein kinase and p38 pathways acting on hypoxia-inducible factor 1alpha. Cancer research **60:**4873-4880.
39. **Tanaka, H., Y. Terada, T. Kobayashi, T. Okado, S. Inoshita, M. Kuwahara, A. Seth, Y. Sato, and S. Sasaki.** 2004. Expression and function of Ets-1 during experimental acute renal failure in rats. Journal of the American Society of Nephrology : JASN **15:**3083-3092.
40. **Thakker, S., P. Purushothaman, N. Gupta, S. Challa, Q. Cai, and S. C. Verma.** 2015. KSHV LANA inhibits MHC II expression by disrupting the enhanceosome assembly through binding with the RFX complex. Journal of virology.
41. **Verma, S. C., K. Lan, and E. Robertson.** 2007. Structure and function of latency-associated nuclear antigen. Curr Top Microbiol Immunol **312:**101-136.
42. **Wang, S., A. B. Aurora, B. A. Johnson, X. Qi, J. McAnally, J. A. Hill, J. A. Richardson, R. Bassel-Duby, and E. N. Olson.** 2008. The endothelial-specific microRNA miR-126 governs vascular integrity and angiogenesis. Developmental cell **15:**261-271.
43. **Wang, X., Z. He, T. Xia, X. Li, D. Liang, X. Lin, H. Wen, and K. Lan.** 2014. Latency-associated nuclear antigen of Kaposi sarcoma-associated herpesvirus promotes angiogenesis through targeting notch signaling effector Hey1. Cancer research **74:**2026-2037.
44. **Watanabe, T., M. Sugaya, A. M. Atkins, E. A. Aquilino, A. Yang, D. L. Borris, J. Brady, and A. Blauvelt.** 2003. Kaposi's sarcoma-associated herpesvirus latency-associated nuclear antigen prolongs the life span of primary human umbilical vein endothelial cells. Journal of virology **77:**6188-6196.
45. **Wu, F., L. Y. Yang, Y. F. Li, D. P. Ou, D. P. Chen, and C. Fan.** 2009. Novel role for epidermal growth factor-like domain 7 in metastasis of human hepatocellular carcinoma. Hepatology **50:**1839-1850.
46. **Xu, H. F., L. Chen, X. D. Liu, Y. H. Zhan, H. H. Zhang, Q. Li, and B. Wu.** 2014. Targeting EGFL7 expression through RNA interference suppresses renal

cell carcinoma growth by inhibiting angiogenesis. Asian Pacific journal of cancer prevention : APJCP **15:**3045-3050.

47. **Ye, F. C., D. J. Blackbourn, M. Mengel, J. P. Xie, L. W. Qian, W. Greene, I. T. Yeh, D. Graham, and S. J. Gao.** 2007. Kaposi's sarcoma-associated herpesvirus promotes angiogenesis by inducing angiopoietin-2 expression via AP-1 and Ets1. Journal of virology **81:**3980-3991.
48. **Ye, F. C., F. C. Zhou, S. Nithianantham, B. Chandran, X. L. Yu, A. Weinberg, and S. J. Gao.** 2013. Kaposi's sarcoma-associated herpesvirus induces rapid release of angiopoietin-2 from endothelial cells. Journal of virology **87:**6326-6335.
49. **Zhang, L., C. Zhu, Y. Guo, F. Wei, J. Lu, J. Qin, S. Banerjee, J. Wang, H. Shang, S. C. Verma, Z. Yuan, E. S. Robertson, and Q. Cai.** 2014. Inhibition of KAP1 enhances hypoxia-induced Kaposi's sarcoma-associated herpesvirus reactivation through RBP-Jkappa. Journal of virology **88:**6873-6884.